UNIVERSITY OF SOUTHAMPTON

PREDICTING TRANSMISSIBILITY OF CAR SEATS FROM SEAT IMPEDANCE AND THE APPARENT MASS OF THE HUMAN BODY

LIN WEI, (B.Sc. M.Sc.)

DOCTOR OF PHILOSOPHY

FACULTY OF ENGINEERING AND APPLIED SCIENCE
INSTITUTE OF SOUND AND VIBRATION RESEARCH

APRIL 2000

UNIVERSITY OF SOUTHAMPTON

ABSTRACT

FACULTY OF ENGINEERING AND APPLIED SCIENCE
INSTITUTE OF SOUND AND VIBRATION RESEARCH

Doctor of Philosophy

PREDICTING TRANSMISSIBILITY OF CAR SEATS FROM SEAT IMPEDANCE AND THE APPARENT MASS OF THE HUMAN BODY

By Lin Wei

A literature review suggested that seat transmissibility could be used to evaluate seat dynamic performance. Using a mathematical model to predict seat transmissibility may be useful, but no standard seat-person model has been developed. This study developed a standard seat-person model based on measured seat impedance and the apparent mass of the human body so as to predict the transmissibility of conventional car seats. There are three parts to this thesis: the development of a human body model, a seat model and a seat-person model.

Many researchers have considered using a linear mathematical model to represent the seated body apparent mass, but researchers have not considered whether this model can represent the body apparent mass in a wide range of vibration environments. It has been reported that the body apparent mass is affected by sitting posture, footrests, vibration magnitude, vibration spectra and backrests, but some factors have not been investigated. Four experiments were conducted to investigate the influences of seat cushion inclination, hard and soft seats, seat backrests and vibration spectra on measured apparent mass. In each experiment, ten subjects were exposed to 60 seconds of random vibration with a frequency range from 0.5 to 25 Hz. The conclusions were: (i) the effects of seat inclination, hard and soft seat and vibration spectra on body apparent mass are not great and so a simple seated body mathematical model is useful, (ii) the seat backrest has a significant influence on apparent mass so the model parameters must be varied for different backrest conditions, (iii) a change of vibration magnitude revealed a non-linear response of the body, so model modifications are needed for different vibration magnitudes. Four linear models were developed to predict body apparent mass and encouraging results were obtained from two models.

Fairley and Griffin (1986) proposed an indenter method to measure seat impedance. An experiment was conducted to compare this method with other seat test methods. It was concluded that an indenter can provide useful results, but the method requires development. There are many factors that may affect test results, such as vibration magnitude, pre-load force, seat cushion inclination, contact area and vibration spectra. Experiments were conducted to investigate the effect of these factors on foam impedance. Five foams were used in each experiment over the frequency range of 0.5 to 30 Hz. The conclusions were: (i) the influence of seat inclination, vibration magnitude and vibration spectra were small, (ii) the effect of pre-load and contact area were significant and must be specified to obtain useful measurements of seat impedance.

A seat-person model was developed based on the above studies. Three experiments were conducted to compare measured and predicted seat transmissibilities. Eight subjects participated in a laboratory study with a seat and a foam over the frequency range from 1 to 30 Hz; six subjects participated in a field study with three car seats over the frequency range from 1 to 50 Hz. It was found that the seat-person model provided good predictions of seat transmissibilities. However a new model, which includes interaction between the seat backrest and the person, should provide improved predictions of seat transmissibility.

ACKNOWLEDGEMENTS

I would like to express my great appreciation to my supervisor, professor M. J. Griffin, for his excellent supervision. His extremely kind support with a lot of advice and suggestions for this research encouraged me and guided my study in the right direction. I would also like to thank to all subjects who participated in the experiments. I am particularly grateful for the friendly working environment provided by every member of the Human Factor Research Unit.

I especially thank my wife, Guo Hong, for her devoted support in providing me a comfortable working atmosphere. I would like to thank my family for their constant support and encouragement.

Notation

List of symbols

c Viscous damping of seat, Ns/m

c_1 Viscous damping of body first subsystem, Ns/m

c_2 Viscous damping of body second subsystem, Ns/m

c_b Viscous damping for seat-person model with backrest, Ns/m

F Force, Newton

f Frequency, in hertz (Hz).

i $\sqrt{-1}$

k Stiffness of seat, N/m

k_1 Stiffness of body first subsystem, N/m

k_2 Stiffness of body second subsystem, N/m

k_b Stiffness for seat-person model with backrest, N/m

m Model frame mass, kg

m_1 Mass of body first subsystem, kg

m_2 Mass of body second subsystem, kg

PSD power spectral density expressed as mean square acceleration per unit bandwidth $(m/s^2)^2/Hz$

PDF probability density function of acceleration amplitudes

r.m.s. root-mean-square

$S(\omega)$ Dynamic stiffness

T Seat transmissibility

θ Phase of seat transmissibility

x (or d) Displacement, in metres (m)

$\dot{x}$ (or v) Instantaneous velocity, in metres per second (ms^{-1}).

$\ddot{x}$ (or a) Instantaneous acceleration, in metres per second squared (ms^{-2}).

ω Circular frequency (radians/s)

CHAPTER 1

INTRODUCTION

People are exposed to vibration environments when they travel in a car, a bus or a train. Such whole-body vibration could have adverse effects on health or could result in discomfort even when sitting on a soft seat. In order to reduce effects of vibration on people, good seat isolation features became an issue in both research and industrial development. Sitting comfort, which depends on seat dynamic properties became, therefore, one of the prime matters in vehicle design.

In order to provide good isolation of vibration at the frequencies to which a seat will be exposed, seat dynamic evaluation techniques were needed. There are many proposed methods for evaluating seat dynamic properties. Seat transmissibility is the most often used tool to express seat dynamic characteristics and performance. However, obtaining a good measurement of seat transmissibility is a difficult task. At the moment, most seat transmissibilities are measured using seated subjects in the field. Using a subject to measure seat transmissibility is a time consuming and expensive method, it also has an inherent risk when exposing the human body to vibration. A laboratory test may improve the repeatability of seat transmissibility measurements because it reduces the existence of any cross-axis coupling, but other problems still exist. Fairley and Griffin (1986) proposed a prediction method to obtain seat transmissibilities. The method used the measured seat impedance and the measured body apparent mass to directly predict seat transmissibility. They showed good prediction results using this method.

The research in this thesis continues the idea of predicting seat transmissibility and further develops it. In this research, a seat-person mathematical model based on the measured seat impedance and the measured human body impedance were developed and then used to predict seat transmissibility. There were three main parts in this study: (i) developing a standard

mathematical model to replace the seated body, (ii) developing a seat model representing seat dynamic characteractics, (iii) using the seat-person model to predict seat transmissibilities. The study concentrates on conventional car seats.

Sitting body model development

The use of a linear mathematical model to replace the seated body has been proposed by many researchers (Vogt *et al.,* 1968; Suggs *et al.,* 1969; Kaleps *et al.,* 1971; Fairley and Griffin, 1986 and International Organization for Standardization, 1981). However, these studies did not consider the effect of changes to apparent mass in different vibration environments. The human body is a complex system. The features of this system are affected by many factors, such as sitting posture, vibration magnitude, seat inclination, hard and soft seat, seat backrest, footrest and vibration spectra, etc. A full understanding of the factors influencing the body apparent mass is needed before setting up a standard body mathematical model. Some factors have been studied by researchers, for example vibration magnitude, sitting posture, footrest and backrest, but some factors have not been investigated, such as the effect of hard and soft seat and seat inclination. The studies here investigate the effect of these factors on measured apparent masses so that a model can be developed to represent the seated body in varied vibration environments.

Many studies revealed that the response of the seated body was non-linear with respect to vibration magnitude. However, the current international standard and some researchers suggest a linear model to represent the seated body. It is unclear whether any revision of these linear models can extend the use of them to include non-linear properties. In other words, it is needed to investigate the relation between the models and the response of the seated body at varied vibration magnitudes. A modified linear model is developed to represent the non-linear response of the sitting body.

It has been found previously that the effect of a backrest on the measured apparent mass was significant. No researchers have been concerned whether

a linear model can represent the change in body apparent mass with changes in backrest angles. Developing a model representing the seated body with varied backrest angles is one of the aims of this thesis. An experiment is conducted to investigate the relation between the linear model and apparent mass with changed backrest angles.

No previous research has focused on the effect of hard and soft seat, and seat inclination on apparent mass. The study of these factors would extend the understanding of responses of sitting subjects to vibration. Two experiments are conducted to investigate the influence of these factors on apparent mass. The findings of the studies can be helpful in model development.

Seat test method and seat model development

Predicting seat transmissibility depends not only on a model of the human body but also on a model of the seat. A seat model based on the measured seat impedance is developed.

However, there are many methods to obtain seat impedance. A new method, proposed by Fairley and Griffin (1986), used an indenter to measure seat impedance. An experiment is conducted to investigate which method can give reliable data.

The indenter rig is complex and there are many factors affecting test results, such as vibration magnitude, pre-load, seat cushion inclination, contact area and vibration spectra. Previous research has not investigated the effect of these factors on the indenter test. Some experiments are therefore conducted in this thesis to investigate the influence of these factors on results obtained with an indenter. The findings will contribute to establishing a standard seat test method.

Predicting seat transmissibility using seat-person model

A seat-person model based on the separately developed human body model and the seat model is then used to predict seat transmissibility. Assessment is

performed through a comparison between the measured and predicted seat transmissibilities. Three experiments are designed to assess the model.

Because most studies were based on laboratory measurements without a seat backrest, it is not surprising that the prediction of seat transmissibility performed in the laboratory without a seat backrest gave encouraging results. However, the model is not suitable for predicting the measurements in the field with a seat backrest. A new model is, therefore, developed to predict seat transmissibility with a conventional car seat backrest.

The general objective of the research is to develop a standard test procedure to predict transmissibility of car seats from seat dynamic properties. The core of the study is the seat-person model development based on a full understanding of the human body apparent mass and the measured seat impedance. Series studies have been conducted to obtain a standard seat-person model and encouraging results were achieved using this model.

Table 1.1 shows experiments and model application in thesis. The thesis is divided into nine chapters. The content of each chapter is summarised as follows:

Chapter 1: The objectives of this research are explained.
Chapter 2: A review of previous studies in related fields is presented. The responses of the seated body and coresponding mathematical models are discussed. The study area was selected.
Chapter 3: The apparatus used for the experiments in this research is described. The data analysis method is also described.
Chapter 4: A preliminary study conducted to select the appropriate research direction is presented. Encouraging data were obtained in limited conditions.
Chapter 5: This chapter describes a method to obtain seat mechanical properties. The seat test methods and factors affecting the seat measurement are discussed.

Chapter 6: Alternative mathematical models representing the sitting body are investigated. A comparison between these models is performed. Models with good predictions of seat transmissibility were produced.

Chapter 7: Factors affecting seated body responses are discussed. Experiments were performed to investigate the influences of these factors on the response of the sitting body. Modified models were developed.

Chapter 8: This chapter describes the prediction seat transmissibilities and comparing with measurements. Encouraging results were obtained in laboratory and in the field.

Chapter 9: The findings of this research are summarised in this chapter. Recommendations for future research are also provided.

Table 1.1 Experiments reported in thesis.

Chapter	Experiments	Factors studied	Model applied
4.2	One foam, indenter test	—	One degree-of-freedom (dof) body model and foam model
5.2.1	Five car seats, static and dynamic indenter tests	Seat dynamic stiffness and static stiffness	Seat model
5.2.2.1	Seat tests using indenter, sand bag and rigid mass	Comparison of seat test methods	Seat model
5.3	Five foams, indenter tests	Effect of contact area, static force, vibration magnitude and inclination on foam dynamic stiffness using indenter test.	Foam model
6	Fairley and Griffin: 60-people apparent mass measurements	—	Body one dof model 1a, 1b and body two dof model 2a, 2b.
7.2	Mansfield: 8-people apparent mass measurements	Effect of input vibration magnitude on apparent mass	Modification of model 2b
7.3	10-subject apparent mass measurements	Effect of seat cushion inclination on body apparent mass	Model 2b
7.4	10-subject apparent mass measurements	Effect of seat backrest on body apparent mass	Modification of model 2b

Chapter	Experiments	Factors study	Model application
7.5	10 subject apparent mass measurements	Effect of hard seat and soft seat as well as vibration spectra on body apparent mass	Model 2b and foam model
8.2	Seat transmissibility measured in laboratory	Effect of seat inclination on seat transmissibility	—
8.3	Foam and seat dynamic stiffness and transmissibility measured in laboratory	Comparison of predicted and measured foam and seat transmissibility	Modified model 2b
8.4	Seat transmissibility measured in field	Compare predicted and measured foam and seat transmissibility	New body model

CHAPTER 2

LITERATURE REVIEW

2.1 INTRODUCTION

The aim of this chapter is to review previous studies of seat and human body dynamic response so as to find out the factors that affect seat transmissibility. The review of previous studies will be helpful to determine the fields of future study and avoid spending time on the road that other people have passed.

Various mechanical responses to whole-body vibration have been measured by many researchers to investigate the effects of vibration on the human body. A number of human body dynamic responses have been obtained through experimental investigations. However, the experimental results are not always consistent because the human body is a complex structure with large variability between subjects and within a subject. Many biodynamic models of the human body response to the vertical vibration have been developed so as to interpret the measured responses with a physical and theoretical understanding, and also to predict dynamic responses of body. It is the purpose of this review to investigate and study the factors that affect the body responses so as to develop a suitable model representing the human body in various vibration environments.

The seat transmissibility gives an insight into the dynamic response of a seat. Seat transmissibility is the frequency response function for vibration transmitted from the base of a seat to the person sitting on the seat. However, the transmission of vibration through a seat is dependent on the mechanical impedance of the body supported on the seat: the seat and the body act as a coupled dynamic system. Many previous seat transmissibility measurements are summarised in this review.

This literature review is a summary of previous studies of the mechanical impedance of the human body, the transmissibility of seats, biodynamic

models of sitting persons and seat test methods. The intention of this review is to find out all important factors affecting the seat dynamic response so as to develop an useful method to predict the seat transmissibility and SEAT values.

2.2 MECHANICAL IMPEDANCE OF THE SITTING HUMAN BODY IN THE VERTICAL VIBRATION

2.2.1 Introduction

The mechanical impedance of a resilient system reflects its dynamic properties. When considering the effects of vibration on a system, it is valuable to have an understanding of the mechanical characteristics of the system. There are two types of mechanical impedance, transfer and driving point mechanical impedance. When the excitation point and the response point are different, they are termed the transfer mechanical impedance. When the response point is the same as the excitation point, they are termed the driving point mechanical impedance. Transfer mechanical impedance of the human body is outside the scope of this study.

For a simple structure, driving-point mechanical impedance is a useful tool to reveal the fundamental natural frequency and the resonances of the major subsystems. Plotting impedance versus frequency, it is possible to calculate the system parameters for the main system or for the subsystem if their resonance peaks can be distinguished clearly.

The driving-point mechanical impedance, $Z(\omega)$, is defined as the ratio of the driving force, $F(\omega)$, acting on a system to the resulting velocity, $v(\omega)$, of the system measured at the same point and in the same direction as the applied force.

$$\text{Mechanical Impedance, } Z(\omega) = \frac{F(\omega)}{v(\omega)} \qquad (2.1)$$

Where Z(ω), F(ω) and v(ω) are the complex values for impedance, force and velocity amplitudes respectively at a given frequency, ω.

In addition to mechanical impedance, apparent mass and dynamic stiffness are also used as a tool to measure system dynamic properties.

The apparent mass M(ω), is defined as the ratio of the driving force, F(ω), at the driving point to the resulting acceleration, a(ω), at the same point.

$$\text{Apparent mass, } M(\omega) = \frac{F(\omega)}{a(\omega)} \qquad (2.2)$$

Where M(ω), F(ω) and a(ω) are the complex values for apparent mass, force and acceleration amplitudes respectively at a given frequency, ω.

The dynamic stiffness S(ω), is defined as the ratio of the driving force, F(ω), at the driving point to the resulting displacement, d(ω), at the same point.

$$\text{Dynamic stiffness, } S(\omega) = \frac{F(\omega)}{d(\omega)} \qquad (2.3)$$

Where S(ω), F(ω) and d(ω) are the complex values for dynamic stiffness, force and displacement amplitudes respectively at a given frequency, ω.

Table 2.1 drawn by Griffin (1990) shows all used terms defined for the measurements of system driving point dynamic response. When the movement is measured at a distant point in the system the term transfer impedance is used.

The three elements of a simple spring-mass-damper system have typical impedance curves as a function of frequency. For a pure mass the impedance is a straight line through the zero-point. Table 2.2 shows dynamic responses of pure masses, dampers and springs.

Table 2.1 Some common measures of dynamic response. From Griffin 1990.

Ratio	Preferred terms	Other terms
Force/acceleration	Apparent mass	Effective weight
	Effective mass	Effective load
Force/velocity	Mechanical impedance	
Force/displacement	Dynamic stiffness	Dynamic modulus
Acceleration/displacement	Accelerance	Inertance
Velocity/force	Mobility	Mechanical admittance
Displacement/force	Dynamic compliance	Receptance

Table 2.2 Dynamic responses of pure masses, dampers and springs ($\omega=2\pi f$) From Griffin 1990.

Element	Modulus		Phase
Mass, m	Apparent mass	$= m$	a and F in phase
	Mechanical impedance	$= i\omega m$	v lags F by 90^0
	Dynamic stiffness	$= -\omega^2 m$	d and F 180^0 out of phase
Damper, c	Apparent mass	$= c/i\omega$	a leads F by 90^0
	Mechanical impedance	$= c$	v and F in phase
	Dynamic stiffness	$= i\omega c$	d lags F by 90^0
Spring, k	Apparent mass	$= -k/\omega^2$	a and F 180^0 out of phase
	Mechanical impedance	$= k/i\omega$	v leads F by 90^0
	Dynamic stiffness	$= k$	d and F in phase

Although driving point mechanical impedance (DPMI) and apparent mass (APMS) both can reveal system dynamic properties, there is a difference between the functions. A recently reported synthesis of selected published data, performed on both DPMI and APMS data, revealed the important differences between the two functions (Wu *et al.* 1997). The two biodynamic functions yield considerably different dominant frequency at which the peak magnitude is observed. The analysis of the data sets, reported in the literature and acquired under similar test conditions, revealed extensive variations in both the resonance magnitude and resonance frequency, irrespective of the

biodynamic function considered, attributed to differences in the test conditions, measurement techniques, data analysis methods, test objectives, subject populations, etc. The analysis of the APMS data, however, revealed a more consistent primary resonance frequency near 4.4 Hz, while this primary resonance frequency derived from the reported DPMI data ranged from 4.0 to 5.6 Hz in the DPMI data. The statistical results of the primary resonance frequency of the human body are summarized in Table 2.3.

Table 2.3 Variation in the primary resonance frequency of the human body derived from 8 data sets (Wu *et al.* 1997).

Function	Mean value (Hz)	Standard Deviation (Hz)	Range (Hz)
DPMI magnitude	4.70	0.51	4.0-5.6
APMS magnitude	4.38	0.46	3.6-4.8

2.2.2 Mechanical impedance of the sitting human

Sensations perceived by the human body in the sitting position when subjected to vertical vibration are due to the deformation and relative movement of organs and body segments (Donati 1983). Indeed, visual observation shows that the human body does not vibrate like a pure mass. Different body parts can be animated with relative movement whose form is a function of frequency, magnitude and axis of vibration.

The mechanical impedance and the apparent mass are the most widely measured driving point responses for whole-body vibration. The driving point (excitation point) of whole-body vibration is the buttocks when a subject is sitting on a seat. When measuring the driving point responses of a seated subject, the subject sits on a seat mounted on a vibrator. Excitation and measurement are usually in the vertical direction. The excitation velocity or acceleration is measured on the seat. Velocity is sometimes integrated from acceleration measured by an accelerometer, if mechanical impedance is used to study body dynamic properties. A force transducer placed between the seat and the buttocks of the subject measures the response force. Mathematical descriptions of the driving point impedance and the apparent mass are

obtained by substituting the output by force and the input by velocity or acceleration (equation 2.1 and 2.2).

It will be realized that knowledge of the mechanical impedance of a body will, at least, give some indication of what force is required to produce a given movement. The apparent mass of the body has the advantage that it can be obtained directly from the signals provided by accelerometers and force transducers. At very low frequency, the value of apparent mass is equal to the human body static mass and the force and acceleration are in phase (Table 2.2).

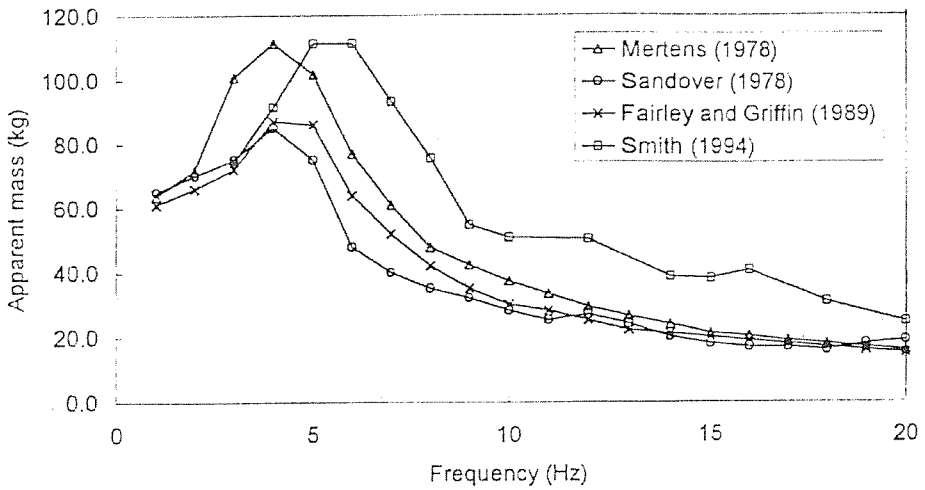

Figure 2.1 Apparent masses of sitting subjects. (Mertens 1978, Sandover 1978, Fairley and Griffin 1989 and Smith 1994). From Mansfield 1998.

Many researchers have measured mechanical impedance or apparent mass of the seated body (e.g. Coermann 1962, Pradko 1968, Suggs *et al.* 1969, Miwa 1975, Sandover 1978 and 1982, Fairley 1986 and 1989, Mansfield 1997). The experiments were conducted in laboratories on mechanical, electrodynamic or hydraulic vibrators. Some of the previously reported data are shown in Figure 2.1. Although authors did not always report subject static weight, the body static masses supported on the seat were equal to the apparent mass at the lowest frequency.

From previous mechanical impedance data, it can be observed that the main resonance frequency of human apparent mass or mechanical impedance is at

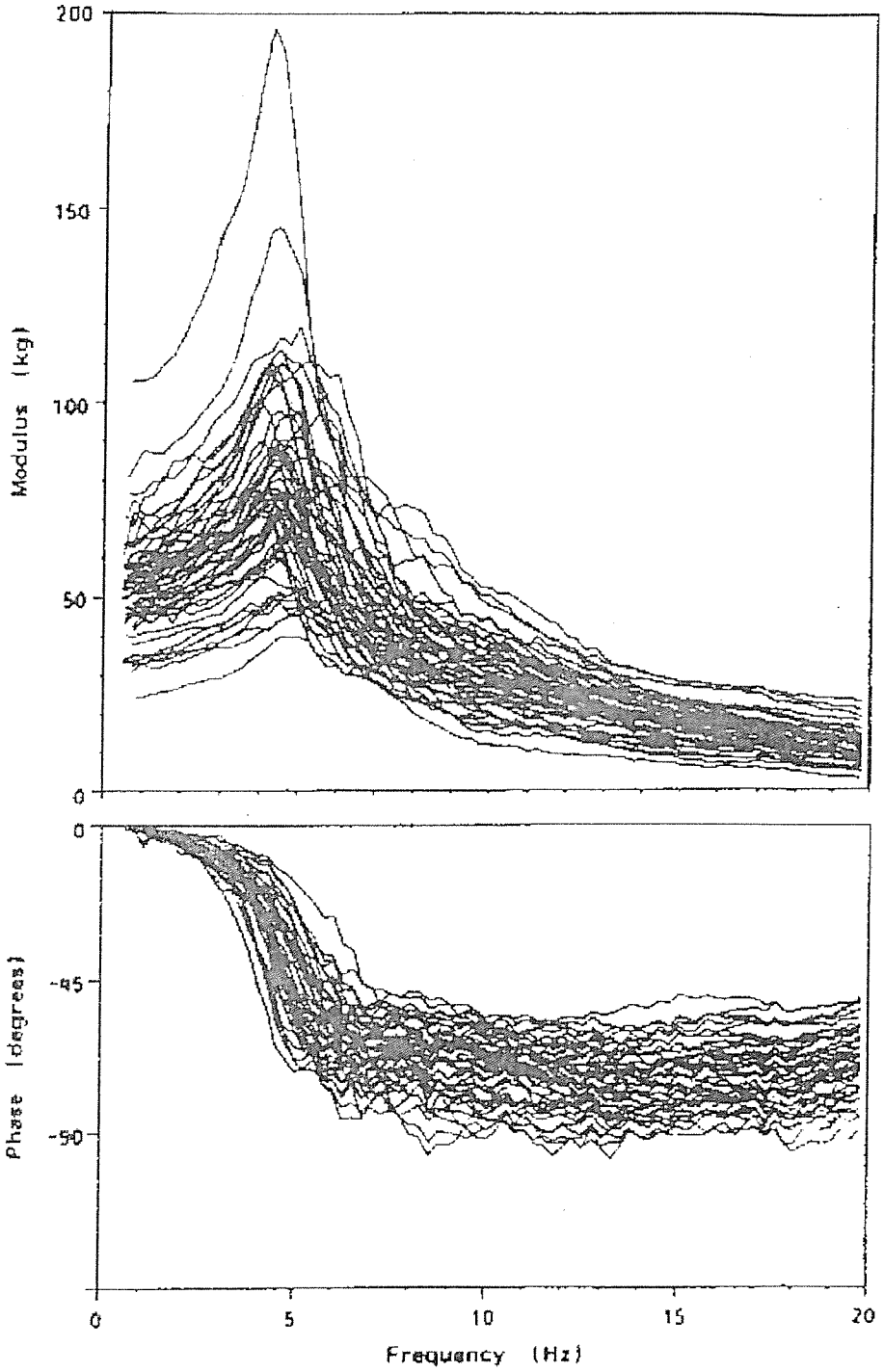

Figure 2.2 apparent masses of sixty people (from Fairley and Griffin 1989)

approximately 5 Hz, which was corroborated by Fairley and Griffin (1989) using 60 people, including 24 male, 24 female and 12 children (Figure 2.2). It could be observed that there were significant differences between apparent mass moduli and phases. The differences may be caused by many factors

which deserve study for further understanding about human body dynamic characteristics.

Most apparent masses show one resonance feature. Coermann (1962) found evidence of a second resonance at approximately 10 Hz for sitting subjects. In International Standard ISO 5982 (1981) the mechanical impedance also shows two resonance frequencies of the human body for vertical vibration (Figure 2.3). Some researchers even thought that there was a third resonance in the human mechanical impedance. Coermann (1962) and Vogt *et al.* (1968) mentioned a third resonance at about 15 Hz in their data. Miwa (1975) suggested that a third resonance was present at about 50 Hz. However, the third resonance peak is small and not clear, and the effect of it is also small.

2.2.3 Factor affecting body apparent mass and mechanical impedance

The sitting body is a complex dynamic system when it is exposed to a variety of vibrations. Therefore, many researchers have measured the response of the sitting body in different conditions to study the system characteristics. Some studies revealed that the response of the sitting body to vertical vibration is non-linear. It has been shown that the sitting posture, footrest, backrest, vibration magnitude and the type of input signal all cause changes of body apparent mass and mechanical impedance. Hence, it is important to study the factors affecting body apparent mass and mechanical impedance.

The driving-point responses are easily measured and indicate the total responses of the body, however they are also affected by many factors. In addition to the above mentioned factors which have a significant influence on the measured responses of the body, external restraints, such as the seat pan, arm rests and seat belts or harnesses have an effect too. These factors may merit attention to obtain the repeatability of results, but they are less important compared to other factors which will be discussed below and they are not included in this research.

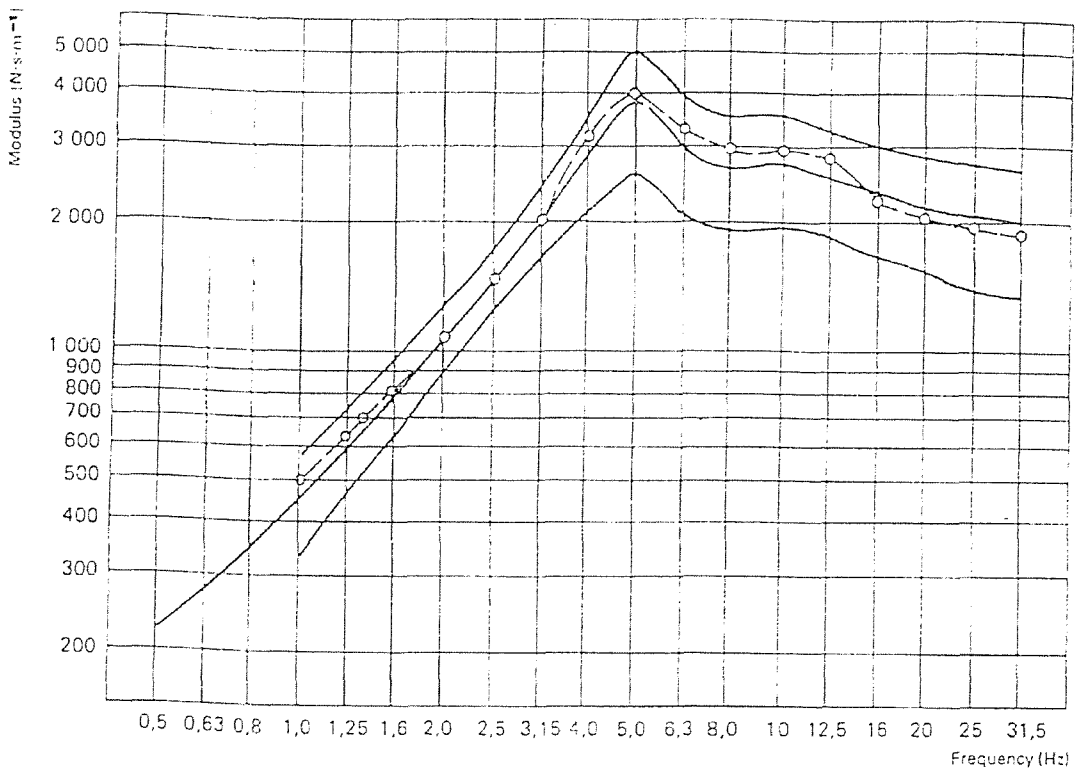

Figure 2.3 Driving point impedance of human in sitting position from ISO 5982 (1981).

2.2.3.1 Effect of posture

Many researchers have investigated the effects of posture on the driving point responses. Coermann (1962) did an experiment with a subject on a hard stiff plate connected to a shaker table supported on force-transducers. The natural frequency of the system, consisting of the mass of the subject and the elasticity of the plate was 6 times higher than the highest frequency in his study. The subject was exposed to vertical discrete sinusoidal vibration in the frequency range from 1 to 20 Hz with a magnitude of 0.1 g, in erect and relaxed postures. Coermann found that there were significant differences between the two sitting postures. In the erect sitting posture, the body had the highest impedance peak and the highest natural frequency and therefore, the lowest damping factor. By relaxing the muscles to a relaxed posture, the first resonance frequency reduced and the damping factor increased.

Miwa (1975) used vertical swept sinusoidal excitation with a magnitude of 0.1 g to measure the driving point impedance of seated subjects over the frequency range 3 to 200 Hz. The impedance was measured on 20 subjects in two postures: erect posture and relaxed. The conclusion from Miwa was that no clear difference exists between the two sitting postures. From the impedance curves, Miwa observed two resonances below 30 Hz and, above 30 Hz, the impedances could be classified into two groups, one group had the resonance at 50 Hz, and the other did not.

Fairley and Griffin (1989) compared the apparent masses of subjects in several postures. Random vibration with four magnitudes (0.25, 0.5, 1.0 and 2.0 ms^{-2} rms) was produced by a 1m stroke hydraulic vibrator. Eight subjects were exposed to vertical vibration in four postures:'normal', 'erect', 'tense' and backrest. 'Normal' means a comfortable upright posture with normal muscle-tension. 'Erect' was a posture the same as 'normal' but with an erect body. 'Tense' was all the muscles in the upper body tensed as much as possible. 'Backrest' was the subjects leaning back slightly so as to rest against a rigid backrest. Figure 2.4 shows results from eight subjects. This appears to be a general trend for the resonance frequencies and the apparent mass at frequencies above resonance to be larger for the 'erect' and 'tense' conditions than the 'normal' condition. The largest changes were for the 'tense' condition, but there was considerable variability between subjects: some subjects were able to increase the stiffness of their body so that they almost doubled their resonance frequency whilst others showed hardly any change, even though they appeared to tense their muscles in the upper body with equal effort. The effect on the second resonance located around 10 Hz was not clear. Further investigation was conducted using one of the subjects. The subject adopted five different postures, slouched, normal, slightly erect, erect and very erect postures. In this study, a clear trend for the resonance frequency to shift from the slouched posture to the very erect posture was observed. The largest shift between the two extreme postures was about 1.5 Hz (Figure 2.5).

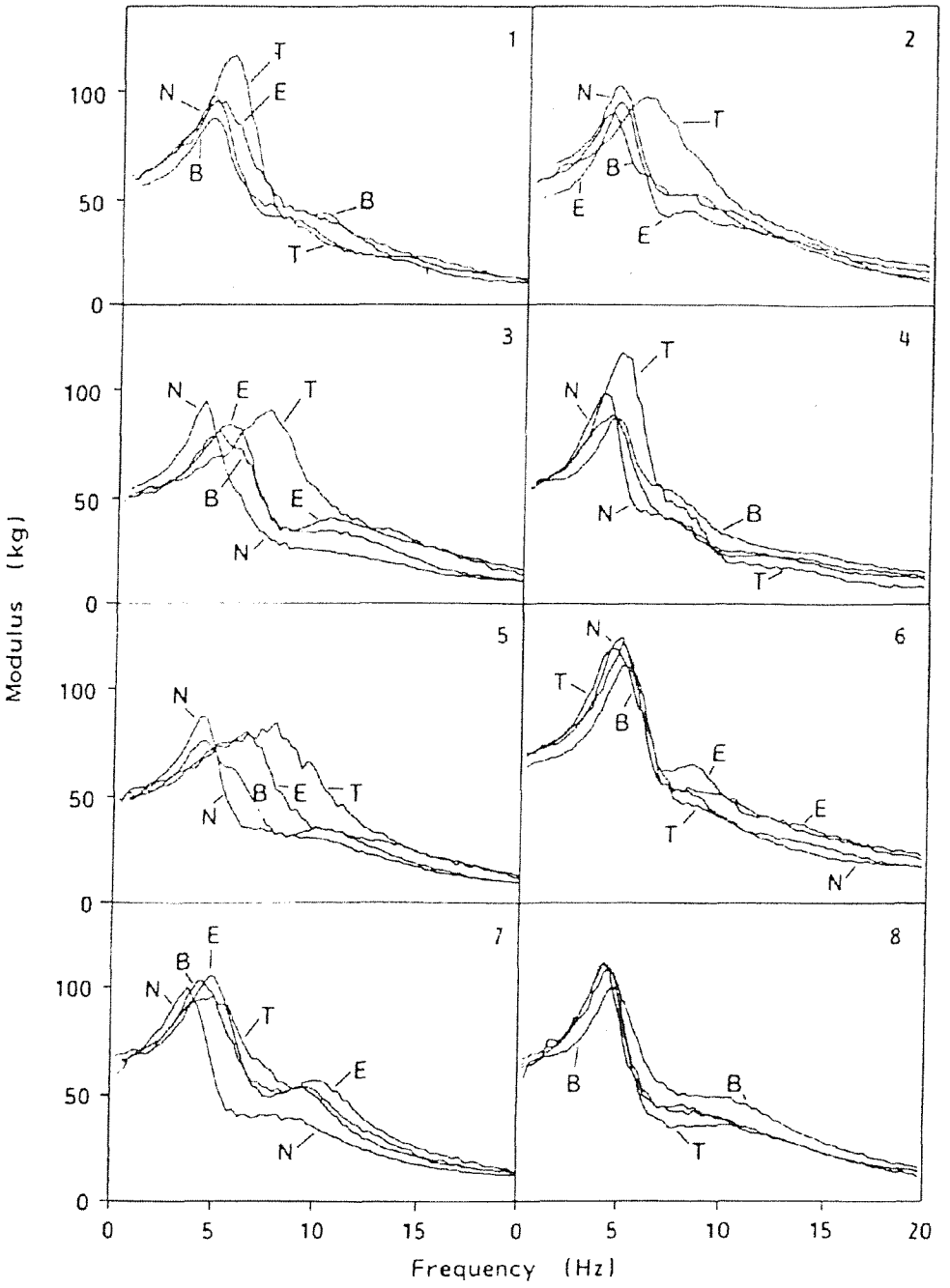

Figure 2.4 Effect of posture and muscle tension on the apparent masses of eight subjects (N=normal; E=erect; B=backrest; T=tense). From Fairley and Griffin (1989).

Kitazaki (1998) also investigated the effect of posture on the apparent mass. Three postures were studied in his paper: slouched, normal and erect postures. Random vibration with constant acceleration power spectra between 0.5 and 35 Hz and a magnitude of 1.7 ms^{-2} rms was generated for 60 seconds by a computer and fed into the vertical axis of a vibrator. The time histories of acceleration and force were acquired simultaneously into a computer with a

sampling rate of 100 samples per second through low pass filters at 35 Hz. Eight male subjects were used in the experiment. The natural frequencies corresponding to the principal and the second principal resonances of the apparent mass in the normal posture were 4.9 and 8.6 Hz when extracted from the mean apparent mass (Figure 2.6). At the principal resonance, when the subjects changed posture from erect to slouch, the frequency of the mean apparent mass decreased from 5.2 to 4.4 Hz with a corresponding decrease in the modulus.

For standing subjects, Matsumoto (1996) revealed that subject posture affected apparent mass. The value of the normalised apparent mass at resonance and resonance frequency both changed between a normal and a knees bent posture.

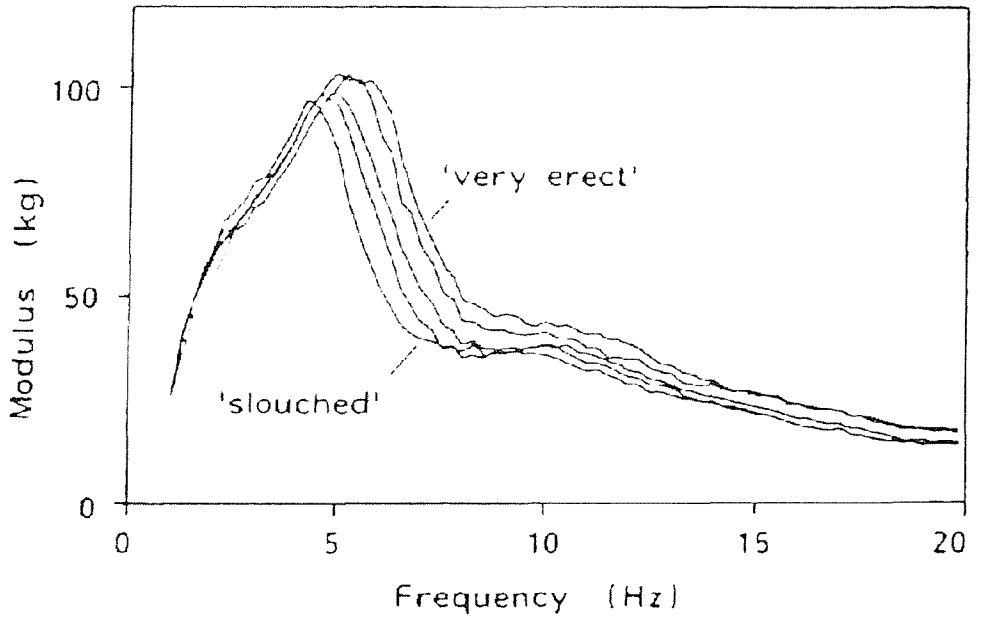

Figure 2.5 Effect of posture on the apparent masses of one subject: (slouched, normal, slightly erect, erect, very erect). From Fairley and Griffin (1989).

Although many previous studies showed that the effect of posture on body impedance and apparent mass is significant, Coermann (1962) reached a contrary conclusion that the posture of the subject did not influence apparent mass. However, the majority of the studies tend to reveal that subject posture affects human body response. It seems clear that when subject posture

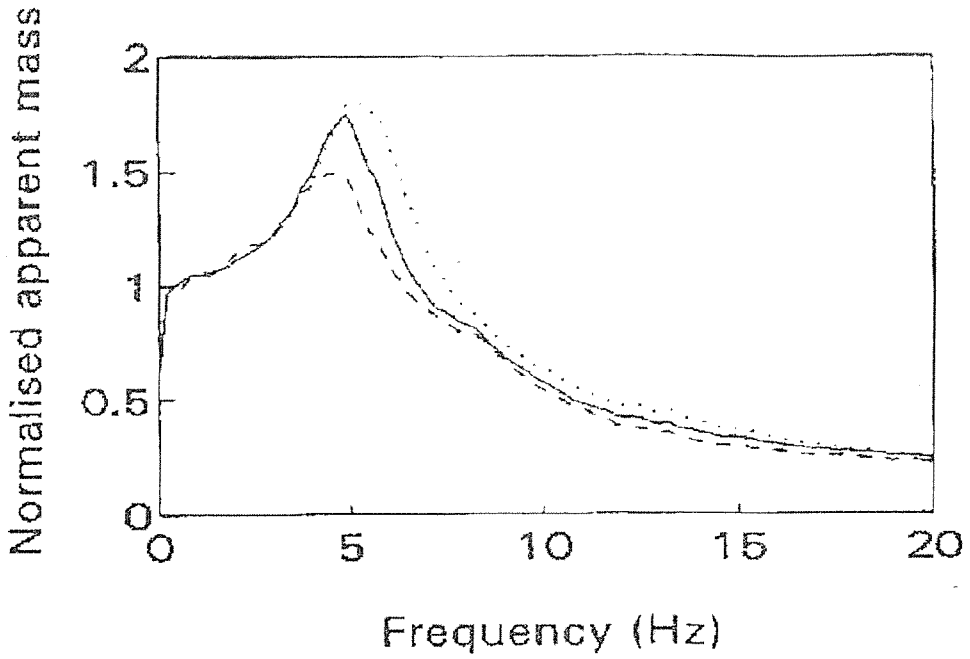

Figure 2.6 Mean normalized apparent mass of the eight sitting subjects (····· erect posture, ——— normal posture, – – – – slouched posture). From Kitazaki and Griffin 1998.

changes from slouched to erect, the resonance frequency increases, the frequency range covered by the peak increases and the peak apparent mass increases (Figure 2.5 and 2.6), but below the resonance frequency there is no change between the different postures.

2.2.3.2 Effect of footrest

Fairley and Griffin (1984) investigated the effect of footrest on the apparent mass. The vertical driving point apparent masses of ten men, sitting on a flat rigid seat without backrest, were measured for 40 seconds on an electrodynamic vibrator. The subjects sat in a normal upright posture with either the feet supported on a stationary footrest, so that the lower leg was vertical and the upper leg horizontal, or with the feet allowed to hang free. Figure 2.7 shows the results of two test conditions and a comparison of the apparent masses between the Fairley and Griffin measurements and International Standard ISO 5982. It can be observed that the modulus of the measured apparent mass is less for the feet supported than for the feet not supported, but the resonance frequency of both conditions is the same.

The effect of a stationary footrest was investigated further by measuring the apparent mass of one subject with eight different heights of a stationary

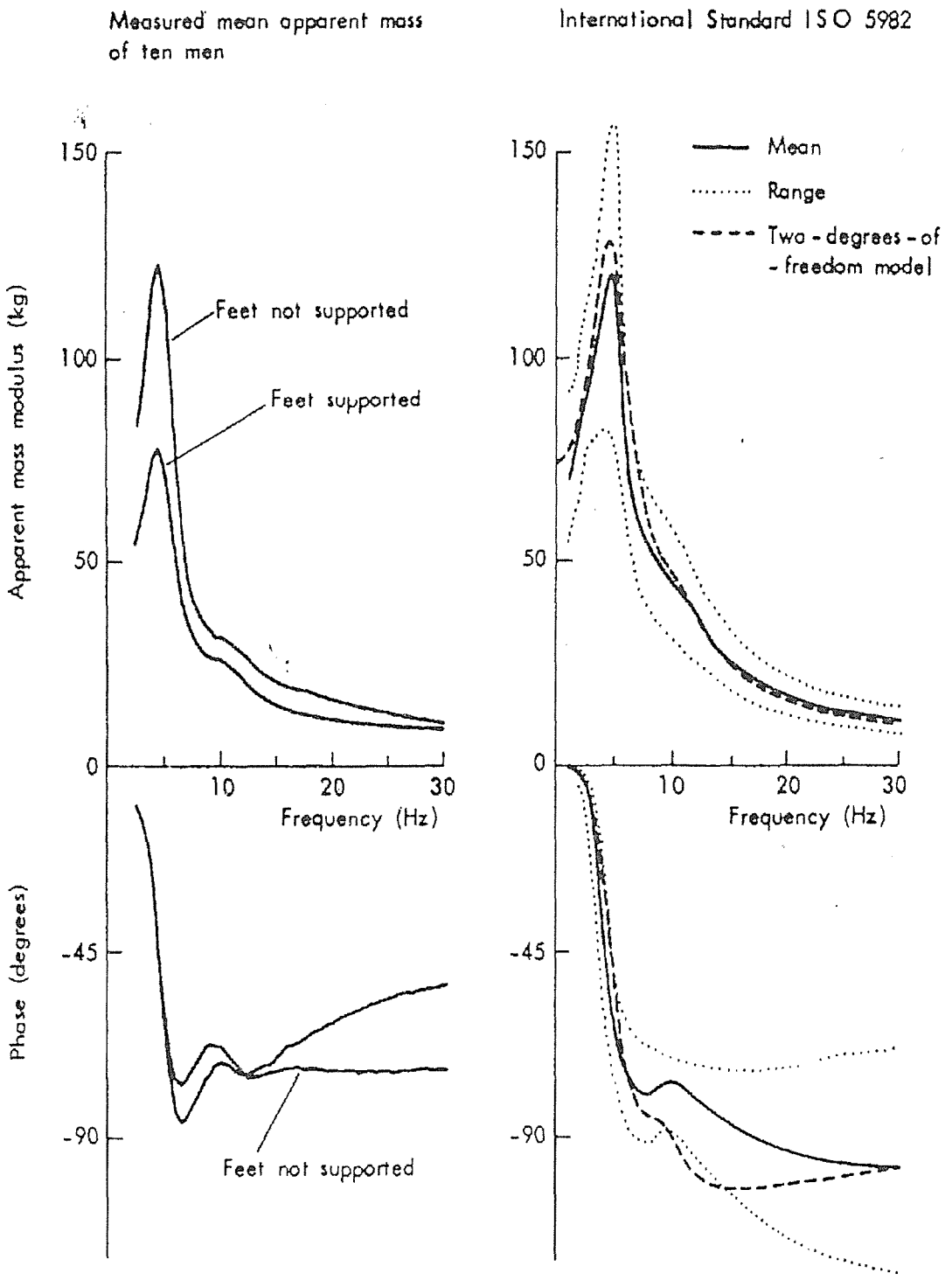

Figure 2.7 Mean apparent mass of ten sitting subjects compared with ISO 5982. From Fairley and Griffin 1984.

footrest (Fairley and Griffin 1989). The results in Figure 2.8 showed that the apparent mass increased slightly at frequencies above about 10 Hz as the footrest was lowered. However, the greatest effect was at low frequencies: the apparent mass at 1 Hz was about 60 kg with a high footrest – close to the

static weight of the person on the platform – but only about 20 kg with the lowest position of the footrest (where the feet were only just able to reach the footrest). Generally speaking, a higher stationary footrest can transfer more subject mass from seat to footrest and the value of apparent mass should be lower at 1 Hz frequency because it represents the mass of the subject. However, this experiment result showed the converse result. Therefore, further study is needed to confirm the finding.

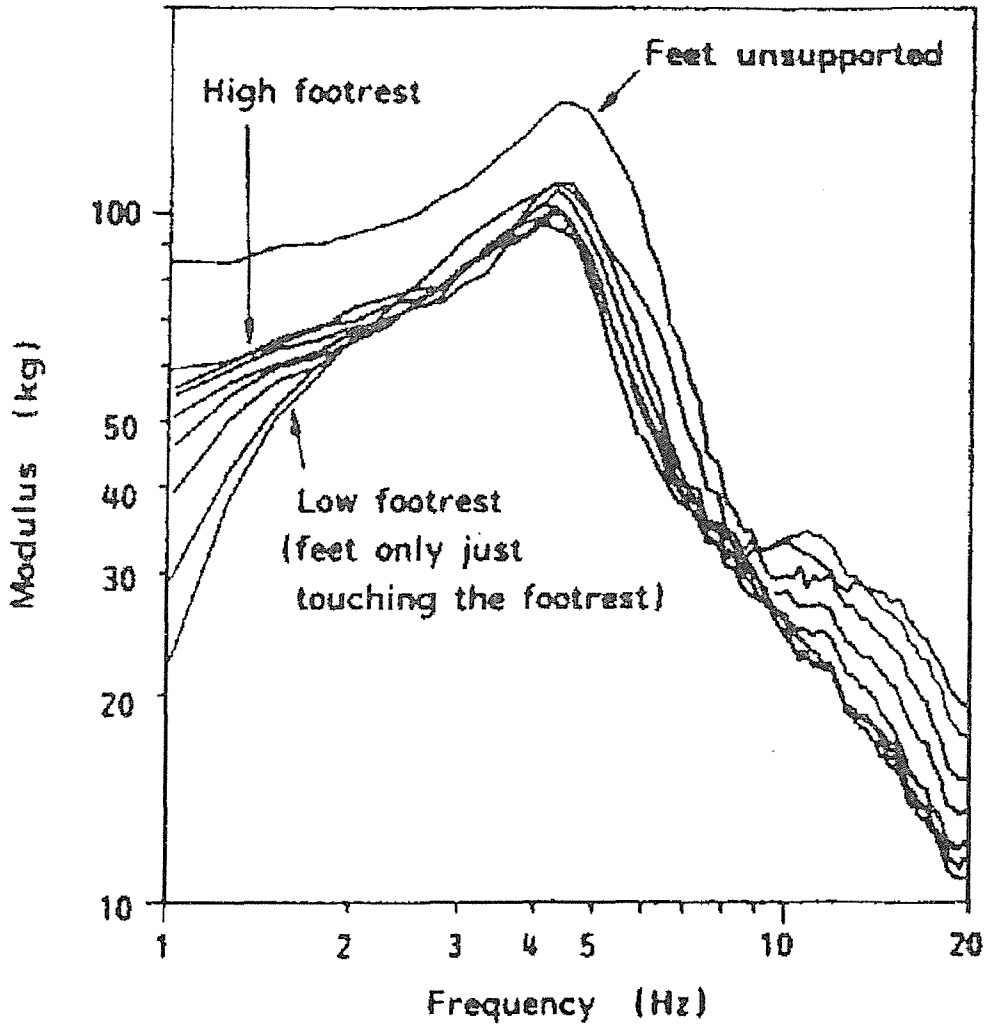

Figure 2.8 Effect of the height of a stationary footrest on the apparent mass of one subject. From Fairley and Griffin 1989.

Fairley and Griffin (1989) also studied the effect of a moving footrest. With a moving footrest, where there was no relative movement between the feet and the platform, it was found that the apparent mass of the body tended towards the static weight on the platform near zero frequency, as expected.

Experimental results showed that the effect of the height of a moving footrest was small compared to the effect of the height of a stationary footrest, the apparent mass of the body above 10 Hz and the static weight on the platform both increased slightly when the height of the moving footrest was reduced.

2.2.3.3 Effect of backrest

There are only a few investigations concerning the effect of a seat backrest on the measured apparent mass, because the influence of the backrest on a seated subject is complex. The force produced by the backrest for a sitting subject is not only in the vertical axis but also in the fore-and-aft axes and it is not at the main drive point. Coermann and Okada (1964) investigated the effect of different backrest angles from zero to fifty degrees from vertical. The results showed no consistent changes in the mechanical impedance of the body with changes in backrest angles.

Fairley and Griffin (1989) made apparent mass measurements of the human body in the vertical direction with and without a rigid backrest. The results showed that there were significant differences between the two conditions (Figure 2.9). When the subject sitting condition changed from 'normal' to 'backrest', that is the subject leant back against the rigid backrest, the resonance frequency increased, the frequency range covered the peak increased and the peak of apparent mass decreased. Meanwhile, the second resonance peak for some subjects became more clear.

Fairley and Griffin (1990) also investigated the effects of a backrest on the apparent mass of the human body in both lateral and fore-and-aft directions. Data were presented at frequencies up to 10 Hz, since above 10 Hz the apparent mass was very small. The measurements made without a backrest showed that the seated body has two heavily damped modes of vibration in both the fore-and-aft and lateral directions. The first mode of vibration had a resonance frequency at about 0.7 Hz in both directions. The second mode of vibration was observed in the lateral direction at 2 Hz and in the fore-and-aft direction at 2.5 Hz. Adding a backrest to the rigid seat greatly affected the apparent mass of the body in the both the lateral and fore-and-aft directions.

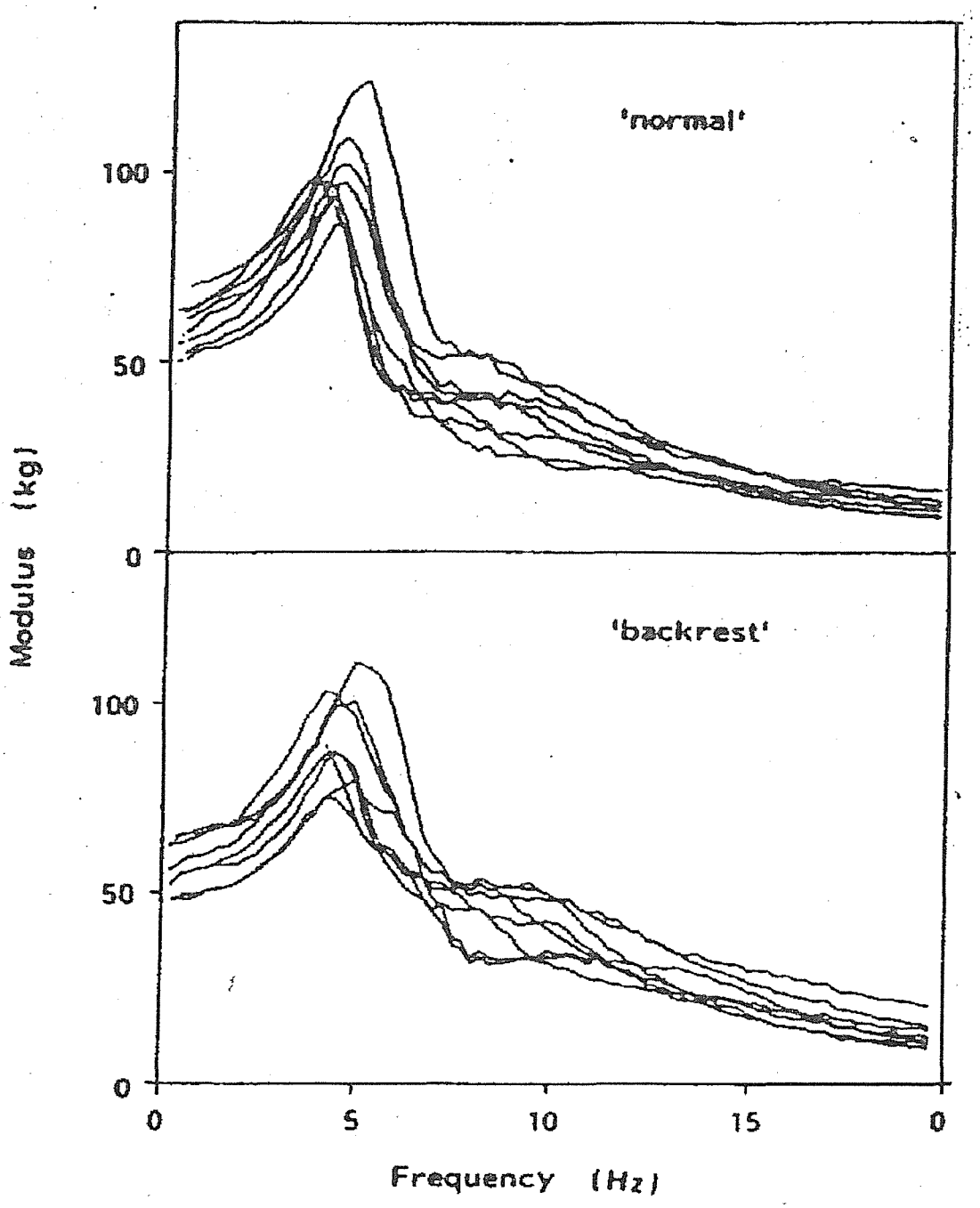

Figure 2.9 Apparent masses of eight people with and without backrest. From Fairley and Griffin 1989.

For fore-and-aft motion, the modulus of the apparent mass was increased across the whole frequency range apart from at 0.8 Hz and there appeared to be only one resonance, which occurred at 3.5 Hz. For lateral motion, there was a single resonance at 1.5 Hz and there was again an increase in the modulus of the apparent mass over the entire frequency range. The authors suggested that the backrest had the effect of both restraining the rocking and swaying motion of the upper body at low frequencies and providing an

additional vibration source for motion at high frequencies. The change in the apparent mass resonance frequency may have been due to the first resonance not occurring for the 'back-on' case and the second resonance being increased.

2.2.3.4 Effect of input signal

The apparent mass or mechanical impedance of the human body is obtained from the measured driving point acceleration and the force. It can be understood that both signals, the measured driving point acceleration and the force, are affected by the input vibration. Therefore, many studies have been conducted to investigate the effect of the characteristics of the input vibration on human body apparent mass and mechanical impedance.

2.2.3.4.1 Vibration magnitude

Many studies have been concerned with the effect of input vibration magnitude on human body apparent mass or impedance. Pradko *et al.* (1966) conducted a study of the effect of vibration magnitude on the mechanical impedance of the seated body. Seven magnitudes of random vibration ranging from 0.35 to 2.0 g peak to peak were used. The author found that the human response was linear when subjects were exposed to different vibration magnitudes. Although the author did not display the experimental data, the finding of this study is clearly different from other later research. A further attempt to investigate non-linearity by varying the intensity of the vibration was made by Sandover (1978). Using a seat with a backrest, the apparent mass of a single seated subject was measured in the frequency range from 1 to 25 Hz. Exposing the subject to vibration at 1 and 2 ms^{-2} rms. Sandover obtained the same conclusion as Pradko: 'any non-linear effects are small'.

Miwa (1975) compared the driving point impedances of a kneeling subject exposed to vertical vibration with two excitation magnitudes of 0.1 and 0.3 g. He found that the higher vibration magnitude shifted the first resonance frequency from about 5 Hz to about 4.5 Hz. Although a kneeling subject is different from a sitting subject, the finding showed that the input vibration

magnitude is important when considering human body mechanical impedance.

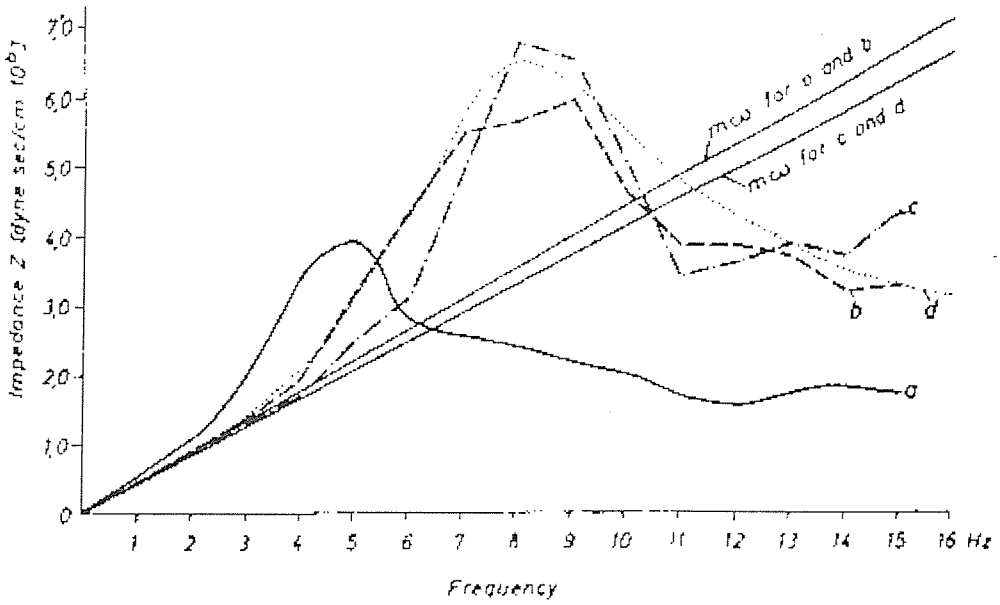

Figure 2.10 The mechanical impedance of the sitting human body; (a) under 1g gravity, (b) under 2g gravity and (c) under 3 g gravity. From Vogt (1968).

Vogt (1968) and Mertens (1978) studied the effect of gravity on the sitting body mechanical impedance. Vogt exposed ten subjects to increased acceleration on a centrifuge. The frequency range used was between 2 and 20 Hz. Measurements of mechanical impedance made at 1, 2 and 3 g are shown in Figure 2.10. The data showed that the resonance frequency of the impedance of the body increased as the static acceleration increased from 1 to 3 g. Mertens explained these shifts as being due to the increasing stiffening of the body under the gravity force. The author suggested that the change in response was primarily due to subjects being unable to maintain an upright posture at high static acceleration levels thereby allowing the spine to change to a curved shape. However, such a change in shape may be expected to reduce the stiffness of the spine to vertical motion, thereby reducing the mechanical impedance resonance frequency with increased static acceleration. A change of static acceleration differs from a change of vibration

magnitude, so the changes of body response caused by these two variables may be different.

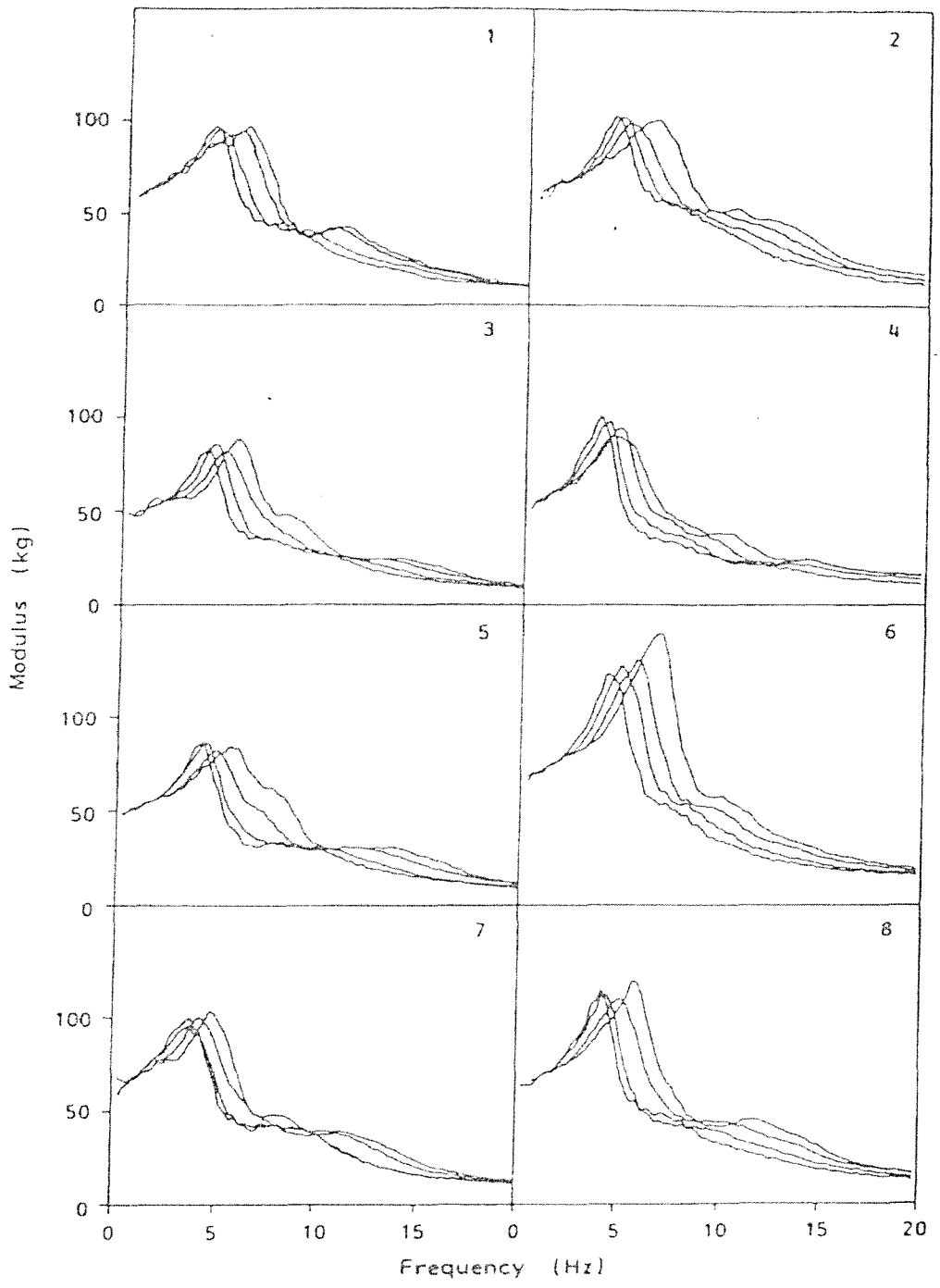

Figure 2.11 Apparent masses of 8 subjects measured at 0.25, 0.5, 1.0 and 2.0 ms^{-2} rms. From Fairley and Griffin (1989).

Hinz and Seidel (1987) compared the apparent masses with two different excitation magnitudes of 1.5 and 3.0 ms^{-2} rms. They used vertical discrete sinusoidal vibration in the frequency range from 2 to 12 Hz to excite four

subjects. It was found that the first resonance frequency, at about 4 Hz with the greater magnitude, was increased to 4.5 Hz with the lower magnitude. Fairley and Griffin (1989) came to same conclusions to those of Hinz and Seidel, but with different experimental conditions. They measured eight people with four different magnitudes of vibration: 0.25, 0.5, 1.0 and 2.0 ms^{-2} rms. The vertical random vibration was used in the frequency range from 0.25 to 20 Hz. They found that the first resonance frequency consistently decreased with increasing input vibration magnitude for every subject (Figure 2.11). The mean resonance frequency reduced from 6 Hz at 0.25 ms^{-2} rms, to 4 Hz at 2.0 ms^{-2} rms. Some subjects showed small changes in the apparent mass at resonance, but there appeared to be no mean effect. The second resonance frequency also decreased with increasing vibration magnitude. The implication of the reduction of resonance frequency is that the human body, a complex dynamic system, becomes less stiff with higher vibration magnitudes

Smith (1994) has also studied the effect of vibration magnitude. Using discrete sinusoidal frequencies between 3 and 20 Hz at selected acceleration levels (0.347, 0.694 and 1.734 ms^{-2} rms), she found that for four male subjects, the driving point mechanical impedance resonance frequency decreased with increases in vibration magnitude. Data from one subject are shown in Figure 2.12. The mean resonance frequency for the first resonance region is shifted downward from 6.8 Hz at 0.347 ms^{-2} rms to 5.9 Hz at 0.694 ms^{-2} rms and to 5.2 Hz at 1.734 ms^{-2} rms. A significant decline in resonance frequency was also observed in the high frequency range (15 to 18 Hz). The figure also showed that there were four relatively distinct peaks in the magnitude profiles between 3 and 20 Hz for the lowest acceleration level (0.347 ms^{-2} rms). However, the number of peaks decreases from 4 at 0.347 ms^{-2} rms to 3 at 0.694 ms^{-2} rms and to 2 at 1.734 ms^{-2} rms. That means the low vibration magnitude excited more vibration modes in human response, but this finding has not been verified by other researchers.

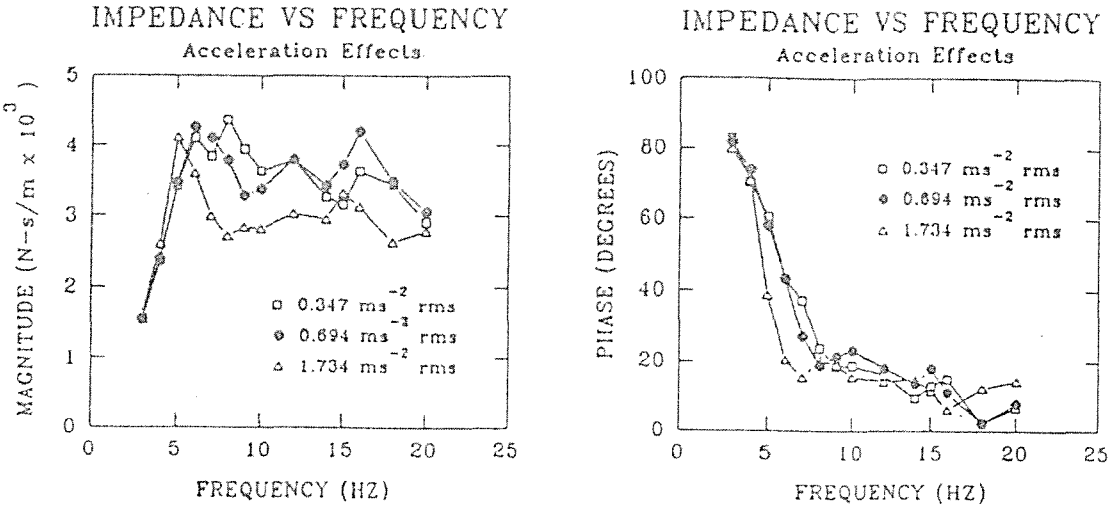

Figure 2.12 Driving point mechanical impedance measured for one subject at 0347, 0.694 and 1.734 ms^{-2} r.m.s, From Smith 1994.

Matsumoto and Griffin (1998) investigated the effect of vibration magnitude for standing subjects. They showed that the main resonance frequency of the apparent mass decreased from 6.75 Hz to 5.25 Hz as the vibration magnitude increased from 0.125 to 2.0 ms^{-2} rms. The 'softening' effect was also found for the second broad peak in the apparent mass. It did not appear that the vibration magnitude influenced the magnitude of apparent mass at resonance.

2.2.3.4.2 Sinusoidal and random vibration

Most early studies reported in the literature were conducted with sinusoidal motions, which are different from the vibration conditions in vehicles. Donati and Bonthoux (1983) compared the driving point impedances in response to a vertical swept sinusoidal vibration and a broad band random vibration of Gaussian distribution. For both of the vibrations, the magnitude was 1.6 ms^{-2} rms and the frequency band was restricted to the 1-10 Hz range. The exposure to each type of signal was 5 minutes. Fifteen male subjects took part in the experiments. The results are shown in Figure 2.13. It can be observed that the random excitation produced a lower modulus of the impedance below 5 Hz and a larger modulus above 5 Hz. Although the first resonance frequency at about 4 Hz did not shift, the second resonance frequency shifted from 6 Hz to 8 Hz when the vibration changed from the

swept sinusoidal to the broad band random motion. Any phase difference is not clear between the two excitations.

2.2.3.4.3 Vibration spectrum

The effect of the vibration spectrum on the mechanical impedance of the seated human body has rarely been considered. Sandover (1978) studied the effect of the input vibration spectrum on the apparent masses of two subjects. A broad band random vibration was used. The stimulus type was changed by having more or less energy at high and low frequencies. Figure 2.14 showed the effect of varying the frequency spectrum for two magnitudes: 1.0 ms^{-2} rms and 2.0 ms^{-2} rms. For the stimulus with more energy at low frequencies there was a slight downwards shift in the resonance frequency compared to the stimulus with more energy at high frequencies. However, these changes were small.

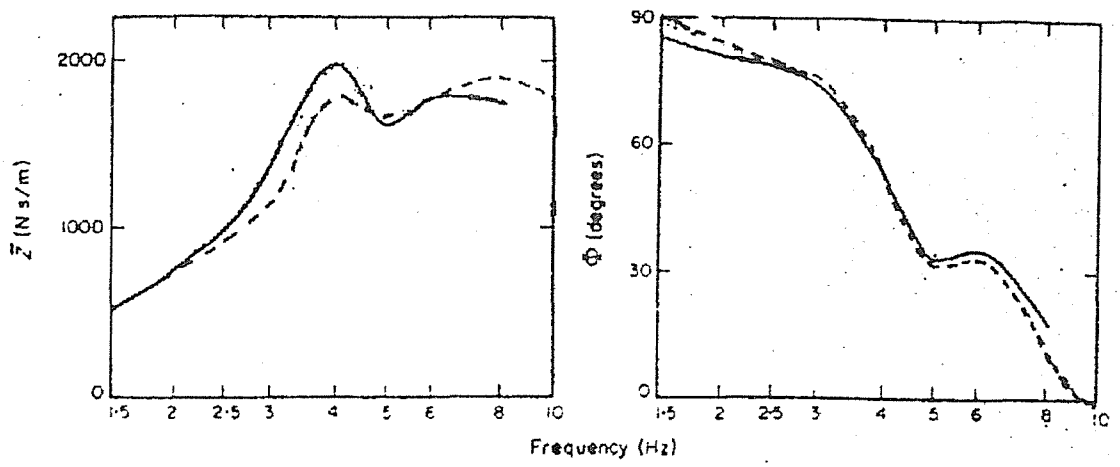

Figure 2.13. Comparison between the mean of the body impedance (modulus and phase) of subjects in the sitting position. ———, Swept sinusoidal motion; – – – –, broad band random motion. From Donati and Bonthoux 1983.

Fairley (1986) studied the effect of adding sinusoidal vibration to random vibration. He measured the apparent mass of a subject with different frequencies (2.5, 5, 10 and 20 Hz) and magnitudes (0, 0.25, 0.5 and 1.0 ms^{-2} rms) of sinusoidal vibration added to 'background' random vibration with a magnitude of 0.25 ms^{-2} rms. The measurements were conducted as separate experiments for each frequency of sinusoidal vibration. It was concluded that the apparent mass at resonance consistently shifted towards lower

frequencies as the magnitude of the sinusoidal vibration was increased for each frequency of sinusoidal vibration.

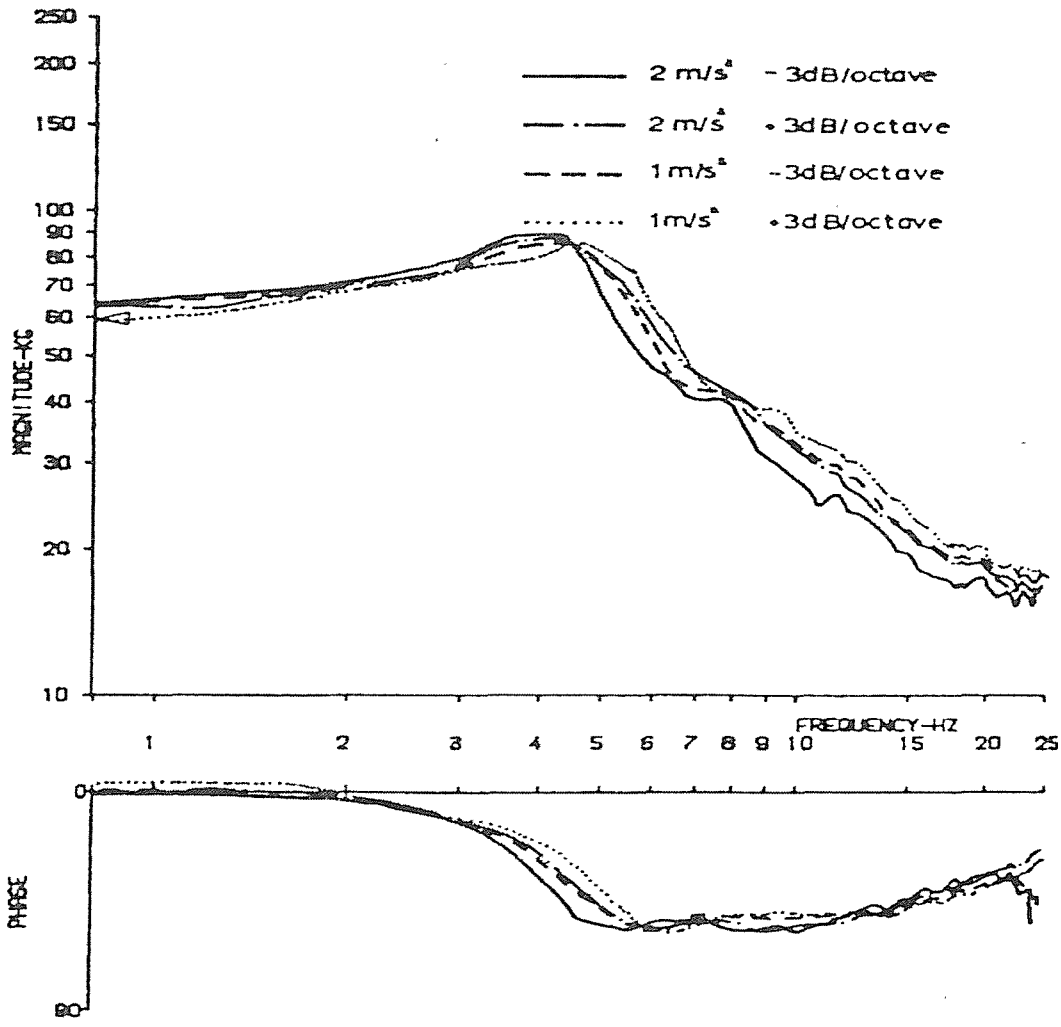

Figure 2.14 Apparent masses of sitting people resulting from different input vibration spectra. From Sandover 1978.

Fairley (1986) also compared the effect of random vibration and a frequency sweep vibration. The apparent mass of a subject was measured with both random vibration and a linear frequency sweep vibration. The magnitude of the vibration was 1.0 ms^{-2} rms in each case. The frequency sweep, from 1.5 to 20 Hz, had a duration of 64 seconds. The results, calculated as the mean of tests, were very similar for the two vibration inputs.

2.2.4 Non-linearity

There are various kinds of non-linearities in the responses of a seated body to vibration. Excitation magnitudes have been considered as the important factor causing the non-linear response of human body by many researchers. Some of the studies which investigated the non-linearity of the driving point response caused by excitation magnitudes have been discussed (see Section 2.2.3.4). Additional research and some reasons for human body non-linearity will be discussed here.

For vibration magnitude, Coermann (1962) expected that the human body had a non-linear characteristic over a large range of acceleration. He exposed a subject to three-vibration magnitudes: 0.1, 0,3 and 0.5 g. He found that the impedance and phase curves remained in the range of ± 10 per cent (which is about the accuracy with which such impedance and phase angle measurements can be taken), this means that the human body is a linear system in different vibration magnitudes. He does not be the only researcher to express that the human body had linear characteristics at different vibration magnitudes. Pradko *et al.* (1966) and Sandover (1978) obtained the same conclusion, but Sandover used a different experimental condition that was a subject sitting on a seat with a backrest, and Pradko measured the mechanical impedance of the seated body on a seat without backrest.

Mansfield (1994) investigated the non-linearity of the body by using different vibration magnitudes. Subjects were exposed to six magnitudes of vibration (0.25, 0.5, 1.0, 1.5, 2.0 and 2.5 m/s^2 rms). Twelve male subjects were used in the experiment with mean height 1.79 m and mean weight of 68.3 kg. One minute of Gaussian random vibration with equal energy at each frequency was used in the experiment in the frequency range of 0.2 to 20 Hz. He noted the same conclusion as Fairley and Griffin (1989), except that the resonance peak value was consistent with different vibration magnitudes (Figure 2.15).

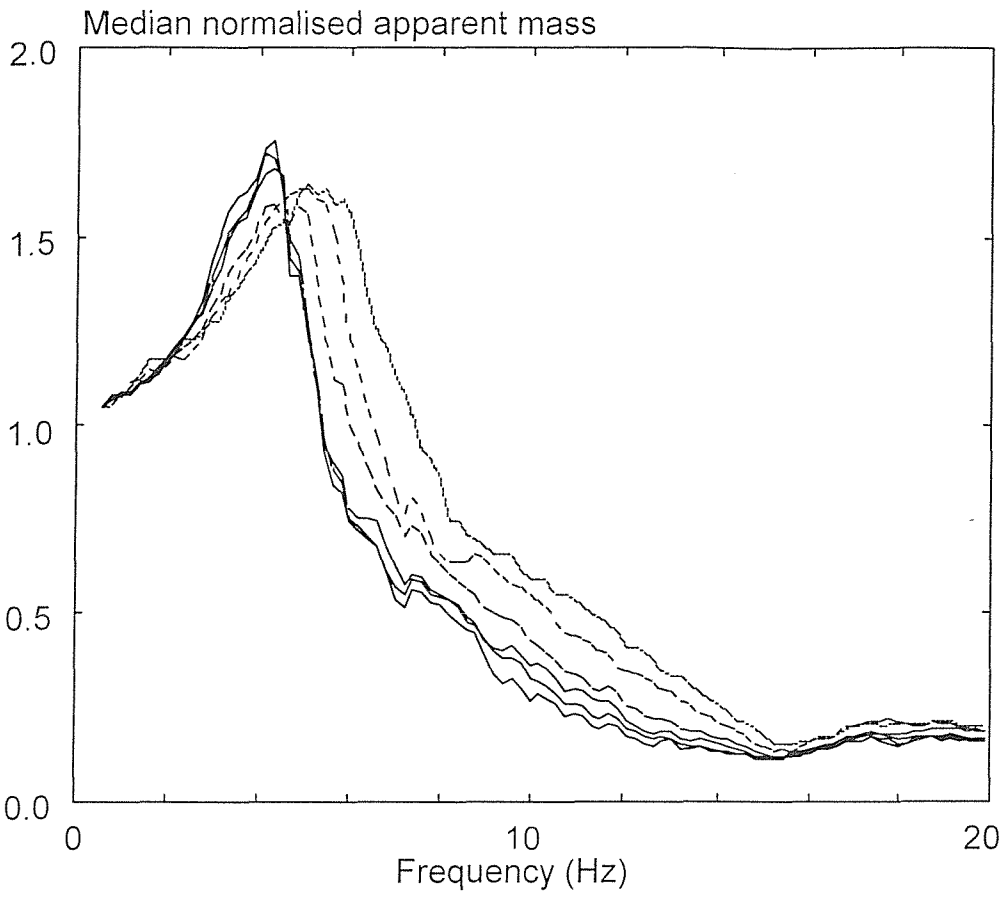

Figure 2.15 Median 12 subjects' apparent mass at 0.25, 0.5, 1.0, 1.5, 2.0 and 2.5 ms^{-2} rms. From Mansfield 1998.

For a vertical impact loading, Wittman and Phillips (1969) used a vertical drop tower to measure the transient driving point impedance. Four subjects participated in the experiment. Two types of vertical impacts with peak acceleration magnitudes of 6-7 g and 12-14 g were compared. The effect of acceleration profile was also investigated. One profile was of 55 msec duration and the other of approximately 120 msec. The impedance curves for these tests is presented in Figure 2.16. The solid curve presents a high acceleration (12-14 g) test of the longer duration waveform, the dashed curve, a low acceleration (6-7 g) test of the shorter duration waveform, and the dotted curve, a high acceleration test also of the shorter duration waveform. The difference between these curves for the same subject reflects the dependence of the human body's mechanical impedance on the test

environment and, therefore, the non-linearity in subject response to impact forces.

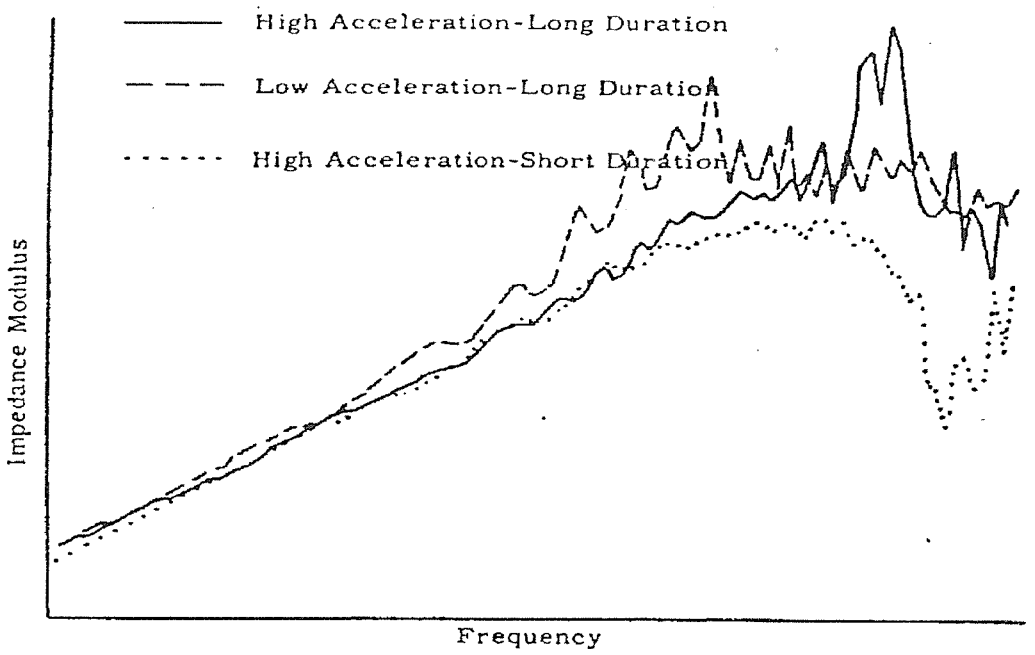

Figure 2.16. Transient mechanical impedance of one subject exposed to three different acceleration environments from wittman and Phillips (1969).

Many researchers have tried to explain why non-linearity appears in the biodynamic response of the body. They considered that non-linearity in the body may be caused by the response of the skeleton or by the response of muscles but these effects have not been proven. The discussions about the reason for non-linearity of the body are helpful to avoid the non-linearity of the body in experiments and are helpful in designing mathematical models for the human body.

1) Skeleton

Coermann (1962) assumed that the response of the body would show stiffening characteristics due to a hardening characteristic of the spine. To the contrary, Fairley (1986) hypothesised that more movement may occur in the skeletal joints of the body with higher magnitudes of motion making the body appear to be less stiff. Mansfield (1998) supports Fairley's hypothesis when he showed a non-linear response with vibration magnitude in the seat to spine and seat to pelvis transmissibilities. However, the reason why the skeleton may change in stiffness is not clear from these data.

2) **Muscle stiffness**

An alternative explanation of the non-linearity in the apparent mass is that the tissue beneath the ischial tuberosities acts as a softening spring (Kitazaki 1994). According to this hypothesis, increasing or decreasing the contact area with the tissue may cause the change of the body response to vibration. Experimental studies were performed by Mansfield (1998) where the pressure on the seat surface was varied by using the 'normal upright' posture, an 'inverted SIT-BAR' and 'cushion' conditions. The measurements were obtained with increasing and decreasing pressure at the ischial tuberosities, respectively. No significant changes in the non-linearity were observed between apparent mass measurements made using the three conditions. These results show that the non-linearity in apparent mass is not dependent on the pressure distribution beneath the ischial tuberosities. Additionally, these data imply that the non-linearity in the dynamic response of the body is not due to inherent characteristics in the tissue beneath the ischial tuberosities.

Fairley (1986), Potemkin and Frolov (1979) and Lakie (1986) all explained non-linear dynamic behaviour of the body as being caused by muscle stiffness. Lakie (1986) investigated the response of muscles to vibration. When exposed to vibration, the forces exerted by muscle fibres were shown to decrease. After the vibration stopped, the muscle took up to 20 seconds to return to the original stiffness. This delay was termed the 'post vibration force recovery'. Such a loosening effect due to vibration could also account for the lower stiffness and hence the lower apparent mass resonance frequencies at higher vibration magnitudes.

Other possible reasons for the non-linear response of the body may be that subjects could not maintain a steady posture (Mertens 1978) or that pelvis motion was the primary contributor (Smith 1994).

2.2.5 Absorbed power for the seated body

Pradko *et al.* (1965, 1966), Lee and Pradko (1968) discussed the concept of absorbed power in whole-body vibration. They presented results from some

investigations which indicated that subjective experience of vibration is related to the amount of vibration energy absorbed by the body. The absorbed power is defined as the product of the force and the velocity (Lundström *et al.* 1995), in contrast to the driving point mechanical impedance, which is defined as the ratio of the force and velocity. The absorbed power, P, transmitted to a structure due to vibration exposure is defined by the dynamic force, F, to which the structure is exposed, multiplied by the resulting velocity, v:

$$\overline{P} = \overline{F} \times \overline{v}$$

where both the force and velocity components are vectors. They have both magnitude and direction. Therefore, the absorbed power, P, is complex. It can be separated into real and imaginary parts.

$$P = P_{Re} + P_{Im} = F * v * \cos(\phi_{f,v}) + F * v * \sin(\phi_{f,v})i$$

where $\phi_{F,v}$ is the phase between the force and the velocity. The real part, P_{Re}, reflects the part of the vibration energy per unit of time absorbed by the structure. The imaginary part, P_{Im}, reflects the part that is returned to the vibration source, (i.e. the energy which is not absorbed by the structure). Practically, this implies that the magnitude of the power not only depends on the force and velocity components but also on the phase difference between them. The maximum absorption of the power occurs when force and velocity are in phase. When the phase between force and velocity is 90^0, the absorption of power is zero.

Lundström *et al.* (1998) made measurements of the absorbed power for 15 male and 15 female subjects during vibration exposure at 1.0 ms^{-2} rms. Subjects sat in erect and relaxed upper body postures while being exposed to frequencies from 2 to 100 Hz. The individual graphs have a similar shape (Figure 2.17). A peak in the absorbed power was observed at about 5 Hz for all measurements. There were significant differences between male and female subjects. For females, there was an indication of an additional peak around 9 Hz. The frequency for maximum absorption was somewhat lower for the relaxed sitting position compared to the erect. Regression and correlation

analysis clearly indicated that absorbed power, over the entire frequency range, increased with increasing body weight.

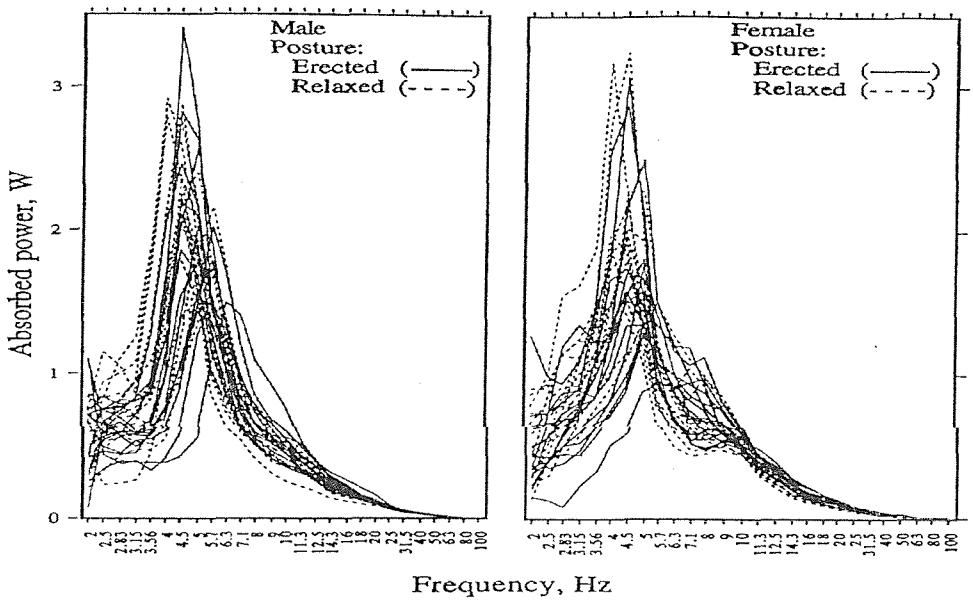

Figure 2.17 Absorbed power for 15 males and 15 females (relaxed and erect), From Lundström *et al.* (1998).

The amount of vibration energy, either absorbed or exchanged between the source and body, may be a measure of the physical stress on the body since it takes into consideration the interplay between the vibration structure and the body in contact with it. However, some doubts exist over the use the value of absorbed power as an indicator of subjective response.

2.2.6 Conclusions

The driving point mechanical impedance and the apparent mass are useful tools to reveal the human body dynamic properties. Many researchers have used these methods to measure human body response in different vibration environments. Previous data showed that the apparent mass, or mechanical impedance, of the seated human body has a resonance frequency at around 5 Hz in the vertical direction. Some subjects show a second resonance between 7 and 12 Hz. However, there are important differences between the two functions: the apparent mass and the mechanical impedance. The two dynamic functions yield different dominant frequencies at which the peak magnitude is observed. If the mechanical impedance is used to measure

human response, two resonances, sometimes three resonances, are observed. If the apparent mass is used, often one resonance appears.

It is clear that there are many factors affecting experimental results when measuring human body responses. These factors can be divided into two groups, one group contains important factors whose effects are clear and cannot be neglected, such as posture, backrest, footrest and input signal. Another group contains general factors whose effects are not important but still need attention to enable results to be repeatable, such as seat pan shape, arm rests, seat belts or harnesses, etc.

Posture

Many studies of the effect of subjects' posture on the response of the body revealed that the response of the body changed in different test postures, except for Coermann's study, which showed a linear characteristic of the sitting body in different sitting posture. Fairley and Griffin (1989) and Kitazaki (1998) both found that the resonance frequency of the apparent mass decreased when the subject posture changed from erect to slouched, but the change was different in their studies. For example, Kitazaki showed a decrease of the peak value at resonance with a posture change from erect to slouch, but Fairley and Griffin (1989) did not find this change.

Backrest

It is not clear if the response of the sitting body is consistent with different backrest angles or with and without a backrest. Coermann and Okada (1964) showed that the mechanical impedance of the body is consistent at different backrest angles from zero to fifty degrees. Fairley and Griffin (1989) revealed that the resonance frequency of the apparent mass increased and the peak of apparent mass value decreased when the sitting condition changed from no backrest to a backrest condition. This means that the apparent mass of the sitting body is changed when the sitting condition varied between with and without backrest conditions. Fairley and Griffin (1990) also showed the change with both lateral and fore-and-aft directions of apparent mass with and without backrest conditions.

Footrest

Although few researchers think the effect of the footrest is important, the investigation of Fairley and Griffin (1989) showed that the effect of the height of a moving footrest was small, but the effect of stationary footrest was significant (see Section 2.2.3.2). At low frequencies (below 2.5 Hz), the apparent mass decreased as the stationary footrest height decreased. The study revealed that the response of a sitting body at different stationary footrest heights is significantly changed.

Vibration signals

For the vertical direction, many researchers have shown that the human body is a non-linear system. Vibration magnitudes and vibration spectra have been recognized as the major factors causing sitting subjects to exhibit a non-linear response, except studies by Coermann (1962), Pradko et al. (1966) and Sandover (1978). They concluded that the effect of vibration magnitude was small and that the body could be considered as a linear system with regard to vehicle vibration. The conclusion from other researchers was that the resonance frequency of the apparent mass increased as the vibration magnitudes decreased. The change of the resonance frequency of the apparent mass with variation of the input vibration magnitude, or the input vibration spectrum, may be caused by the response of the skeleton or by the response of muscles but this has not been proven.

With variations of static acceleration magnitude, Vogt *et al*, (1968), and Mertens (1978) found a non-linearity which differs from the non-linearity described above. They found that the resonance frequency of the impedance of the body increased as the static acceleration increased from 1 to 3 times gravity: the main resonance frequency increased from 5 to 8 Hz and the mechanical impedance at resonance increased slightly.

The vibration spectrum and input waveform, such as random or sinusoidal, also affect the apparent mass. However, the research in this field does not give conclusive evidence or reasons for the changes.

2.3 DYNAMIC PROPERTIES OF SEATS

Vehicle seats are exposed to vibration which depends on the vehicle type, vehicle speed, road surface, etc. A seated occupant in a vehicle is mainly exposed to vibration transmitted by the seat, so seating dynamics are an important factor when considering vibration exposure. The vibration is also transmitted to occupants by their feet and hands, but the main problems focus on the seat.

The seat should have the optimum dynamic properties so as to minimize the unwanted vibration response of the occupant in the relevant vibration environment. As far as we know, there are three factors combining together to determine the seat dynamic efficiency: the vibration environment, the seat dynamic response and the response of the human body. In general, the optimum dynamic response of a seat depends on both the vibration spectrum in the environment and the relevant criterion (maintenance of comfort, minimization of the disturbance of activities or preservation of health). The seat transmissibility is a useful tool to represent the interaction of the seat dynamics with the dynamics of the body

2.3.1 Seat transmissibility

The transmissibility of a seat is the frequency response function for vibration transmitted from the base of the seat to the person sitting on the seat. The transmissibility of a seat is defined as the motion at the seat surface divided by the motion at the base of the seat. The motions both at the seat surface and at the base can be expressed in times of displacement, velocity or acceleration. Using Fourier transform techniques, the frequency content of the two digitized time histories can be determined and the transmissibility, or transfer function, of the seat calculated by their division. This division may involve Fourier transforms, power spectra or cross spectra according to the assumptions made and the facilities which are available.

The transmissibility of the seat, T(f), is defined as the ratio of the power spectral density (PSD) measured at the seat surface and to the power spectral density measured at the floor:

$$T(f) = \left[\frac{G_{oo}(f)}{G_{ii}(f)}\right]^{1/2}$$

where G_{oo} (f) is the PSD at the seat surface and G_{ii} (f) is the PSD at the floor. This method assumes that there is only one cause of the measured output motion and T(f) is only the modulus of the transmissibility.

An alternative method to obtain seat transmissibility is to use the cross-spectral density method. In this method, the seat transmissibility, T(f), may be determined from the PSD, G_{ii} (f), of the input (seat base motion) and the cross-spectral density, G_{io} (f), of the input (seat base motion) and output (seat surface motion). T(f) is a complex quantity which can yield the modulus $|\,T(f)\,|$, and the phase, ψ(f), of the transfer function.

$$|T(f)| = \left\{[\mathrm{Re}(T(f))]^2 + [\mathrm{Im}(T(f))]^2\right\}^{1/2}$$

where Re[T(f)] and Im[T(f)] are the real and imaginary parts of the complex transfer function T(f), respectively.

These calculations are useful for determining the system transfer function. However, they cannot give any information about relationship between the input and output signals. For example, assuming two irrelevant signals (i.e., one is measured acceleration in fore-and-aft axes and another is measured acceleration in vertical axes) were obtained from an experiment, what is the meaning of the transfer function calculated from these two signals? To assist the explanation of the transfer function, the information of coherency between the signals is needed. The coherency function can be calculated by:

$$\gamma_{io}^2(f) = \frac{|G_{io}(f)|^2}{G_{ii}(f) * G_{oo}(f)}$$

The value of coherence γ_{io}^2(f) is always in the range 0-1. For a linear system and no noise, the coherence will have its maximum value of unity at all

frequencies. If the system has a poor signal-noise (e.g., background noise) ratio, that is the noise occupied a large proportion in measured signal, the value of coherence $\gamma_{io}^2(f)$ will be lower than unity.

If the seat transmissibility is linear, the motion of the seat surface can be predicted from the motion at the base of the seat at any frequency. The seat transmissibility gives an insight into the dynamics of the seat and can give an indication of possible areas of the seat that could be improved. However, the seat transmissibility is not a universal method of determining seat dynamic properties. A drawback is that it is often difficult to identify a better seat when comparing two or more seat measurements (e.g., although 16 seat transmissibilities are shown in Figure 2.18, it is difficult to say which seat gives a good isolating function from these calculated transmissibility curves).

2.3.2 Assessment of seats

A seat is only required to provide good isolation of the vibration at the frequencies to which it will be exposed when in use. There are two methods by which this may be measured. The seat may be exposed to the appropriate vibration and the motion on the seat assessed either objectively or subjectively in terms of comfort, activity disturbance, or health effects. Alternatively, the seat transfer function may be determined and used to calculate the vibration which will occur on the seat with a given input spectrum. Seat transmissibility is a good method to appraise the seat isolation function because it includes all three important factors: the vehicle floor vibration spectrum, the seat response and the occupant response, at all frequencies where there is significant vibration.

It is often difficult to identify the best seat through comparison between measured seat transfer functions. The seat transfer function is a dynamic characteristic over a frequency range and not a single value. Therefore, one seat may have the lower transmissibility at some frequencies but higher transmissibility at other frequencies. A widely used method of comparing the responses of different seats is the SEAT value (the seat effective amplitude transmissibility).

The SEAT value is given by (From Griffin 1990):

$$SEAT\% = \left[\frac{\int G_{ss}(f)\, W_i^2(f)\, df}{\int G_{ff}(f)\, W_i^2(f)\, df} \right]^{1/2} \times 100$$

Where $G_{ss}(f)$ and $G_{ff}(f)$ are the seat and floor acceleration power spectra and $W_i(f)$ is the frequency weighting for the human response to vibration which is of interest: this is the weighting for vibration occurring on the seat and not the weighting for vibration on the floor.

Using a frequency weighting appropriate to vibration discomfort, a SEAT value of 100% indicates that, although the seat may have amplified the low frequencies and attenuate the high frequencies, there is no overall improvement or degradation in vibration discomfort produced by the seat. Therefore a SEAT value of 100% means that sitting on the floor (or on a rigid seat) would produce similar vibration discomfort. If the SEAT value is greater than 100%, the vibration discomfort has been increased by the seat. If the SEAT value is less than 100%, it indicates that the seat provides a useful isolation.

If the seat transfer function, T(f), is known, the seat effective amplitude transmissibility (SEAT) may be calculated from the floor vibration spectrum. The SEAT is given by:

$$SEAT\% = \left[\frac{\int G_{ff}(f) |T(f)|^2\, W_i^2(f)\, df}{\int G_{ff}(f) W_i^2(f)\, df} \right]^{1/2} \times 100$$

This is a very useful method to calculate the seat effective amplitude transmissibility (SEAT) because it does not depend on the acceleration signal measured at seat surface. If the seat transmissibility has been obtained (e.g., predicted seat transmissibility), this method can be used to predict the SEAT value in a different car which has a different floor vibration or one car driving on different roads which also gives different floor vibration. This method is important for seat design and seat improvement because the seat designer

can obtain the SEAT value by varying seat parameters which result in different seat transmissibility and lead to different SEAT values. The transfer function of the seat from a vehicle may be determined either on the road or in the laboratory.

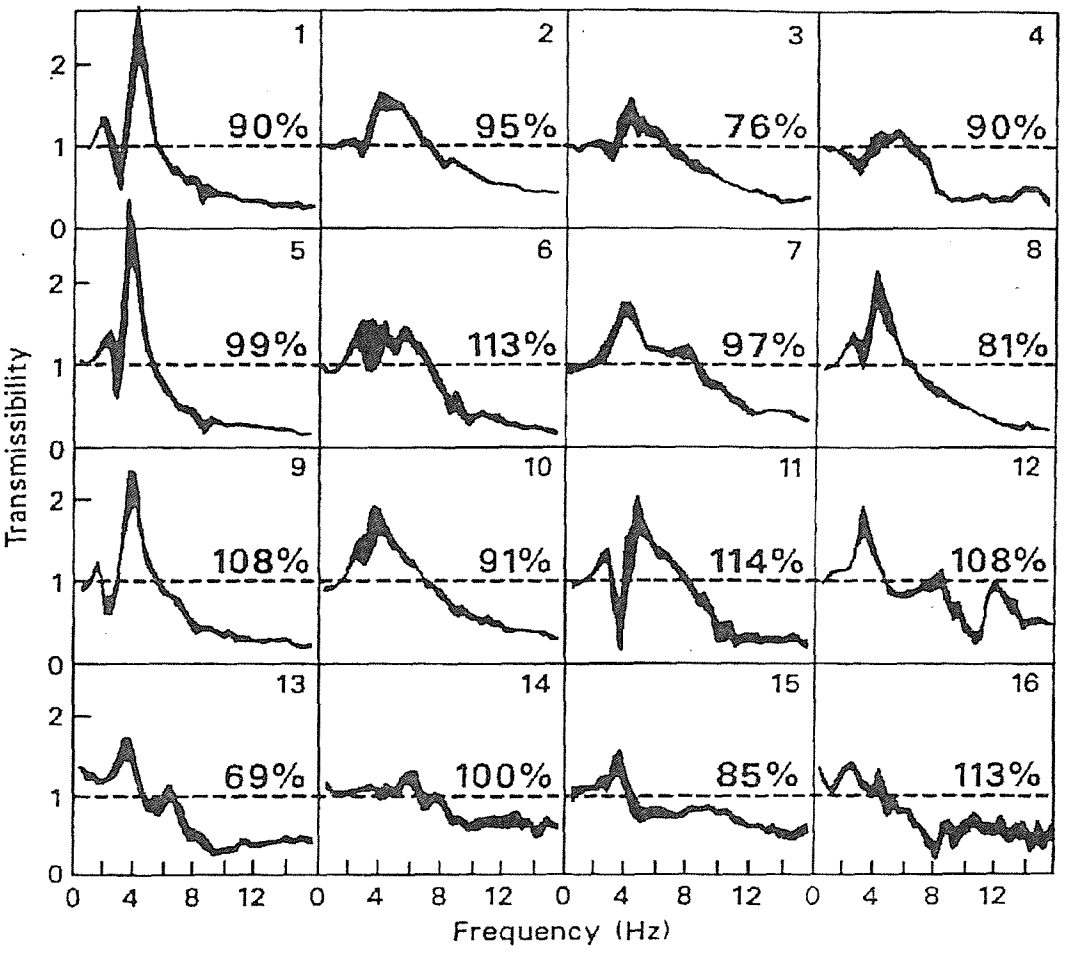

Figure 2.18. Veritical seat transmissibilities and SEAT values in 16 vehicles (black bands indicate 10% to 90% confidence intervals. From Griffin (1978).

If the motion on either the floor or the seat have a high crest factor, the SEAT value should be obtained using vibration dose value (from Griffin 1990):

$$SEAT\% = \frac{\text{VDV on the seat}}{\text{VDV on the Floor}} \times 100$$

The crest factor and vibration dose values (VDV) are given by:

$$\text{Crest factor} = \frac{\text{peak acceleration}}{\text{r.m.s acceleration}}$$

$$\text{VDV} = \left[\int_{t=0}^{t=T} a^4(t)\, dt \right]^{1/4}$$

For sinusoidal vibration the crest factor is $\sqrt{2}$. Typical vibration in a vehicle on a good road may have a crest factor in the approximate range 3 to 6, but this will increase if the measurement period includes any shock motion. In the VDV equation, the symbol, a(t), is the frequency-weighted acceleration time history, the symbol, T, is the period of time over which vibration may occur. The VDV on the floor is calculated using the same frequency weighting applied to the vibration occurring on the seat.

The SEAT value and seat transmissibility are different but both are ways of expressing the performance of seats. The SEAT value gives an indication of the overall benefit of the seat and the transmissibility identifies in which frequency ranges the benefits occur.

Griffin (1978) compared the measured SEAT values and seat transmissibilities for 16 different vehicles. Figure 2.18 shows the transmissibilities of the seats in 16 vehicles and the vertical SEAT values obtained using the ISO 2631 (1974) frequency weighting.

Other evaluation techniques have been suggested by Varterasian (1982) who developed an objective measure of automobile seat ride comfort, or a ride number, based on both the vibration spectrum and human sensitivity to mechanical vibration. The ride number depended on the natural frequency of the seat transfer function, f_n, the peak value of transmissibility, A, and the amplitude of the transmissibility at 10 Hz, B. A further variable, k (a seat comfort constant), was used which varied with seat type (such as split seat, bucket seat, bench type seat, etc.). The ride number is defined as:

$$R = \frac{k}{f_n A B}$$

Varterasian (1981) considered the ride number very useful in seat parameter study because it includes the amplitude of the transmissibility at 10 Hz. He found that the ride number was sensitive to seat durability because of the fact that seat foam (polyurethane) degradation occurred most noticeably in the 10 Hz range where the ride number was tuned.

Ebe (1995) used comfort scores to evaluate seat performance. The subjects were required to compare static and dynamic comfort between the seats. They assessed the relative discomfort of each sitting in terms of category numbers or category words as below:

+3 : 1st very much more comfort than 2nd
+2 : 1st definitely more comfort than 2nd
+1 : 1st slightly more comfort than 2nd
+0 : 1st the same comfort with 2nd
-1 : 1st slightly less comfort than 2nd
-2 : 1st definitely less comfort than 2nd
-3 : 1st very much less comfort than 2^{nd}

The comfort score for different seats was obtained by the calculation of category numbers for each subject. The higher comfort scores correspond to better sitting comfort.

2.3.3 Measurements of seat transmissibility

A vehicle seat occupied by a passenger comprises two coupled dynamic systems: the seat and the person. The transmissibility of a seat is the ratio of the vibration at the seat surface to the vibration at the base of the seat. The transmissibility should be measured at a position that gives a representative and repeatable result. An accelerometer placed on the surface of the seat may cause discomfort to the subject, thereby inducing a different posture, and cause a change of the transmissibility. Therefore, a suitable measurement

device is needed in measuring seat transmissibility. Miwa and Yonekawa (1971) studied the methods of measuring seat transfer functions. As the deflection of the seat cushion may influence seat dynamics, a large rigid transducer on the seat surface is not satisfactory for accurate measurements. They concluded that a 1.3 kg bakelite box 300mm by 300mm by 30mm provide the most useful mount. Although a flat mount of this size could not easily be made to fit some car seats, their results also suggest that the differences obtained with a 230mm by 180mm by 45mm bakelite box of the same weight were not large.

The Society of Automotive Engineers (SAE 1974) recommended a semi-rigid disc containing accelerometers to measure the vibration on a seat surface. It is now called the "SAE-pad". According to its statement, the design of the SAE-pad was to "provide a suitable mounting for the accelerometers, not disturb operator comfort, and not significantly distort the buttock-cushion load distribution." The shaped disc is placed midway between the ischial tuberosities and taped to the cushion in situations of high vibration exposure. Figure 2.19 shows this device.

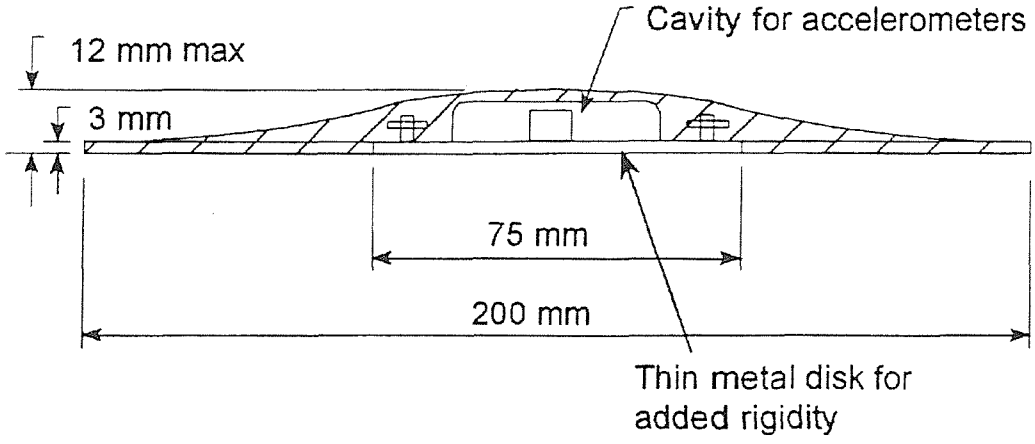

Figure 2.19 SAE-pad for measuring seat vibration (From SAE J1013, 1974)

Whitham and Griffin (1977) tested three accelerometer mounts. They were an aluminium bar (290 by 45 by 20mm), a semi-rigid SAE pad and a SIT-BAR. The SIT-BAR is shown in Figure 2.20. Its upper end of the bracket is located

at a convenient position providing space for the attachment of rotational accelerometers. The accelerometers used to measured vertical acceleration can be mounted on its upper surface. Whitham and Griffin (1977) found that both the SAE-pad and the SIT-BAR gave similar results and were suitable for transmissibility measurements in the frequency range of 2 to 32 Hz (Figure 2.21).

In vehicles, there are different vibrations at the different floor parts. This can be due to the vehicle not being entirely rigid in structure or a pitch mode occurring. Measurements made at the fixing point of one seat may not be representative of the vibration transmitted to another seat in the same vehicle. Messenger *et al.* (1992) suggested that the accelerometer placed on the vehicle chassis should be located within a circle of 200 mm diameter centred directly beneath the seat accelerometers. In addition, the position for mounting of the accelerometer should be a rigid part of the vehicle such that it is not affected by structural motion.

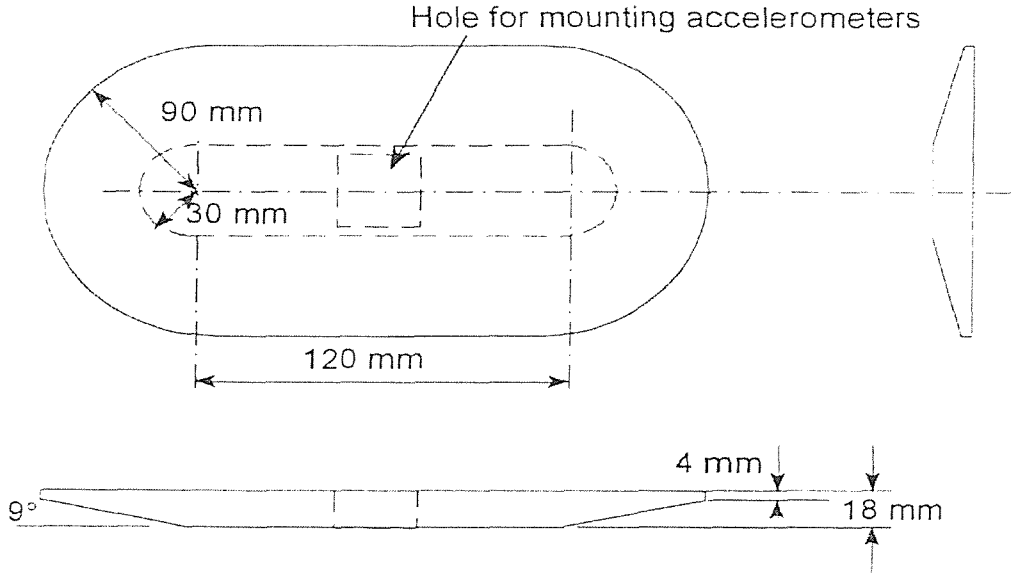

Figure 2.20 Design of the SIT-BAR (after Whitham and Griffin 1977).

Bruns and Ronitz (1971) found that measuring the transmissibility of vehicle seats in a laboratory was more repeatable than tests in vehicles. The measurement of the seat transmissibility in vehicles can be impeded by the unsuitability of the vibration input for the determination of a transfer function.

The input may not contain sufficient energy at all frequencies and may not be representative of other typical inputs. The visibility of these problems depends on the analysis methods employed and the extent of any repeatability measures. There are two methods for measuring the transmissibility (see Section 2.3.1): the power-spectral density (PSD) method and the cross-spectral density (CSD) method. Griffin (1990) showed the difference between two methods in measuring seat transfer function (Figure 2.22). Differences may arise for several reasons but they most often occur at frequencies where there is little vertical vibration in the vehicle. In consequence, the differences may have little effect on the overall magnitude of vibration occurring on the seat and have little influence on measures of seat isolation efficiency. Figure 2.22 also showed a poor coherency in a vehicle because of multiple axis input vibration. With an ideal linear system and no noise, the coherence should have its maximum value of unity at all frequencies.

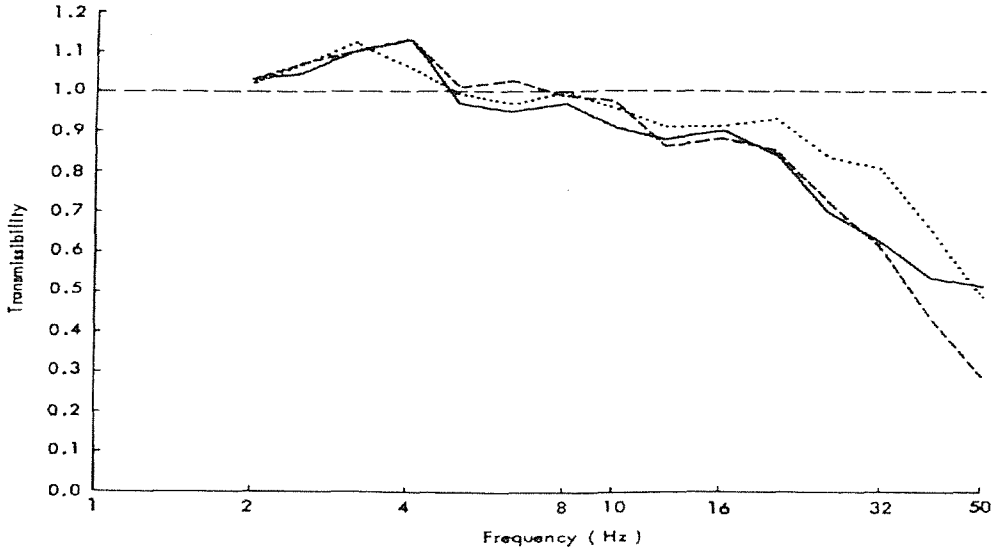

Figure 2.21 Transmissibility of the 100mm foam with the aluminium bar (dotted line), the SIT-BAR (broken line and the SAE-pad (continuous line) from Whitham and Griffin 1977.

2.3.4 Factors affecting seat transmissibility

When measuring the seat transmissibility, it should be remembered that the seat transmissibility is affected by many factors. The seat transmissibility may be intentionally changed, for example, by changing the properties of seat components in order to improve the dynamic characteristics of a seat. In other

cases, the transmissibility is unintentionally affected, for example, by the measuring conditions, such as vibration characteristics, the variance of subjects and so on. Therefore, it is important to understand the factors which could affect the seat transmissibility so as to avoid misinterpreting the results of experimental data.

2.3.4.1 Seat type and properties

Every vehicle needs a seat for the driver and any passengers. There are many types of seat but they can be divided into three categories: full-foam cushion seat, spring plus foam seat and suspension seat. The spring plus foam seat consists of spring, polyurethane foam and a seat cover. The full-foam seat is shaped thicker foam with a seat cover. The suspension seat has a suspension system which consists of a damper, spring, end-stop rubber and a seat cushion. These three types of seat have different dynamic characteristics due to their different seat constructions.

Leatherwood (1975) compared the comfort and seating dynamics of aircraft tourist class seats, aircraft first class seats and a bus seat in the frequency range of 1 to 30 Hz. He used a mock-up of a passenger cabin of an aircraft and 92 subjects. Measurements showed that there were significant differences in the transmissibilities of the aircraft seats and the bus seats but the vertical transmissibility for the aircraft tourist and first class seats appeared to be very similar. He analysed the result and explained that the aircraft seats were softer than the bus seats and amplified more of the floor vibration over the frequency range below 8 Hz and less at the higher frequencies.

Corbridge and Griffin (1989) measured the transmissibilities of ten alternative railway seat cushions. Each seat cushion was tested using a random motion with a magnitude of 0.6 ms^{-2} rms. Of the ten seat cushions, three were constructed from spring cases (A, B, C), four from foam blocks (D, E, F, G), one from rubberized hair material (H) and two consisting of layers of mounded foam 60 mm and 30 mm thick covering solid wooden bases (Cushion I and J respectively). The spring cases had the highest transmissibility at the resonance around 4 Hz and the foam-wooden cushions had the lowest

transmissibility at the resonance but a higher transmissibility above 6 Hz (Figure 2.23). Corbridge and Griffin (1991) compared the transmissibilities between a spring case seat cushion and two prototype cushions consisting of 60 mm and 30 mm thickness moulded foam on a rigid base. The experimental data showed that the three seat cushions had very different transmissibilities to vertical vibration.

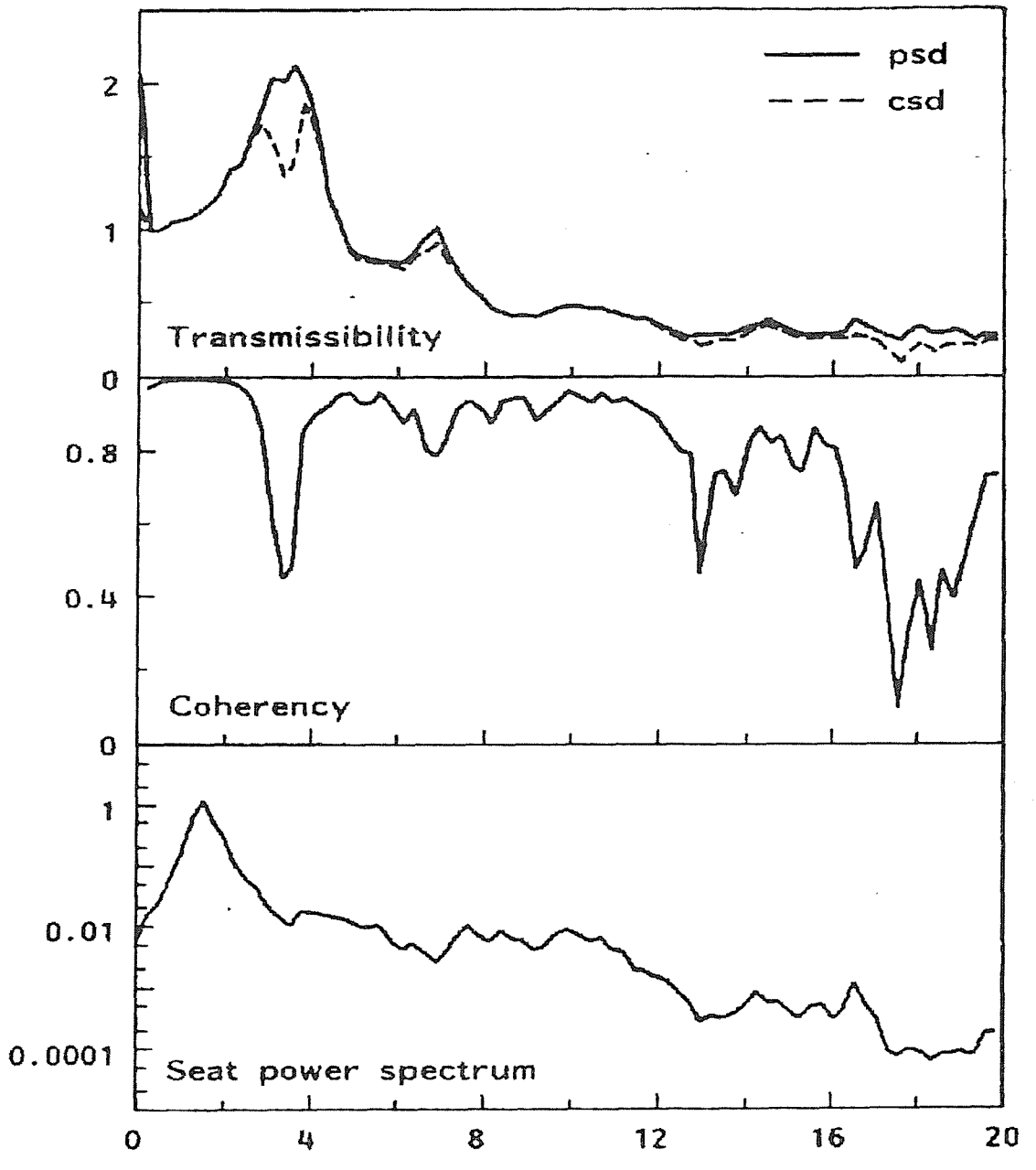

Figure 2.22 Vertical seat transmissibility determined with CSD and PSD methods. From Griffin 1990.

If we study vertical vibration spectra on a vehicle floor, it can often be seen from the vehicles that there is a peak in the frequency range from 3 to 5 Hz where conventional seats always amplify the vibration. However, this can be avoided by using a suspension seat. A suspension seat consists of a conventional seat mounted on a separate isolation mechanism with a lower natural frequency. Usually the suspension mechanism has a resonance at around 2 Hz, thereby attenuating the vibration above $\sqrt{2}$ times the resonance frequency.

Corbridge (1981) studied the transfer function of a suspension seat to vertical vibration. The results showed several features of suspension seats. Firstly, the natural frequency of the seat reduced from 3.25 Hz without a suspension system to 2.0 Hz with the suspension system but varied with the subject's weight. Secondly, the transmissibility was attenuated at frequencies over 3 Hz.

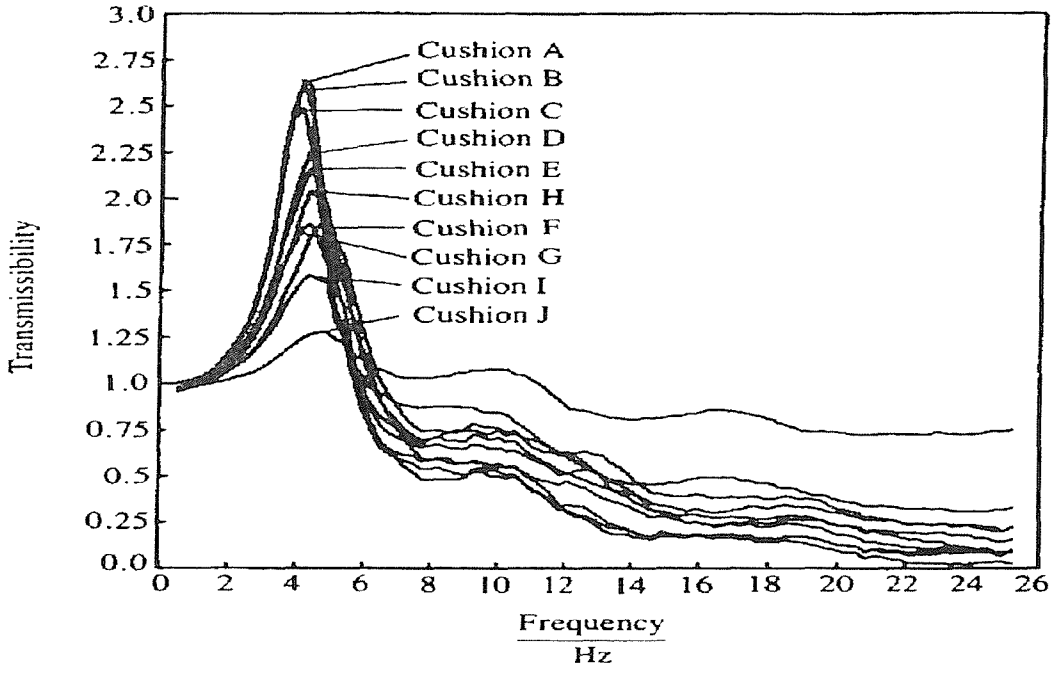

Figure 2.23 Transmissibility of ten seat cushions. From Corbridge and Griffin (1989).

The response of a typical suspension seat compared to a foam and metal sprung seat and a rigid seat is shown in Figure 2.24 (Griffin 1990). It can be

observed that the suspension seat dramatically improved the seat dynamic characteristics compared with the foam and metal sprung seat or a rigid seat in the frequency range from 4 to 8 Hz in which human are most sensitive to vibration. However, according to Wu (1994), there is a problem with suspension seats hitting end-stops at the extremes of their travel and exposing the occupant to shocks. Sometimes it may cause the occupant more discomfort and a greater health risk than the vibration itself. Another problem caused by suspension seats is that the subject mass affects the transmissibility of the suspension. Stayner (1972) compared the seat transmissibilities of four drivers of different weight (62.5, 74, 77 and 100 kg) with three suspension seats. As expected, greater subject mass produced a lower resonance frequency. This change was probably due to the dynamics of the seat suspension system rather than the seat cushion. Wu *et al*, (1994) mentioned that active suspension systems with varying dynamic parameters have been developed to solve the above problems but these have not yet come into general use due to the prohibitive costs and complexity involved.

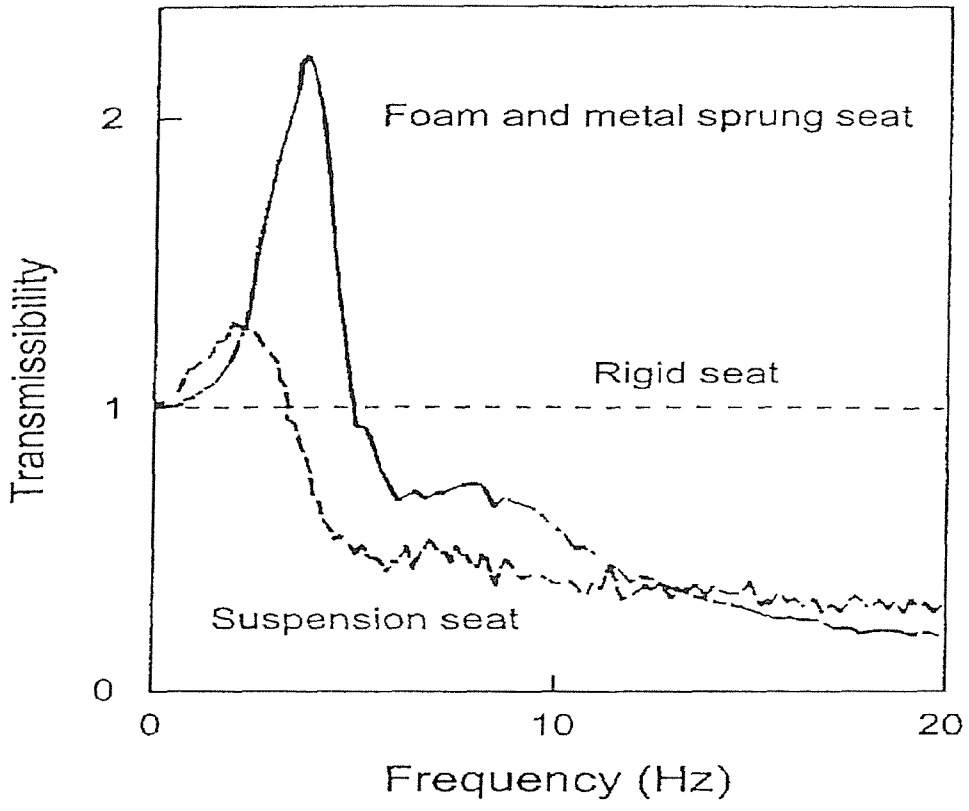

Figure 2.24 Comparison of the transmissibilities of a foam and metal sprung seat, a suspension seat and a rigid seat. From Griffin 1990.

It can be concluded that there are significant differences in the transmissibilities between the three seat categories. Regarding comfort, the suspension seat appears to perform with a good isolation of vibration for many vehicles, it not only provides low resonance frequency but also it has low transmissibility over a larger important frequency range (ISO 2631/1- 1985). However, it is difficult to adopt the suspension seat for all vehicles. In general, the suspension seat is costly and needs a large space below the cushion in order to install the suspension system. This means that the suspension seat cannot be used for compact cars. Therefore, when a suitable type of seat is chosen for a vehicle, the cost, the vibration environment and the space used for fitting the seat must be taken into account.

In addition to the seat type affecting the seat dynamic properties, the seat cushion components, such as the foam, spring and seat cover, etc., are also important for the seat dynamic characteristics. Not many studies of the effect of seat cushion components on the seat dynamic characteristics have been reported. However, there has been some research intentionally modifying the seat components in order to change the static or dynamic characteristics of the seat so as to improve seat comfort or reduce the seat cost. Messenger (1988) investigated the effect of foam hardness on the seat transmissibility. She compared the vertical vibration transmission of two similar helicopter seats with different foam hardnesses in both the seat pan and the backrest. When the foam was changed to be firmer than the original foam, the transmissibility at frequencies from 1.25 to 4.75 Hz increased significantly. However, in a different frequency range, such as from 5.75 to 30 Hz, the transmissibility was lower. The cushion thickness effect can be observed from Figure 2.23 where cushion I is a 60 mm foam and cushion J is a 30 mm foam. Corbridge and Griffin (1989, 1991) found that the thickness effect is significant in the cushion transmissibility. They compared a 30 mm thickness mounded foam with a 60 mm thickness mounded foam. The experimental data showed that the 60 mm foam had higher peak transmissibility around 5 Hz, but lower transmissibility in the frequency range above 6 Hz (Figure 2.23). Corbridge *et al.* (1989) studied the effect of a seat cover on seat transmissibility. They measured the transmissibility of a railway seat with a seat covering material

and without a seat covering material. It was found that the cover had little influence on the seat transmissibility.

Ebe (1993 and 1994) studied the effect of composition of polyurethane foam on the vibration transmissibility of automotive seats. The characteristics of the four foams are listed in Table 2.4. He used comfort score to evaluate seat performance. Figure 2.25 shows comfort scores for the different seats. It is clear that there was a significant difference among the four seats and that the effect of foam composition on seat dynamic property is significant.

Table 2.4 characteristics of the foam in the automotive seats (From Ebe 1994)

Type	Hardness (kg)	Density (kgm^{-3})	Comment
A	20.8	45	Low density type
B	21.1	52	Standard type
C	21.2	55	Long durability type
D	21.0	65	Soft feeling type

Seat dynamic properties are affected by the environment such as temperature and relative humidity as well as their change while measuring. Hence, when measurements of seat dynamic properties are obtained the temperature and relative humidity, as well as their change, must be controlled in a required range.

Ebe (1995) studied the effect of foam pad construction on vibration transmission. Four similar seats with different foam pads, which were defined as HR, PP, SF and HOT foam, were used to investigate the influence of the construction of the polyurethane foams on vibration transmission. The experiments were conducted on a bumpy road at a speed of 30 m.p.h and a motorway at a speed of 70 m.p.h for a period 30 seconds. The comfort scores were used to assess the performance of the seats. It was found and that there were differences between four seats comfort scores.

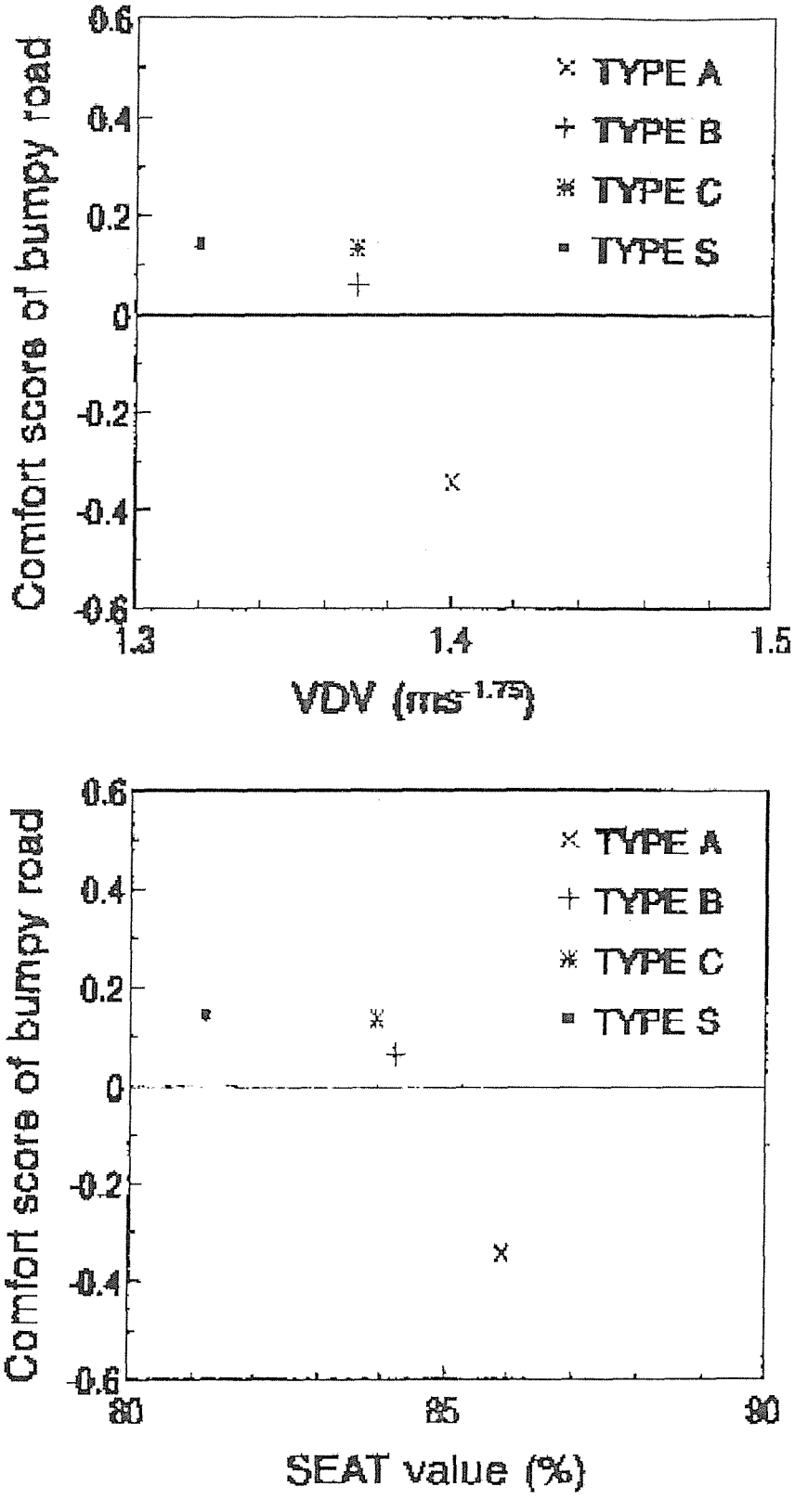

Figure 2.25 comfort scores for different seats (From Ebe 1994)

The effect of density of polyurethane foam on vibration transmission was

investigated by Ebe (1994). Five foams with different density were used in experiments. The experiment was conducted using an electro-hydraulic vertical vibrator having a maximum stroke of 1 metre. The input vibration had a flat acceleration power spectrum over the frequency range 0.8 to 20 Hz and was presented at 1.0 ms^{-2} rms magnitude for two minutes duration. Eight subjects participated in the study. The conclusion was that the density of polyurethane foam did not affect either the transmissibility at resonance, the resonance frequency or the vibration transmission ratio.

2.3.4.2 The loading on the seat

It has been noted by many researchers that a person cannot be replaced by a rigid mass when measuring seat transmissibility. Leatherwood (1975) exposed a seat to vertical vibration with sandbags and human subjects. The experimental data showed that the peak transmissibility of the seat with the sandbags was greater than that with the subjects. The resonance frequency was also higher for a mass than that for subjects. Ashley (1976) showed that at low frequencies the transmissibility of a suspension seat was similar whether it was loaded with a mass or a person, but considerably different at high frequencies. Although Lowe (1972) suggested that suspension seats should be tested with a mass instead of a person in the interest of repeatability and comparability, Fairley and Griffin (1983) pointed out that the transmissibility of the seat depended upon the dynamics of the body on the seat as well as the dynamics of the seat and demonstrated the effect with a comparison of seat transmissibility loaded with mass and a man. Griffin (1990) showed typical seat transmissibilities obtained when loaded with a person or loaded with a rigid mass of the same weight as the person (Figure 2.26).

Matthews (1967) developed a one degree-of-freedom mechanical dummy to replace a seated person. The dummy consisted of a mass suspended by four elastic bands from a rigid frame. The total mass was 55 kg, including the frame, and the natural frequency was 5 Hz. The damping was adjusted so that the transmissibility of a suspension seat measured with the dummy had the best agreement with the transmissibility when a person was on the seat. Agreement was fairly good at high vibration magnitudes, but at low vibration

magnitudes the transmissibility with the dummy was higher than the transmissibility with a person. The possibility of there being significant friction and other non-linearities in the dummy was not considered.

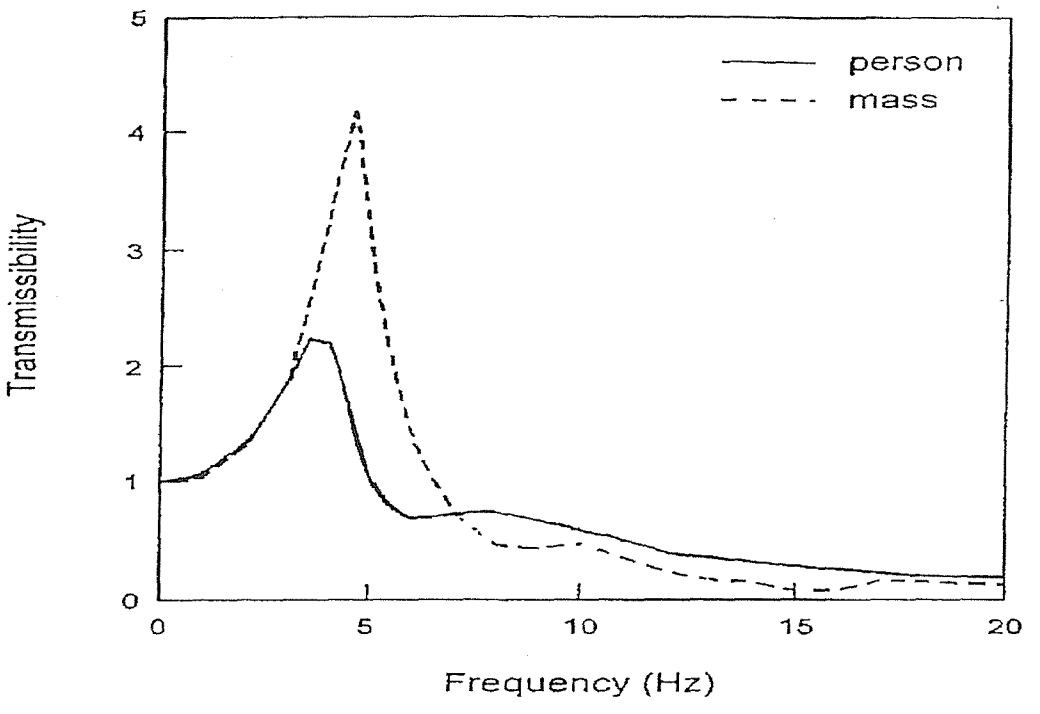

Figure 2.26 comparison of seat transmissibilities loaded with a person and a rigid mass. From Griffin 1990.

Suggs *et al.* (1969) found two resonances at about 5 and 8 Hz in the driving point impedance of a sitting subject and then developed a more complicated two degree-of-freedom dynamic dummy based on a lumped parameter model that was fitted to measurements of the mechanical impedance of the body. Suggs *et al.* (1969) built the model, which had a common rigid frame from which two uncoupled masses were suspended by springs and dampers (Figure 2.27). The lower mass was larger and represented the pelvis and the abdomen, while the smaller upper mass represented the head and the chest. The rigid frame was analogous to the spinal column. The weight of the unsprung components was 6 kg. The dummy had a glass-fibre base that was moulded to represent the buttocks of a person. The authors also used the dummy to simulate the human loading on a seat to measure the seat transmissibility. The comparison between the dummy and the subject in

different sinusoidal vibration magnitudes showed that agreement was good in some frequency ranges (Figure 2.28).

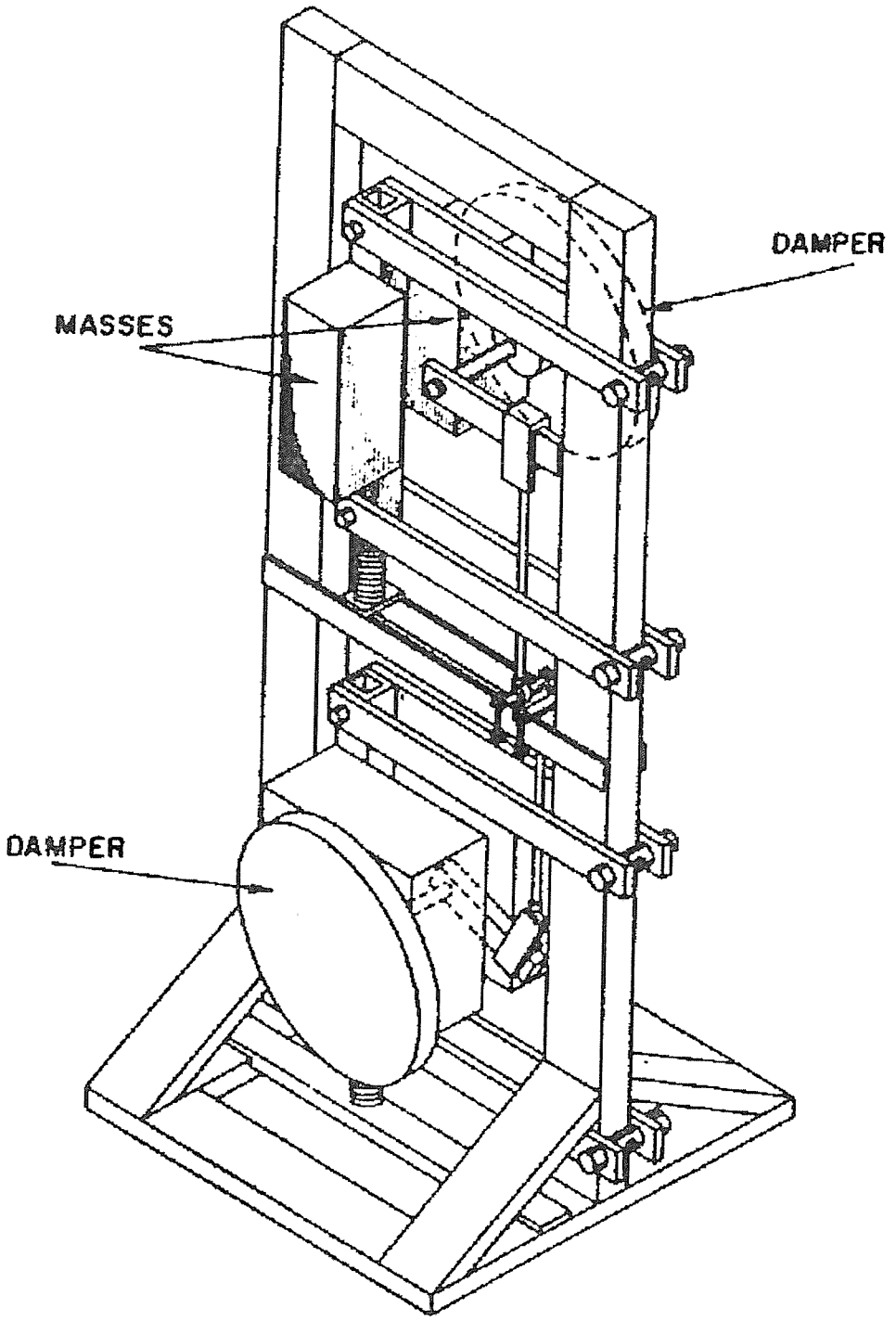

Figure 2.27 Two degree-of-freedom dummy. From Suggs *et al.* 1969.

For the routine testing of seats it might be attractive to use a mass or an anthropodynamic dummy having representative impedance characteristics in

place of a subject. However, there are significant differences between a seat response loaded with a mass and a person. The human subject is a complex dynamic system. When a person sits on a seat the interaction between the human subject and the seat affects the seat dynamic response. Although anthropodynamic dummies have been developed, they are not yet in general use because there are difficulties in maintaining the response of such systems in calibration and it may not be easy to restrain a dummy to the correct position in a seat.

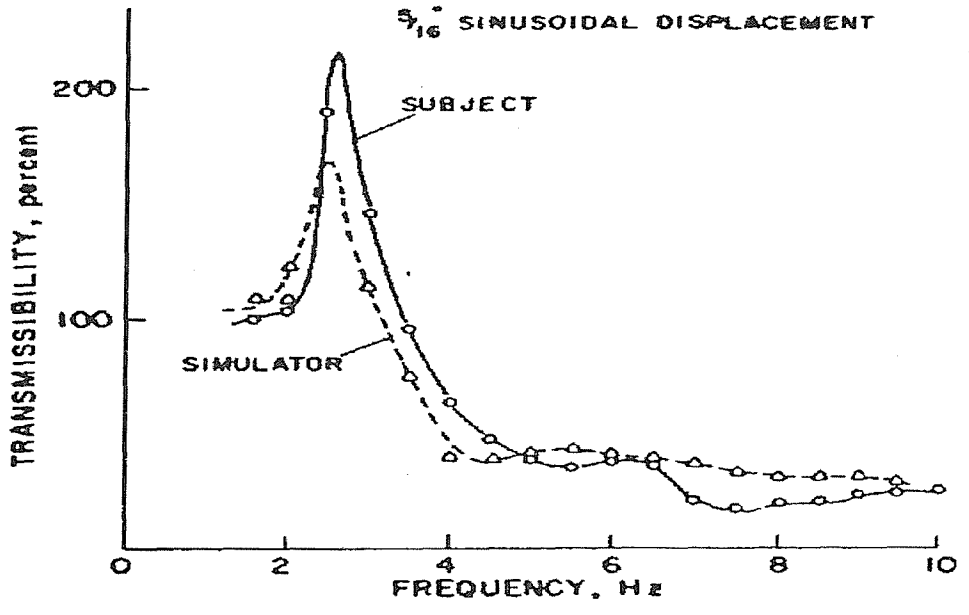

Figure 2.28 Transmissibility comprison of a seat loaded with a person (solid line) and with the dummy (dashed line), From Suggs *et al.* 1969.

Mansfield (1998) and Lewis (1998) developed a serious of anthropodynamic dummies for the simulation of the vertical dynamic response of the seated human body. The dummy was based on the model of human impedance as suggested by Fairley and Griffin (1989). These dummies will be discussed in Section 2.5.5.

2.3.4.3 Effect of subject variability

Many researchers have investigated the effect of the occupant characteristics on seat transmissibility. It has been found that different subjects give different seat transmissibilities. Subject weight and size, subject posture, contact with the backrest, foot support position and arm support all may influence the

measured seat transmissibility. However, previous studies suggest that several of these factors are less important than might be expected.

1) Subject weight and gender

Matthews (1967), Stayner (1971) and Burdorf and Swuste (1993) showed that the subject's weight affected suspension seat transmissibilities. They found heavier subjects usually tended to be better isolated by a suspension seat than light subjects due to the lowering of the suspension natural frequency under increased load. Other researchers, such as Corbridge (1981), Fairley (1986) and Corbridge *et al.* (1989), provided evidence that subject mass generally has a small effect. Corbridge (1981) studied the effect of two subject variables: weight and sex, on the transmissibility of a suspension seat to vertical vibration. The results showed that the suspension system was relatively insensitive to the differences in subject weight and sex. Varterasian and Thompson (1977), also investigated the effect of subject weight and sex. They measured the transmissibilities of an automotive seat with 9 male and 6 female subjects. The study showed that there was no effect of subject mass or sex on the transmissibility of conventional seats as there were only small differences in the resonance frequency and transmissibility at resonance, even though the subject mass supported by the seat had a range of 31 kg to 72 kg. The standard deviation of the resonance frequency of the seat and the transmissibility at the resonance of the seat were small.

2) Footrest

Fairley (1986) measured the transmissibility of a seat with one person with different heights of a stationary footrest. Initially, the footrest was in the highest position, where there was little contact between the thighs and the seat. The footrest was then lowered by a total of 0.32m in 0.04m steps. He found that the transmissibility increased slightly at frequencies above resonance as the footrest was lowered (Figure 2.29). Fairley thought that the reason for this result was likely to be a consequence of the increased contact between the person's thighs and the front of the seat cushion. Increasing thigh contact means that more vibration is transmitted to the thighs. A change in the dynamic response of the body would be expected as a result. However, this

was just an investigation of the effect of stationary footrest on the transmissibility. In general, the footrest moves with the seat, so further investigation about how moving footrest heights affect seat transmissibility is needed.

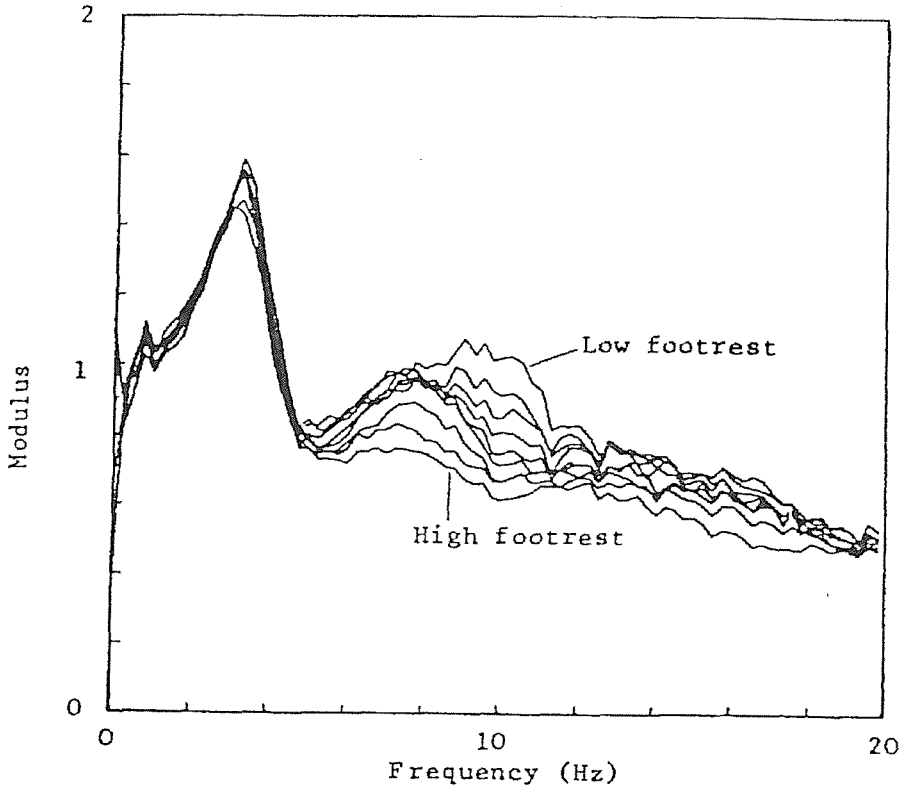

Figure 2.29 Effect of stationary footrest heights on the transmissibility of a seat. From Fairley 1986.

3) Backrest

Fairley (1986) investigated the effect of a backrest on seat transmissibility. He measured a car seat with four people under three different conditions: no backrest, lumbar back contact and full back contact. The angle of the backrest was fifteen degrees from vertical. Figure 2.30 shows the comparison between three test conditions. Increasing backrest contact caused the transmissibility of the seat to increase at frequencies above resonance; although, above 10 Hz the increase for full back contact was not as great as the increase for just lumbar contact. The resonance frequency, and the transmissibility at resonance, also increased slightly with increasing backrest contact. The effect of increasing the angle of the backrest from 0 to 50 degrees from vertical, at

10 degree steps, was also investigated with one person (Figure 2.31). When the angle of the backrest increased from 0 to 50 degrees, the resonance frequency increased slightly and the transmissibility at resonance decreased a little, but the transmissibility increased a lot in the frequency range from 5 to 10 Hz. The reason for the above changes may be that the presence of a backrest changed the dynamic response of the body. With a subject against the backrest, the force produced by backrest might tend to restrain the motion of the subject's upper body.

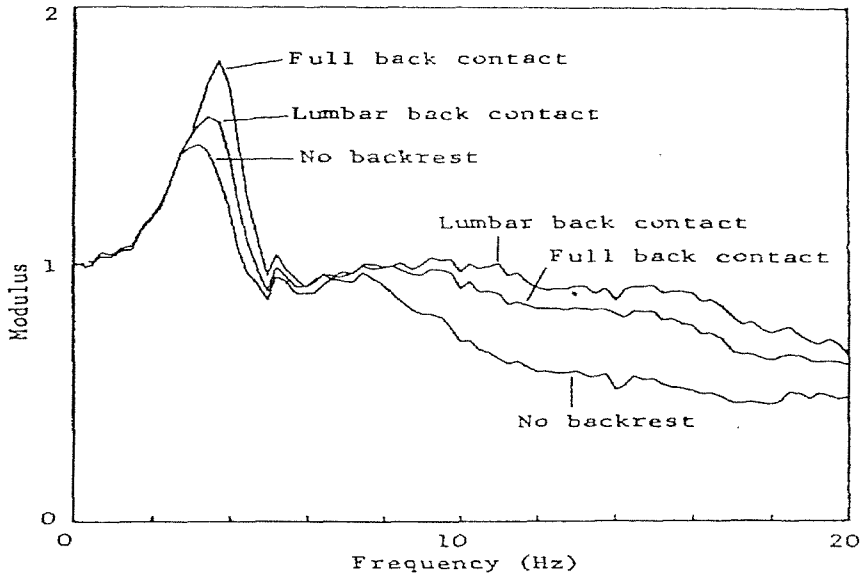

Figure 2.30 Effect of backrest contact on the transmissibility of a seat (mean results for four subjects), From Fairley 1986.

Lewis and Griffin (1996) tested the transmissibility of one seat with a fixed backrest and a moving backrest. The seat was mounted on a rigid frame attached to the platform of a vertical vibrator. The seat back angle was adjusted to 20^0 from the vertical. The moving backrest allowed the seat backrest cushion to move up and down along the backrest frame or a simple spring suspension. Figure 2.32 compares transmissibilities for two subjects with a fixed and with a moving backrest and with the 'back off' condition. The resonance frequency appeared similar with both the moving backrest and the 'back off' condition and was about 0.5 Hz higher with fixed backrest than the above two conditions. The transmissibility at resonance was also higher with the seat back fixed.

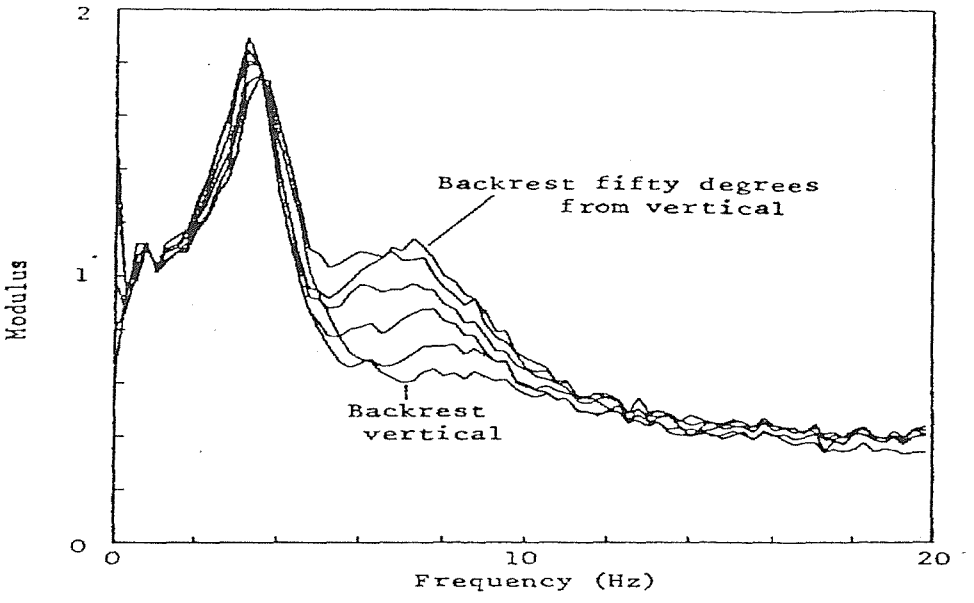

Figure 2.31 Effect of increasing backrest angle on the transmissibility of a seat, From Fairley 1986.

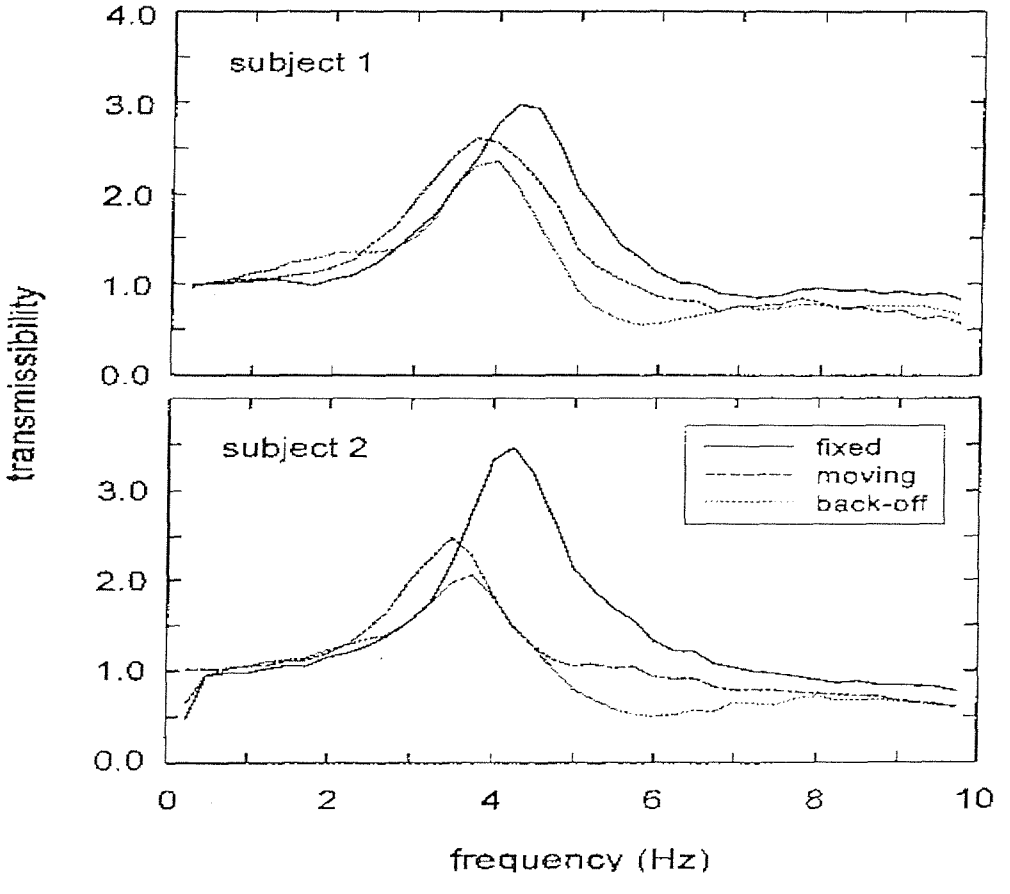

Figure 2.32 Comparison of vertical transmissibilities with three conditions. From Lewis and Griffin 1996.

4) Effect of subject posture

The posture of subjects has been shown to have some effect on the transmissibility. Corbridge and Griffin (1986) reported that the upper body might have a significant effect on the transmissibility of a seat, particularly when there was no contact with the seat backrest. They found that changing the contact with the seat by leaning against a backrest or leaning forward or by resting the arms on the armrests also changed the transmissibility of the seat. They mentioned that the position of the arms had a significant influence on the measures of seat transmissibility; when subjects placed their arms on the armrests, the peak mean transmissibility was lower than when the hands were on their laps. Corbridge *et al.* (1989) continued his study in this field. The conclusion was that changes in upper body position gave greater changes in measured transfer function than changes in lower body posture.

2.3.4.4 Effect of vibration characteristics on seat transmissibility

The type of vibration to which a seat is exposed can affect the seat transmissibility. However, only a few studies have been performed in this field. Fairley (1983) compared the transmissibilities of a seat with two types of transient vibration input (a series of single frequency impulses and a rapid frequency sweep) and a continuous input of Gaussian random vibration were given. It was found that the transmissibilities obtained with these vibration inputs were similar. Burdorf and Swuste (1993) measured the transmissibilities in the laboratory and in the workplace. They found that there were differences between the transmissibilities obtained in both conditions. These may be caused by the differences of the input vibration spectrum.

a) Vibration magnitude

The effect of vibration magnitude is important for transmissibility, as has been recognized by many researchers. Stayner (1972), Leatherwood (1975), Ashley (1976), Fairley (1983, 1986), Corbridge (1987) and Fairley (1990) have provided evidence that vibration magnitude affects seat transfer functions. However the seats they studied were different, Stayner (1972), Ashley (1976) and Fairley (1990) analysed the effect of vibration magnitude on suspension seats and others analysed conventional seats. Because the studies gave similar results, a typical experimental result is demonstrated here for the effect

of vibration magnitude on seat transmissibility. Fairley (1986) measured the transmissibility of a car seat with eight different people using six different magnitudes of vibration: 0.2, 0.5, 1.0, 1.5, 2.0, 2.5 ms^{-2} rms. The mean results (Figure 2.33) showed a consistent effect of vibration magnitude - as did all the individual results. The resonance frequency decreased from about 5 to 3 Hz, and the transmissibility at resonance decreased from about 1.9 to 1.5 as the magnitude of the vibration was increased. A second resonance frequency was apparent. It also decreased with increasing vibration magnitude - from about 10 to 7 Hz. The author thought that the changes of transmissibility may arise from changes in the dynamic response of either the seat or the person; although, it is unlikely that the dynamic response of a seat could, by itself, be responsible for the observed changes - there is no reason to expect that a simple seat fabricated from foam with wire springing should have such large non-linearities in its stiffness and damping.

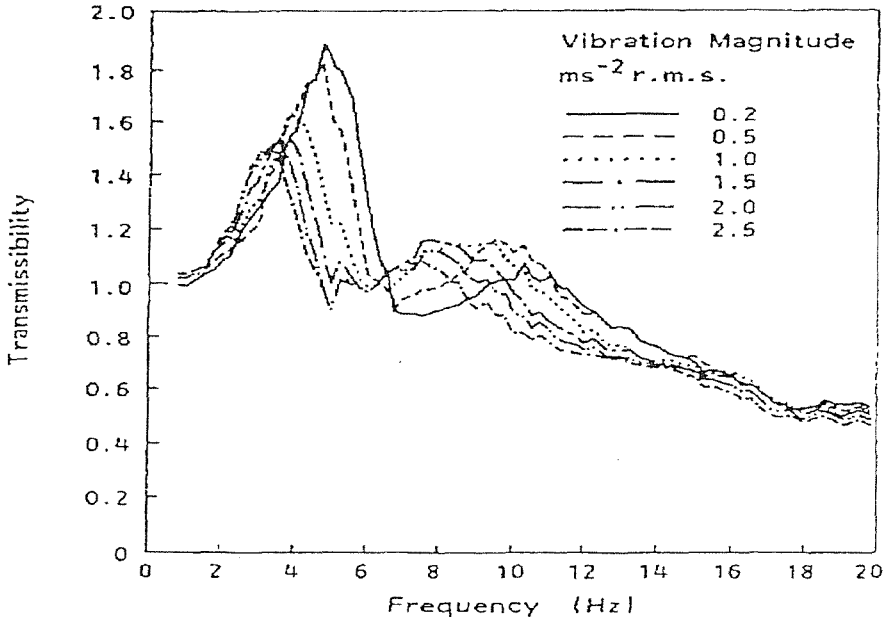

Figure 2.33 Transmissibility of a seat meaured with six different magnitudes of random vibration. From Fairley 1986.

Fairley (1990) also studied suspension seat non-linearity. He measured a typical air suspension seat (Grammer, type LS95H/90Ar) with a subject. The results are shown in Figure 2.34. Because a suspension seat is composed of a cushion and a suspension system, Fairley measured transmissibilities of a

cushion, a suspension and the complete seat with different vibration magnitudes which were 0.35, 0.7 and 1.4 m/s^2 rms. The non-linearity of a cushion was similar to that of a conventional seat shown in Figure 2.33, but there was different non-linearity with the suspension system. When vibration magnitude increased, the resonance frequency of the suspension system was unchanged but the peak value increased. However, the transmissibility modulus of the suspension decreased with increased vibration magnitude over the frequency range above 2 Hz. The non-linearity of the complete seat was composed of both the non-linearity of the cushion and the non-linearity of suspension, but it was mainly affected by the latter.

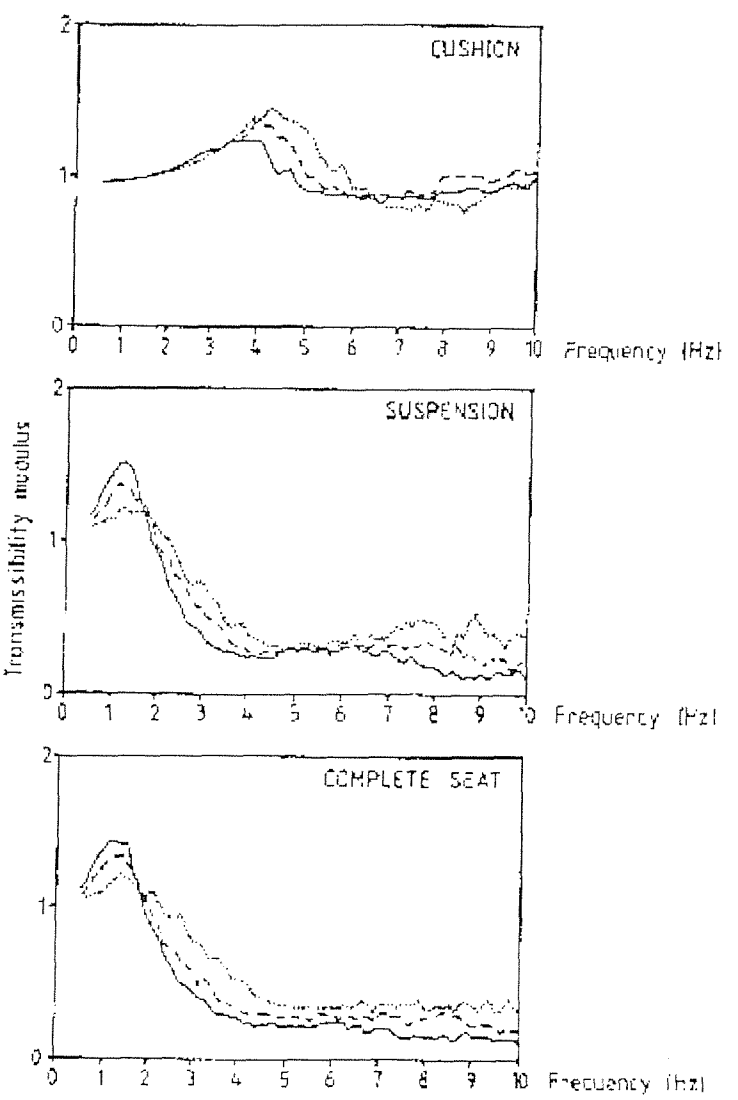

Figure 2.34 Transmissibility of a suspension seat measured at different vibration magnitudes (From Fairley 1990).

Figure 2.34 shows the non-linearity of a suspension seat at normal vibration magnitudes. If the vibration magnitude is great enough, a non-linear end-stop impact will affect the seat transmissibility. Wu and Griffin (1995) proposed a suspension model including a non-linear end-stop system (Figure 2.35).

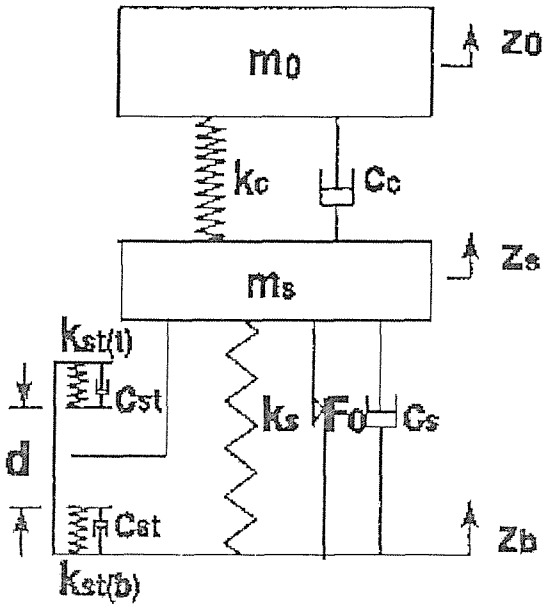

Figure 2.35 Non-linear end-stop suspension seat model (From Wu 1995)

2.3.5 Effect of multi-axis input

Laboratory seat testing is often carried out using only vertical vibration. However, the existence of any cross-axis coupling in the dynamic response of a seat-person system could have important implications for field measurements in vehicles where vibration occurs in many axes. Fairley (1986) investigated whether the transmission of vertical vibration through a seat would be affected by the presence of fore-and-aft vibration. He mounted a seat on a slip-table driven simultaneously in the vertical and fore-and-aft axes by two electrodynamic vibrators. The magnitude of the random vibration in each axis was 1.0 ms^{-2} rms. The input time history for the vertical vibration was the same as the input time history for the fore-and-aft vibration except that it was reversed so that the vibration in the vertical axis was uncorrelated with the vibration in the fore-and-aft axis. Figure 2.36 shows how the vertical

vibration at the seat-person interface was caused by the vertical and fore-and-aft vibration at the base of the seat. The cross-axis coupling, as implied by the transfer function for fore-and-aft vibration at the base of the seat transmitted to vertical vibration at the seat-person interface, was small. The multiple coherency function was close to unity at all frequencies from 1 to 20 Hz, indicating that almost all of the vertical vibration measured at the seat-person interface was accounted for by the two inputs measured at the base of the seat. Because the vertical vibration on the seat surface was not fully caused by vertical vibration on the seat base, the coherency between the two vertical vibrations does not equal to unity (see Section 2.3.3).

2.3.6 Conclusion

The optimization of seat dynamics involves the minimization of the transmission of vibration through seats. In order to provide good isolation of the vibration at the frequencies to which a seat will be exposed, suitable seat evaluation techniques should be adopted. The seat transmissibility and SEAT value are useful tools to represent the seat dynamic characteristics and performance of seats. Other evaluation techniques such as absorbed power and measurements of seat ride comfort have also been used by some researchers, but these have not yet come into general use.

The transmissibility of a seat loaded with a rigid mass is not representative of the transmissibility when a person sits on the seat: the transmissibility of a seat depends upon the dynamic characteristics of both the seat and the person sitting on the seat. Therefore, when researchers study seat dynamic performance, they should not only pay attention to the seat properties but also to the human body response in different vibration environments.

The transmissibility of a seat is affected by many factors, however it can be seen that most of the factors are same as the factors affecting human body apparent mass, or mechanical impedance. The reason is that the transmissibility of a seat depends upon the dynamic characteristics of both the seat and the person sitting on the seat.

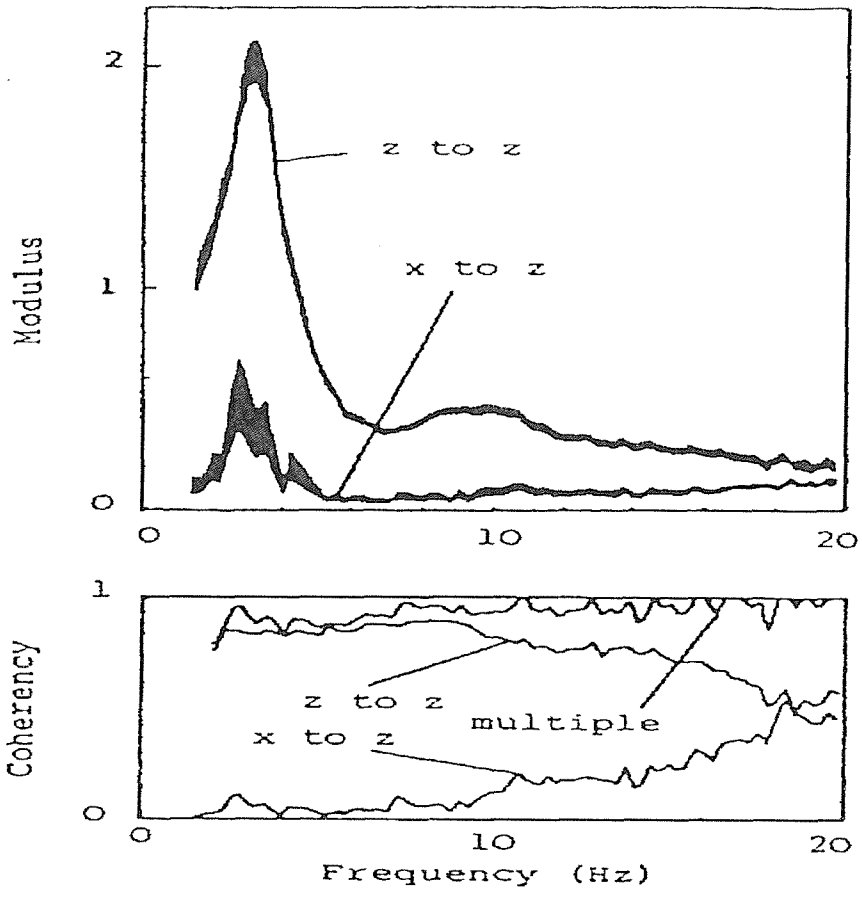

Figure 2.36 Transfer function and coherency function for vertical and fore-and-aft vibration (black bands indicate 95% confidence intervals), From Fairley 1986.

Through the review of literature, it can be concluded that the main factors affecting seat transmissibility are: seat type and properties, subject posture, backrest, vibration magnitude and multi-axis input. Among these factors, subject posture, backrest and vibration magnitude are the three factors which have the most important influence on the seated person response, so it can be assumed that the effect of these factors on seat transmissibility are caused by the seated person who influences these three factors. It cannot be assessed that the effect of multi-axis input on the seat transmissibility is caused by seated subjects because no researches concerned with the effect of multi-axis input on the human body apparent mass. The effects of seat type and seat properties on the seat dynamic response are the only factors which seat designers feel able to control. The seat designers can optimise the seat dynamics properties through changing these factors.

Other factors such as subject weight, gender, footrest, etc. did not appear to have large effects on the transmission of vertical vibration, so we do not need to pay more attention to these factors.

Measuring the performance of a seat requires a person to load the seat other than with a rigid mass. Most conventional seats show a peak in the vertical transmissibility at 3 to 5 Hz while suspension seats have their primary vertical resonance frequency occurs at a frequency of 1 to 3 Hz. An 'SAE pad' is the standard device for measuring the acceleration on the surface of seats, although other devices have been shown to give reliable and repeatable results.

2.4 Biodynamic modelling of seated persons

2.4.1 Introduction

Griffin (1990) explained the importance of biodynamic models for human response to vibration and listed their applications (Table 2.5). Many biodynamic models have been developed due to the variability of model applications. Dynamic models for the human body can be categorised into three types: lumped parameter models, continuum models and discrete models. The lumped parameter models are models where masses of the human body structure are concentrated into a few lumped masses interconnected by springs and dampers. Although there are many limitations, lumped parameter models are useful to interpret measured data with a physical and theoretical understanding so that underlying phenomena or mechanisms may be found, by focusing only on the phenomena of interest.

Continuum models and discrete models are distributed parameter models in contrast to the lumped parameter models. The continuum models treat the body or spine as a homogeneous rod or beam, whereas the discrete models treat the body or spine as a layered structure of rigid elements representing the vertebral bodies. Internal stress or strain within the spine in response to vibration or shock may be predicted, using the models, so as to investigate the process of spinal injuries. Both types of model are developed principally

based on anatomy, including the geometry of the human body such as the spinal curvature. The development of the finite element method has made it possible to create more accurate models in geometry. However, the more accurate the models become, the more the lack of data in the material properties is found. There are also some material properties which are not easy to be obtained, such as stiffness of live tissue. The discrete model is outside the scope of this study, so we will not discuss it.

Table 2.5 Applications of biodynamic models (from Griffin 1990)

To predict movement or forces caused by situations too hazardous for an experimental determination
To predict movement or forces caused by situations too numerous and varied for an experimental determination
To understand the nature of body movements
To provide information necessary for the optimization of isolation systems and the dynamics of other systems coupled to the body
To determine standard impedance conditions for the vibration testing of systems used by man
To provide a convenient method of summarizing average experimental biodynamic data
To predict the influence of variables affecting biodynamic response

This section will mainly introduce the biodynamic models developed by previous studies based on measured sitting body apparent mass. Only the models for the human body exposed to vertical vibration will be reviewed.

2.4.2 Lumped parameters models

A simple single degree-of-freedom model for the human body was proposed by Payne (1965), which consisted of a mass representing the head and the upper torso, and a spring and a damper located in parallel representing the spinal column. The stiffness and damping of the spinal column were determined based on driving point impedance data. Vogt *et al.* (1968)

extended Payne's approach by suggesting a generic model for measurements made using one subject. It was shown that up to 8 Hz the mechanical impedance of the body could be represented by a single degree-of-freedom system with a resonance frequency at 5 Hz and a damping ratio of 0.575. It was shown that the resonance frequency increased under sustained acceleration but that the damping factor remained unchanged at approximately 0.575.

Fairley and Griffin (1989), who fitted a lumped parameter model to the mean normalised apparent mass of 60 subjects, suggested a lower damping ratio. The authors measured the apparent mass of 60 subjects (Figure 2.37) and, minimizing the sum of squared differences at each frequency, obtained the parameters of a moving mass of 45.6 kg, and damping ratio of 0.475. A better fit with the measured data was obtained by adding a static frame mass of 6.0 kg to the model, representing the parts of the body which do not move during whole body vertical vibration. In the frequency range of 0 to 20 Hz the normalized apparent mass and the phase of the model lay within plus and minus one standard deviation of the mean normalised subject apparent mass.

Although the impedance of single degree-of-freedom models shows a fairly close agreement with Fairley's mean subject data, most measurements of impedance or apparent mass show two resonance characteristics. Coermann (1962) found evidence of a second resonance frequency at approximately 10 Hz for sitting subjects. In International Standard ISO 5982 (1981) the mechanical impedance also shows evidence of two resonance frequency characteristics for the human body in response to vertical vibration. Suggs *et al.* (1969) found two resonances at about 5 and 8 Hz in the driving point impedance of a sitting subject and, therefore, developed a two degree-of-freedom model. The model had a common rigid frame, from which two uncoupled masses were suspended by springs and dampers (Figure 2.38). The lower mass was larger and represented the pelvis and the abdomen, while the smaller upper mass represented the head and the chest. The frame was analogous to the spinal column. The resonances of the lower and the upper masses corresponded to the 5 Hz and 8 Hz resonances respectively

and the model parameters were determined so that the driving point impedance at the base of the rigid frame coincided with the measured impedance of the human body.

International Standard 5982 (1981) includes a similar two degree-of-freedom model for calculating the driving point impedance of the human body in sitting and standing positions. However, some restrictions apply to this standard for seated human body. First, the whole-body z-axis input mechanical impedance of the seated human body was based on a limited number of subjects. Although the experimental values related to 39 subjects with a range of whole-body weights from 53 to 93.8 kg, the values related to an upright posture were based on only 10 subjects, other values were derived from poorly defined subject postures. Second, it has been said in the standard "the mechanical impedance curves come from sinusoidal vibration of the body. Due to the possibility of non-linearities occurring, the curves from sinusoidal vibration should not be taken to apply to other forms of motion". Third, the model mass (m_1+m_2) of 75 kg in this standard seems heavier than the model mass 51.6 kg from Fairley and Griffin (1989). The reason for this can be seen in the standard: "One would expect the impedance magnitude to be greater in those cases where the feet were not supported".

Payne and Band (1971) developed a four degree-of-freedom model. The model consisted of the pelvic mass, visceral mass, upper torso mass and the head mass with springs and dampers interconnecting between the masses (Figure 2.39). The mass distribution of the model was said to be based on anthropometry. Initial values for stiffnesses were based on data reported in the literature rather than experimental data. The stiffnesses and the damping ratios were adjusted by comparing the model predictions with experimental data. He concluded that the driving point impedance data reflected only the motion of the lower part of the body such as the pelvis and the buttocks, and more data on the response of each body segment would be required to develop a more validated whole body model.

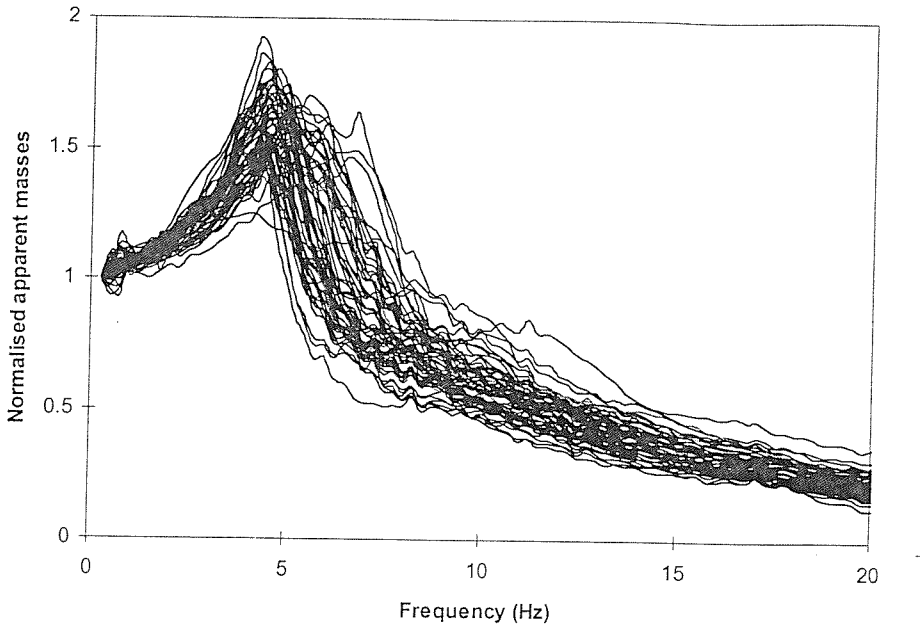

Figure 2.37 Normalised apparent masses of 60 seated subjects in the vertical axis (From Fairley and Griffin 1989).

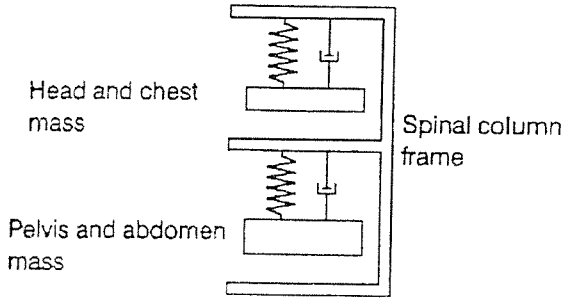

Figure 2.38 A two degree-of-freedom model for sitting person. From Suggs *et al.* 1969.

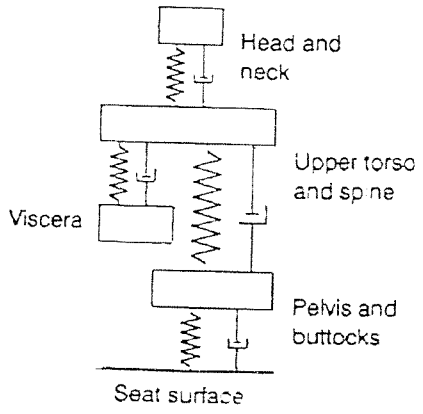

Figure 2.39 A four degree-of freedom model developed by Payne and Band.

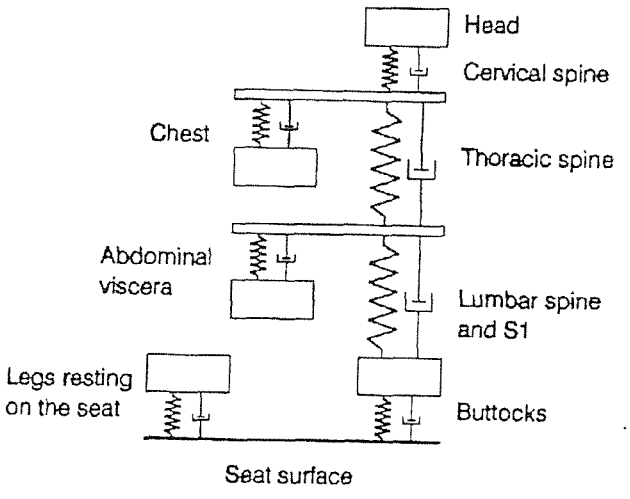

Figure 2.40 A five degree-of-freedom model developed by Mertens and Vogt (1979).

Mertens and Vogt (1979) proposed a five degree-of-freedom model (Figure 2.40). The model consisted of masses for the head, chest, abdomen, buttocks and some part of the legs. The mass distribution was based on anthropometry. The stiffnesses for the spinal springs were chosen from the static and dynamic measurements of the spinal responses, and the stiffness for the abdominal spring was chosen from the abdominal pressure response data reported in the literature. The stiffnesses for the remaining parts and all the damping coefficients were estimated, comparing the driving point impedance and the seat-to-head transmissibility of the model with experimental data.

2.4.3 Continuous models

Liu and Murray (1966) proposed a continuous model, which included a head mass at the upper end of a uniform homogeneous elastic rod (Figure 2.41). The rod represented the human torso from the lumbar spine to the neck. The study concentrated on a theoretical formulation of the model response and the model parameters seemed to have been chosen arbitrarily. They investigated the longitudinal wave propagation and calculated the stress distribution in response to an axial step acceleration input. The effect of damping was studied. However, inclusion of the damping term did not greatly affect the

response, except that it increased the stress in the lumbar region slightly. It was concluded that the stress and the acceleration in the spine were different and a maximum acceleration criterion for spinal injuries should be replaced by the maximum stress criterion. A similar continuous model was developed by Ji (1995) for a standing person.

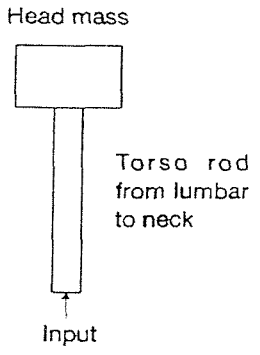

Figure 2.41 A continuous model developed by Liu and Murray (1966).

Li *et al.* (1971) developed a simplified continuum dynamic model representation of the curved spine with the torso mass uniformly distributed along its length. The model consisted of a sinusoidally curved beam, representing the spine from the upper lumbar region to the cervical region, with the upper end fixed to a head mass. The spinal beam possessed a constant cross section which was determined, considering the additional contribution of the supporting vertebral structure. The material properties and the geometrical data were chosen from the literature on compressive wave propagation in the spine, measurement of the natural frequency of the spine, and compression and bending tests of inter-vertebral discs. The calculated undamped compressive wave velocity and the axial natural frequency were 36.6 m/s and 13.5 Hz respectively.

2.4.4 Non-linear models

It has been confirmed that the response of the sitting body to vertical vibration is non-linear. Therefore, developing a non-linear system model representing the human body in vibration environments has attracted several researchers.

Hopkins (1971) considered the non-linear behaviour of the abdominal viscera in his three degree-of-freedom non-linear model (Figure 2.42). The model consisted of the upper torso mass, lower torso mass, visceral mass, and springs and dampers interconnecting the masses. The other parts included in the model were a piston in a cylinder with an orifice interconnecting the upper torso mass and a visceral mass which represented the lungs. The model possessed tension cut-off non-linear connections between the visceral mass and the abdominal wall spring and between the visceral mass and the lung piston, assuming that vertical visceral motion would neither pull down the diaphragm nor pull up the pelvis. The equation of state of air inside the lung cylinder was incorporated into the equations of motion of the model. The model parameters were determined from comparisons of the dynamic responses of the model with corresponding experimental data reported in the literature, such as the driving point impedance, seat-to-head transmissibility, and the abdominal strain and pressure responses. The model produced a non-linear excitation magnitude dependent, driving point impedance, in which a higher magnitude decreased the modulus of the impedance at most frequencies.

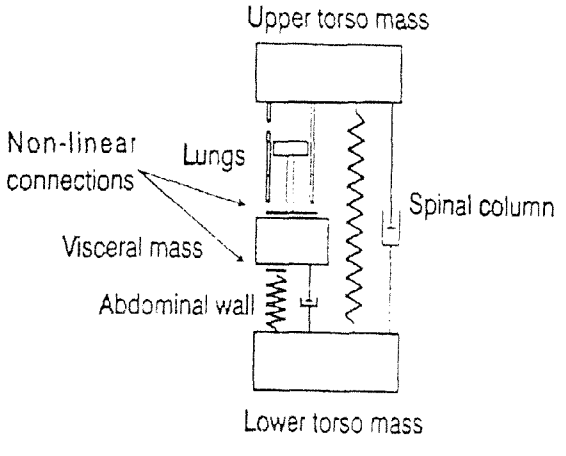

Figure 2.42 A three degree-of-freedom non-linear model developed by Hopkins (1971).

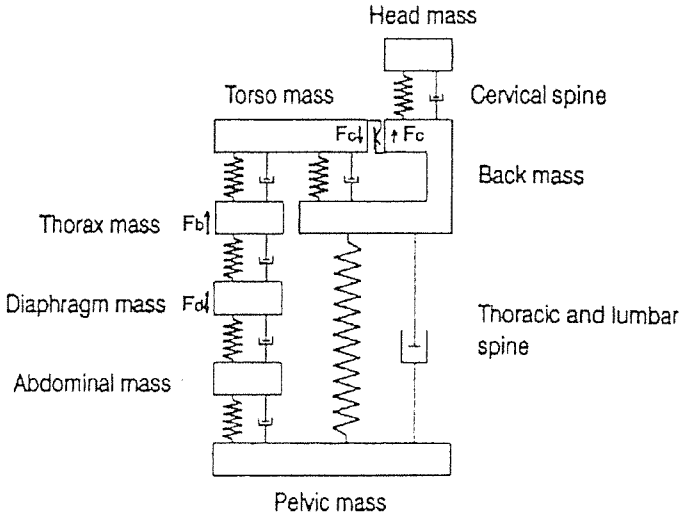

Figure 2.43 A seven degree-of-freedom non-linear model developed by Muksian and Nash 1974.

Muksian and Nash (1974, 1976) developed a seven degree-of-freedom non-linear model which included masses for the head, torso, thorax, diaphragm, abdomen, back and the pelvis (Figure 2.43). The mass distribution was determined from the literature as 5.44kg for the head, 47.17kg for the body and 27.22 kg for the pelvis (which included the legs) based on a total mass of 79.83kg. The stiffnesses and damping ratios were estimated through comparing the driving point impedance and the seat-to-head transmissibility of the model with experimental data. The authors showed that the model gave a close agreement with experimental data up to 6 Hz using linear dampers and above 6 Hz using non-linear dampers. They concluded that an appropriate model of the body could be found by having frequency-dependant non-linear parameters in the model.

2.4.5 Transmissibility models

Transmissibility of the whole body has been investigated by many researchers through studying the relation between vertical vibration of a seat and the resulting vertical vibration at the head. Paddan and Griffin (1988, 1996) studied the transmission of vibration from the seat to the head. The resonance frequency of the measured body transmissibility was around 5 Hz. A six-axis 'bite-bar' was used to measure the acceleration at the head. The 'bite-bar'

was same as that previously used by Griffin (1975) to measure rotational motion.

A single degree-of-freedom model was firstly developed by Latham (1957) to represent the transmissibility of the body. It was a lumped parameter model composed of two masses connected by a spring. Griffin *et al.* (1979) developed another single degree-of-freedom model which had a natural frequency of 14 Hz and a damping ratio of 0.6 and gave a result which lay between the 5th and 95th percentile of subject data (18 subjects) in the frequency range 1 to 100 Hz.

International standard 7962 (1987) proposed a four degree-of-freedom model to represent the transmissibility of the body. The model in the standard is suitable for vibration in the frequency range 0.5 to 31.5 Hz and magnitude range of 2 to 4 m/s^2 rms. It applies to sitting or standing subjects in the vertical direction. The model was based on the measurement of 50 subjects. The model response is showed in Figure 2.44. The model parameters can be obtained from Table 2.6.

Table 2.6 Parameters for model of seat-to-head transmissibility (from ISO 7962 1987)

Mass	M1	8.24 kg
	M2	8.05 kg
	M3	44.85 kg
	M4	13.86 kg
Stiffness for seated body	K1	22×10^8 Nm^{-1}
	K2	20.13×10^4 Nm^{-1}
	K3	88.56×10^3 Nm^{-1}
	K4	36.47×10^3 Nm^{-1}
Stiffness for standing body	K1	36.0×10^7 Nm^{-1}
	K2	65.0×10^9 Nm^{-1}
	K3	52.34×10^4 Nm^{-1}
	K4	69.3×10^3 Nm^{-1}
Damping	C1	748.1 Nsm^{-1}
	C2	578.0 Nsm^{-1}
	C3	2964.0 Nsm^{-1}
	C4	901.8 Nsm^{-1}

2.4.6 Conclusion

Biodynamic models for human response to vibration are useful due for specific applications (Griffin, 1990). Many different models have been developed to represent the body in different vibration environments. The models range from linear single degree-of-freedom lumped parameter model to non-linear and finite element models. The degree of complexity of the model should be dictated by the application for which the model is designed. For example, if the model is only designed to simulate the driving point impedance of the body then there is no need to have an accurate representation of transmissibility to other parts of the body. It must be decided whether the model should represent the response of a single individual or a population as a whole, due to differences in response between subjects.

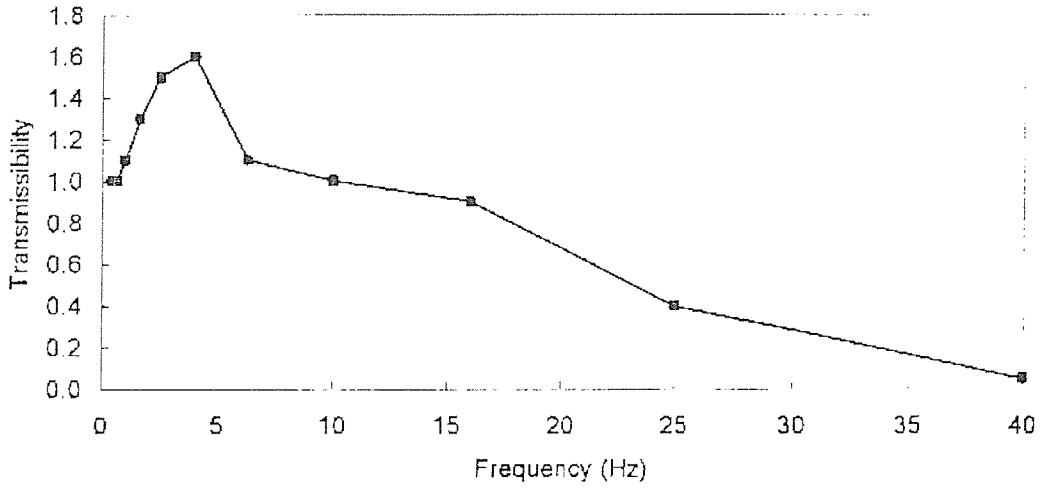

Figure 2.44 Transmissibility of four degree-of-freedom human body model (from ISO 7962 1987)

Accurate models of human biodynamics are not usually general purpose. Most models are specifically designed for an application, such as representing apparent mass, mechanical impedance or the seat-to-head transmissibility. In general, models representing the driving point mechanical impedance have one or two degree-of-freedom. Transmissibility models are more complex. Non-linear representations of the body have been made, but most were not designed to represent the non-linearity in the apparent mass of subjects. The complexity of many models is unwarranted for simple applications, as there may be sub-systems that only have influence outside the specified frequency

range. Alternatively, an almost identical response may be achieved using fewer degree-of-freedom. It is clear that the more complex the model is, the more parameters there are to be determined and the more difficulties involved, such as Nigam and Malik's 15 DOF mass-spring model (Nigam and Malik 1987), where most of model parameters must be estimated through the literature.

Although many continuous models and non-linear models have been developed, they are still in the study stage and require further verification.

2.5 SEAT TEST PROCEDURES

2.5.1 Introduction

The measurement of the transmission of vibration through seats currently requires that a human subject sits on a seat and is exposed to vibration. This is unsatisfactory since results may differ between subjects and may be affected by posture and other factors. Laboratory tests require the availability of vibration simulators that are safe for human exposure.

Ethical and safety considerations make it desirable that a test is developed in which seat transmissibility can be determined without exposing the human body to vibration. Therefore, seat testing has been carried out with alternative forms of loading in place of human subjects. Tests have been made with rigid masses, anthropomorphic dummies and force measuring indenters. The following discussion summarises the three methods.

2.5.2 Measurement quantities

The seat dynamic stiffness is often used to represent the seat dynamic characteristics. The dynamic stiffness (see Section 2.2.1) has the advantage that it can be obtained most directly from the signals provided by displacement transducers (or indirectly from accelerometers) and force transducers. For measuring vertical seat dynamic properties, measuring the vibration at the interface between the person and the seat as well as the body and the backrest is necessary. This requires the insertion of a device between

the seat and the body. It is important that a seat-person interface device does not change the way the seat transmits vibration to the person - either because of its extra mass or because it changes the contact of the body with the seat. Since the seat-person interface is not necessarily rigid, a variety of points, or an average, measurement is possible. Whatever vibration is measured, it must be a suitable measure of the vibration actually received by the person.

2.5.3 Static properties

A common method of reporting seat static characteristics is the load-deflection curve. Many studies of the load-deflection curve have been carried out. Hilyard (1983) studied strain-stress characteristics of foam based on the geometry and compression process of the foam cell. Fairley and Griffin (1986) measured load-deflection curves for both a conventional seat and a suspension seat (Figure 2.45). The force-deflection curve provides useful information regarding the seat characteristics. For example, the gradient of the curve indicates spring characteristics of a seat, the enclosed area corresponds to the hysteresis loss which shows the damping characteristics of a seat. A standard method for measuring the load-deflection curve for a cellular foam is defined in International Standard (ISO 3386/1:1986). Although this standard is not specifically for measuring seat load-deflection curves, it can be applied to a seat.

The force-deflection curve has attracted many researchers interest because it reveals seat static properties and can be changed by varying seat characteristics, such as foam density, hardness and thickness, etc. It is a useful tool for seat designers.

Although the force-deflection curve contains useful information, it is obtained by compressing the seat or foam with a shaped plate. This is different from the real condition in which a person sits on a seat. The pressure distribution on a seat is used to represent real sitting conditions and is widely adopted for predicting the seat static comfort, but it is outside the scope of this study.

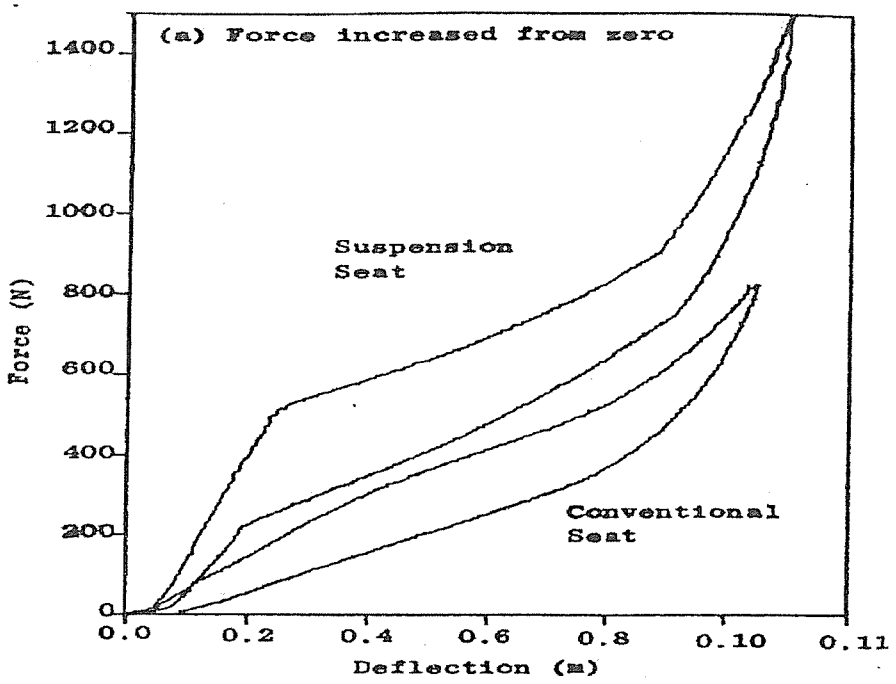

Figure 2.45 Load-deflection curve for a conventional seat and a suspension seat. From Fairley and Griffin 1986.

2.5.4 Testing with rigid masses

Static properties of a seat are important because they have a relationship to seat static comfort. However, for vehicle seats, dynamic properties are also important. While being driven, passengers are exposed to vibration which comes through the seat, floor and steering wheel. Among these vibrations, the vibration coming through the seat is often the largest and most concerned with the passenger comfort. Therefore, a vehicle seat should provide a good isolation. The seat dynamic properties are important for seat designers hoping to optimize seat dynamic performance and provide good isolation of the vibration at the frequencies to which the seat will be exposed.

Rigid masses have been used for testing the dynamics of conventional seats and suspension seats. However, the results of these tests have proved to be inaccurate when compared to tests made using human occupants. Griffin (1990) showed a typical seat transmissibility obtained when loaded with a person or loaded with a rigid mass of the same weight as the person (Figure 2.26). The results were very different. In this case the transmissibility at resonance was higher when using the mass. However, the resonance

frequency appeared to be little affected by the use of a mass on conventional seats.

Wu and Griffin (1996) showed that a sandbag gave the same resonance frequency of a suspension seat as a person, but the magnitude of the transmissibility at resonance was different. The vibration dose value (VDV) measured using the sand bag was higher than the VDV measured using a human subject at all frequencies for tests using sinusoidal motion from 1.0 to 3.15 Hz at all magnitudes.

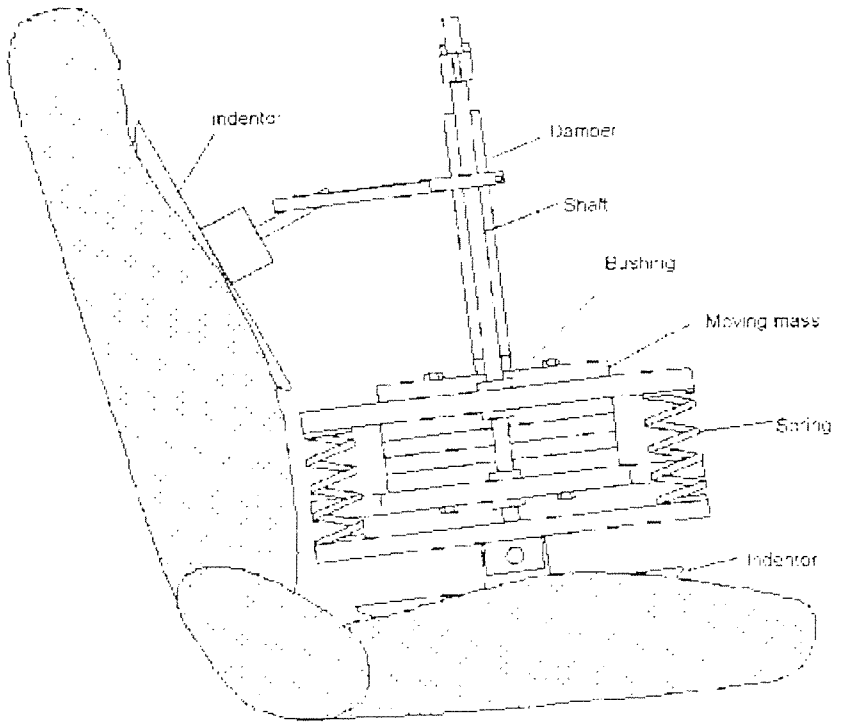

Figure 2.46 Stage four anthropodynamic dummy mounted in a car seat (from Mansfield 1998)

2.5.5 Testing with dummies

A dummy simulates the human body dynamic characteristics in vibration environments. Several researchers have designed a dummy according to mathematical model parameters derived from the human body impedance, or apparent mass. The dummy is used in place of a human subject when testing the seat in vibration conditions. Matthews (1967) developed a single degree-of

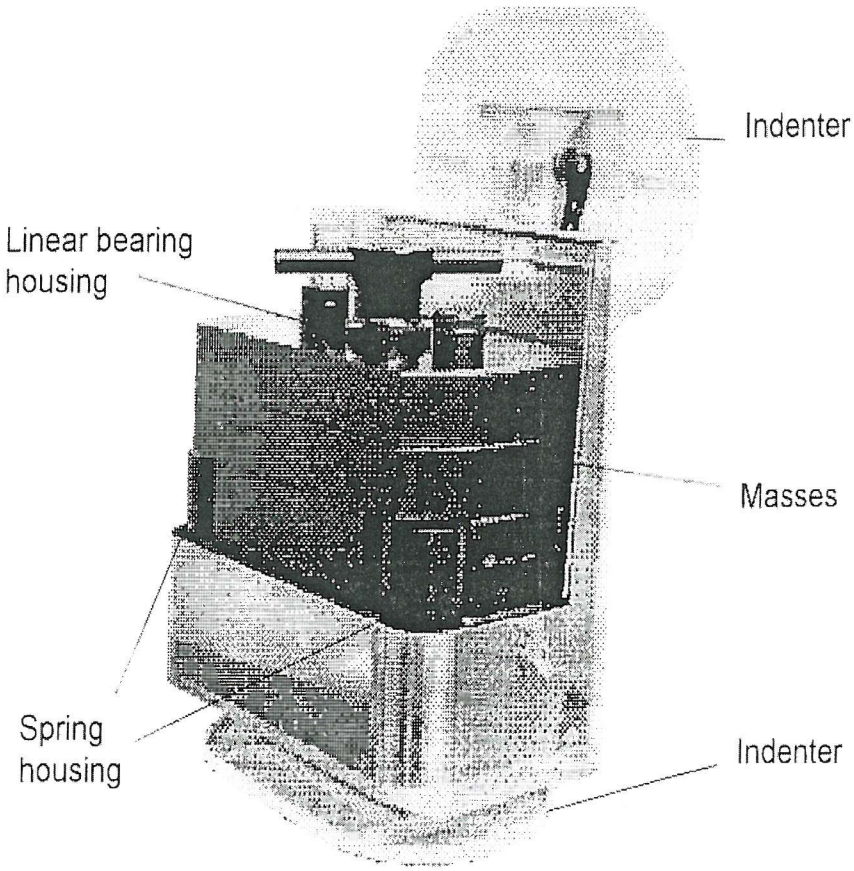

Figure 2.47 Stage five anthropodynamic dummy mounted in a car seat (from Mansfield 1998)

freedom dummy based on the work of Coermann (1959). The mass of the dummy was not reported. The transmissibility using the dummy gave agreement only up to 3 Hz for a seat with low suspension friction. Above this frequency the transmissibility measurements diverged.

Mansfield (1998) built a series anthropodynamic dummies for the simulation of the vertical dynamic responses of the seated human body in the laboratory of the Human Factors Research Unit (HFRU), the Institute of Sound and Vibration Research (ISVR), the University of Southampton. All the dummies were based on the model of human impedance as suggested by Fairley and Griffin (1989). Two of these anthropodynamic dummies are shown in Figure 2.46 and 2.47. They were stage 4 and stage 5 dummies. The apparent

masses of the two anthropodynamic dummies and the apparent masses of 12 subjects measured at 1.0 m/s^2 are shown in Figure 2.48.

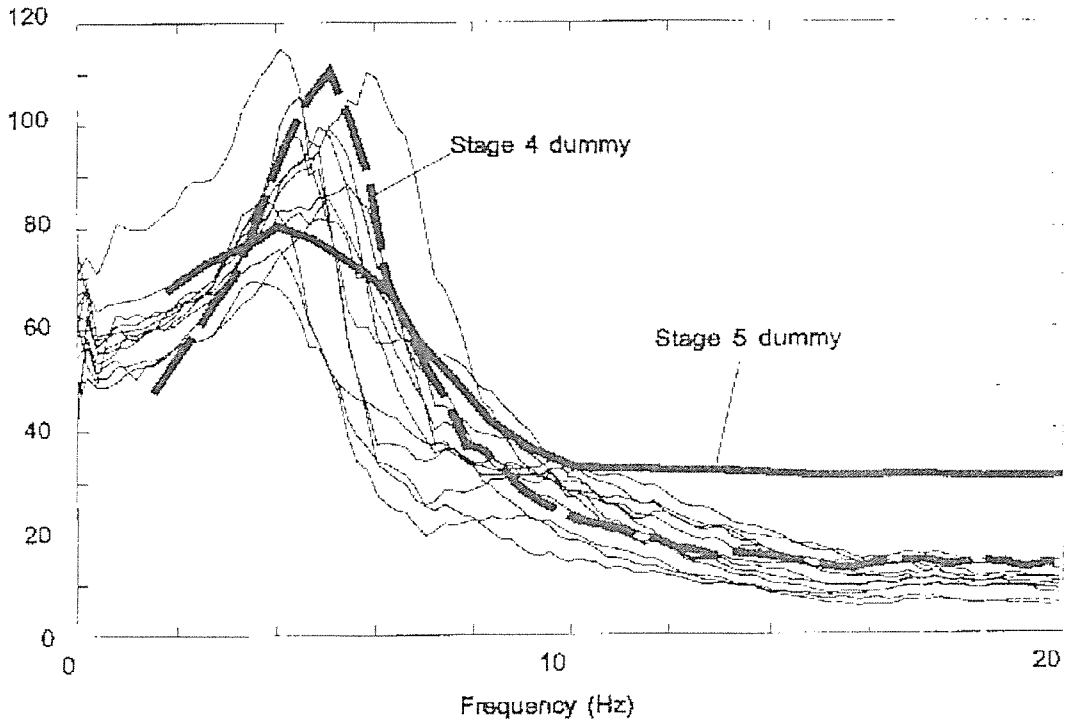

Figure 2.48 Apparent masses of two anthropodynamic dummies and 12 subjects measured at 1.0 m/s^2 rms. (from Mansfield 1998)

The measured transmissibilities of seats for six cars and six different subjects over a normal road are compared with measured transmissibilities obtained with the anthropodynamic dummy in Figure 2.49. These data showed that the variability in the results using the dummy was smaller than the inter-subject variability. It can also be concluded that the transmissibility of a car seat measured using an anthropodynamic dummy was closer to that obtained using a subject than that achieved using a rigid mass.

Although anthropodynamic dummies, based on a mass-spring-damper system, have been proposed for testing seats, some performance limitations due to non-linear phenomena such as friction impede their use in seat transmissibility measurement. Lewis (1998) investigated the factors that are likely to limit dynamic performance in tests of the vertical vibration isolation of vehicle seats. Figure 2.50 showed that the magnitude of the apparent mass was affected markedly by the vibration magnitude at most frequencies

between 1 Hz and 20 Hz. At lower magnitudes of vibration the response was increasingly influenced by friction. It can be seen that there is a lower apparent mass in the region of the resonance frequency and higher apparent mass at frequencies above 6 Hz with lower vibration magnitudes. It is clear that most of the friction in the mechanism could be attributed to the damper, even though the damper used had been specially designed to minimise friction.

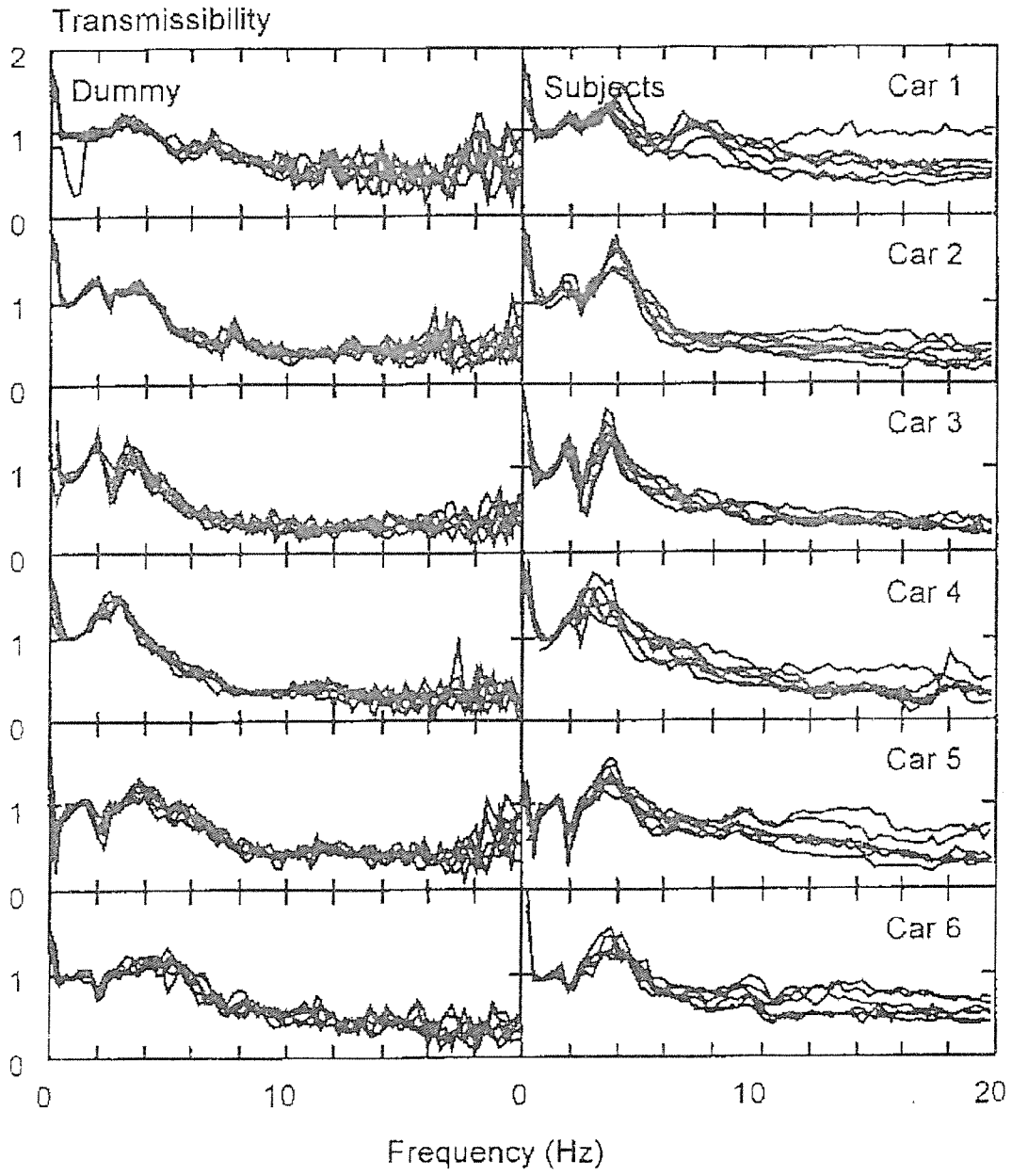

Figure 2.49 Transmissibilities of six car seats measured using a dummy and six people (from Mansfield 1998).

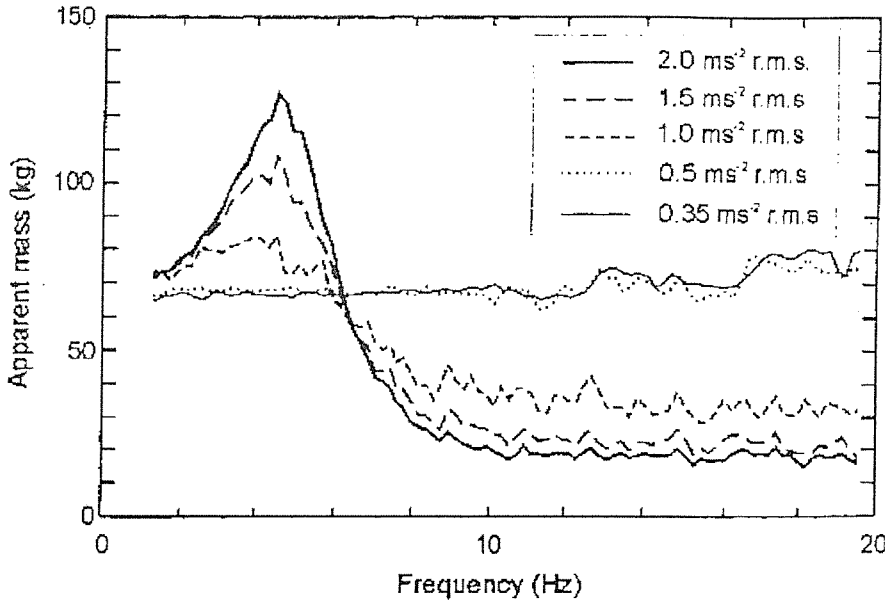

Figure 2.50 Apparent mass of prototype dummy with conventional oil-filled damper measured at five vibration magnitudes (from Lewis 1998).

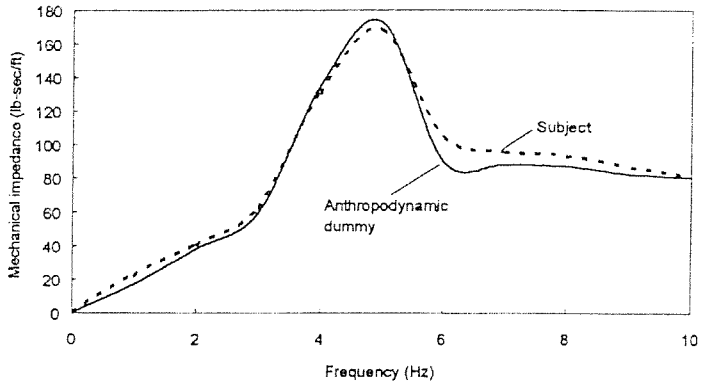

Figure 2.51 Mechanical impedance of the dummy and mean of 11 people, from Suggs *et al.* 1969.

A more complicated two degree-of-freedom dummy was developed by Suggs *et al.* (1969) consisting of coil springs and adjustable rotational dampers as shown in Figure 2.27. The two sub-systems had resonance frequencies of 4.5 and 5.5 Hz. Measured impedance showed a close agreement to the measurements made with 11 human subjects in the frequency range of 1.5 to 10 Hz (Figure 2.51). The measurements were made on a typical tractor seat. It was shown that there were slight differences of the seat transmissibility at resonance around about 4 Hz and significant differences at frequencies over 6 Hz between the subjects and the simulator.

2.5.6 Prediction method

Fairley and Griffin (1986) showed that it was possible to make predictions of the transmissibility of a vehicle seat. They measured the impedance of a seat using an indentor (Figure 2.52). The indenter, had the shape of a SIT-BAR (Whitham and Griffin 1977) which could be screwed up and down until the required force on the seat was reached and then locked in position. This was to simulate the static force experienced by the seat when loaded with a human subject. An Entran piezoresistive accelerometer was mounted on the vibration platform beneath the seat. The force on the indenter and the acceleration at the base of the seat were measured during random vibration produced by the electrodynamic vibrator. The surface of the seat did not move due to the rigid indentor.

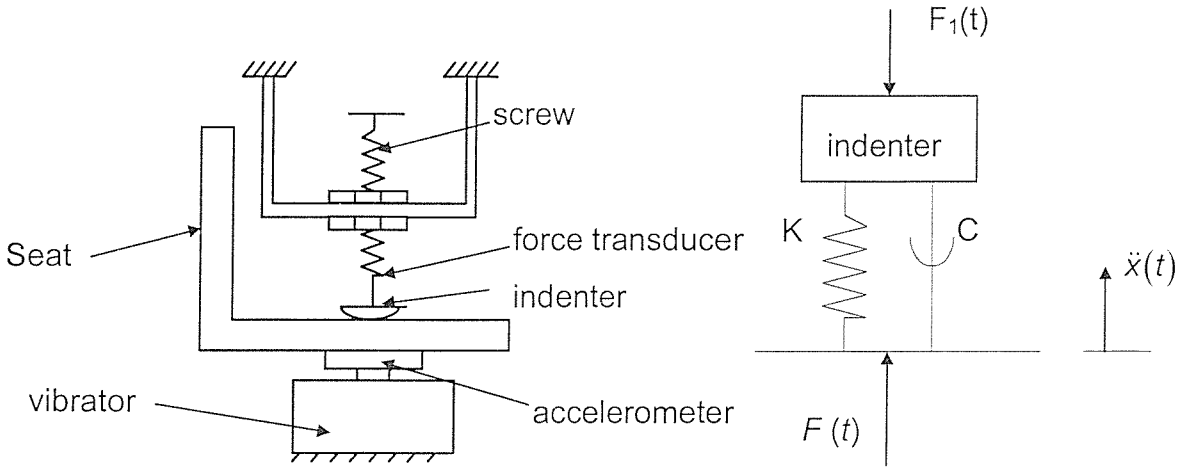

Figure 2.52 Using indenter to test a seat

Using the indenter to load the seat, the response of seat and foam system is given by:

$$F_1(t) = c\dot{x} + kx$$

where x is the displacement $\dot{x}$ is the velocity and $F_1(t)$ is the force measured by the indenter. From this equation the complex ratio of force to displacement is given by:

$$S(\omega) = \frac{F(\omega i)}{x(\omega i)} = k + c\omega i$$

The ratio of the force to the displacement, $S(\omega)$, is called the dynamic stiffness, a complex quantity. Dynamic stiffness was used in preference to the mechanical impedance, the ratio of the force to the velocity, because by using the dynamic stiffness the equivalent stiffness k, and the equivalent damping c, are more easily seen.

Fairley and Griffin (1986) measured the transmissibilities of one seat with eight subjects and eight seats with one subject. The input vibration had a flat spectrum and an acceleration magnitude of 1.0 ms^{-2} rms. The seat backrests were used and the subjects were in lumbar back contact with the seat. They measured the apparent masses of eight subjects in the same vibration environment. The dynamic stiffness of each seat was also measured with the rigid indenter. A pre-load of 600N was used and it was assumed to be equivalent to the static weight of the person on each seat. The dynamic stiffness of each seat and the apparent mass of the person measured on the hard seat were used to predict the seat transmissibilities. The measured and predicted seat transmissibilities are compared in Figures 2.53 and 2.54. The predicted transmissibilities had a good agreement with measurements for some of the subjects and some of the seats but not for all people and all seats. It was concluded that the prediction method is useful but needed further study to verify the method.

2.5.7 Conclusion

In general, human subjects are used in seat test procedures to determine the transmission of vibration through seats. However, there is a drawback using this method that is that the test results may vary between subjects because of the effect of subject variability.

Many researchers attempted to use a rigid mass to replace real subjects, but they could not obtain a good agreement between the seat test results by using the human body and a rigid mass.

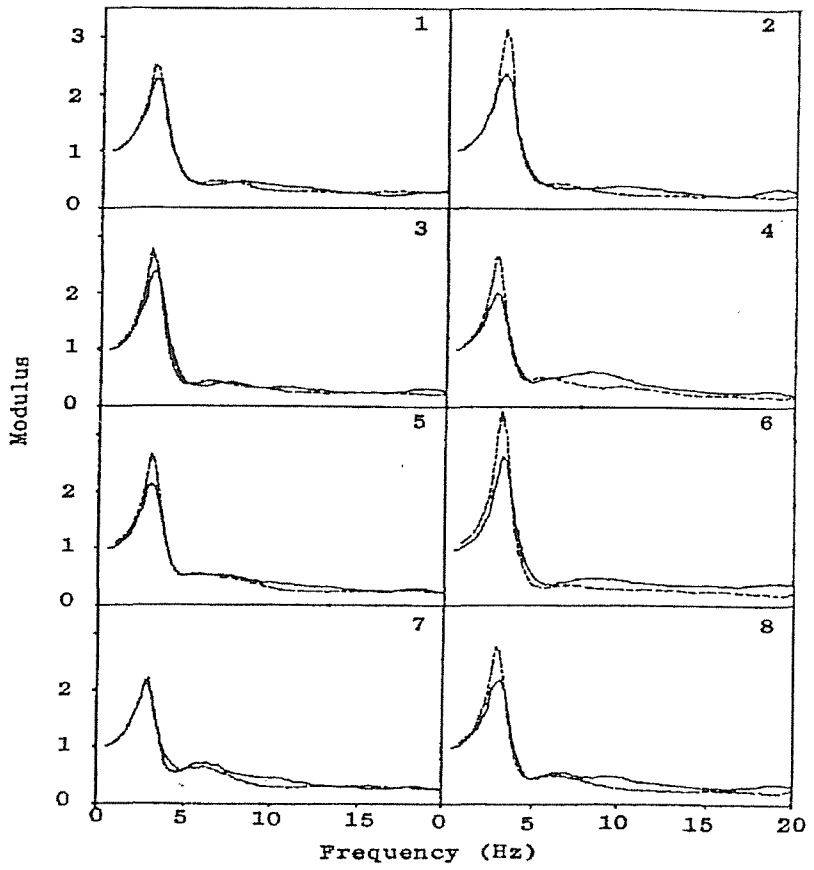

Figure 2.53 Comparison of measured (solid lines) and predicted (dashed lines) transmissibilities of a seat for eight different people, From Fairley 1986.

The use of an anthropodynamic dummies was proposed by Matthews (1967) and Suggs (1969), and was continued by Mansfield (1998), but dummies are not in general use, even though they may sometimes give transmissibility measurements similar to those obtained using human subjects over a limited frequency range. There could be difficulties in maintaining the response of such systems in calibration and it may not be easy to restrain a dummy to the correct position in a seat.

Prediction methods show a good agreement between measured and predicted seat transmissibilities for some subjects and some seats. A further study is needed before this method can be recognised.

2.6 CONCLUSION

The driving-point mechanical impedance and the apparent mass are useful tools to reveal the human body dynamic characteristics. It has been shown

that the response of the seated body in the vertical direction has a main resonance frequency in the frequency range from 4 to 6 Hz. Some researchers have found a second resonance of the body in the frequency range from 7 to 12 Hz.

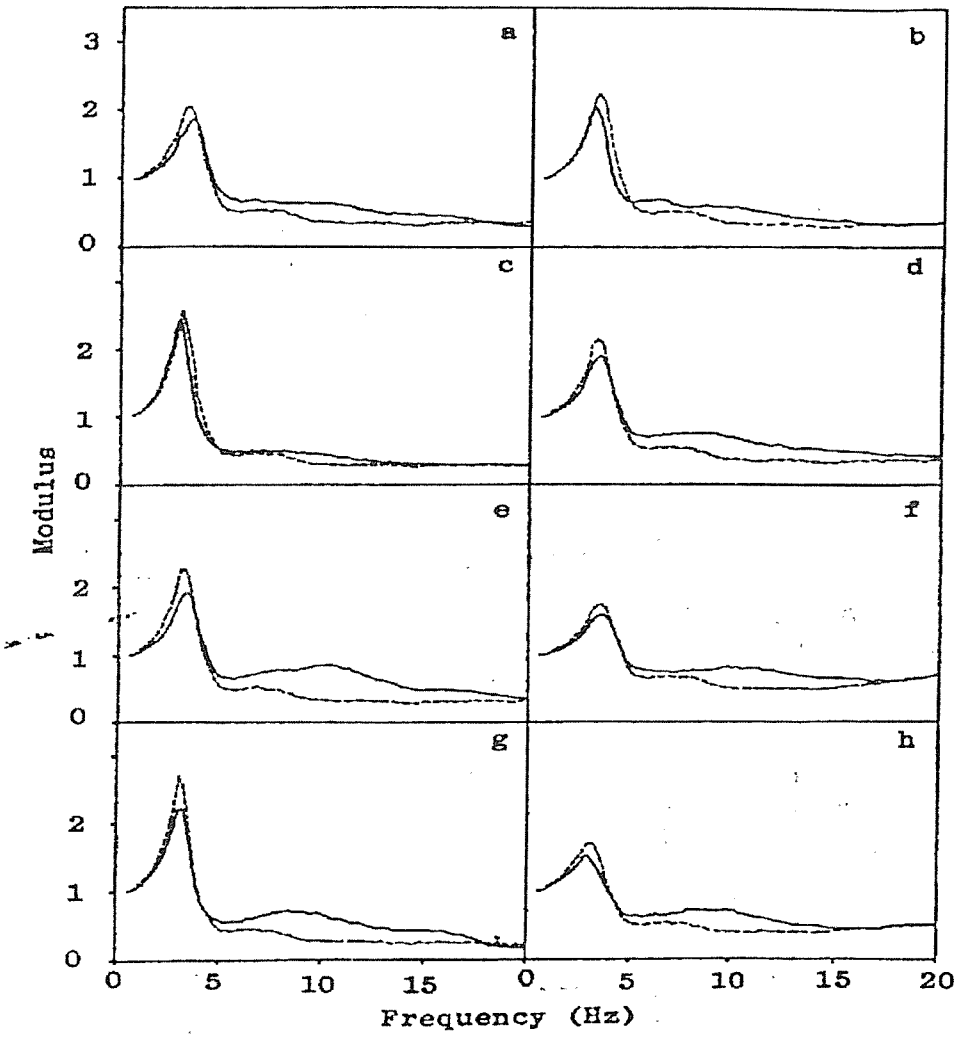

Figure 2.54 Comparison of measured (solid lines) and predicted (dashed lines) transmissibilities for eight different seats and one subject, From Fairley 1986.

International Standard ISO 5982 (1981), defines a two degree-of-freedom lumped-parameter model, but a one degree-of-freedom model would appear to suffice. The standard is based on limited data and appears to be mostly applicable to the people whose legs are hanging free (see Section 2.4.2).

Data show that the apparent mass of the body can change within a person due to subject variability, such as changes in posture, backrest, footrest,

subject weight and gender. Subject posture and seat backrest are two factors which affect the response of the body significantly. External restraints, for example the seat pan, armrest and seat belts or harness also affect the experimental results. Although the effects of external restraints are small, attention to these factors are still needed in experiments to make the results repeatable. A change of vibration magnitude causes a non-linear response of the human body.

Various seat-person interface devices have been used to measure seat transmissibilities. Some of them have been shown to make an appropriate measure of the vibration input to the body and to not affect the way the seat transmits vibration. Transmissibility resonance frequencies of conventional seats are in the frequency range from 3 to 6 Hz and the resonance frequencies for suspension seats are usually 1 to 3 Hz.

There are many factors affecting the seat transmissibility, but the important factors are the same factors that have significant effects on human body apparent mass and mechanical impedance.

Biodynamic models of human response to vibration are useful and have several applications. Most models are specifically designed for one application and so many models have been developed. Models representing the driving point mechanical impedance or apparent mass generally have one or two degree-of-freedom, because this is sufficient to give a good agreement with the measured response of the body. Non-linear models should be developed to represent the non-linear properties of the sitting person.

The seated human body cannot be replaced by a rigid mass while measuring seat transmissibility. An alternative method using a dummy to replace people has been investigated. Non-linearities in the responses of the dummies and their failure to reproduce the non-linearities in the response of the human body currently make them a doubtful means for directly determining seat transmissibility.

Methods of predicting seat transmissibility are needed because they avoid using human subjects in seat tests. However, further investigation and study is needed before a prediction method can be defined for general use.

CHAPTER 3

EXPERIMENTAL APPARATUS AND DATA ANALYSIS

3.1 Introduction

There are many experiments that have been conducted in this research. The laboratory studies were carried out in the laboratories of the Human Factors Research Unit (HFRU), the Institute of Sound and Vibration Research (ISVR), the University of Southampton. The experiments were carried out using similar apparatus. This chapter describes the equipment used in the experiments, such as the vibrators and transducers. Data analysis methods for testing data, including statistical and signal processing techniques, are also described in this chapter.

3.2 Apparatus

3.2.1 Transducers

A variety of accelerometers, force transducers and displacement transducers were utilised in this research. They will be described separately.

3.2.1.1 Accelerometers

The motions of seat base and seat surface were measured in the laboratory and field using a variety of transducers such as Entran EGCSY-240D-10, Entran EGCS-DO*-10 and Endevco 2265-20. The Entran EGCSY-240D-10 had a sensitivity of approximately 13 mv/g with an operating range of ±10 g. The Entran EGCS-DO*-10 had a sensitivity of approximately 10 mv/g with an operating range of ±10g. The sensitivity of the Endevco 2265-20 was around 32 mV/g and its operating range was about ±20 g.

Measurements of acceleration at seat surfaces were made using SAE pads containing three mutually perpendicular Entran EGCS-DO*-10V

accelerometers. The SAE pads met the specification set out in ISO 10326-1 (1992).

Accelerometers were calibrated before each experiment and checked during and after experiments. Calibration was carried out according to ISO 5347 (1993) for the transducers which all had a response at zero frequency.

3.2.1.2 Force transducer

A Kistler 9821B force platform made from four matched quartz piezo-electric force cells mounted at the corners of a rectangular welded steel frame was used to measure the driving force whilst testing subjects. An aluminium alloy plate, 0.6m long, 0.4m wide and 0.02m thick was bolted on the pre-loaded force transducers. The weight of the plate was approximately 16kg. The force corresponding to this mass was subtracted when calculating the measured apparent mass or calibrating with a standard mass. The signals from each vertical force cell were summed to provide a single signal and were amplified using a Kistler KIAG5001 charge amplifier. The lowest resonance frequency of the force platform was 320 Hz in the vertical direction.

The force platform was calibrated statically and checked dynamically. Static calibration was carried out by placing and removing a rigid mass from the surface of the platform.

In order to calibrate the dynamic load, the measuring system was checked by measuring the apparent mass of the platform using random vibration in three conditions: no load, load 1 and load 2. As the system should be rigid, the modulus of the apparent mass of the platform should not be frequency dependent. If any frequency dependency was observed it would indicate that the system was not mounted rigidly. The apparent mass for the no load condition indicated the mass of the top plate on the force transducer. It should be 16 kg. The apparent masses measured using load 1 and load 2 were equal to the mass of each load plus the mass of the top plate of the force transducer.

A Kistler 9321 force cell was used to measure the driving force whilst testing the seat using the indenter. The sensitivity of the force cell was approximately ±4.0 pc/N with a temperature range – 40^0 to 120^0. The measuring range was ±10,000N. The signal from the force transducer was amplified using a Kistler KIAG 5000 charge amplifier. There was also a static and dynamic calibration for this force cell. The method of its calibration was similar to the calibration of the Kistler 9821B force platform.

3.2.1.3 Displacement transducers

Motion of the vibrator platforms can also be measured using a variety of LVDT displacement transducers such as DC-LVDV D2/200A and DC-LVDV D2/3000. The DC-LVDV D2/200A had a sensitivity of approximately 0.16 v/mm with an operating range of ±10 mm and DC-LVDV D2/3000 had a sensitivity of approximately 0.4 v/mm with an operating range of ±50 mm.

The seat force-deflection loop were also measured using DC-LVDV D2/3000, however DC-LVDV D2/3000 is not suitable to measure the motion over 20 Hz. For dynamic experiments, the DC-LVDV D2/200A was used.

3.2.2 Vibrators

Two kinds of shaker were used during experimental work. They were all situated in the laboratories of the Human Factors Research Unit, Institute of Sound and Vibration Research, University of Southampton.

3.2.2.1 Electro-magnetic vibrator

A Derritron VP85 was used to measure seat dynamic properties and seat transmissibilities. The VP85 electro-magnetic shaker was powered by a 1 kW Derritron amplifier. The vibrator had a 25.4 mm (1 inch) peak to peak displacement and could be used in a frequency range from 1.5 to 3700 Hz. The maximum force produced by the shaker was 3.3 kN and the maximum acceleration was 45g. The vibrator was mounted in a rigid frame (called trunion) which allowed it to be fixed at any angle between vertical and horizontal. The trunion-mounted vibrator could also be fixed to an experimental rig for indenter tests. It was used vertically in this research.

Mechanical and electrical stops were fitted to the vibrator. Emergency stop buttons were also accessible to the experimenter adjacent to the vibrator.

3.2.2.2 Electro-hydraulic vibrator

An electro-hydraulic vibrator was used in many experiments. The vibrator consisted of an actuator which was capable of producing a vertical displacement of up to 1 metre, a vibration table, electronic control panel and hydraulic power supply. The vibrator could be operated in the frequency range between 0.05 to 50 Hz with the acceleration waveform distortion specified as below 5%. A flat aluminium plate with dimensions of 1.50 by 0.90 metres was fixed to the vibration table, which can provide enough space to arrange experimental equipment. The vibrator had a capability of producing a dynamic force of up to 10 kN and a static force of up to 8.8 kN.

The vibrator's performance was in accordance with BS 7085 (1989) (Guide to safety aspects of experiments in which people are exposed to mechanical vibration and shock). Specific safety measures were incorporated into the hydraulic, mechanical and electrical parts of the system. Emergency stop buttons were situated within reach of the experimenter and subject at all times.

3.2.3 Data acquisition system

The *HVLab* data acquisition system and signal generation system, was developed at HFRU, ISVR, the University of Southampton. The *HVLab* system can acquire up to 16 channels of time-varying analogue signals generated from accelerometers, force transducers and displacement transducers whilst simultaneously outputting up to 2 channels of analogue signals to vibrators, Data acquisition uses a 12-bit Advantech PCLabs PCL-818 card. The number of output and input channels, sampling rate and duration can all be controlled by the *HVLab* software. An Onsite Instruments Techfilter TF-16 anti-aliasing card was used in the systems as a low pass filter giving -70 dB/octave attenuation at the software controlled cut-off frequency. The *HVLab* system was used both in the laboratory and field studies.

The *HVLab* system including software and hardware which contains the data acquisition and anti-aliasing cards running on a personal computer. The external signal amplification and conditioning box are used to connect the transducers and the PC which has *HVLab* system. Figure 3.1.shows the whole arrangement for *HVLab* measure system.

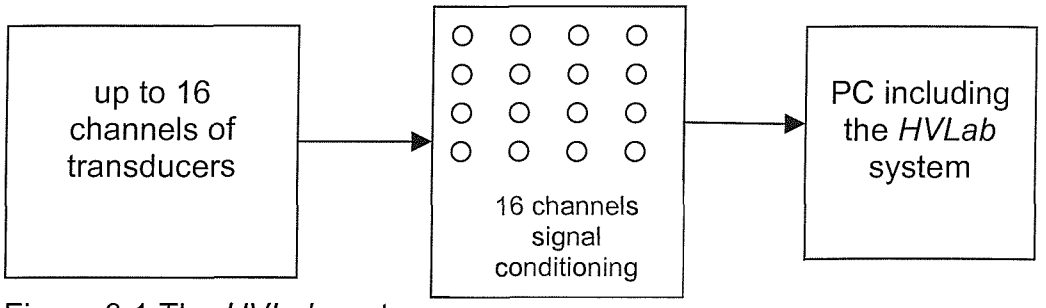

Figure 3.1 The *HVLab* system

Either a.c. or d.c. transducer calibration is allowed in the *HVLab* system. For example, with a piezoresistive accelerometer, the d.c. calibration procedure is appropriate, using the acceleration due to gravity to give signals corresponding to ±1g (±9.81 m/s^2) when the transducer is turned over. With a piezoelectric accelerometer, however, which will not respond at very low frequencies, it is necessary to perform a.c. calibration using a sinusoidal vibration excitation of known r.m.s. acceleration magnitude. The F2 key may be used to switch the system between the a.c. and d.c. calibration modes.

The maximum sample rate of the *HVLab* system for one channel was approximately 62,000 samples/second. If the channels increased up to 16, the rate reduced to 3,750 samples/second for signal acquisition. The maximum samples per channel of the *HVLab* system depend on the sample rate, computer basic memory and sampling duration.

3.3 Experimental data analysis

Experimental data analysis can be executed using *HVLab* software. The time history of experimental data is easily exported to ASCII format which can be used by other software. Some methods of data analysis such as: PSD (power spectral density), CSD (cross-spectral density), transfer function, coherency and frequency weighting filter etc. are possible in the *HVLab* system. The

frequency resolution, the frequency intervals in the spectrum, is easily selected. MATLAB software has similar functions, however the graph functions of the *HVLab* system are more powerful, for example, using *HVLab* system can merge many figures in one figure.

3.3.1 Frequency response functions

Frequency response is that the output signal from a system expressed as a function of the frequency of the input signal. Frequency response functions are useful to analyse the dynamic system over a frequency range.

3.3.1.1 Seat transmissibility

The transmissibility of a seat is the frequency response function for vibration transmitted from the base of the seat to the person sitting on the seat.

The transmissibility of the seat, T(f), is defined as the ratio of the cross-spectral density, G_{io} (f), (CSD) between the acceleration at the input and output point to the power spectral density, G_{ii} (f), measured at the floor (the input):

$$T(f) = \frac{G_{io}(f)}{G_{ii}(f)} = \mathrm{Re}[T(f)] + \mathrm{Im}[T(f)]j$$

where T(f) is the seat transmissibility, G_{io},(f) is the cross spectrum between the input and the output, G_{ii} (f) is the power spectrum at the floor, Re[T(f)] and Im[T(f)] are the real and imaginary parts of the complex transfer function.

Because T(f) is a complex quantity, the modulus |H(f)|, and the phase, θ(f), of the transfer function can be generated by:

$$|T(f)| = \left\{[\mathrm{Re}(T(f))]^2 + [\mathrm{Im}(T(f))]^2\right\}^{1/2}$$

$$\theta(f) = \tan^{-1}\frac{\mathrm{Im}[T(f)]}{\mathrm{Re}[T(f)]}$$

These calculations are useful for determining the system transfer function. However, they are not sufficient to give a relationship between the input and output signals. For example, assuming two irrelevant signals obtained from experiment, what is the meaning the transfer function calculating from these signals? To assist the explanation of the transfer function, the coherency between the signals is needed. The coherency function can be calculated by:

$$\gamma_{io}^2(f) = \frac{|G_{io}(f)|^2}{G_{ii}(f) * G_{oo}(f)}$$

Where $G_{oo}(f)$ is the power spectral density at the seat surface.

The value of coherence $\gamma_{io}^2(f)$ is always in the range 0-1. For a linear system and no noise, the coherence will have its maximum value of unity at all frequencies. If the system has not a good signal-noise ratio, that is the noise occupied a large proportion of the measured signal, the value of coherence $\gamma_{io}^2(f)$ will be lower than unity. If the measured data at the output is not linearly related to the input, then the coherence will be less than unity. It is possible for the output data not to be linearly related to the input if the system is non-linear or if there is a low signal-to-noise ratio in one or both of the signals at any frequency. A coherence of zero would indicate that the output signal was not correlated to the input signal.

3.3.1.2 Apparent mass

The apparent mass is a driving point frequency response function. The apparent mass of the subject, M(f), is defined as the ratio of the cross-spectral density, $G_{af}(f)$, between the acceleration as the input and force as the output signal to the acceleration power spectral density, $G_{aa}(f)$, measured at the input.

$$M(f) = \frac{G_{af}(f)}{G_{aa}(f)}$$

The apparent mass of the subject differs from that of a rigid mass because the subject is a multi-degree-of-freedom system that has a retroaction on the base

motion. If an apparent mass is measured for a rigid mass, the result equals the mass of the rigid mass. Therefore, when the apparent mass of a subject is measured using the force platform, the weight of the force platform should be subtracted from the calculated result.

The measured apparent mass of a subject is a curve over a frequency range. However it must equal to the subject weight at zero frequency. The apparent mass at the lowest frequency can represent approximately weight of the subject.

The apparent masses of subjects vary a lot because of variations between the weights of the subjects. Hence, the normalised apparent masses are often used in analysis of the apparent masses. The normalised apparent mass is defined as the ratio between the measured apparent mass and the apparent mass at the lowest frequency. The normalised apparent masses assists the comparison of apparent masses across subjects.

3.3.1.3 Seat dynamic properties

Seat dynamic properties may be determined using a rigid mass. The advantage of using rigid mass to measure seat dynamic property is that it can provide repeatable experimental results. A variety of rigid masses can be used in determining seat dynamic responses such as a sand bag, shaped rigid mass (bottom shape) and square rigid mass.

A seat with a rigid mass system is shown in Figure 3.2. The seat transmissibility is defined as:

$$T(f) = \frac{A_{io}(f)}{A_{ii}(f)}$$

where $A_{ii}(f)$ is the power spectral density of the acceleration at the seat base and $A_{io}(f)$ is the cross power spectral density between the acceleration at the input and output point at the seat surface.

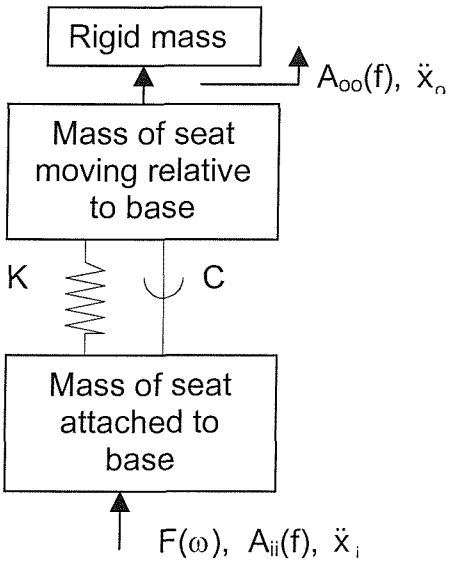

Figure 3.2 A seat and rigid mass dynamic system

If the mass of the seat moving relative to the base is neglected, the seat to rigid mass system equation of motion is:

$$m\ddot{x}_o + c(\dot{x}_o - \dot{x}_i) + k(x_o - x_i) = 0$$

Where $\ddot{x}_o$ is the acceleration measured at seat surface and $\ddot{x}_i$ is the acceleration measured at seat base.

Invoking the Laplace transform, the seat to rigid mass system transmissibility in the frequency domain becomes:

$$T(f) = \frac{A_{io}(f)}{A_{ii}(f)} = \frac{k + c\omega i}{k - m\omega^2 + c\omega i}$$

The seat stiffness, k, and damping, c, can be determined by curve fitting from the seat and rigid mass transmissibility.

Another method to obtain seat stiffness and damping is to use an indenter test procedure. Figure 3.3 shows how to use an indenter to measure seat dynamic properties.

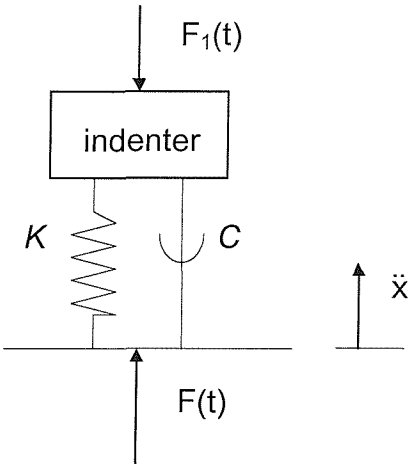

Figure 3.3 Using an indenter to load the seat.

When using an indenter to load a seat, the response of the seat and foam system is given by:

$$F_1(t) = c\dot{x} + kx$$

where x is the displacement (it can be obtained from acceleration by double integration or from measurements by a displacement transducer), $\dot{x}$ is the velocity and $F_1(t)$ is the force measured by the indenter. From this equation the complex ratio of force to displacement is given by:

$$S(\omega) = \frac{F_1(\omega i)}{x(\omega i)} = k + c\omega i$$

The ratio of the force to the displacement, $S(\omega)$, is called the dynamic stiffness, a complex quantity. Dynamic stiffness was used in preference to the mechanical impedance, the ratio of the force to the velocity, because by using the dynamic stiffness the equivalent stiffness k, and the equivalent damping c, are more easily seen. They are just the real part and the imaginary part of the seat dynamic stiffness.

3.3.2 Statistical functions

Statistics helps us draw inferences about populations based on observations obtained from random samples, or samples in which the characteristics and relationship of interest are independent of the probabilities of being included in the samples. Non-parametric statistical tests are used in this study, as it was not assumed that data sets had a normal distribution. An advantage of non-

parametric statistical methods over parametric methods is also that they are generally very easy to understand. A knowledge of only the most elementary mathematics is all that is necessary to gain a relatively full understanding of most non-parametric statistical techniques. Non-parametric statistical tests make relatively few assumptions about the nature of the population distribution, and so they are widely applicable. SPSS statistical analysis software (version 6.1) was used to calculate statistical functions.

3.3.2.1 Friedman two-way analysis of variance

Friedman two-way analysis of variance is a non-parametric statistical method. When the data from k matched samples are in at least an ordinal scale, the Friedman two-way analysis of variance by ranks is useful for testing the null hypothesis that k samples have been drawn from the same population.

Since the k samples are matched, the number of cases is the same in each of the samples. The matching may be achieved by studying the same group of subjects under each of k conditions. For example, whether or not the seat stiffness differs at several vibration magnitudes can be tested by the Friedman two-way analysis of variance.

Table 3.1 Example seat stiffness data for Friedman two-way analysis of variance.

Seat	Vibration magnitudes (m/s^2)			
	0.5	1.0	1.5	2.0
1	75105	71754	68267	65370
2	64299	61263	58970	56703
3	53905	53315	52218	50065
4	50530	51315	50657	48739

For the Friedman test, the data are cast in a two-way table having N rows and k columns. The rows represent the various subjects or matched sets of subjects, and the columns represent the various conditions.

Table 3.1 lists the stiffnesses of four seats measured at four vibration magnitudes. Here k=4 and N=4. To perform the Friedman test on these data, the first process is to rank the scores in each row. We may give the lowest score in each row the rank of 1, the next lowest score in each row the rank of 2, etc. The scores in each row are then ranked separately in a range from 1 to 4. The ranks of the stiffness for each subject are shown in Table 3.2. It can be observed that the ranks in each row of Table 3.2 range from 1 to k=4.

If the stiffnesses of the seats were independent of the vibration magnitudes, the set of ranks in each column would represent a random sample from the discontinued rectangular distribution of 1, 2, 3 and 4, and the rank totals for the various columns would be about equal. If the stiffnesses of the seats were dependent on the vibration magnitudes (i.e., if the null hypothesis that all the samples – columns - came from the same population, H_0, were false), then the rank totals would vary from one column to another.

The Friedman test determines whether the sum of the ranks (R_j) differ significantly. This is done by calculating a statistic, F_r using (Siegel and Castellan, 1988):

$$F_r = \frac{12}{Nk(k+1)} \sum_{j=1}^{k} (R_j)^2 - 3N(k+1)$$

where: N is the number of rows

k is the number of columns

R_j is the sum of the ranks in jth condition

$\sum_{j=1}^{k}$ sum s of ranks over all k conditions

Table 3.2 Ranks of the seat stiffness under 4 vibration magnitures

Seat	Vibration magnitudes (m/s^2)			
	0.5	1. 0	1.5	2.0
1	4	3	2	1
2	4	3	2	1
3	4	3	2	1
4	2	4	3	1
R_j	14	13	9	4

For the example, the value of F_r is 9.3. Probabilities associated with various values of F_r, have previously been calculated and tabulated for various samples and various numbers of variables (Siegel and Castellan 1988). The probability associated with F_r =9.3 when N=4, k=4 is p=0.012 (i.e., p<0.05). With these data, therefore, the null hypothesis that the stiffnesses of the seats were dependent on the vibration magnitudes (i.e., the four samples – columns - were drawn from the same population) could be rejected at the 0.012 level of significance.

3.3.2.2 Wilcoxon matched-pairs signed ranks test

The Wilcoxon matched-pairs signed ranks test was useful to make the judgement of "greater than" between any pair of two performances and make the judgement between any two difference scores arising from any two pairs. This is also a non-parametric test which tests the null hypothesis that the distributions of the two variables are the same. For example, we can use the Wilcoxon matched-pairs signed ranks test to determine if there are differences between the measured and predicted modulus of the seat transmissibility at one frequency for different subjects. The experimental data and predicted data at one frequency are shown in Table 3.3.

Table 3.3 Moduli of measured and predicted transmissibility at one frequency

Subject	Measured seat transmissibility	Predicted seat transmissibility	Difference	Rank of difference
1	87.2	84.3	2.9	7
2	65.8	63.9	1.9	5
3	72.5	71.3	1.2	2
4	83.2	81.8	1.4	3
5	92.1	90.4	1.7	4
6	100.6	96.4	4.2	8
7	64.8	64.1	0.7	1
8	85.7	82.9	2.8	6

Using the Wilcoxon matched-pairs signed ranks test to compare the seat transmissibility in two conditions for N=8 subjects, the null hypothesis is that the change between the methods to obtain seat transmissibility has no effect on the moduli of the seat transmissibility. If this is true, it would be expected that the sum of those ranks having positive values is approximately equal to the sum of those ranks having negative values. For each of the subjects, the difference between the measured and predicted seat transmissibility at one frequency is obtained and listed in Table 3.3. The sum of those ranks having plus values (signs) is $T_+=36$, while the sum of those ranks having negative values (signs) is $T_-=0$.

For small samples (i.e., N<25), T= the smaller sum of like-signed ranks. That is, T is either the sum of the positive ranks or the sum of the negative ranks, whichever sum is smaller. Probabilities associated with various values of T have previously been calculated and tabulated for various samples and two variables (Siegel and Castellan 1956).

The probability associated with $T=T_-=0$ and N=8 is $p=0.01$ (i.e., $p<0.05$). With these data, therefore, the null hypothesis could be rejected.

3.3.2.3 Spearman rank-order correlation

The Spearman rank correlation coefficient statistic is a measure of association which requires that both variables be measured in at least an ordinal scale so that the objects or individuals under study may be ranked in two ordered series. This statistic is commonly used as a non-parametric measure of correlation between two ordinal variables. For all of the cases, the values of each of the variables are ranked from smallest to largest, and the Spearman rank – order correlation coefficient is computed.

For example, the stiffnesses of one seat measured at one pre-load, one vibration magnitude and five different indenter areas are showed in Table 3.4. The null hypothesis for this example was that the stiffness measured at one static force and one vibration magnitude and five different indenter areas is independent of indenter contact area (i.e., there is not a correlation between the indenter head area and the foam stiffness).

The Spearman rank-order correlation coefficient, r_s, can be calculated using (Siegel and Castellan, 1988):

$$r_s = 1 - \frac{6\sum_{i=1}^{N} d_i^2}{N^3 - N}, \quad d_i = X_i - Y_i$$

Where X_i is the value of the ranks of the measured seat stiffnesses and Y_i is the value of the ranks of the indenter areas. They are shown in Table 3.5. To test whether the ranks are different, the differences, d_i, for each pair of ranks are calculated.

Table 3.4 Example the Spearman rank-order correlation test

Indenter head	Measured seat stiffness	Indenter areas cm^2
Disk 15	68267	176
Disk 20	52684	314
Disk 25	85063	490
SIT-BAR	48454	280
Buttocks	65280	540

Table 3.5 Ranks of stiffnesses and indenter areas

Indenter head	Measured seat stiffness	Indenter areas cm^2	Stiffness rank	Indenter area rank
Disk 15	68267	176	4	1
Disk 20	52684	314	2	3
Disk 25	85063	490	5	4
SIT-BAR	48454	280	1	2
Buttocks	65280	540	3	5

A problem occurs where the difference, d_i, is equal to zero. If the proportion of the ties compared to the non-tied data is small, then the effect is negligible.

Calculating the Spearman rank coefficient for the example data gives a value of r_s of 0.2. Probabilities associated with various values of r_s have previously been calculated and tabulated for various samples and two variables (Siegel and Castellan 1956). Therefore, the probabilities associated with the value of r_s =0.2 for 5 indenter areas is 0.74>0.05, the decision is in favour of the null hypothesis (i.e., there is not a correlation between the indenter head area and the foam stiffness).

3.3.2.4 Mann-Whitney U test

The Mann-Whitney U test may be used to test whether two independent groups have been drawn from the same population. It is the most popular of the two-independent-samples tests. It is equivalent to the Wilcoxon matched – pairs signed ranks test and the Kruskal-Wallis test for two groups. The Mann-Whitney statistic tests whether two sampled populations are equivalent. The observations from both groups are combined and ranked, with the average rank assigned in the case of ties. The number of ties should be small relative to the total number of observations. If the populations are identical in location, the ranks should be randomly mixed between the two samples. The number of times a score from group 1 precedes a score from group 2 and the number of times a score from group 2 precedes a score from group 1 are calculated. The Mann-Whitney U statistic is the smaller of these two numbers.

For example, we have different aged subjects from two groups to join experiments. They are male group A and female group B. The null hypothesis is that the subject ages of the group A and B have the same distribution or there are no differences in the subject age between the two groups. Table 3.6 shows the age of all subjects from two groups and the ranks of the age for each subject.

Table 3.6 Example for the Mann-Whitney U test

Subjects to attend experiments	Age of men	rank	Age of women	rank
1	26.00	20	24.00	15.5
2	16.00	1.5	56.00	45.5
3	39.00	33.5	22.00	9.5
4	38.00	30	45.00	39
5	34.00	27	55.00	44
6	33.00	26	52.00	43
7	29.00	23	25.00	18
8	25.00	18	23.00	12.5
9	45.00	39	40.00	36
10	51.00	42	23.00	12.5
11	16.00	1.5	17.00	4.5
12	27.00	21.5	35.00	28
13	56.00	45.5	25.00	18
14	17.00	4.5	39.00	33.5
15	69.00	48	21.00	7.5
16	27.00	21.5	38.00	30
17	39.00	33.5	24.00	15.5
18	39.00	33.5	31.00	24.5
19	50.00	41	59.00	47
20	45.00	39	21.00	7.5
21	17.00	4.5	41.00	37
22	23.00	12.5	38.00	30
23	23.00	12.5	22.00	9.5
24	17.00	4.5	31.00	24.5
		R_1=583.5		R_2=592.5

This is a large samples test because the numbers of $n_1=n_2=24>20$. The value of U, the statistics in the Mann-Whitney U test, and the value of z, the deviation of the observed value of U, can be calculated using:

$$U = n_1 n_2 + \frac{n_1(n_1+1)}{2} - R_2, \qquad z = \frac{U - \mu_u}{\sigma_u}$$

Where, μ_u is the population mean and σ_u is the standard deviation of the population. They are decided by:

$$\mu_u = \frac{n_1 n_2}{2}, \qquad \sigma_u = \sqrt{\frac{n_1 n_2 (n_1 + n_2 + 1)}{12}}$$

For this example, U=283.5 and z=-0.093. Probabilities associated with values as extreme as observed values of z in the normal distribution have been calculated and tabulated. Therefore, a two-tailed probability associated with the value of z = -0.093 under null hypothesis is *p*= 0.926, the decision is in favour of the null hypothesis.

CHAPTER 4 PRELIMINARY STUDY

4.1 Introduction

In a vehicle, a seat is a suspension system that can be designed to reduce the effects of the vehicle vibration on the occupant. The transmissibility of a seat is often used to evaluate seat performance or seat isolation efficiency. Therefore, an important thing for seat designers is to obtain reliable seat transmissibility. There are three main methods to obtain seat transmissibilities. They are measuring seat transmissibility using a subject, using a mechanical dummy or a rigid mass and predicting seat transmissibility through a mathematical model. As discussed in literature review, most researchers have used subjects to measure seat transmissibility in the laboratory and field, but it is time consuming work. Suggs *et al.* (1969), Matthews (1967) and Mansfield 1998 used a mechanical dummy to replace human subjects to obtain seat transmissibilities. As the results showed, there were some problems, such as dummy fixing and the influence of the backrest. Because there was no ideal method to obtain seat transmissibility, Fairley and Griffin (1986) put forward a new method to predict seat transmissibility. It was a seat transmissibility prediction method in which the seat transmissibility could be obtained directly using the measured seat impedance and the measured human body apparent mass. The problem for this method is that the subject response to vibration still needs to be measured. The aim of the study here is to further develop this method so that it can become a standard seat test method.

Previous studies have revealed that the transmissibility of a seat not only depends on the impedance of the seat but also depends on the impedance of the body supported on the seat. In the literature review, it has been discussed that there are many factors that affect seat transmissibility, such as the vehicle floor vibration spectrum, the seat response and the occupant response. Researchers have found that it was difficult to obtain repeatable seat experimental results because of the effect of the seat occupant. Even if the

same subject is adopted in an experiment, subject posture and subject physical conditions also affect experimental results.

Figure 4.1 shows seat transmissibilities measured in a car driven over eight different roads. The seat was mounted in a Ford Mondeo car and driven at different speeds. Although the subject kept the same posture on the seat, the differences of seat transmissibilities in different vibration environments are large.

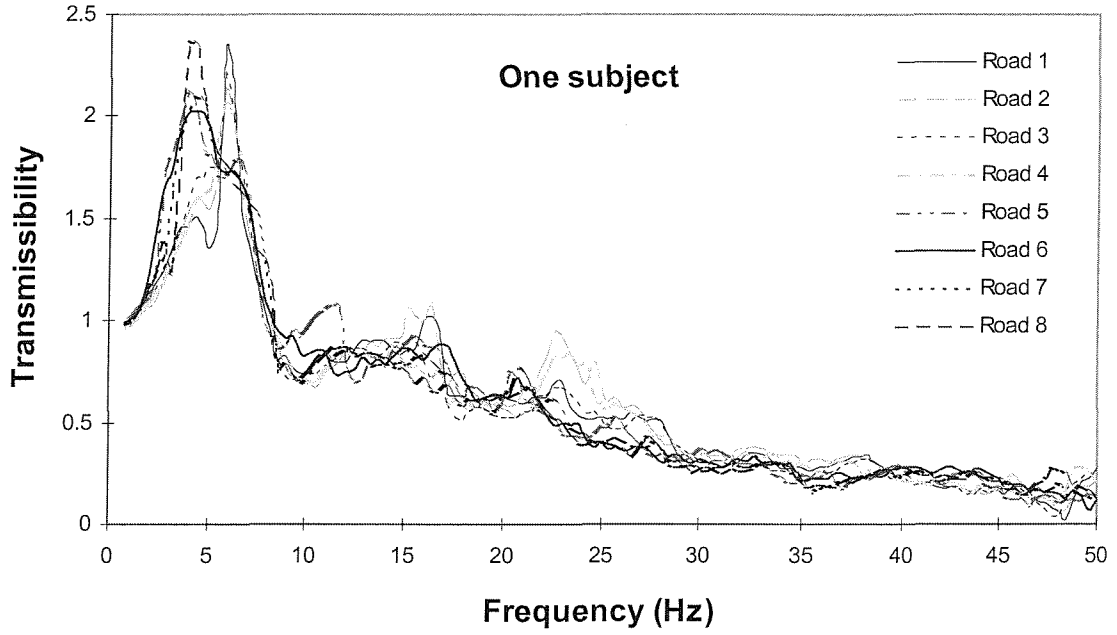

Figure 4.1 Ford Mondeo seat transmissibilities measured over eight different roads with the same person.

Figure 4.2 shows seat transmissibilities with the same passenger seat measured with six passengers on the same road. The seat was also mounted in a Ford Mondeo car and driven at the same speed. The experimental data show that there are big differences in seat transmissibilities when using different subjects.

As mentioned above, the seat transfer function may be determined using a rigid mass. Although many researchers have proved that the rigid mass cannot represent the real person, it is still a useful method to measure the seat response. The advantage of using a rigid mass is that it can provide

repeatable experimental results. A variety of rigid masses can be used to determine seat dynamic response such as a sand bag, a shaped rigid mass (bottom shape) and a square rigid mass.

The transmissibility of a seat supporting a rigid mass is sometimes measured in the laboratory and used to predict the ride in a vehicle. However, the seat-person system is complex: the vibration that is transmitted to a seated person depends upon the dynamic response of the person as well as the dynamic characteristics of the seat. Consequently, seat design cannot be optimised using solely the dynamic response of a seat loaded with a rigid mass.

Seat transmissibility variations are mainly caused by changes of dynamic characteristics of human subjects from person to person. Using either a rigid mass or a mechanical dummy as the load will avoid this problem, but fixing the mass or the dummy in the seat and to the backrest may cause problems. Furthermore, while such measurements may indicate the response of the seat-person system, they reveal little about the underlying dynamic response of the seat which is the subject of the design.

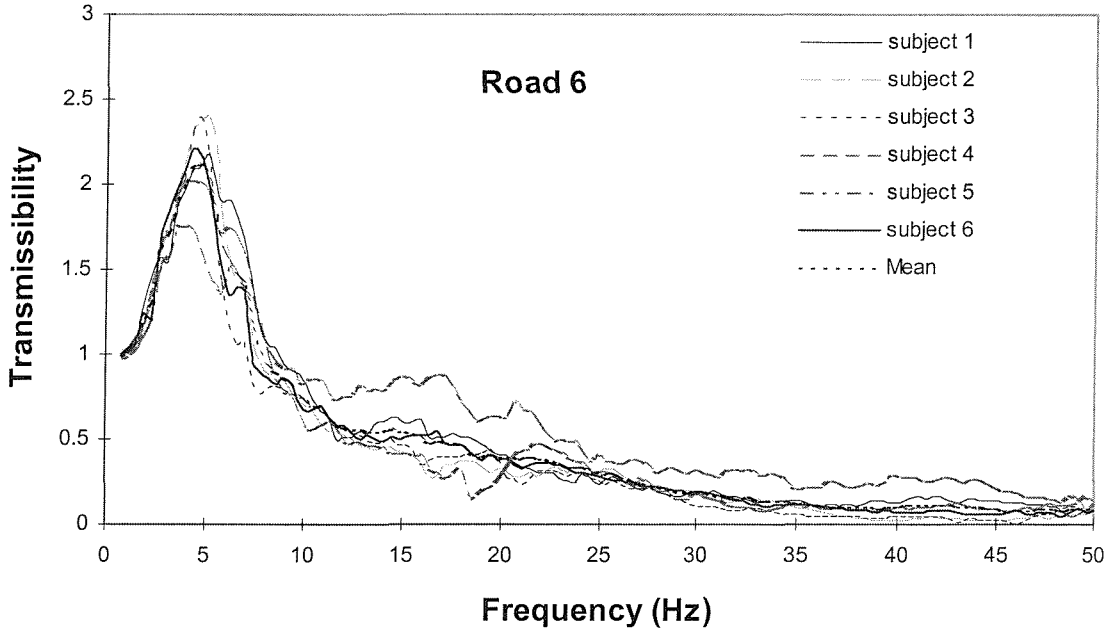

Figure 4.2 Ford Mondeo seat transmissibilities measured with six persons over the same road.

A seat transmissibility prediction method (Fairley and Griffin 1986) could give good predicted seat transmissibility. It is a procedure in which separate measurements of the impedance of a seat and the impedance of the human body are combined to predict the transmissibility of the seat supporting the human body. The method is based on the following theory. A preliminary study will be reported in this chapter to investigate this method.

4.2 Method

This method includes two parts. One is the measurement of the seat dynamic stiffness, the other is the measurement of human body apparent mass. Then, the seat transmissibility can be obtained through the combination of the two measurements.

4.2.1 Measurement of foam impedance with an indenter

Consider a seat with a displacement $x(t)$ under the influence of a force, $F(t)$. An indenter attached to a rigid steel frame was screwed up and down on to the top surface of a block of foam (500 mm by 420 mm by 120 mm) so as to vary the applied static force between indenter and foam. The indenter had loading corresponds to subjects of various weights. The indenter was mounted on a bearing, so that it would not rotate relative to the seat as the indenter was screwed up and down. For different static loading, the dynamic force on the indenter was measured with a piezo-electric force link while the surface supporting the foam was vibrated.

$\ddot{x}(t)$: Acceleration measured at base of seat

$F(t)$:Force provided by vibrator

$F_1(t)$ Force measured from indenter

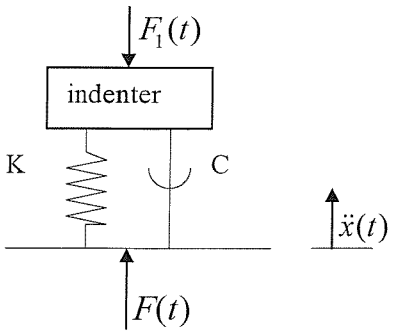

Figure 4.3 The arrangement of the apparatus, where *K* and *C* represent the damping and stiffness of the foam.

The force on the indenter and acceleration beneath the foam were measured during 100 seconds of random vibration (0.5 ms^{-2} r.m.s. over the frequency range 1.0 to 30 Hz) produced by an electrodynamic vibrator. The constant bandwidth acceleration spectrum was flat to within plus and minus ten per cent of the nominal acceleration spectral density.

4.2.2 Theory

If the force measured on the indenter is $F_1(t)$, the response of the system is given by:

$$F_1(t) = c\dot{x} + kx \tag{4.1}$$

Where x is the displacement and $\dot{x}$ is the velocity of the surface supporting the foam. Since mechanical impedance is a function of frequency, it is helpful to transform this equation by means of the Laplace transform to the frequency domain. Taking the Laplace transform of Eq. (4.1), and setting the initial conditions equal to zero since the steady state is the case of interest, gives:

$$F_1(s) = (cs + k)x(s) \tag{4.2}$$

The real frequency response is obtained by setting $s = \omega i$ where $i = \sqrt{-1}$ and ω is the frequency in radians:

$$\omega = 2\pi f \tag{4.3}$$

From this equation the complex ratio of force to displacement is:

$$F_1(\omega i) = (k + c\omega i)x(\omega i) \tag{4.4}$$

Mechanical impedance, Z(ω), is the complex ratio of force to velocity; dynamic stiffness, S(ω), is the complex ratio of force to displacement:

$$S(\omega) = \frac{F(\omega i)}{x(\omega i)} = k + c\omega i \tag{4.5}$$

This expression for dynamic stiffness is a complex equation with real and imaginary components, or with magnitude and phase angle. These components are more than mathematical constructs in that they have important physical significance. The real part, $|S|\cos\theta$, is due to those components that do not dissipate power but simply store energy either in

kinetic or potential form. The imaginary part, $|S|\sin\theta$, or the damping coefficient, c, in Eq. (4.5), is proportional to the power dissipated by the foam, mainly as heat (Suggs *et al* 1971).

The modulus of the dynamic stiffness of the measured foam is shown in Figure 4.4 for preload forces from 300 to 800 newtons. According to Eq. (4.5):

$$|S| = \sqrt{k^2 + (c\omega)^2} \tag{4.6}$$

$$\theta = \arctan\left[\frac{c\omega}{k}\right] \tag{4.7}$$

Equations (4.6) and (4.7) can be used to determine the response of a given system to an exciting force. In addition, by computer techniques the system parameters for a desired response can be determined by making successive approximations. That is fitting a non-linear function to a set of experimental data (Figure 4.4). We can programme software (Appendix A) that implements the Nelder - Mead simplex algorithm and use it to minimise a non-linear function of variables, in this case the frequency and dynamic stiffness.

4.2.3 The apparent mass of the seated human body

The apparent mass of the body determined by Fairley and Griffin (1989) was used in this study. The apparent mass frequency response function is defined as:

$$\text{apparent mass } M(\omega) = \frac{F(\omega i)}{\ddot{x}(\omega i)} \tag{4.8}$$

Fairley and Griffin (1989) studied subjects sitting on a rigid flat seat secured directly to the platform of a vertical vibrator. The mean normalised apparent mass of the sixty subjects obtained by Fairley and Griffin is shown in Figure 4.5. Although the dynamic response of the seated human body is extremely complex, due to the mass, damping and resiliency being distributed rather than lumped, a single degree-of-freedom system was able to account for most of the response observed in the low frequency range. The single degree-of-freedom system is applicable because, for low frequency vibration, the resonance in the apparent mass is due to parameters which act as if they were lumped rather than distributed.

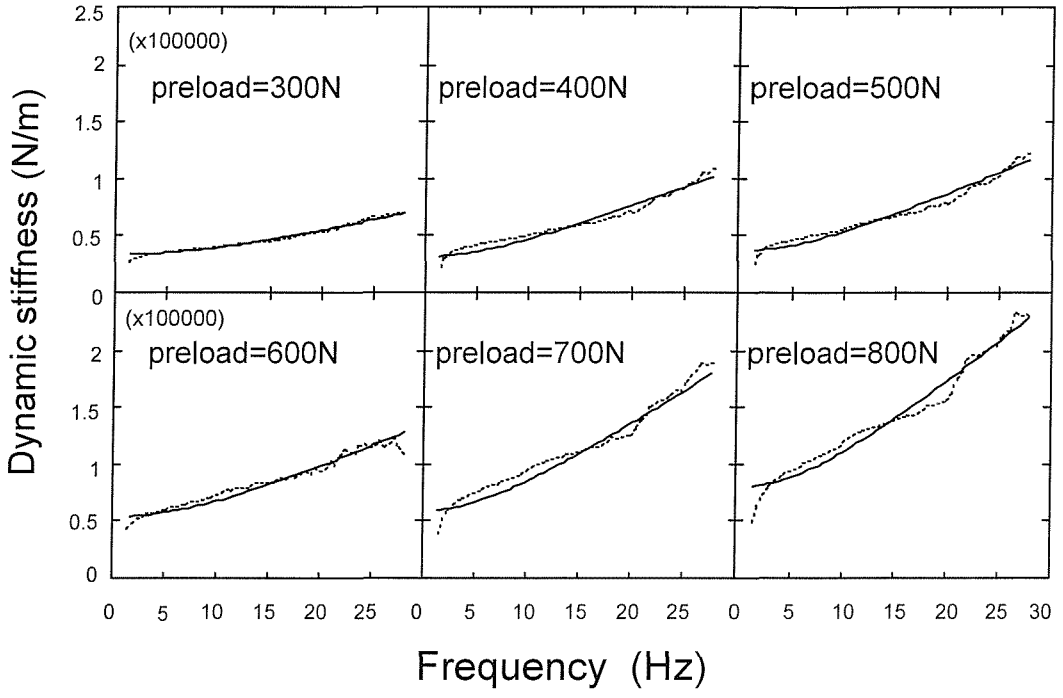

Figure 4.4 Dynamic stiffness of foam block and fitted model for preload forces from 300N to 800N. (------ measured values; —— fitted values).

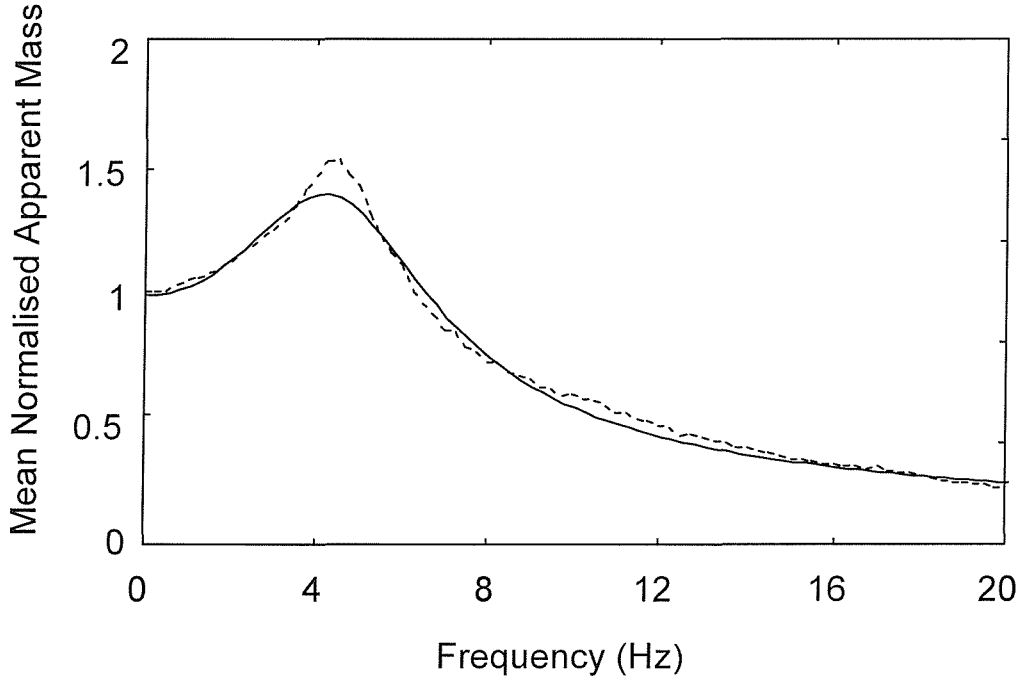

Figure 4.5 The mean normalised apparent mass of the sixty subjects from Fairley and Griffin (1989) and values from fitted model (------ measured values; —— fitted values).

Because the measured human body mechanical impedance showed simple mechanical system property, Matthews (1967) and Suggs *et al.* (1968, 1969) developed a mathematical model and constructed a dynamic simulator to replace the seated subject (see Chapter 2).

Based on the same reason, a single-degree-of freedom model was considered here as a simulator of the human body, the results of Fairley and Griffin (1989) can be represented by Figure 4.6.

The response of the system is given by

$$F(t) = m_1\ddot{x} + m_2\ddot{x}_1 \qquad (4.9)$$

The only force which can be transmitted to the simulator is the sum of the inertial forces, F(t).

Invoking the Laplace transform we get for the steady state case.

$$F(s) = m_1 s^2 x(s) + m_2 s^2 x_1(s) \qquad (4.10)$$

The acceleration and the velocity of the simulator, when transformed, will be:

$$\ddot{x}(s) = s^2 x(s) \;; \qquad \dot{x}(s) = s\,x(s) \qquad (4.11)$$

In order to arrive at a term that corresponds to the mechanical impedance we seek to solve for $x_1(s)$ in terms of $x(s)$ by Newton's second law of motion.

$$m_2\ddot{x}_1 = k_1(x - x_1) + c_1(\dot{x} - \dot{x}_1) \qquad (4.12)$$

Taking the Laplace transforms and substituting ωi for s, the model in the frequency domain is:

$$x_1(\omega i) = \frac{k_1 + c_1\omega i}{k_1 - m_2\omega^2 + c_1\omega i}\, x(\omega i) \qquad (4.13)$$

Substituting for $x_1(\omega i)$ above gives

$$F(s) = \left[m_1 + m_2\left(\frac{k_1 + c_1\omega i}{k_1 - m_2\omega^2 + c_1\omega i} \right) \right] \ddot{x}(s) \qquad (4.14)$$

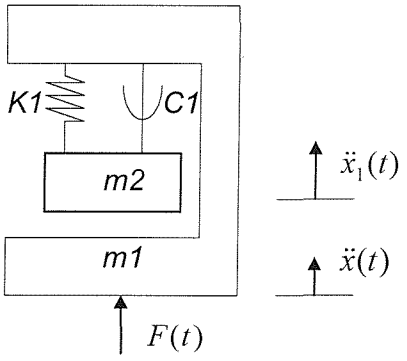

Figure 4.6 Simulator of human body

The term in the bracket, being the ratio of $F(s)$ to $\ddot{x}(s)$, is called apparent mass. This is identical to the equation of Fairley and Griffin.

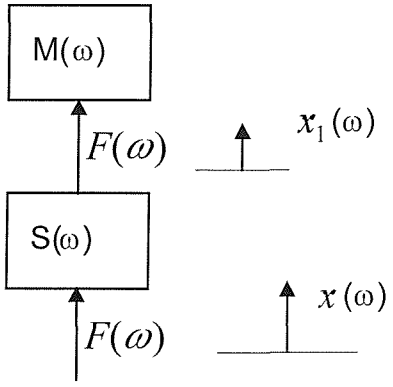

Figure 4.7. Seat loaded with a person

Using the Nelder—Mead routine in MATLAB, we can fit equation (4.14) with four parameters (m_1, m_2, K_1, C_1) to the normalised apparent-mass for 60 subjects as shown in Figure 4.5. The optimisation was conducted separately for each subject in the present experiment such that sitting weight ($m_1 + m_2$) corresponded to 75% of the subject's weight. This was necessary as the apparent mass ($F(s)/\ddot{x}(s)$) is not simply related to the sitting weight ($m_1 + m_2$), (see equation 4.14).

4.2.4 Measurement of seat transmissibility with human subjects

With eight male subjects (Table 4.1), acceleration was measured at the foam-person interface and on the platform of the vibrator beneath the foam (Figure 4.7). Vibration was generated in the vertical direction by an electrodynamic vibrator with the same characteristics as used to measure the dynamic

stiffness of the foam (0.5 ms^{-2} r.m.s. from 1 to 30 Hz). Vibration was measured at the interface between the foam and the body with a SIT-BAR (Whitham and Griffin, 1977).

Table 4.1 Subject Characteristics

subject	age (years)	stature (m)	total weight (kg)
1	37	1.66	58
2	35	1.66	53
3	33	1.65	52
4	23	1.84	63
5	23	1.85	65
6	32	1.70	70
7	38	1.68	63
8	30	1.70	75

The following frequency response function can be defined:

Seat transmissibility, $T(\omega)$:

$$T(\omega) = \frac{\ddot{x}_1(\omega)}{\ddot{x}(\omega)} \tag{4.15}$$

Massless dynamic stiffness of seat $S(\omega)$:

$$S(\omega) = k + c\omega i = \frac{F(\omega) * \omega^2}{\ddot{x}_1(\omega) - \ddot{x}(\omega)} \tag{4.16}$$

So the force transmitted to the seated person is:

$$F(\omega) = S(\omega) \times \omega^{-2}(\ddot{x}_1(\omega) - \ddot{x}(\omega)) \tag{4.17}$$

From equation (4.8) we get:

$$\ddot{x}_1(\omega) = \frac{F(\omega)}{M(\omega)} \tag{4.18}$$

Substituting for $F(\omega)$ above gives:

$$\ddot{x}_1(\omega) = \frac{S(\omega) * (\ddot{x}_1(\omega) - \ddot{x}(\omega))}{M(\omega) * \omega^2} \tag{4.19}$$

So, for the seat transmissibility, we get:

$$T(\omega) = \frac{\ddot{x}_1(\omega)}{\ddot{x}(\omega)} = \frac{S(\omega)}{S(\omega) - M(\omega) * \omega^2} \tag{4.20}$$

The seat transmissibility modulus is given by:

$$\left|\frac{x_1(s)}{x(s)}\right| = \sqrt{\frac{[kk_1 - (m_2k + cc_1)\omega^2]^2 + \{[(kc_1 + k_1c) - m_2c\omega^2]\omega\}^2}{[(k - (m_1 + m_2)\omega^2)k_1 + B\omega^2]^2 + [(kc_1 + k_1c - A\omega^2)\omega]^2}} \quad (4.21)$$

Where:

$$A = m_1c_1 + m_2c + m_2c_1 \quad (4.22)$$

$$B = m_1m_2\omega^2 - km_2 - cc_1 \quad (4.23)$$

The phase angle can then be expressed as:

$$\theta = \arctan\left[\frac{(kc_1 + k_1c - m_2c\omega^2)\omega}{kk_1 - (m_2k + cc_1)\omega^2}\right] - \arctan\left[\frac{(kc_1 + k_1c - A\omega^2)\omega}{(k - (m_1 + m_2)\omega^2)k_1 + B\omega^2}\right] \quad (4.24)$$

4.2.5 Prediction of the foam transmissibility

The measured foam impedance and the apparent mass reported by Fairley and Griffin (1989), were used to determine the relevant parameters of the foam and the human body. Equations (4.21) and (4.24) were then employed to predict the foam transmissibility. That is, using all parameters (m_1, m_2, k_1, c_1, k, c) obtained from the experimental data fitting (Figures 4.4 and 4.5) in equations (4.21) and (4.24). The predicted transmissibility was then compared with the real transmissibility measured with human subjects seated on the foam (Figure 4.8).

4.3 Results

For each of the eight subjects, Figure 4.8 compares the measured foam transmissibility with the transmissibility predicted from the measured dynamic stiffness of the foam and the single degree-of-freedom model of each subject's apparent mass calculated from the data of Fairley and Griffin. The measurements differ among the eight subjects, probably because of differences in subject apparent mass. The predictions differ because the parameters representing the dynamic characteristics of subjects and the foam are different according to the different of subjects' masses (from Figures 4.4 and 4.5).

It may be seen that the resonance frequency and the transmissibility at resonance are generally well predicted by the model. In some subjects, the prediction differs from the measurements at frequencies around 8 Hz, probably as a result of the absence of a second degree-of-freedom in the model of subject apparent mass (see Section 2.4).

Figure 4.9 compares the median measured and median predicted foam transmissibility. Statistical analysis showed that in different frequency regions the effects of using the mathematical model for predicting the foam transmissibility is different (Table 4.2). In the frequency region 1.4 to 2.8 Hz, the predicted values are significantly lower than the experimental values (p <0.025), but the difference is small in size. In the resonance region from 3.2 to 5.2 Hz, and also from 9.8 to 10.8 Hz there was no significant difference between the measured and predicted transmissibilities. From 5.6 to 9.3 Hz the predicted values were significantly lower, and at frequencies above 11.2 Hz the predicted values were significantly higher than the measured values (p < 0.05, Wilcoxon matched-pairs signed ranks test)

4.4 Discussion

Two methods have been mentioned for the prediction of seat or foam transmissibility. The first is using equation 4.20 to obtain seat transmissibility. This method does not need any understanding of the seat or body dynamic response. The prediction can be achieved directly using the measured seat dynamic stiffness and the measured human body apparent mass. Fairley and Griffin (1986) proposed this method and obtained good prediction results. However, there are disadvantages in this method. First, it needs two measurements, seat dynamic stiffness and human body apparent mass. Second, this method cannot give out any useful information for seat designers, such as seat stiffness or seat damping on how to affect seat transmissibility and how to achieve ideal seat transmissibility by changing them.

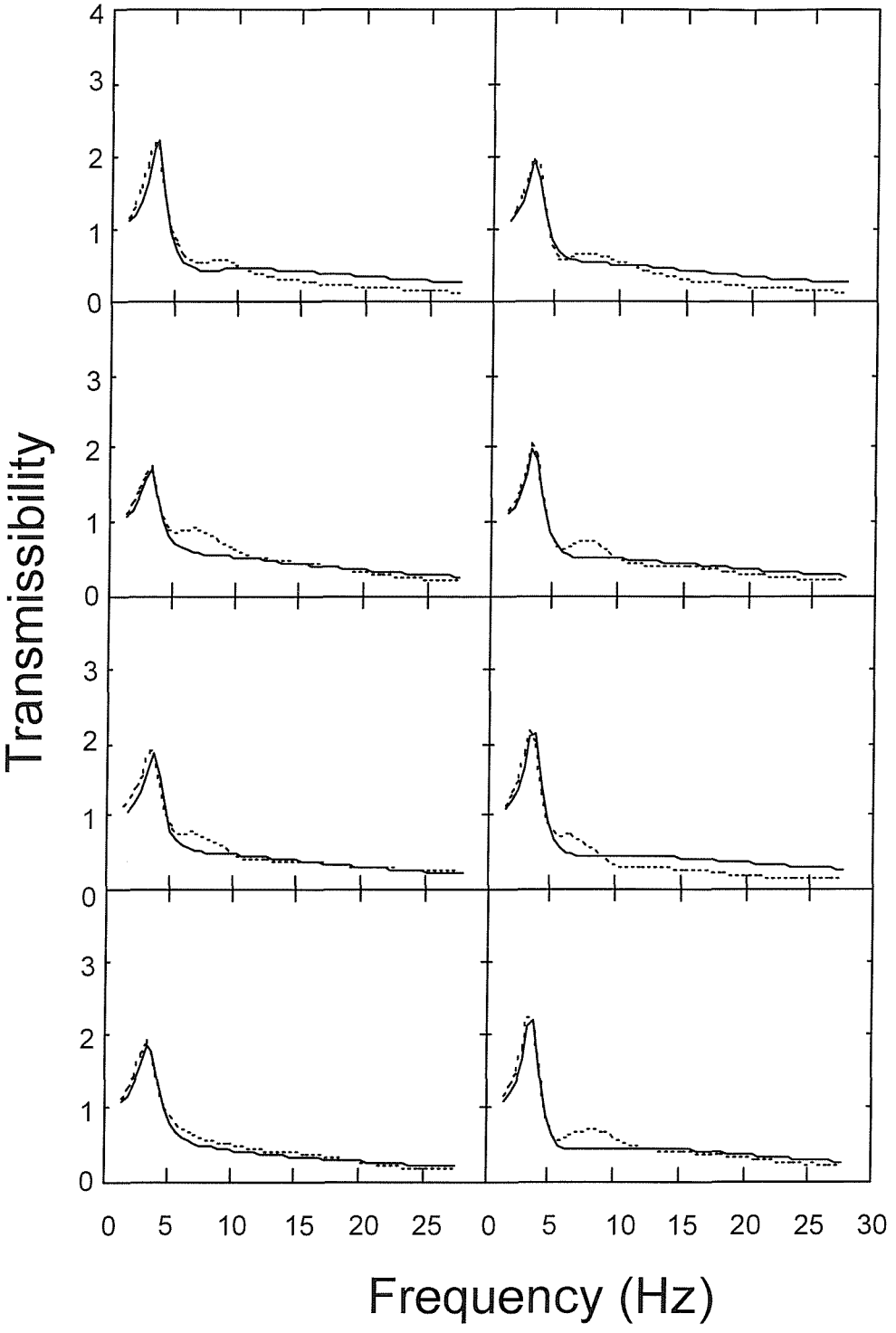

Figure 4.8 Comparison of measured and predicted foam transmissibility for eight different male subjects (------measured transmissibility; ——predicted transmissibility).

Table 4.2 Comparison of measured and predicted transmissibilities (Wilcoxon matched-pairs signed ranks test).

frequency (Hz)	significance level p	frequency (Hz)	significance level p	frequency (Hz)	significance level p
1.41	0.0173	10.78	0.4838	20.16	0.0117
1.88	0.0117	11.25	0.0929	20.63	0.0117
2.34	0.0117	11.72	0.0929	21.10	0.0117
2.81	0.0251	12.19	0.0687	21.57	0.0117
3.28	0.5754	12.66	0.0251	22.04	0.0117
3.75	0.8886	13.13	0.0251	22.51	0.0117
4.22	0.2626	13.60	0.0251	22.97	0.0117
4.69	0.4008	14.07	0.0357	23.44	0.0117
5.16	0.2076	14.54	0.0357	23.91	0.0117
5.63	0.0173	15.00	0.0500	24.38	0.0117
6.10	0.0117	15.47	0.0357	24.85	0.0117
6.56	0.0117	15.94	0.0357	25.32	0.0117
7.03	0.0117	16.41	0.0357	25.79	0.0117
7.50	0.0117	16.88	0.0357	26.26	0.0173
7.97	0.0117	17.35	0.0251	26.75	0.0173
8.44	0.0117	17.81	0.0251	27.19	0.0173
8.91	0.0173	18.29	0.0251	27.66	0.0173
9.38	0.0251	18.75	0.0173		
9.85	0.1614	19.22	0.0117		
10.32	0.6744	19.69	0.0117		

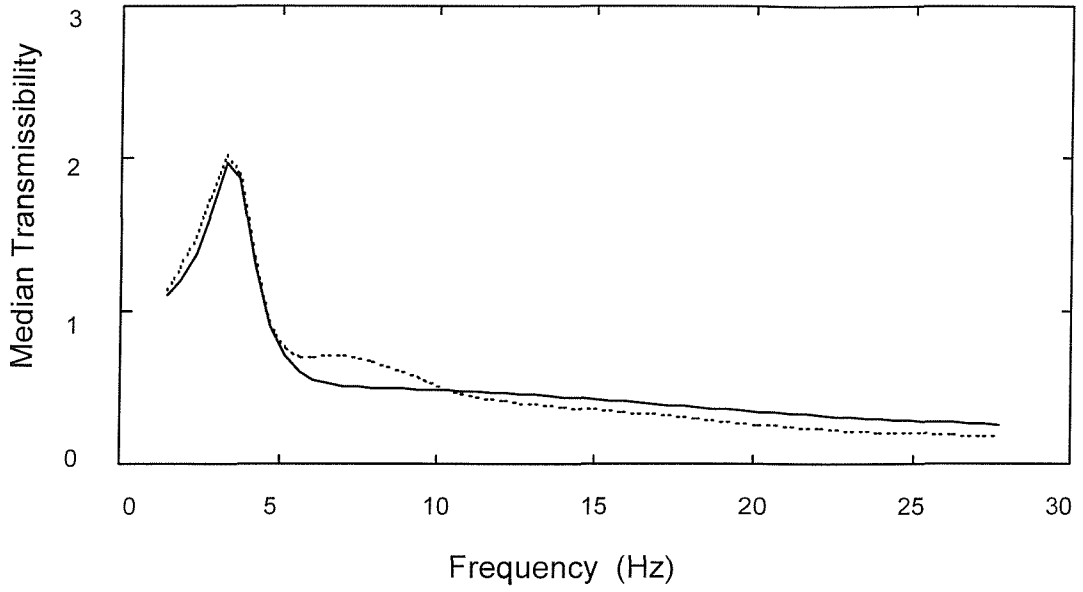

Figure 4.9 Comparison of median measured and median predicted seat transmissibility (------ measured transmissibility; —— predicted transmissibility).

The second method proposed by Wei and Griffin (1995) is expressed by equation 4.21 and 4.24. It was a lumped parameter model which was used to predict seat transmissibility. The model was set up based on an understanding of seat dynamic properties and a sketchy understanding of human body dynamic performance. A one degree-of-freedom model was used to represent the human body dynamic response to vertical vibration, but it was not intended to represent the locations or mechanisms of body movement. The model was only intending to reproduce the measured apparent mass. A simple seat model was also proposed in this method, which included only stiffness and damping and the moving mass of the seat was neglected. There were many advantages for this method. First, it was based on a human body lumped parameter model, so the measuring of the human body can be avoided. It is beneficial not to measure with human subjects since this eliminates the inherent risks of shaking subjects and, therefore, the need for vibration facilities deemed safe for human experimentation. Second, it was a parameter model to predict seat transmissibility, and so the function of any parameters can be observed. Third, the effect of seat composition on seat transmissibility, such as seat stiffness and damping, can be easily obtained,

so it is a good method for the seat designer to optimize seat parameters. Additionally, the measurement of the seat material impedance will be helpful when it becomes possible to predict seat dynamic properties from the physical and chemical properties of seat materials. Ultimately, it should be possible to select the seat components from a knowledge of the desired seat impedance. Finally, the variation of seat transmissibility in different measuring environments is mainly caused by subjects, so this method can give repeatable results due to avoiding of the inter-subject variability.

The dynamic responses of both the human body and some seats are non-linear. The non-linearity results in different seat transmissibilities with different vibration spectra. It will be necessary to quantify the non-linearity of both the human body and the seat material if predictions of seat transmissibility are to be accurate.

Using an indenter to obtain the seat dynamic properties and predict seat transmissibility is only one of several methods of determining seat transmissibility. It is desirable to compare this method with the results obtained by other procedures.

Although the results obtained by this method are promising, further study with a wider range of seats and subjects is required to show that the procedure has general applicability.

The contact area between the body and the seat, and between the indenter and the seat is likely to be important. Further study may be required to investigate the influence of indenter size and shape on the measured seat impedance.

4.5 Conclusion

The experimental results show that it is possible to obtain reasonably accurate predictions of the transmissibility of foam from separate measures of the impedance of the foam and the reported impedance of the human body. This suggests that a single degree-of-freedom simulation of the human body may

reflect the impedance of the human sufficiently at low frequencies to predict seat transmissibility. An improved model may be required at high frequencies.

Measures of foam impedance showed that the stiffness of the foam increased with increasing static load.

Using an indenter to obtain measures of seat dynamic response may be a useful means of predicting seat transmissibility. It may also encourage the development of methods of predicting the influence of the properties of foam (and other material) on vehicle ride.

4.6 Future research

Although useful predictions of the foam transmissibility have been achieved, they were obtained in special conditions. For example, the foam transmissibility was measured in strict conditions, such as the subjects keeping upright posture, no backrest, equal energy spectrum input vibration with one vibration magnitude, limited exposure duration, etc. The seat dynamic properties were also measured in strict conditions, such as the same input vibration which was used for apparent mass measurement, a shaped indenter head (SIT-BAR), no inclination of foam surface, etc.

Further studies of the indenter test will focus on investigating the effect of the indenter area, pre-loads, vibration magnitudes, input vibration spectrum and inclination of the seat on seat dynamic stiffness. A standard indenter test procedure will be developed after this series of studies.

Further study of human body models will focus on model development and investigating the effect of vibration magnitudes, input vibration spectra, backrest and backrest angles as well as hard and soft seats on body apparent mass. A suitable body model will be developed for seat transmissibility prediction.

The final aim of this study is a generally applicable prediction method. So a field experiment will be performed to test the method.

CHAPTER 5

SEAT MECHANICAL PROPERTY MEASUREMENT

5.1 Introduction

There are many methods to measure seat mechanical properties, such as measuring the seat transmissibility with a rigid mass, with an indenter and with subjects. However, as discussed in the literature review, no standard method has been developed to measured seat dynamic properties. The prediction method, as a new method proposed by Fairley and Griffin (1986), was selected here to obtain the seat transmissibility. Assessment and development of this method have been made in Chapter 4. Although good results have been achieved, there were still some limitations, such as limitations in measuring seat impedance and limitations in obtaining seated body apparent mass. The good measurement of the seat impedance and good measurement of the seated body apparent mass are key to obtaining corresponding seat and body models which can be used to obtain good predictions of seat transmissibility.

The aim of this chapter is to define a good method to obtain seat mechanical properties which can be used in seat transmissibility prediction and to develop a seat mathematical model based on authentic seat measurements. The indenter method was the preferred method used in this chapter to measure seat mechanical properties.

The indenter method is described in Appendix A and in Section 4.2. Although, in theory, using an indenter test rig can provide good seat properties, the method has not been verified, and so it is not yet in general use. Some studies of factors affecting test results must be conducted so that the method can be fully understood. Another aim of this chapter is to investigate the effect of various factors on seat mechanical properties measured by an indenter.

The study here will contribute knowledge to this method and enable it to be a general used seat test method.

5.2 Seat mechanical property measurement

Seat mechanical properties consist of two parts: static properties and dynamic properties. The static property of a seat is generally measured using an indenter, but the dynamic property (i.e., mechanical impedance) of a seat can be measured by a rigid mass or an indenter.

5.2.1 Seat static property

An indenter static test procedure for foam was defined in ISO-3386 (1986). The rectangular shaped foam was compressed with a 200 mm diameter circular plate at a speed of 100mm/minute up to 75% of the foam thickness or up to a load of 110 kgf. However, the test procedure is only suitable for a simple rectangular shaped foam. A standard method for complex shaped foam and seats has not been established. Complex shaped foam and seat surfaces are not horizontal or flat and their thickness varies in different parts so that their stiffness cannot reliably be measured using a 200 mm diameter circular plate is changed.

In order to investigate seat static properties, five different seats were measured using an indenter. The indenter head differed from ISO-3386 (1986), because a 200 mm diameter circular plate indenter can only give good results for a simple square foam (a simple square foam has equal stiffness at any parts) and it seems unsuitable for a shaped seat or foam (the flat circular plate differs from the subject bottom). For a complex shaped foam or a seat, a SIT-BAR (Figure 2.20) or a buttocks shape (Figure 5.1) as the indenter head may be more reasonable. Ebe (1998) did an experiment to investigate the effect of foam thickness on foam static properties. Four different thickness foams (50, 70, 100 and 120 mm) were used in the experiment, and had the same foam composition and density. Results are shown in Figure 5.2. As expected, thicker foams had larger deflections and less gradient on the load-deflection curves for a given load compared to thinner foams. This means that thicker foams behaved as if they were softer than thinner foams. A seat, or a

shaped foam, has significant differences in thickness on different parts along the fore-and-aft axis and slightly different along the left-and-right axis, so using a SIT-BAR or a buttocks as the indenter head is more suitable to obtain reliable results. In this study, a buttocks indenter was used as the indenter head to measure seat load-deflection curves.

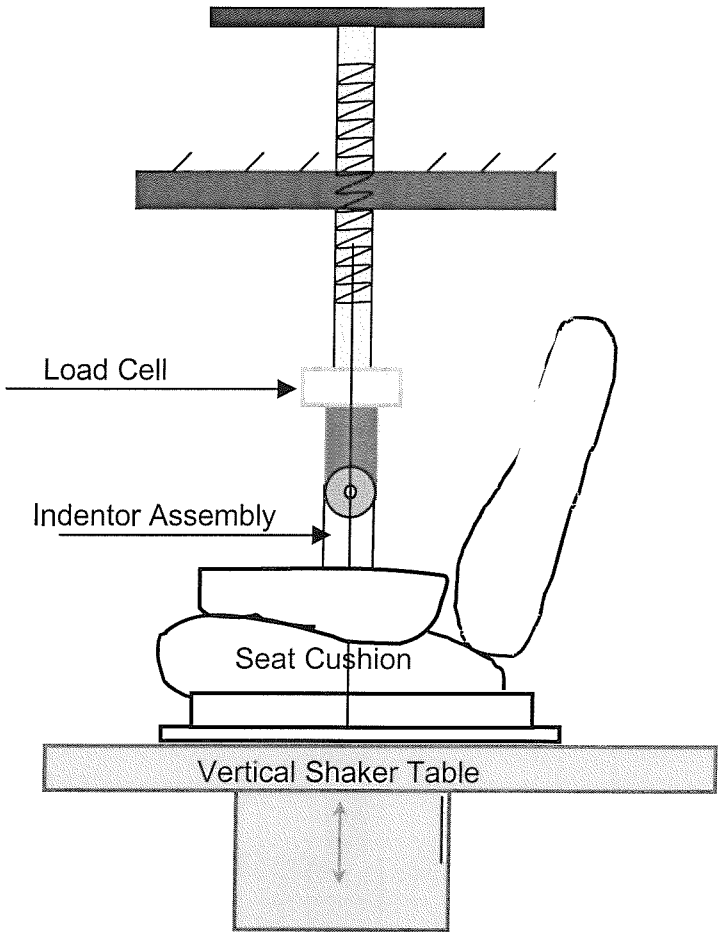

Figure 5.1 Testing rig for seat deflection-load curve

A Kistler 9321 force cell which had a sensitivity of approximately ±4.0 pc/N and a displacement transducer DC-LVDV D2/3000 which had a sensitivity of approximately 0.4 v/mm with an operating range of ±50 mm were used to measure the driving force and deflection whilst testing the seat using indenter. Three compression repeated cycles were performed for each test condition at a speed lower than 100mm/min. The tests were performed at controlled climatic conditions, which were 23 ^{0}C (±2 ^{0}C) temperature and 40% (±5 %) relative humidity. Two-channel signals, which had 5 samples per second sampling rate and 350-second duration, were acquired using *HVLab* software.

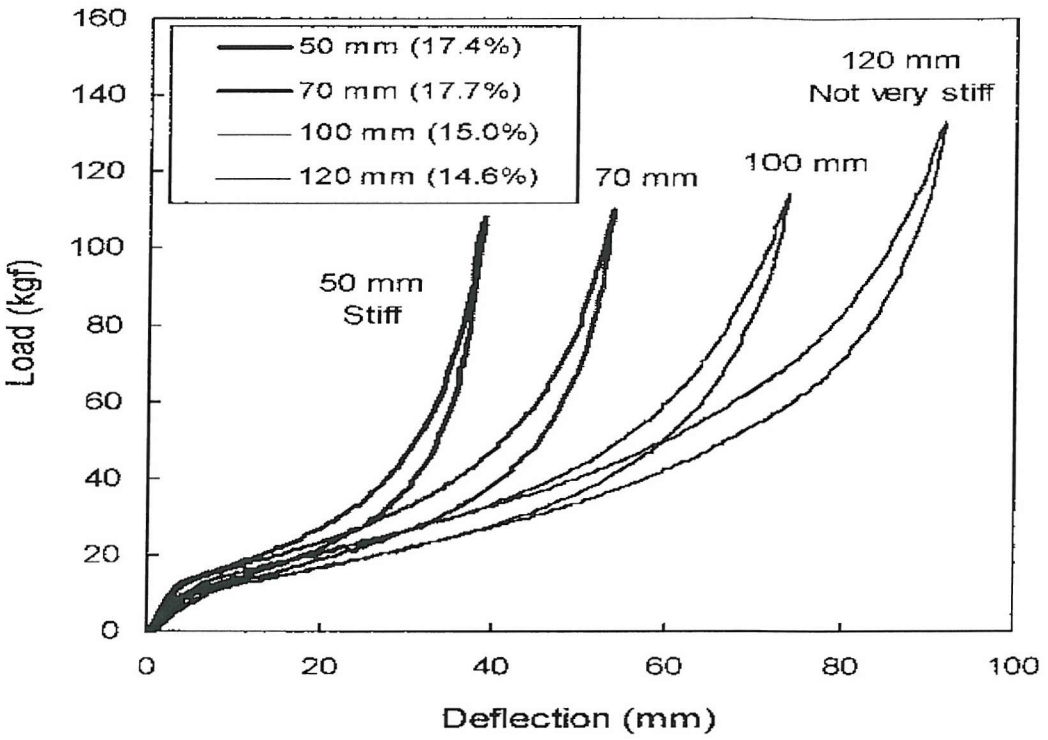

Figure 5.2 Load-deflection curves for different thickness foams (From Ebe 1998).

Test arrangements for five seats and the buttock shaped indenter are shown in Figure 5.1. Seat types are listed in Table 5.1. The measurement for one seat static properties are shown in Figure 5.3.

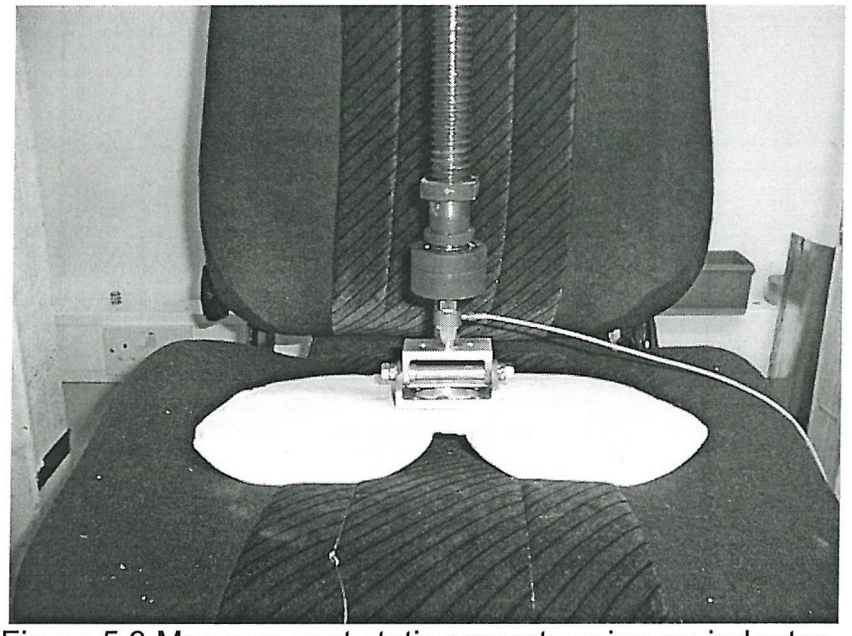

Figure 5.3 Measure seat static property using an indenter

Table 5.1 Seat type and fixing parameters

SEAT	SEAT TYPE
A	Car
B	Car
C	Truck
D	Van
E	Van

One measured seat load-deflection curve is shown in Figure 5.4. The looped area in the load-deflection curve shown in Figure 5.4 is called a hysteresis loop. It is caused by energy dissipation due to the viscoelastic characteristics of the polyurethane foam (Ebe 1998). The hysteresis loss is a ratio of loss of energy and energy applied to the foam per cycle of load and unload during the compression procedure. Hilyard *et al.* (1984) mentioned that the hysteresis loss resulted from the collapse of the cell struts and subsequent recovery during the unloading phase, which was related in some way to the cellular geometry and the viscoelastic behaviour of the base polymer.

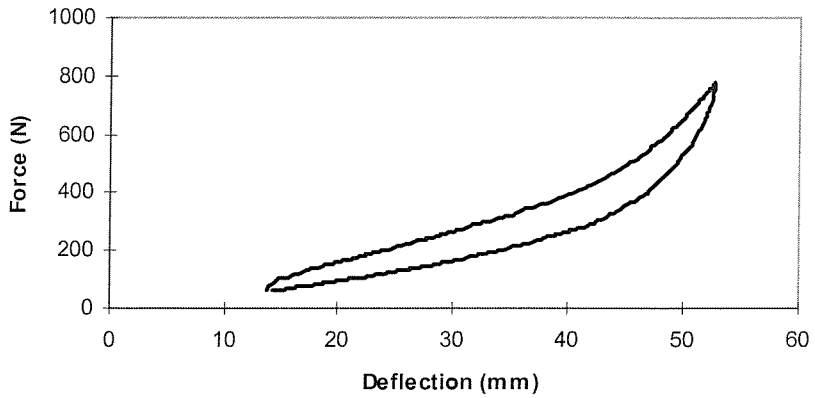

Figure 5.4 Measured seat B load-deflection curve

5.2.2 Seat dynamic properties

A vehicle seat should provide not only good static comfort but also good vibration isolation. Seat dynamic properties are important for seat designers hoping to optimize seat dynamic performance and provide good isolation of the vibration at the frequencies to which the seat will be exposed.

5.2.2.1 Method and analysis

As discussed in the literature review, there are many methods to obtain seat dynamic properties. An experiment was conducted to investigate the adaptation of these methods to acquiring seat physical values which represent dynamic seat characteristics.

The experiments were conducted separately with a car seat and with a rectangular sample of foam. The car seat was the driving seat from a modern small family car. It was constructed from a steel frame with moulded foam supported from beneath by a contoured steel seat pan. The TDI foam in the seat had a density of 50 $kg.m^{-3}$. The rectangular sample of foam was 500mm wide by 420mm deep and 120mm thick. It is described as a 'soft feeling type' polyurethane foam used for car seating. It had a density of approximately 40 $kg.m^{-3}$ and a hardness of about 7.0 kPa. An electrodynamic vibrator, Derritron VP85, was used and three types of measurements were undertaken.

5.2.2.1.1 Measurement of seat mechanical impedance with an indenter

A seat is supported on a vibrator with its upper surface deflected by an indenter attached to a Kistler 9321A force transducer (Figure 2.52). The indenter, having the shape of a SIT-BAR (Whitham and Griffin, 1977) was screwed down until the required force on the seat was reached and then locked in position. An Entran piezoresistive accelerometer (type EGCSY-240*-10) was mounted on the vibrator platform beneath the seat. The force on the indenter and the acceleration at the base of the seat were measured during a 100 s period of random vibration (0.5 ms^{-2} r.m.s.) produced by the electrodynamic vibrator. The vibration had a flat acceleration power spectral density over the range 1.0 to 30 Hz (± 10%).

The measurements were obtained with each of 6 pre-loads (300N to 800N) applied to the surface of the seat and the foam sample. Signals from the force transducer and the accelerometer were signal conditioned and acquired at 100 samples per second into an *HVLab* system.

The whole system of the seat (or foam) was considered a simple system, which comprised only stiffness and damping. Therefore, when using the indenter to load the seat, the response of the seat and foam system is given by:

$$F_1(t) = c\dot{x} + kx \qquad (5.1)$$

Where x is the displacement (in this experiment the displacement was less than $\pm$ 4mm), $\dot{x}$ is the velocity and $F_1(t)$ is the force measured by the indenter. From this equation the complex ratio of force to displacement is given by:

$$S(\omega) = \frac{F(\omega i)}{x(\omega i)} = k + c\omega i \qquad (5.2)$$

The ratio of the force to the displacement amplitudes, S(ω), is called the dynamic stiffness, a complex quantity. Dynamic stiffness was used in preference to the mechanical impedance, the ratio of the force to the velocity, because by using the dynamic stiffness the equivalent stiffness, k, and the equivalent damping, c, are more easily seen.

A curve fitting method was used to obtain seat parameters k and c (i.e. the effective stiffness and damping) from the real and imaginary components of S(ω) (see Section 4.2.2). The least square error method with an optimisation algorithm were utilised (Dierckx 1995). The parameters in the above equation were refined to minimise the function

$$error = \frac{1}{N}\sum_{i=1}^{N}\left(S_f(i) - S(i)\right)^2 \qquad (5.3)$$

Where S_f(i) is the corresponding dynamic stiffness from the curve fit at the i th frequency point and S(i) is the dynamic stiffness in the measured data. Using values for the parameters chosen at random as starting values, the parameters were varied systematically using the optimisation algorithm. The measured and calculated values of the modulus of the dynamic stiffnesses ($\sqrt{k^2 + (c\omega)^2}$) of the foam and the seat over the range of pre-load conditions

are presented in Figures 5.5 and 5.6. The calculated values of stiffness and damping are tabulated in Table 5.2.

The stiffness and the damping of both the seat and the foam changed with variations in the pre-load (see Figures 5.7 and 5.8). The measurements with the indenter show that when the pre-load increased, the stiffness and the damping of both the seat and the foam increased.

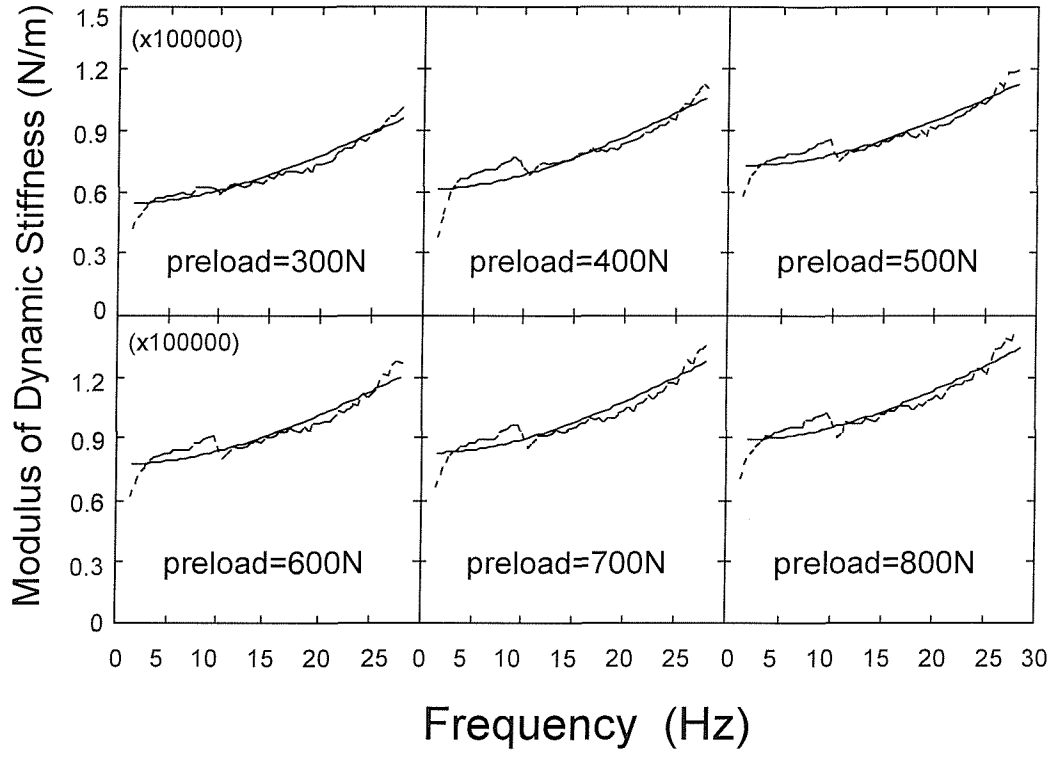

Figure 5.5 Dynamic stiffness of seat and fitted model for pre-load forces from 300N to 800N. (------ measured values; —— fitted values).

5.2.2.1.2 Measurement of seat transmissibility with a sand-bag

Seat or foam transmissibility can also be used to obtain the seat or the foam physical values, but the transmissibilities of the seat and the foam must be measured while they support a mass, such as sand-bag or a rigid mass (Figure 5.9), not a person. Five different masses of sand-bag (30 to 70 kg) were used while the base of the seat was excited by a 100 second period of random vibration at 0.5 ms^{-2} r.m.s. Two Entran piezoresistive accelerometers were mounted on the vibration platform beneath the seat and seat surface.

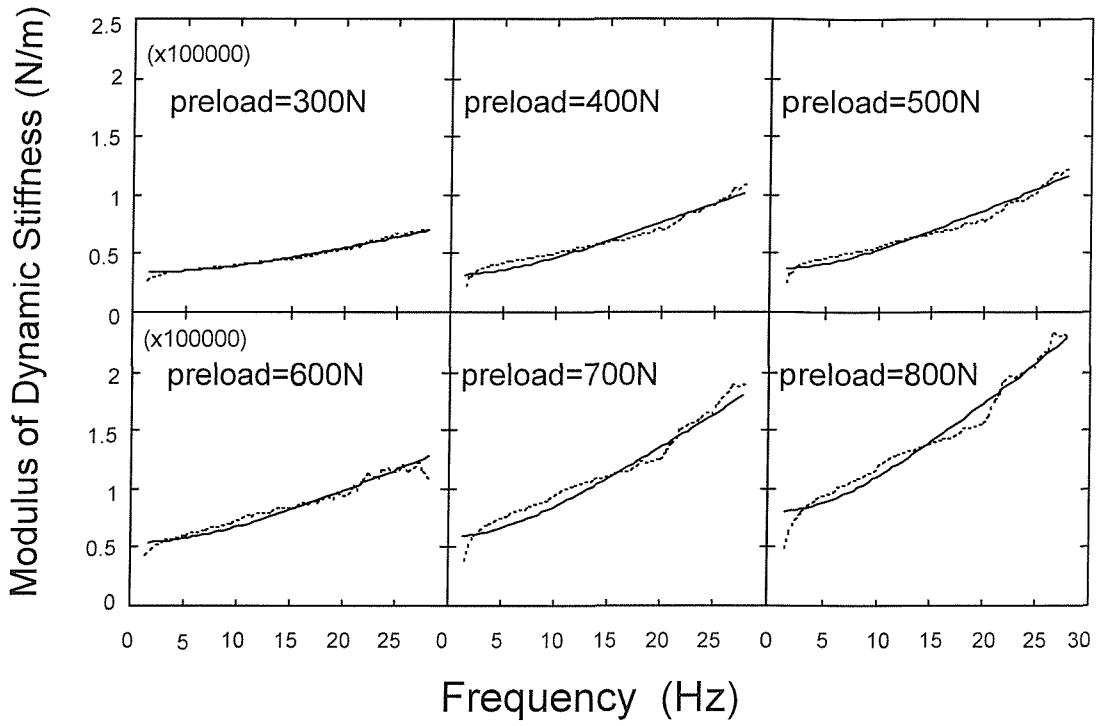

Figure 5.6 Dynamic stiffness of foam block and fitted model for pre-load forces from 300N to 800N. (------ measured values; —— fitted values).

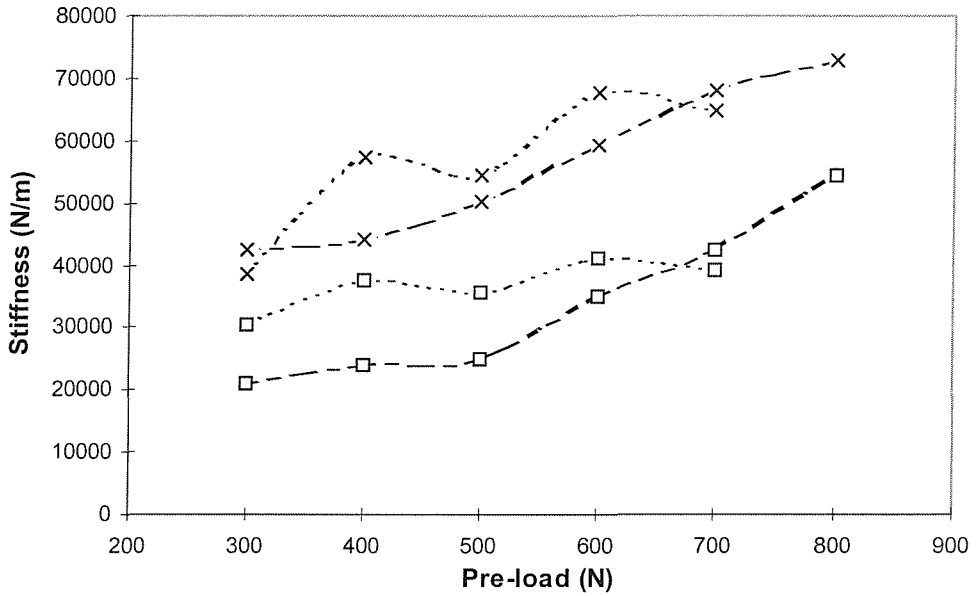

Figure 5.7 The stiffness of the foam and seat with different pre-load (– –□– – foam using indenter as load, · · ·□· · · foam using sand-bag as load, – –×– – seat using indenter as load, · · ·×· · · seat using sand-bag as load).

The transmissibility was calculated from the acceleration measured beneath

the seat (or foam) and the acceleration measured between the sand-bag and the surface of the seat (or foam).

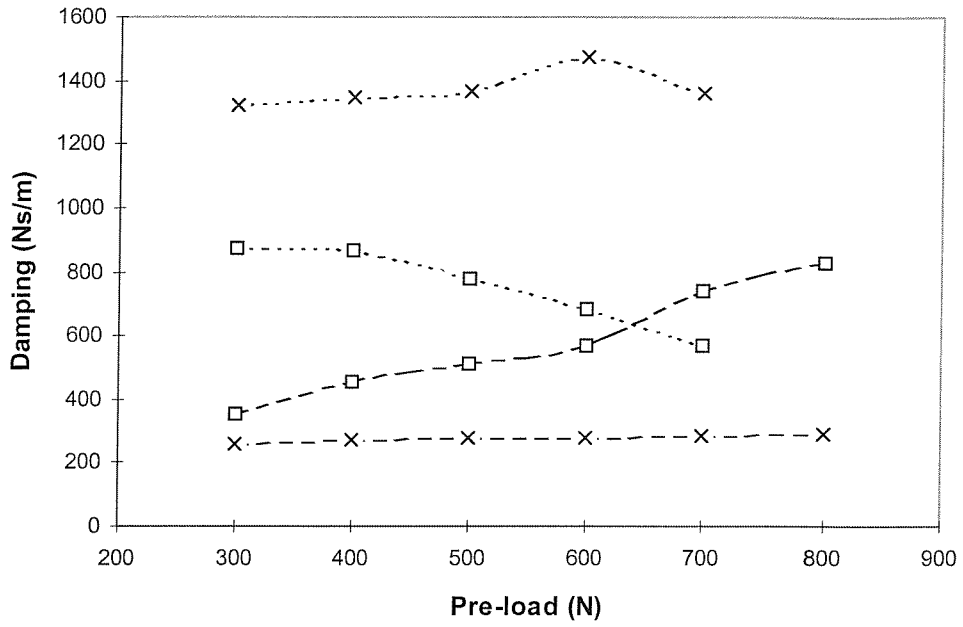

Figure 5.8 The damping coefficient of the foam and seat with different pre-load (– -□- – foam using indenter as load, · · ·□· · · foam using sand-bag as load, – –×– – seat using indenter as load, · · ·×· · · seat using sand-bag as load).

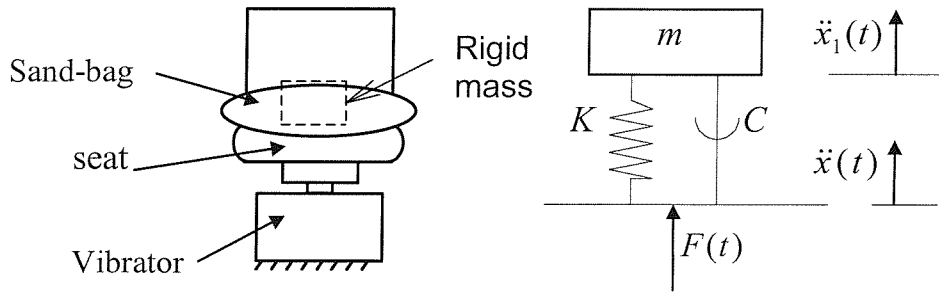

Figure 5.9 Sand-bag and rigid mass as the load on the seat

With the sand-bag used as a load on the seat, the response of seat and foam system is given by:

$$m\ddot{x}_1 = F(t) \qquad (5.4)$$

$$m\ddot{x}_1 + c(\dot{x}_1 - \dot{x}) + k(x_1 - x) = 0 \qquad (5.5)$$

The seat transmissibility is then:

$$T(\omega) = \frac{\ddot{x}_1(\omega)}{\ddot{x}(\omega)} = \frac{k + c\omega i}{k - m\omega^2 + c\omega i} \qquad (5.6)$$

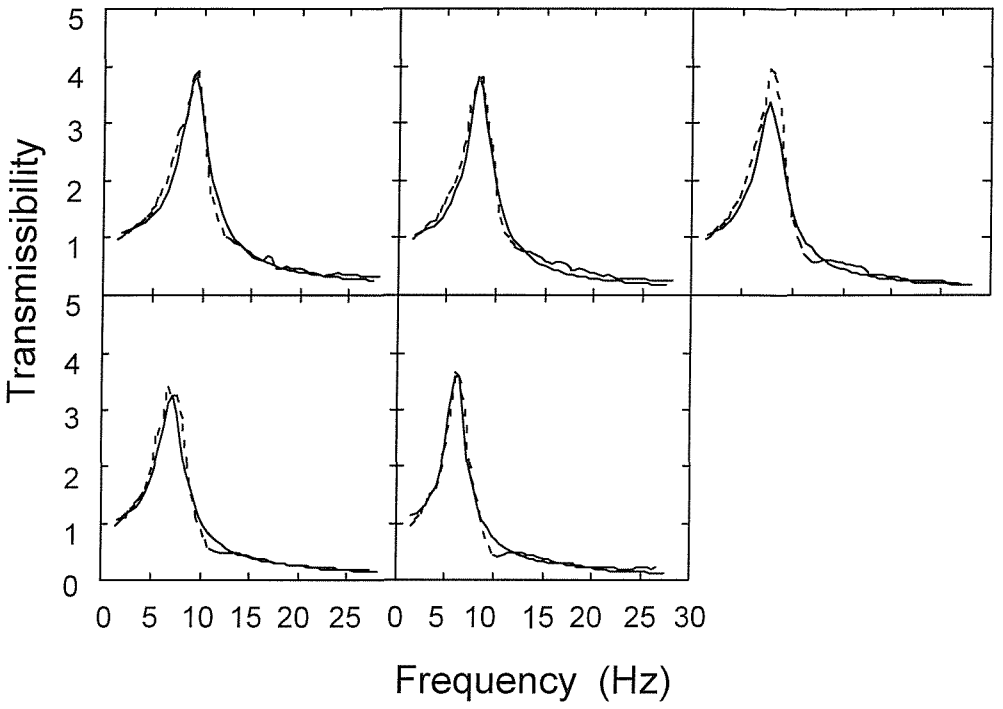

Figure 5.10 The seat transmissibility using sand-bag as the load from 300N to 700N and values from fitted model. (------measured values; —— fitted values).

Again, the seat and foam parameters *k* and *c* were obtained using curve fitting. Figure 5.10 compares the measured transmissibilities and those predicted from the fitted values of *k* and *c*. Table 5.2 lists the values of *k* and *c* obtained with the five different masses of sand-bag. Figure 5.10 shows that using the sand-bag instead of the human-body gave a transmissibility curve unlike the result with a subject, especially the transmissibility at resonance is much greater (see Section 2.3.4.2). For the measurements shown here, the resonance frequency was appreciably higher with the sand-bag than with human subjects, as shown in Section 8.3.1.1.2.

It can be seen again that the stiffness and damping of the seat and foam changed with variations in the pre-load (see Figures 5.7 and 5.8). The

stiffness values were similar to those obtained with the indenter, but the indenter seemed to provide the more consistent values. The damping coefficients were very different for the two methods, especially at low pre-load forces where a much higher damping was indicated from measurements obtained with the sand-bag. The difference may possibly have arisen because the sandbag had a larger contact area than the indenter. The inconsistent effects of increased load may have arisen because increases in mass of the sandbag resulted in increased size of the sand-bag. Figure 5.10 shows only the transmissibilities for the seat-sandbag system; the transmissibilities for the foam-sandbag system were similar, but the resonance frequency was lower and the transmissibility at resonance was higher. When the load on the seat (or the foam) increased, the resonance frequency decreased and the transmissibility at resonance increased.

5.2.2.1.3 Measurements of seat transmissibility with a rigid mass

The transmissibilities of the seat and the foam were also measured while they supported each of two rigid masses 22 mm wide by 14 mm deep by 15 mm (or 30 mm) thick (as for the sand-bag in Figure 5.9). The weights of the rigid masses were approximately 30 kg and approximately 50 kg. The seat was again excited by a 100 second period of random vibration at 0.5 ms^{-2} r.m.s. Two accelerometers were used for these measurements, mounted in the same places on the seat (or foam) as described above.

The procedure used with the sand-bag was also followed using the data obtained with the two rigid masses. This provided the stiffness and damping of the seat for loads of 300 N and 500 N (see Table 5.2). The transmissibilities obtained with rigid masses were the same as those with the sand-bag, except that the transmissibilities at resonance were higher. Comparing both seat and foam experiments, the foam had a slightly lower resonance frequency and a slightly lower transmissibility at resonance.

5.2.2.1.4 Discussions

Using the indenter and various masses the impedance of the seat and the seat response can be measured and provide seat parameters, such as seat

stiffness and damping. These parameters, or their corresponding dynamic stiffness, S(ω), (equation 5.2) will be used to predict seat transmissibility.

Table 5.2 The stiffness and damping coefficient of the seat and foam with different pre-loads.

	Seat					
	indenter		sand-bag		mass	
	k	c	k	c	k	c
300N	42300	260	38471	1323	35786	204
400N	44121	270	57426	1345		
500N	50210	276	54327	1364	47481	301
600N	59300	280	67838	1475		
700N	68000	285	64782	1357		
800N	73000	293				
Foam						
	indenter		sand-bag		mass	
	k	c	k	c	k	c
300N	21167	354	30381	870	18576	235
400N	23904	457	37643	868		
500N	25082	515	35787	777	23187	492
600N	34903	570	41062	681		
700N	42340	740	39186	570		
800N	54363	831				

In order to obtain good seat transmissibility predictions, it is necessary to select a good method of determining seat parameters, or seat dynamic stiffness. A comparison in this study between using an indenter and various masses shows that the indenter is a good method to obtain seat dynamic stiffness.

The rigid mass gave similar seat dynamic stiffness to that obtained with the indenter. However, the indenter is preferable as it provides a more controlled condition: a mass tends to rotate and move when placed on a seat during exposure to vibration.

A sand-bag of the correct mass had an excessively large contact area with the seat (including the edges of the seat) and this can influence the measured dynamic properties.

5.2.2.2 Measurement of seat dynamic properties

The dynamic properties of five seat were measured to investigate the correlation between seat dynamic properties and static properties (see Section 5.2.1). the same indenter test rig and electrodynamic vibrator were used. Two types of measurement were undertaken, with random and sinusoidal excitations. The random vibration had constant acceleration power spectra between 0.5 and 30 Hz and a magnitude of 0.5 ms^{-2} rms generated for 300 seconds by a computer and fed into the vertical axis of the vibrator. Five constant displacements of sinusoidal vibration ranging from 0.2 to 5.0 mm were also used. They were 0.2, 0.5, 1.0, 2.0 and 5.0 mm step sinusoidal vibration with frequency ranges from 1 to 30, 1 to 26, 1 to 19, 1 to 14 and 1 to 8 Hz, respectively. Every frequency duration was 5 seconds.

The dynamic stiffnesses of five seats exposed to random vibration are shown in Figure 5.11. The seat mount and indenter test rig were similar to the seat static test (Figure 5.1 and 5.3). A 500 N pre-load was applied to the seat surface to represent the weight of seated person. Signals were acquired by a computer with a sampling rate of 180 samples per second through low pass filters at 50 Hz.

Figure 5.12 shows the measured force-deflection curve for one seat (Seat A) at different frequencies (2Hz, 5Hz and 14 Hz) with a 500 N pre-load. It is clear that the seat stiffness and damping changed at different frequencies. Similar results could also be seen from measured seat dynamic properties during random vibration (Figure 5.11).

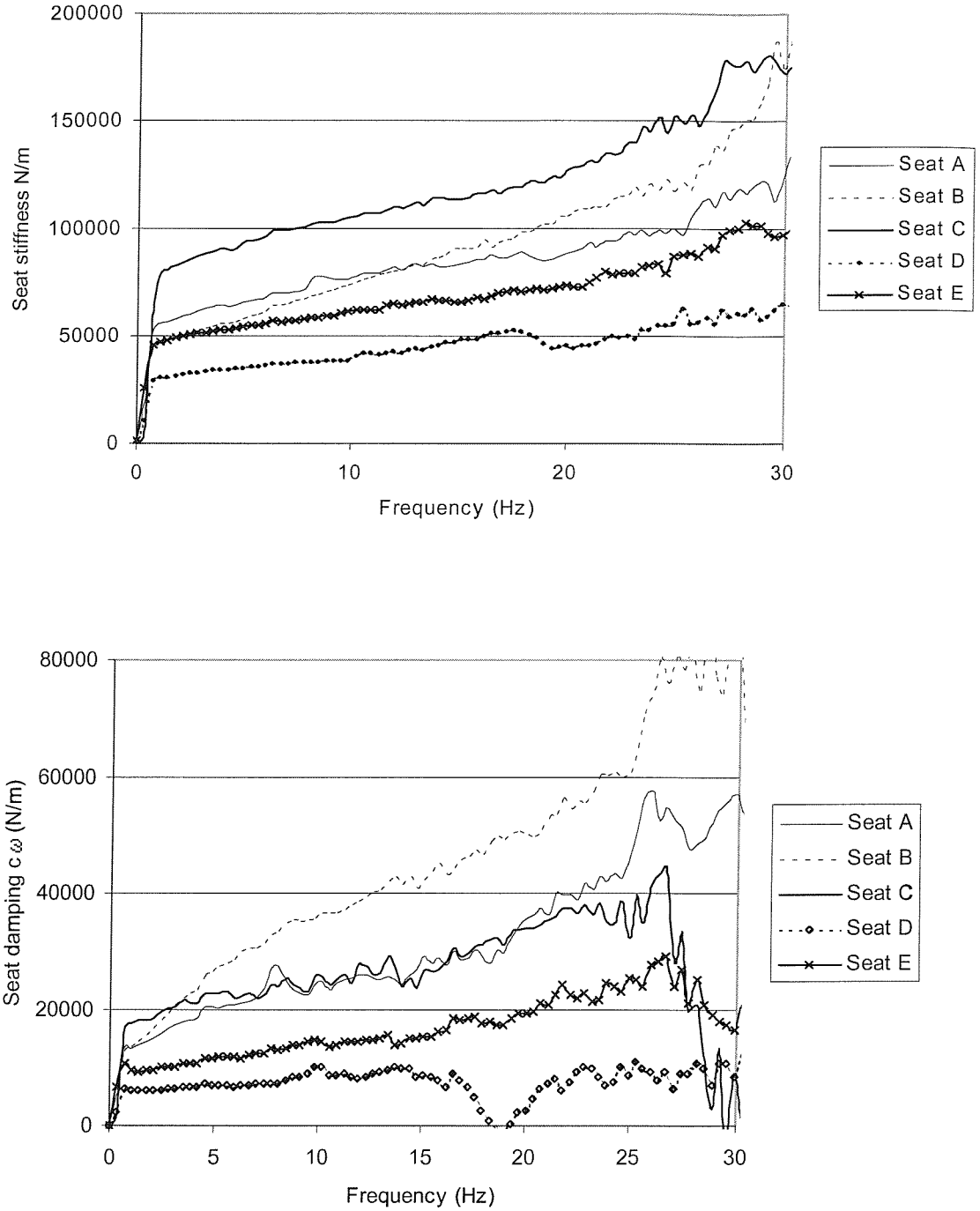

Figure 5.11 Measured dynamic stiffnesses of five seats

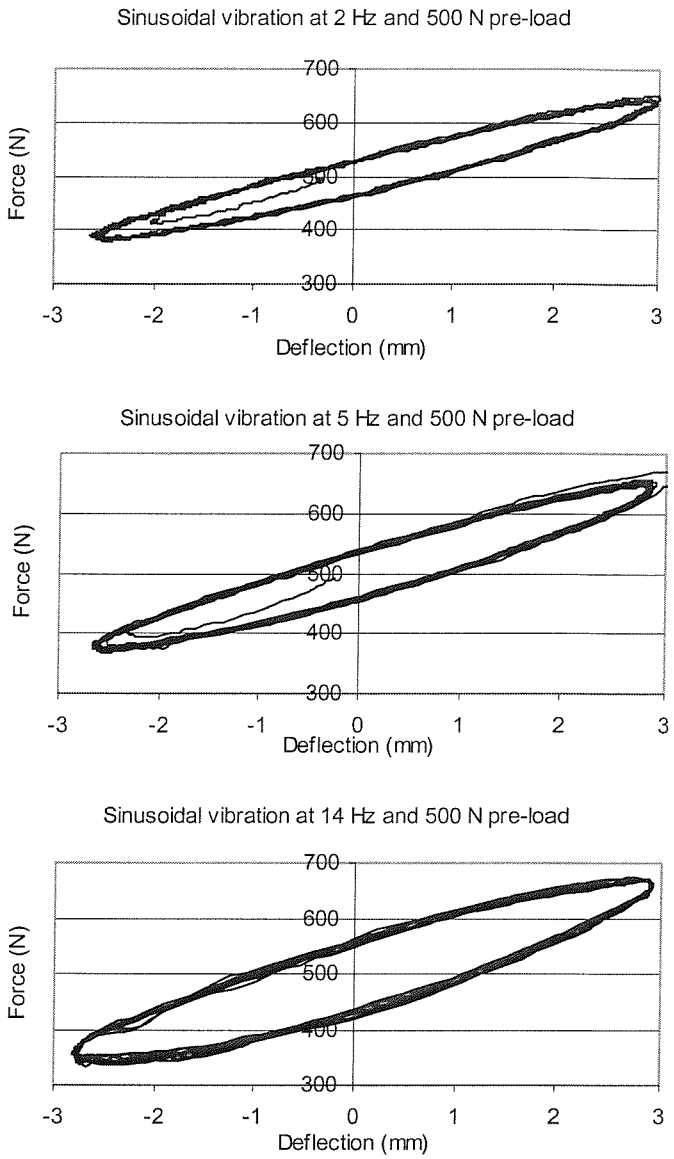

Figure 5.12 Force-deflection curve for seat A at different frequencies with a 500 N pre-load.

Figure 5.13 shows the measured dynamic stiffness for one seat (seat E) at different amplitudes with a 350 N pre-load. It can be observed that the seat stiffness consistently decreased with increasing sinusoidal vibration amplitudes. The seat damping values were also changed at different vibration amplitudes, but there were no consistent variations.

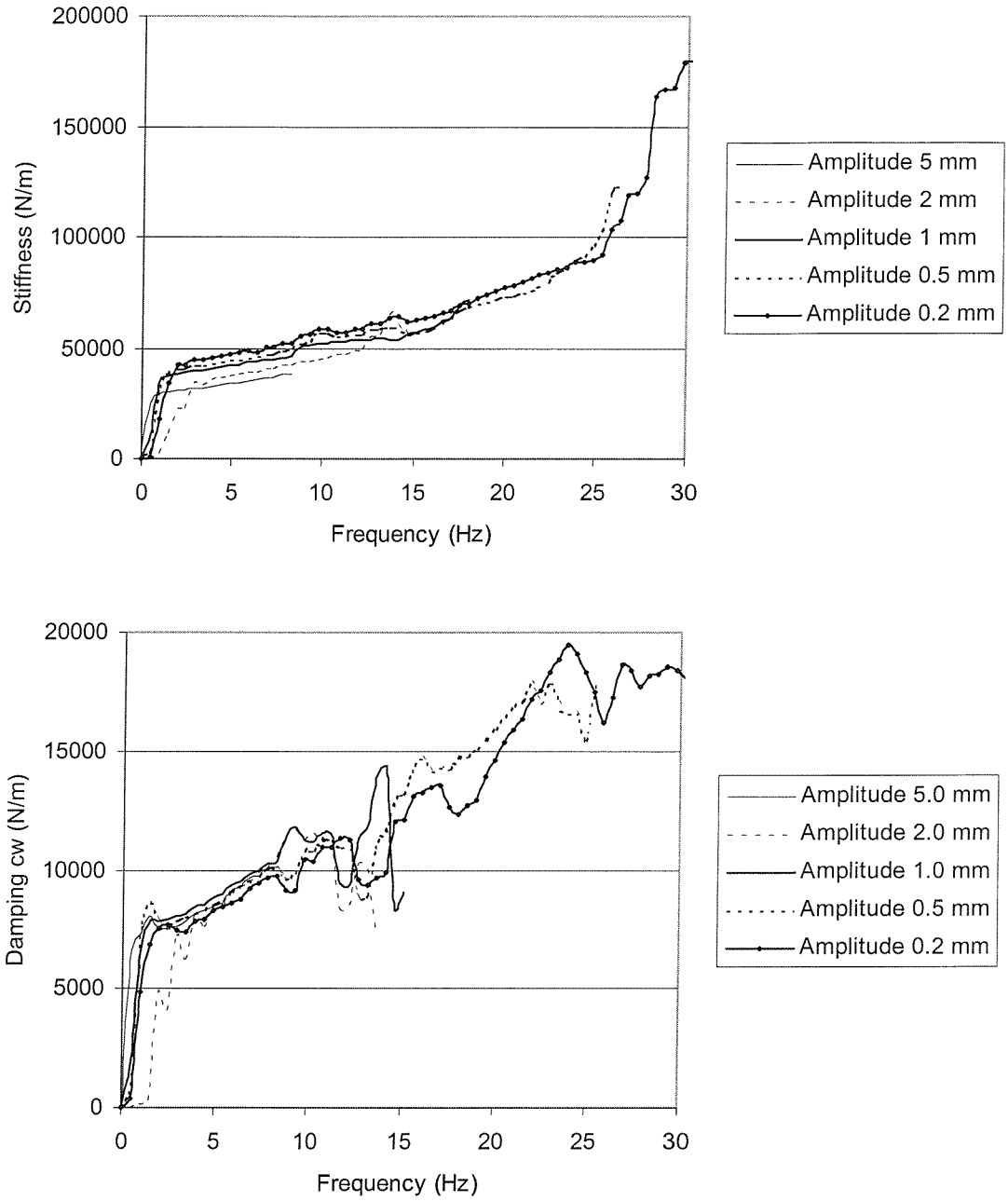

Figure 5.13 Dynamic stiffnesses for seat E measured at different sinusoidal amplitudes with a 350 N pre-load.

Figure 5.14 shows measured static stiffness versus dynamic stiffness for five seats. The static stiffness of seat is calculated from measured seat static property in a cycle of load and unload from 400 to 600 N. It is a ratio between mean varied force and varied displacement. The dynamic stiffness is obtained from measured dynamic stiffness at 500N pre-load (Figure 5.11). It is an

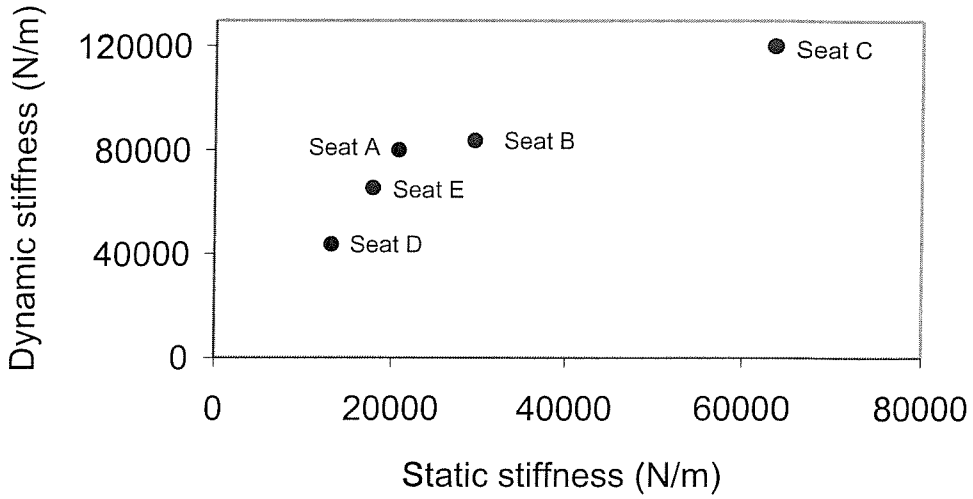

Figure5.14 Measured dynamic stiffness versus static stiffness for five seats

average value in a frequency range from 3 to 30 Hz. As expected, seats with greater static stiffness also have greater dynamic stiffness.

There were many problems when using the buttock as an indenter head to measure seat stiffness in the vertical direction. The first problem was horizontal movement caused by the seat and the indenter inclination. The second problem was twist force caused by large contact area in the fore-and-aft direction. The effect of these factors would result to a low coherency between measured input displacement and the output force.

The resonance of the seat backrest was around 10 Hz. When the seat was measured, if its backrest could not be adjusted to a vertical condition, a peak will appear on the measured curve.

5.3 Factors affecting indenter test results

5.3.1 introduction

The indenter method has been selected as a convenient tool to measure the stiffness and the damping of seats instead of a rigid mass (see Section 5.2.2.1). It is clear that this method can achieve good test results by avoiding many of the defects of using a rigid mass to measure seat characteristics. When using an indenter as the load on a seat, it is necessary to select an appropriate indenter shape and size as well as an appropriate pre-load. The

purpose of this study was to investigate the effect of the contact area, static force, inclination and vibration magnitude on seat response so as to select a suitable static force and vibration magnitude for an indenter-foam test, as well as to confirm the hypothesis that there is a correlation between the indenter head area and the foam stiffness and damping.

Five foams and five different indenter head shapes were used to obtain the foam dynamic stiffness. Five different pre-loads from 300N to 700N, representing different weights of the human body, were applied to the surfaces of the foams. Six different input magnitudes of vibration and five different inclination angles from 0^0 to 20^0 were used. A foam mathematical model and a curve fitting technique were employed to determine the stiffness and the damping of the foam.

5.3.2 Experimental method

Five different seating foams were used with the parameters listed in Table 5.3. Figure 5.15 shows the shape of the foam.

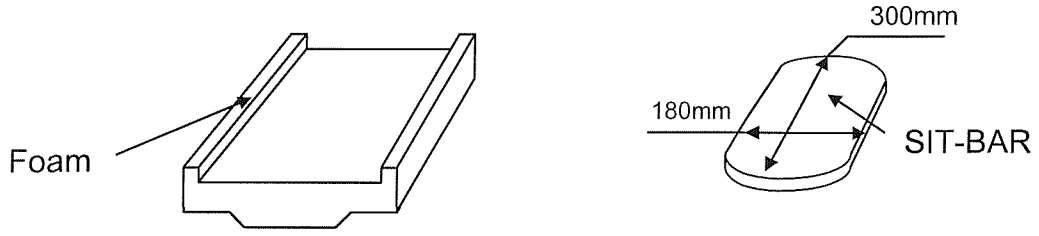

Figure 5.15 The shape of the foam and the shape of the SIT-BAR.

Table 5.3 The characteristics of the five different foams.

Foam No.	Shape	Thickness (mm)	Foam composition	Density (kg/m^3)	Hardness (kPa)
22	Figure 5.15	109	TDI	40	8.9
23	Figure 5.15	109	TDI	50	8.9
24	Figure 5.15	109	TDI	60	8.9
25	Figure 5.15	109	MDI	75	9.1
26	Figure 5.15	94	MDI	75	9.2

The vertical dynamic stiffnesses of the foams were measured using an indenter (Wei and Griffin, 1995) applied to the foam. A force transducer was attached to the indenter with five different indenter heads designated as buttocks, SIT-BAR (Figure 5.15), disk 15, disk 20 and disk 25 (Table 5.4). The buttock's shape was moulded from a HYBRID III Exterior (General Motors 1978). The indenter heads, in increasing order of area were: disk 15, disk 20, SIT-BAR, disk 25 and buttocks.

Table 5.4. The characteristics of the three different indenter disks

	Diameter (mm)	Thichness (mm)
disk 15	150 mm	15 mm
disk 20	200 mm	20 mm
disk 25	250 mm	20 mm

Five different pre-loads from 300N to 700N were applied to the upper foam surface using each of the indenter heads while the foam was exposed to vertical vibration from beneath. The force on the indenter and acceleration beneath the foam were measured during 60 seconds of random vibration.

Six magnitudes of vibration (0.25, 0.5, 1.0, 1.5, 2.0 and 2.5 m/s² r.m.s.) were used in the experiment over the frequency range of 0.5 to 30 Hz.

Five different foam inclinations, which were 0^0, 5^0, 10^0, 15^0 and 20^0, were applied to a SIT-BAR indenter test rig. The input vibration, which had 1.5 m/s² r.m.s. magnitude, and 580 N pre-load were applied to investigate the effect of foam inclinations on indenter test results. Figure 5.16 shows the measurement system to obtain foam dynamic stiffness at different foam inclinations.

5.3.3 Mathematical model and data fitting

5.3.3.1 Model of the foam-indenter system

Figure 5.17 illustrates the arrangement of the apparatus, where c and k represent the damping and stiffness of the foam:

$\ddot{x}(t)$: acceleration measured at the base of the foam

$F(t)$: force provided by the vibrator

$F_1(t)$: force measured on the indenter

Foam provides a complex non-linear system. Gurram *et al.* (1995) showed that the seat composed by a foam cushion is a highly non-linear system whose response is dependent on the input excitation and the weight of the occupant. Patten *et al.* (1998) also revealed that the response of open cell polyurethane foam was non-linear. Therefore, using a simple stiffness *k* and damping *c* to represent a foam or a seat composed of foam may not be suitable, because static forces and vibration magnitudes at different frequencies both may have a significant effect. However, only a few studies have investigated the non-linearity of foam and tried to use a non-linear model to represent foam. The non-linear model has not given better prediction of foam (Patten *et al.* 1998) than simple model (see Section 5.2.2.1.2 and Figure 5.10), so most researchers are still using a simple stiffness *k* and damping *c* to represent foam or a seat. The study here used an indenter to measure foam dynamic response. The effect of input excitation level on measurements was small (see Section 5.3.5.3). Therefore, two factors causing a non-linear response of a seat or a foam are eliminated (Gurram *et al.* 1995), because the static force is fixed during the indenter test. The simple foam system, as in Figure 5.17, still utilized an indenter test as a convenient approximation.

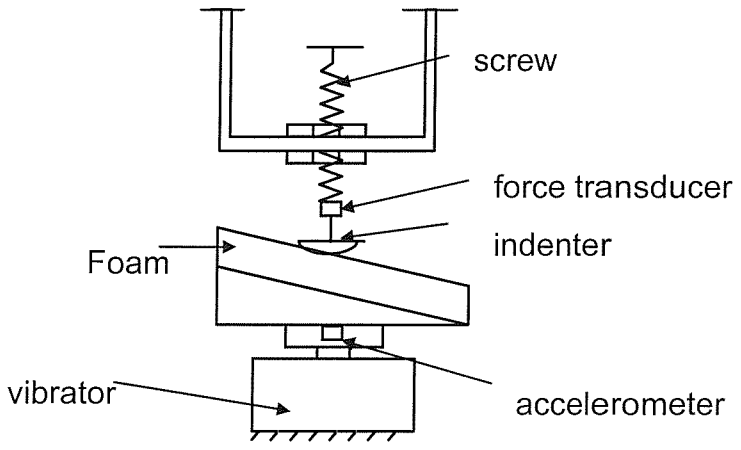

Figure 5.16 Indenter test rig for different foam inclinations

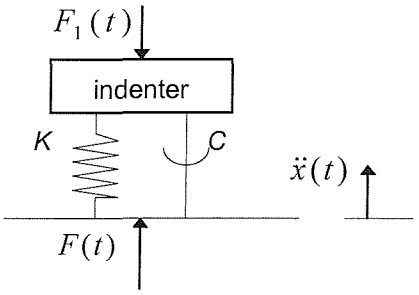

Figure 5.17 Representation of experimental measurements.

The model of the foam-indenter system in Figure 5.17 shows the rigid indenter connected to the vibrating base by a spring, *k*, and a damper, *c*.

5.3.3.2. Results and Data fitting

Examples of the modulii of the dynamic stiffnesses of one foam measured with one indenter at six vibration magnitudes are shown in Figure 5.18 for pre-load forces from 300 to 700 Newtons.

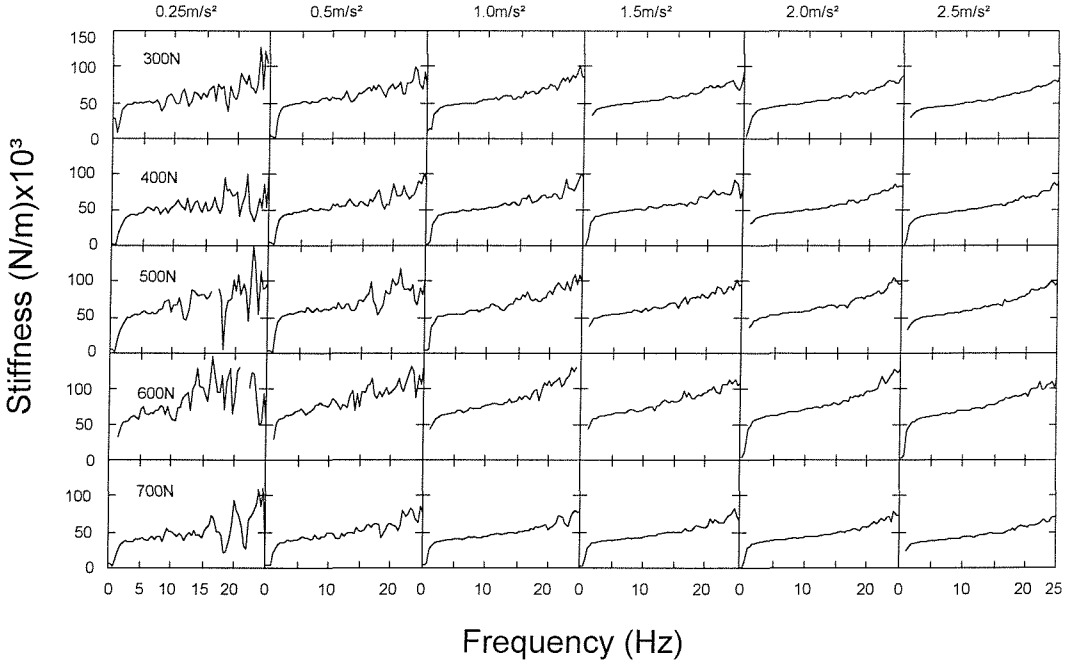

Figure 5.18. Disk 20 and foam 23 at six different vibration magnitudes and five different static forces.

Examples of the modulii of the dynamic stiffnesses of one foam measured with a SIT-BAR at five inclination angles are shown in Figure 5.19 for pre-load forces of 580 Newton.

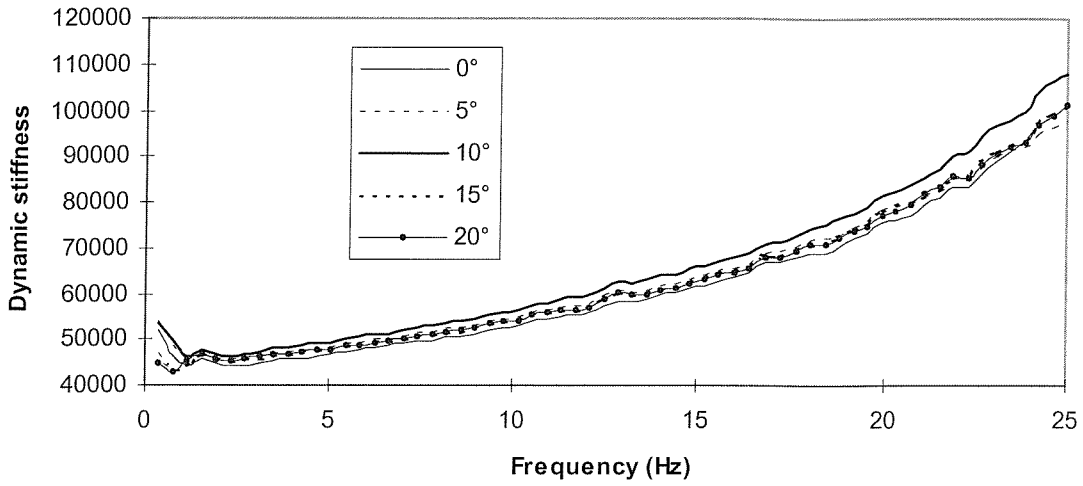

Figure 5.19 Measured dynamic stiffness of a foam at five different inclinations with a 580N pre-load and 1.5 m/s² r.m.s. input magnitude.

The mathematical model of the foam-indenter system was used to fit the experimental data. The least squares method was used to find the values of the parameters in the equation, by minimising the sum of the squared deviations of the measured values of the modulus and phase (See Section 4.2.1).

All model parameters obtained for the foams with different contact areas, pre-loads and magnitudes, are listed in Table 5.5. Examples of the fitted curves and the experimental curves are compared in Figure 5.20. There are too many figures to show the effect for all the different contact areas, magnitudes and foams, so only a typical set of data are illustrated here.

Using the fitted data, the values of equivalent stiffness and damping of the five foams can be seen for different vibration magnitudes and the 500N static force in Figure 5.21. Figure 5.22 shows the equivalent stiffness and damping of the five foams with the 1.5 m/s² input vibration and static forces from 300N to 700N.

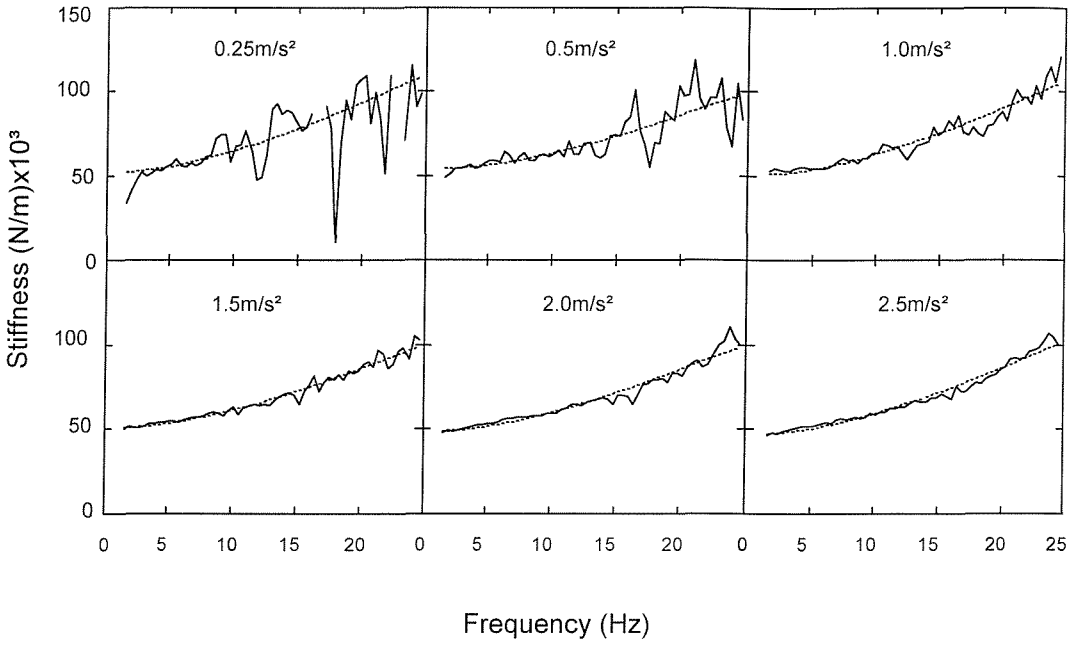

Figure 5.20. Foam 23, disk 20 and static force 500N experimental data compared with value obtained by curve fitting.

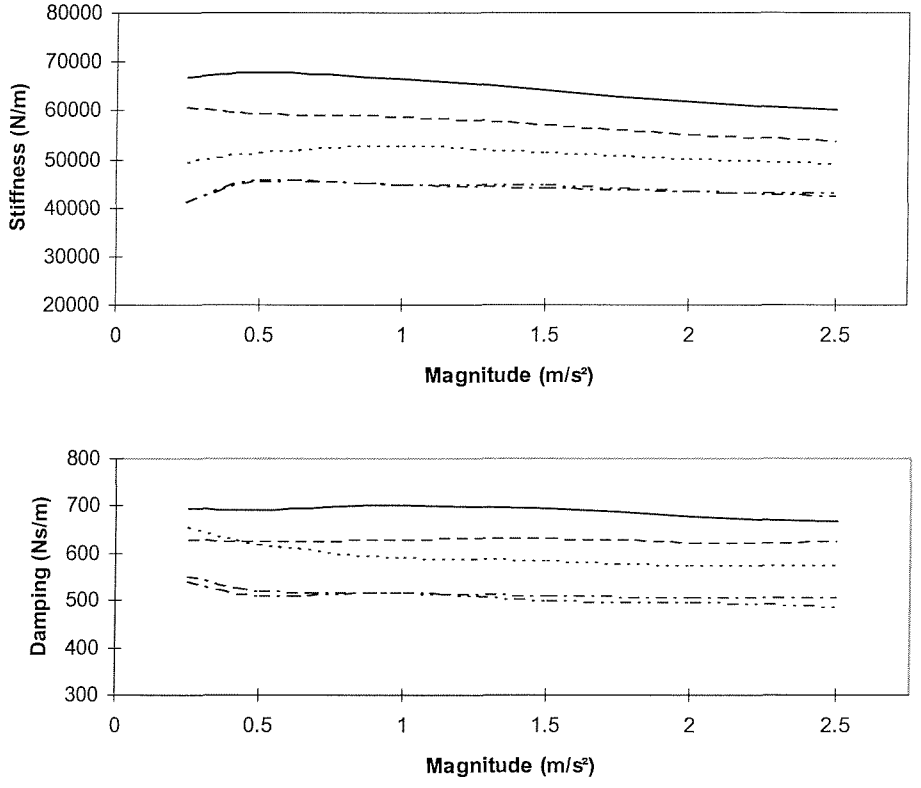

Figure 5.21. Effect of vibration magnitude on measured foam stiffness and damping with the mean of five different contact areas at a static force of 500N (foam 22 ———, foam 23 - - - - , Foam 24 · · · · · · · , foam 25 - - - - - - - - , foam 26 - · - · - · - · - · - · -).

The model parameters of foam 23, which were obtained with different inclination angles, are listed in Table 5.6. Figure 5.23 shows the equivalent stiffness and damping of the foam 23 with the 1.5 m/s² input vibration, 580 N static force and inclination angles from 0^0 to 20^0. There are no consistent differences in stiffness between different inclination angles except for foam 22, but there is a damping peak at 10 degree of inclination angle.

Table 5.5. The stiffness and damping of foam with different static forces, vibration magnitudes and contact areas.

		foam 22		foam 23		foam 24		foam 25		foam 26	
Force	Magnitude	*k*	*c*	*k*	*c*	*k*	*c*	*k*	*c*	*k*	*c*
disk 15											
500N	0.25 m/s²	70819	745	63982	661	52672	756	47515	682	53556	600
500N	0.5 m/s²	75105	666	64299	635	53905	665	50530	652	57475	598
500N	1.0 m/s²	71754	733	61263	662	53315	612	51315	586	55258	600
500N	1.5 m/s²	68267	732	58970	635	52218	580	50657	561	54393	574
500N	2.0 m/s²	65370	705	56703	639	50065	589	48739	581	52648	593
500N	2.5 m/s²	63085	702	55084	636	49272	578	47638	573	52823	560
300N	1.5 m/s²	66519	704	60884	658	58447	649	54291	578	54393	574
400N	1.5 m/s²	63186	690	59004	616	55536	621	51065	570	53309	567
500N	1.5 m/s²	68267	732	58970	635	52218	580	50657	561	54393	574
600N	1.5 m/s²	69837	747	62094	671	57628	686	52834	646	56065	630
700N	1.5 m/s²	65254	704	52924	629	48333	592	45772	563	49913	577
buttocks											
500N	0.25 m/s²	74414	386	61126	518	44358	495	36105	292	36691	391
500N	0.5 m/s²	66026	729	54333	639	44052	482	38800	337	35303	448
500N	1.0 m/s²	64930	710	55816	566	44615	501	35852	391	35887	406
500N	1.5 m/s²	65280	676	53598	592	42703	495	35156	382	35437	399
500N	2.0 m/s²	62186	677	52087	582	42368	448	33813	388	34503	382
500N	2.5 m/s²	61462	656	50120	593	41563	453	33224	382	34700	370
300N	1.5 m/s²	37392	381	34669	295	26083	284	22380	224	23557	229
400N	1.5 m/s²	48026	442	37822	395	33090	368	26573	262	26407	295
500N	1.5 m/s²	65280	676	53598	592	42703	495	35156	382	35437	399
600N	1.5 m/s²	93799	1001	75454	811	56897	708	47705	583	50093	577

Force	Magnitude	*k*	*c*	*k*	*c*	*k*	*c*	*k*	*c*	*k*	*c*
700N	1.5 m/s^2	42010	422	32330	354	27401	336	27824	316	30825	342
disk 20											
500N	0.25 m/s^2	49820	825	51633	616	37732	642	31776	490	42343	518
500N	0.5 m/s^2	57577	594	53556	531	44779	594	38690	427	48032	507
500N	1.0 m/s^2	55648	608	50444	592	46530	535	37894	458	46591	554
500N	1.5 m/s^2	52684	596	50432	549	46697	530	37093	448	46759	530
500N	2.0 m/s^2	50791	574	48357	554	44683	535	36923	434	45980	524
500N	2.5 m/s^2	48476	573	46868	572	43720	535	36306	433	45289	516
300N	1.5 m/s^2	43758	442	43607	442	40017	454	33245	387	36693	416
400N	1.5 m/s^2	44261	511	42999	451	40541	470	32731	388	41500	444
500N	1.5 m/s^2	52684	596	50432	549	46697	530	37093	448	46759	530
600N	1.5 m/s^2	62995	700	61235	629	55261	675	45924	548	52582	568
700N	1.5 m/s^2	42833	448	34746	436	32221	380	34958	437	31771	366
disk 25											
500N	0.25 m/s^2	87452	956	78676	804	72420	803	58555	811	43007	667
500N	0.5 m/s^2	89159	904	75813	718	72815	844	61546	712	49485	565
500N	1.0 m/s^2	88352	909	74113	756	73532	811	61101	710	48592	578
500N	1.5 m/s^2	85063	916	71077	809	71711	805	59487	708	48534	554
500N	2.0 m/s^2	82003	903	69294	785	69846	800	59500	686	48025	534
500N	2.5 m/s^2	79958	886	68377	772	68644	802	57500	703	45963	565
300N	1.5 m/s^2	63849	670	52719	561	53831	599	47531	536	39377	409
400N	1.5 m/s^2	75239	767	63656	694	64549	706	54093	640	44856	490
500N	1.5 m/s^2	85063	916	71077	809	71711	805	59487	708	48534	554
600N	1.5 m/s^2	102080	1127	75991	846	73789	869	61235	765	49372	594
700N	1.5 m/s^2	52081	566	42436	482	38351	443	32483	410	33999	414
SIT-BAR											
500N	0.25 m/s^2	50447	562	48273	553	40758	591	31613	478	29709	527
500N	0.5 m/s^2	50497	561	50003	611	42667	517	38208	479	39091	433
500N	1.0 m/s^2	51168	539	52105	578	45599	512	38842	446	38658	451
500N	1.5 m/s^2	48454	558	50856	574	44216	517	38072	459	38442	440
500N	2.0 m/s^2	47731	531	49215	553	43243	501	37902	444	37204	448
500N	2.5 m/s^2	47071	521	48341	554	42067	510	37229	443	36973	430
300N	1.5 m/s^2	56550	572	44127	498	41132	475	35811	440	35263	397

Force	Magnitude	*k*	*c*	*k*	*c*	*k*	*c*	*k*	*c*	*k*	*c*
400N	1.5 m/s²	63631	685	45028	496	38971	450	34373	397	34271	391
500N	1.5 m/s²	48454	558	50856	574	44216	517	38072	459	38442	440
600N	1.5 m/s²	112610	1205	54985	611	49353	553	39114	502	42284	490
700N	1.5 m/s²	58689	661	48651	558	39893	486	33033	437	36105	449

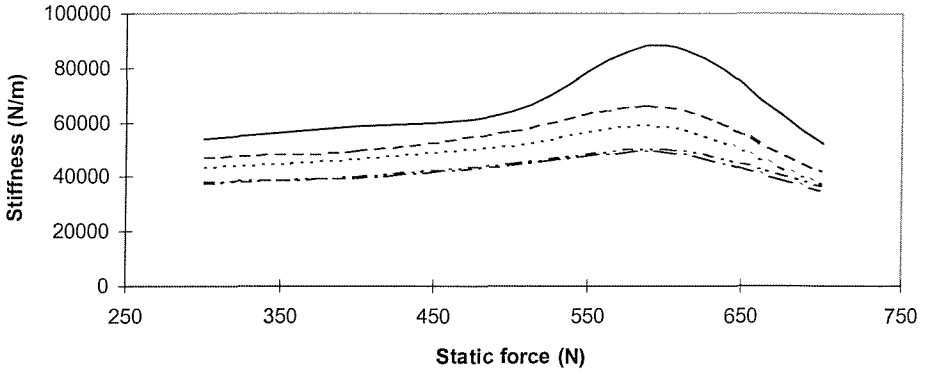

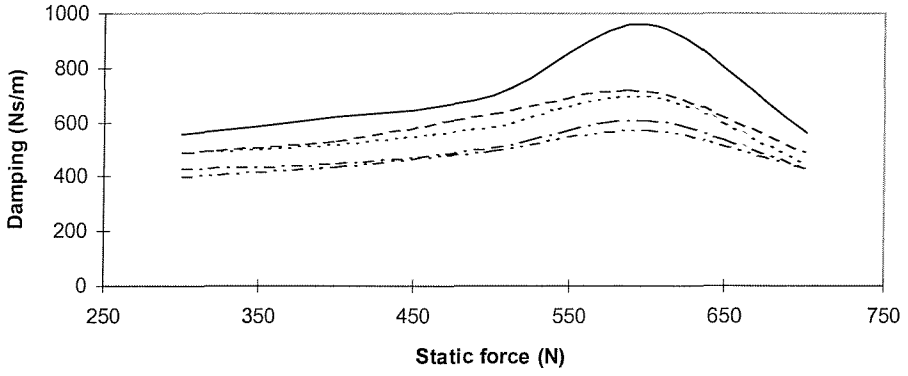

Figure 5.22. The effect of static force on measured foam stiffness and damping with the mean of five different contact areas at an input magnitude of 1.5 m/s² (foam 22 ———, foam 23 - - - - - -, Foam 24 · · · · · · · ·, foam 25 - · - · - ·, foam 26 - · - · - · - · - ·).

Figure 5.24 shows the mean variation in the stiffness and damping of the foams with the different indenter contact areas. It can be observed that the stiffness and damping of the foams increased with the pre-load increasing from 300 N to 600 N, except for indenter disk 15.

5.3.3.3 Statistical correlation between indenter head and foam stiffness, indenter head and foam damping

5.3.3.3.1. Hypothesis

The null hypothesis was that the stiffness and damping measured at one static force, one vibration magnitude and with different indenter areas is independent of indenter contact area. In other words, there is not a correlation between the indenter head area and the measured foam stiffness and damping.

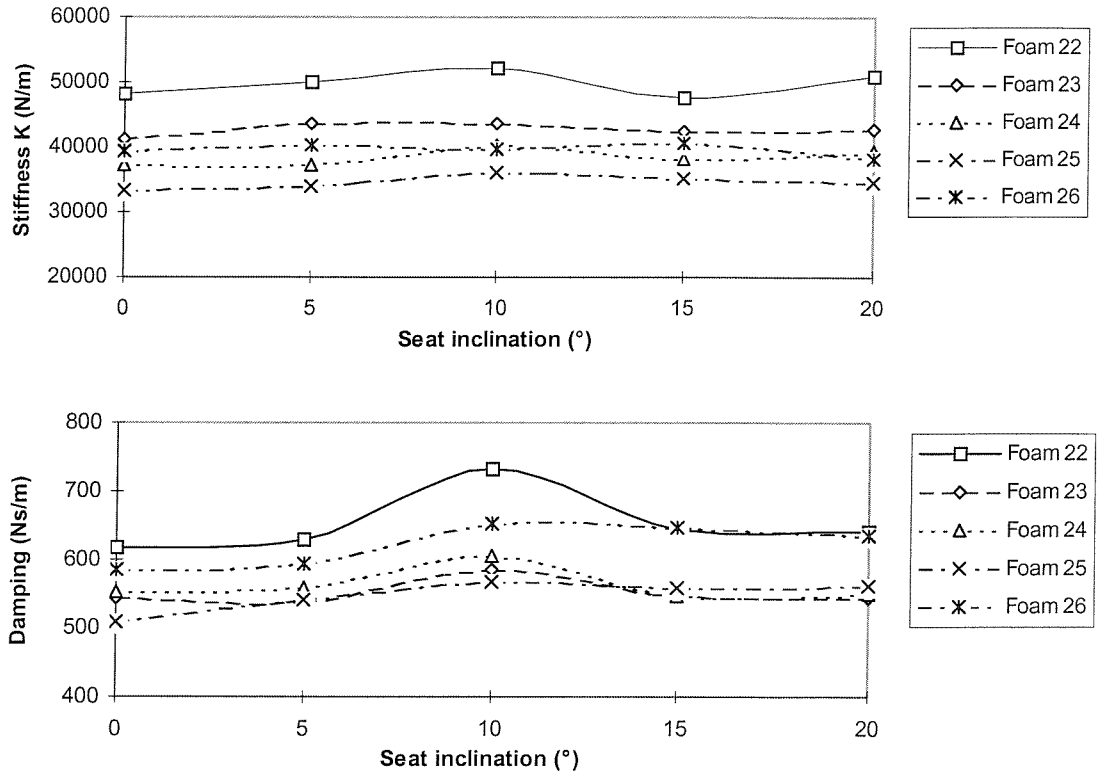

Figure 5.23 The effect of inclination angles on measured foam stiffness and damping with SIT-BAR indenter at an input magnitude of 1.5 m/s².

5.3.3.3.2. Statistics result

Table 5.7 shows that there was no consistent correlation between the indenter head area and the foam stiffness or damping (p>0.188 in Table 5.7, Spearman nonparametric correlations two-tailed test). The hypothesis proposed above is confirmed.

Table 5.6 Foam stiffness and damping at different inclinations

	foam 22		foam 23		foam 24		foam 25		foam 26	
inclinations	K N/m	C Ns/m	K	C	K	C	K	C	K	C
0^0	48278	619	41190	545	37237	554	33412	510	39274	586
5^0	50111	629	43624	539	37207	559	33874	542	40317	595
10^0	52041	732	43654	584	40205	606	35965	569	39788	652
15^0	47703	643	42554	546	38179	546	35081	560	40512	648
20^0	51030	640	42602	544	39366	550	34475	563	38299	634

Table 5.7 The Spearman correlation between indenter head area and the foam stiffness and damping.

			K -v- contact area		*C* -v- contact area	
Static force	vibration magnitude	Foam	Correlation coefficient range (-1 to 1)	Significance level, *p*	Correlation coefficient range(-1 to 1)	Significance level, *p*
500N	1.5 m/s²	foam 22	0.1	0.873	0.1	0.873
500N	1.5 m/s²	foam 23	0.2	0.747	0.2	0.747
500N	1.5 m/s²	foam 24	-0.4	0.505	-0.4	0.505
500N	1.5 m/s²	foam 25	-0.3	0.624	-0.3	0.624
500N	1.5 m/s²	foam 26	-0.7	0.188	-0.7	0.188

5.3.4 Predicting foam transmissibility

The equivalent stiffness and damping of the foams as determined from the experimental data showed that with different contact areas and different static forces these parameters varied greatly. In order to find a reasonable contact area for foam testing, the various parameters were used to predict the foam transmissibility. Wei and Griffin (1995) have previously used this method to predict the transmissibility of both foams and seats using a SIT-BAR indenter. At first, one subject's apparent mass was measured, and the data used to obtain a two-degree-of-freedom mathematical model of the subject (Wei and Griffin 1998). Secondly, the subject's mathematical model was combined with the foam model to predict the foam transmissibility. Finally, the foam transmissibility was measured with the subject and compared with the prediction. The results are shown in Figures 5.25 to 5.29.

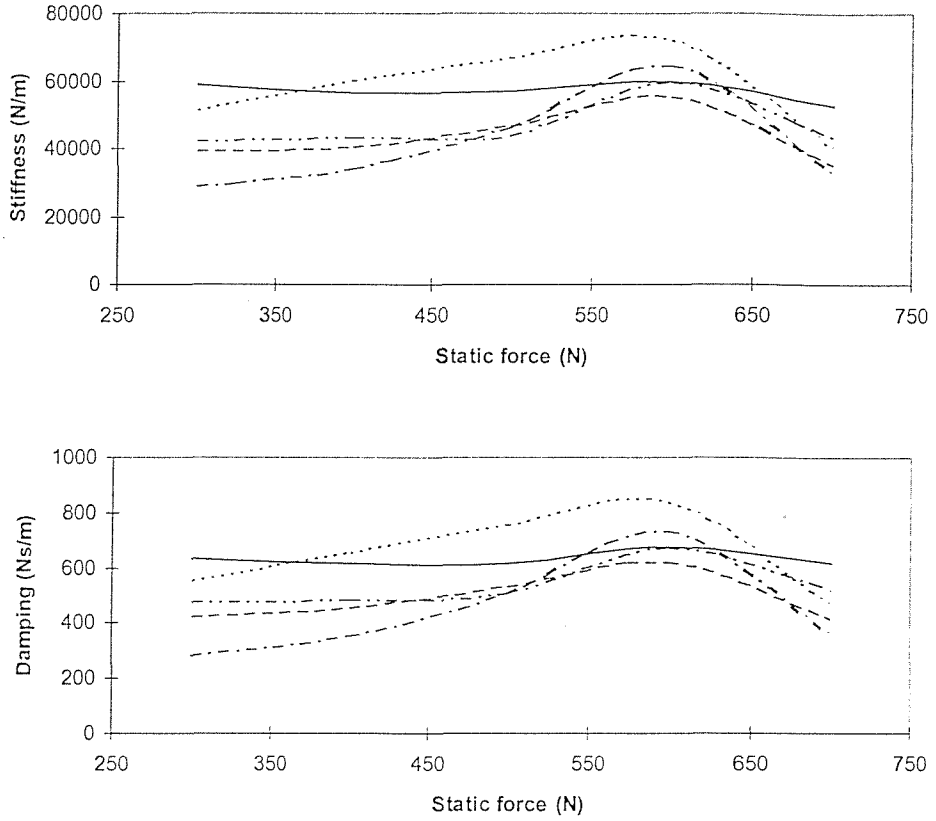

Figure 5.24. The effect of static force on measured foam stiffness and damping with the mean of five different foams at an input magnitude of 1.5 m/s² (disk 15 ———, disk 20 - - - - - -, disk 25 · · · · · · · ·, buttocks - - - - - - - -, SIT-BAR - - - - - - - - - -).

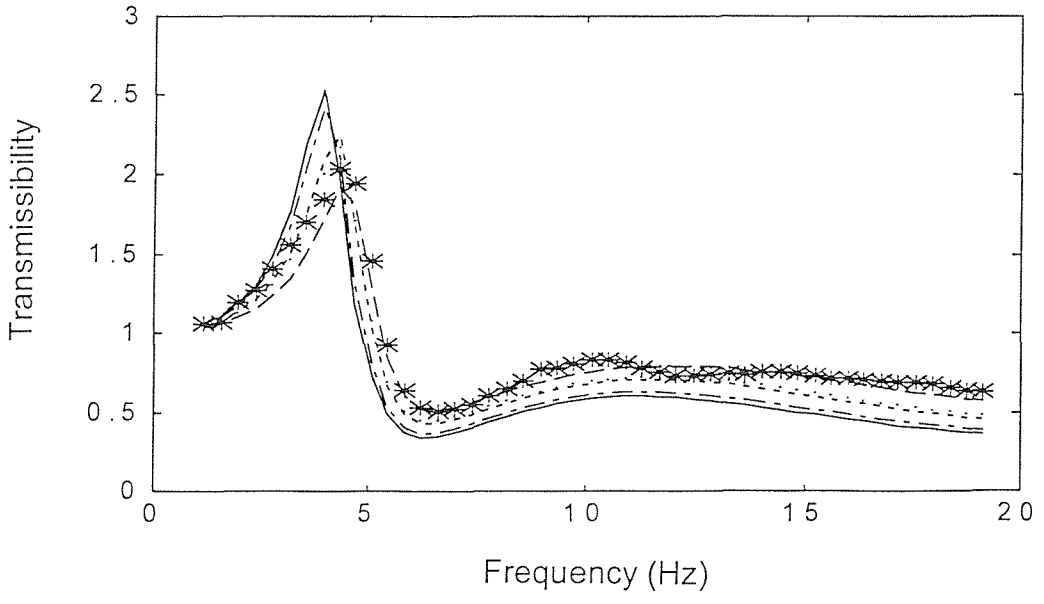

Figure 5.25. Foam 22 comparison of measured transmissibility using one subject with that predicted using five different contact areas. (Disk 15; Buttocks · · · · · · · ·, Disk 20 - - - - - - - -, Disk 25 — — — —, SIT-BAR———, Real subject ***).

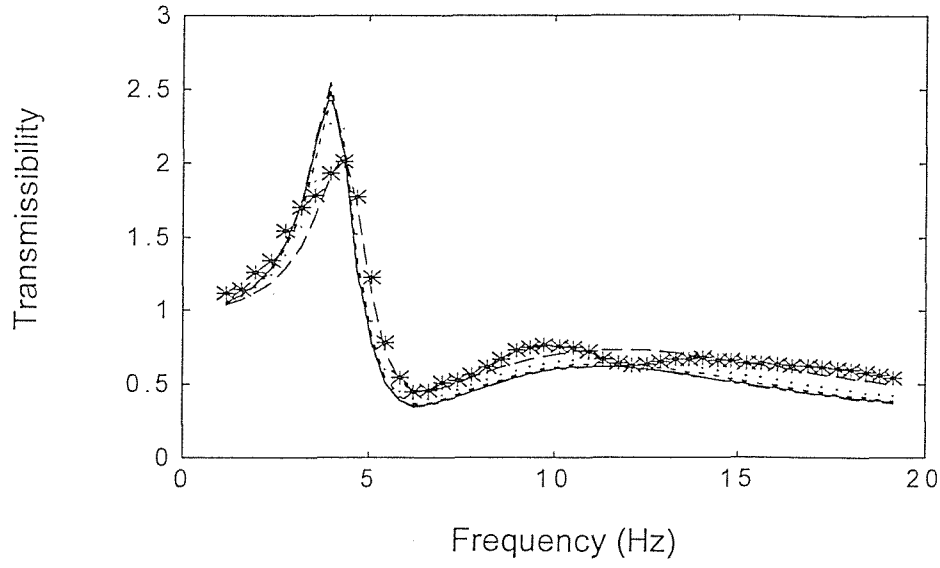

Figure 5.26. Foam 23 comparison of measured transmissibility using one subject with that predicted using five different contact areas. (Disk 15; Buttocks · · · · · · · ·, Disk 20 - - - - - - - -, Disk 25– – – –, SIT-BAR———, Real subject ***).

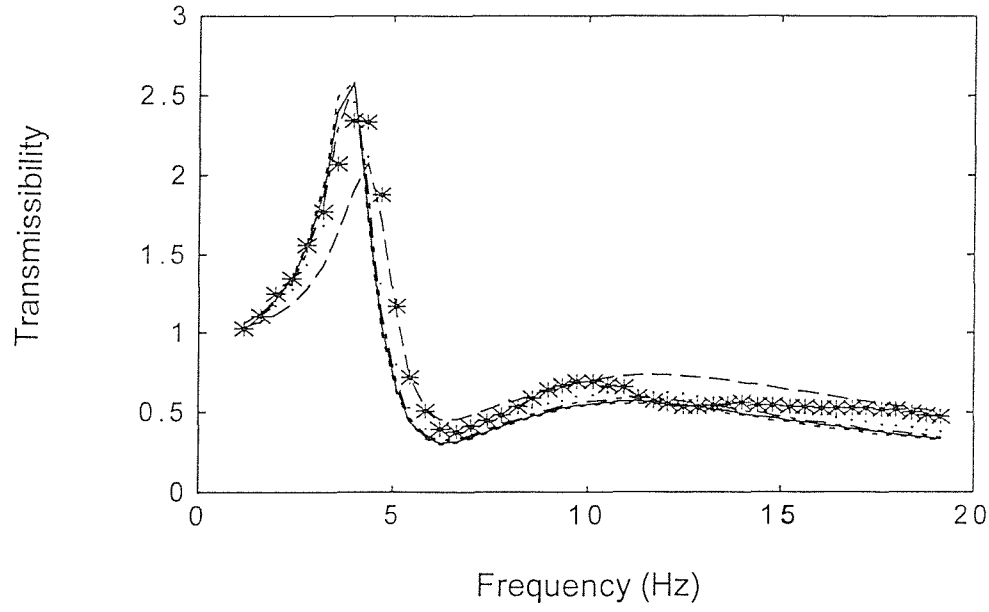

Figure 5.27 Foam 24 comparison of measured transmissibility using one subject with that predicted using five different contact areas. (Disk 15; Buttocks · · · · · · · ·, Disk 20 - - - - - - - -, Disk 25– – – –, SIT-BAR———, Real subject ***).

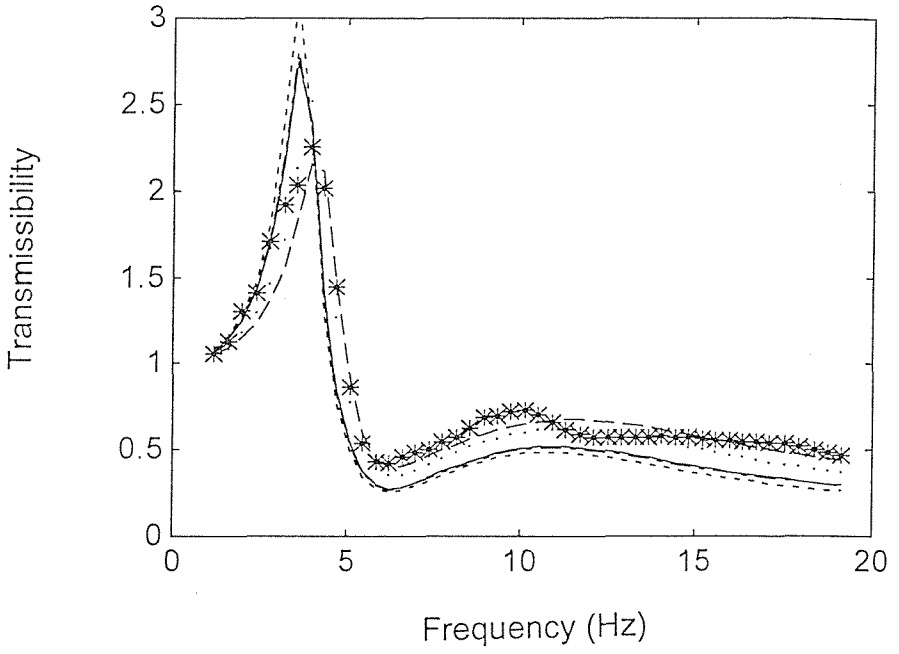

Figure 5.28. Foam 25 comparison of measured transmissibility using one subject with that predicted using five different contact areas. (Disk 15; Buttocks · · · · · · · ·, Disk 20 - - - - - - - -, Disk 25– – – –, SIT-BAR———, Real subject ***).

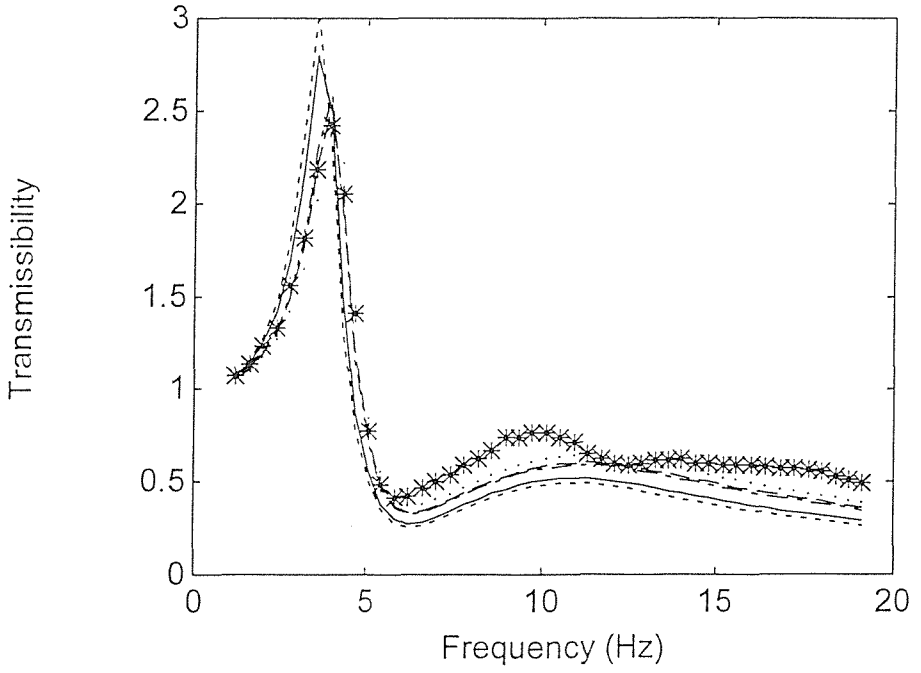

Figure 5.29. Foam 26 comparison of measured transmissibility using one subject with that predicted using five different contact areas. (Disk 15; Buttocks · · · · · · · ·, Disk 20 - - - - - - - -, Disk 25– – – –, SIT-BAR———, Real subject ***).

Figures, 5.25 to 5.29, show that the data measured from the disk 25 can give better foam transmissibility predictions than the data measured from other indenter shapes. Although a buttocks has a similar shape to the subject, the data measured from it could not give a good foam transmissibility prediction.

5.3.5 Discussion

5.3.5.1 Contact areas

The shape of the HYBRID III exterior had the largest contact area, but using a 250 mm diameter disk produced a greater foam stiffness and a greater damping. However, it is impossible to say which contact area produced the greatest or least dynamic parameters for the foam. This suggests that the stiffness and damping of the foam were not only affected by the contact area.

The shape of the HYBRID III buttocks is approximately the same as the seated human body, except that it was rigid and the tissue of the body is flexible. If we do not consider other factors, it is reasonable to use this for foam testing. However, in this experiment the buttocks appears to offer different foam dynamic stiffness than that obtained with the subject, so we cannot currently recommend it for obtaining a good prediction of foam transmissibility. The previous study (5.2.2.2) showed also problems when measuring seat dynamic properties using a buttocks.

5.3.5.2 Static forces

With the different static forces used in this study, the stiffness and damping increased with some increases in force, but this was not consistent.

5.3.5.3 Vibration magnitudes

It is well known that different input magnitudes affect seat or foam transmissibility when measured with human subjects, but in this study we cannot see a large or consistent difference in the parameters with increases in vibration magnitude (Table 5.5 and Figure 5.21). This indicates that the non-linearity in foam transmissibility may be affected mostly by the human body,

whose dynamic properties change with different applied vibration magnitudes (Fairley 1989; Mansfield and Griffin 1998; Wei and Griffin 1998).

5.3.5.4 Inclination angles

With the different inclination angles used in this study, the stiffness and damping changed only a little as the inclination increases.

5.3.5.5 Different foams

Two kinds of foam were used in this study, TDI and MDI. Among the TDI foams, when the density increased, the damping and stiffness decreased (Table 5.5).

This study only investigated foams. It is recommended that selected seats and more subjects are used to investigate the effects of contact area, contact force and vibration magnitude more completely.

5.3.5.6 Foam test method

Using five differently shaped heads for the indenter to obtain the foam or seat dynamic properties is only one of several methods of determining foam response to vibration. It is desirable to compare the results using this method with the results obtained when using a rigid mass or a mechanical dummy (see Section 5.2.2.1).

5.3.6 Conclusion

5.3.6.1 Contact areas

The contact area between the indenter and the foam or seat is important, because with different indenters the foam dynamic response varied (see Table 5.5).

With different contact areas the foam dynamic response changed greatly (Figure 5.24). In the present tests, disk 25 appeared to provide the most reasonable contact area for a foam test. When using this contact area, the

best prediction of foam transmissibility was achieved for one subject (Figures 5.25 to 5.29). This needs to be confirmed using more subjects.

5.3.6.2 Vibration magnitudes

The foam dynamic property varied slightly when the input vibration magnitude increased. From the foams tested it appears that similar results would have been achieved with any reasonable magnitude (for example 1 to 5 ms^{-2}) of vibration.

The effect of vibration magnitude on results of the indenter test for seats (Figure 5.13) is also small. When the sinusoidal vibration amplitude increased (i.e. the magnitude of vibration increase greater), the seat stiffness consistently decreased. Although the damping values were also changed at different vibration amplitude, there were no consistent variations.

5.3.6.3 Static forces

The parameters of the foams (Table 5.5, Figure 5.22) showed that the stiffness and the damping increased with increasing static load, but when the static force reached about 600N the stiffness and damping would fall again. It is recommended that an appropriate static force is needed when determining the foam or seat dynamic stiffnesses.

5.3.6.4 Inclination angles

The foam dynamic property varied only slightly when the input inclination angles increased. This confirms that the inclination angle is not an important factor in simple foam indenter tests.

5.3.6.5 Foam test method

Using an indenter to obtain foam dynamic properties is useful. It can provide appropriate parameters for the foam through setting up a foam mathematical model using data fitting techniques.

5.4 Conclusions

There are many methods to measure seat or foam dynamic properties, but the indenter method gives more reasonable results than some alternatives.

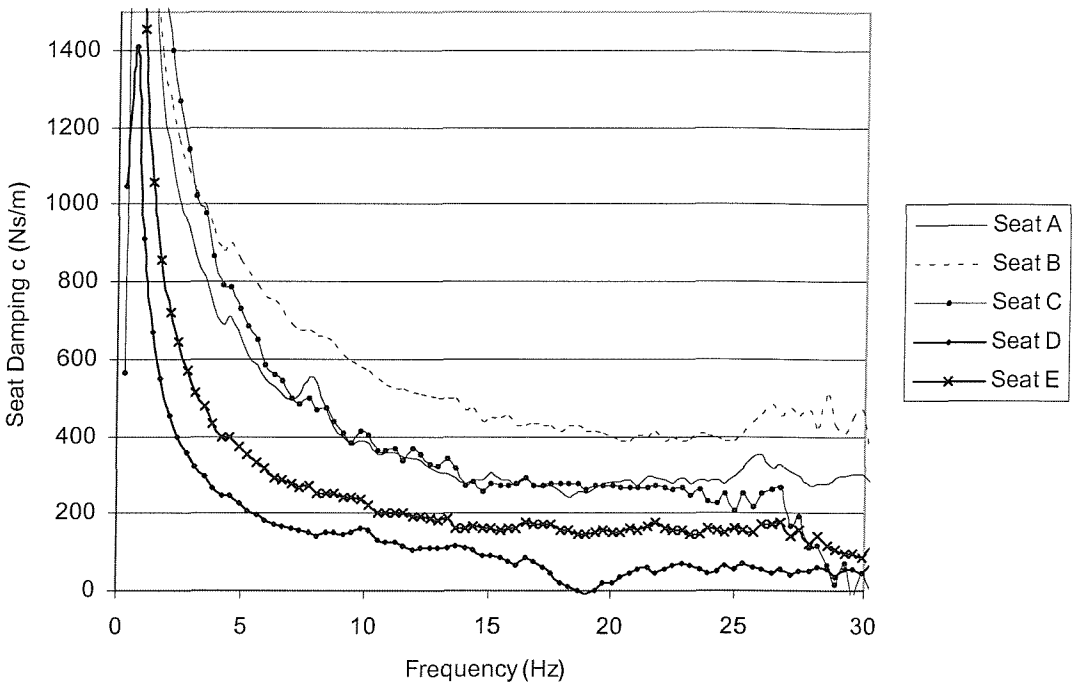

Figure 5.29 Measured damping of 5 car seats

There are correlations between seat static and seat dynamic stiffness. Seats with greater static stiffness seem to also have higher dynamic stiffness (see Section 5.2.2.2), but this precept is not true for seat damping (see Figure 5.30).

Seat stiffness, *k*, increases with frequency increase (Figure 5.11 to 5.13) but seat damping, *c*, decreases with frequency increase from 2 to 15 Hz. (Figure 5.30). The measured seat damping, c, is shown in Figure 5.30 which comes from Figure 5.11.

Vibration magnitude is not very important in foam dynamic stiffness measurement if the change of vibration magnitudes is not large (Figure 5.21), but when vibration amplitude has a large change, such as Figure 5.13 showed, the change of vibration amplitude will affect foam dynamic stiffness. Greater vibration amplitude produces lower foam dynamic stiffness.

Static force, or pre-load, plays a large role in determining seat dynamic stiffness and damping. So the correct pre-load must be selected for any seat or foam test.

The effect of inclination angle is small for foam indenter tests. The stiffness and damping of the foam change a little with different inclination angles.

The type or composition of foam has a significant effect on seat physical values, so optimising foam composition may be used to obtain good seat static and dynamic comfort.

The choice of indenter head is also important in determining seat or foam physical values. The buttocks had a similar shape to the human subject, but the results when using the buttocks are not satisfactory. Using the buttocks causes many problems in measuring seat dynamic properties (see Section 5.2.2.2). In the present tests, disk 25 appeared to provide the most reasonable contact area for a foam test, but it will result in same problem with buttocks in measuring seat dynamic property (both cause big twist force). The SIT-BAR is more reasonable for seat tests.

The effect of factors on indenter tests have been conducted for only shaped foams in this study. So similar investigations are needed for various seats so that a standard method can be developed for seat tests.

CHAPTER 6

MODELLING MECHANICAL RESPONSES OF THE SEATED HUMAN BODY IN THE VERTICAL DIRECTION

6.1 Introduction

The biodynamic responses of the human body influence the manner in which vibration causes discomfort and injury and interferes with activities. Purely numerical considerations of body dynamics have been reported, but the complexity of the human body dictates a vital role for experimentation in the development of understanding of human responses to vibration. There are currently insufficient data to derive a 'complete' mathematical model of the movement of the body during exposure to vibration and also insufficient information to fully justify the form of complex models of body responses. The development of complex models of the responses of the body requires an understanding of the modes of oscillation of the body.

Biodynamic models may either seek to explain the form of body motion caused by vibration or seek to provide a simple mathematical summary of the effect of this response. For example, a model which explains the seat-to-head transmissibility of the human body will be exceedingly complex (Kitazaki and Griffin 1997), but for some purposes a single degree-of-freedom model may adequately summarise the transmissibility of a group of people (Griffin *et al.* 1979). The aim in this chapter is to present a model for the driving point apparent mass of the seated human body without proposing the mechanisms and movements of the body responsible for this apparent mass.

Driving-point frequency response functions, such as mechanical impedance and apparent mass, have been determined at the seat-person interface for vertical whole-body vibration in various studies, but only a few investigations have resulted in a mathematical model or fully investigated the parameters of the model. The mechanical impedance of the human body could be

represented by a discrete system of masses, springs and dampers (e.g., models proposed by Vogt *et al.* 1968; Suggs *et al.* 1969; Kaleps *et al.* 1971; International Organization for Standardization 1981) or a distributed parameter model (e.g., Liu *et al.* 1973; Cramer *et al.* 1976). The number of degrees of freedom required in a model depends on the purpose of the model: a model explaining the motion of the human body will tend to be more complex than the simplest model giving an approximation to the driving point impedance. For example, the 15 degree-of-freedom model proposed by Nigam and Malik (1987) and the finite element model derived by Kitazaki and Griffin (1997) are overly complex for the prediction of the average point impedance of a person sitting in a single posture and exposed to a single type of motion. Unless the sophistication of complex models is used to predict variations in impedance (e.g., with variations in posture or vibration magnitude) or to predict the motions of other body parts, they appear to have no advantage over simple models. For a simple model of the driving point apparent mass, the motions of body parts which do not contribute to the driving point apparent mass over the frequency range of interest can be ignored. Further, it may also be possible to represent a complex motion by a simpler motion that gives a similar apparent mass. Unnecessarily complex models are unnecessarily difficult to calculate and tend to present unfounded speculation on how the body moves.

The main purpose of the present study was to obtain an improved model of the apparent mass of the seated human body for use in procedures for predicting seat transmissibility. In a previous experiment, Fairley and Griffin (1989) measured the apparent masses of 60 seated subjects and derived a single degree-of-freedom model to fit the measured data. This model has been used successfully to predict seat transmissibility from measures of the dynamic stiffness and damping of seats (Fairley and Griffin, 1986). However, seat transmissibilities obtained with human subjects often show evidence of a two-degree-of-freedom response in the human body. This study involved a re-analysis of the earlier data so as to obtain an improved fit to the measured apparent masses of subjects.

6.2 Previous experimental results

The vertical (i.e. z-axis) whole-body driving-point apparent masses of sixty persons (12 children, 24 men, 24 women) were obtained with the subjects seated on a rigid force platform without a backrest (Fairley and Griffin, 1989). Subjects were exposed to 1.0 ms^{-2} r.m.s. random vertical vibration over the range 0.25 to 20 Hz. The subjects sat in a normal upright posture with their feet supported on a footrest which vibrated in phase with the seat. The force platform incorporated quartz piezo-electric force transducers mounted at the corners of a rectangular welded steel frame (Kistler 9281B). The top plate of this platform, on which the subjects sat, was 0.02m thick, 0.6m wide and 0.4m deep; it was 0.46 m above the footrest. The acceleration of the platform was measured on the top plate using an accelerometer.

The apparent mass frequency response function was presented in preference to other force response relationships (such as mechanical impedance or dynamic stiffness) because at zero-frequency it indicates the static weight of a person on the seat.

Fairley and Griffin calculated a 'normalised apparent mass' for each subject by dividing the apparent mass of each subject by the apparent mass at 0.5 Hz. The normalised apparent masses calculated from their sixty subjects are shown in Figure 2.37. The dynamic properties (i.e., mass, stiffness and damping) of a structure may be determined from suitable experimental frequency response data (Lee and Dobson 1991). However, current experimental data are insufficient to define the relevant movements of the human body during vibration and, therefore, they are also insufficient to determine the relevant masses, stiffness and damping of a structure that moves like the body during vibration. The experimental data suggest that just one or two degrees of freedom might accurately represent a subject's apparent mass over the 0 to 20 Hz frequency range; it is therefore reasonable to seek a model which does not move internally in the same way as the human body but has the same apparent mass. In this study, the simplest possible mathematical models having similar apparent masses to those of

human subjects were sought. It appears from Figure 2.37 that some subjects have apparent masses showing one degree of freedom while others show two degrees of freedom. For the present study, all reasonable one and two degree of freedom of systems were investigated as representations of subject apparent mass.

6.3 Derivation of mathematical impedance models

6.3.1 Single degree-of-freedom models.

A simple linear single degree-of-freedom model (model 1a) is shown in Figure 6.1. The mass, *m,* represents the weight of the person which is supported by tissues represented by the spring, *K,* and damping, *C.*

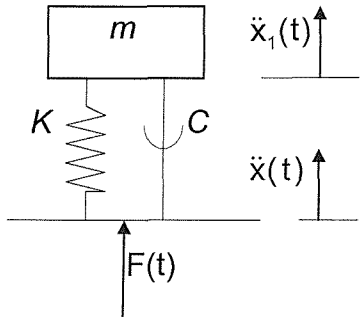

Figure 6.1 Single degree-of-freedom model (model 1a)

The equations of motion of this model are given by:

$$m\ddot{x}_1 = F(t) \qquad (6.1)$$

$$m\ddot{x}_1 + c(\dot{x}_1 - \dot{x}) + k(x_1 - x) = 0 \qquad (6.2)$$

The only force which can be transmitted to the model is *F(t).* Invoking the Laplace transform, one obtains for the steady state case:

$$F(s) = ms^2x_1(s) \qquad (6.3)$$

The acceleration and the velocity of the simulator, when transformed, will be:

$$\ddot{x}(s) = s^2x(s) \qquad (6.4)$$

$$\dot{x}(s) = s\,x(s) \qquad (6.5)$$

In order to arrive at a term that corresponds to the apparent mass one seeks to solve for $x_1(s)$ in terms of $x(s)$ by Newton's second law of motion:

$$m\ddot{x}_1 = k(x - x_1) + c(\dot{x} - \dot{x}_1) \qquad (6.6)$$

Upon taking the Laplace transforms and substituting ωi for *s*, the model in the frequency domain becomes:

$$x_1(\omega i) = \frac{k + c\omega i}{k - m\omega^2 + c\omega i} x(\omega i) \qquad (6.7)$$

Substituting for $x_1(\omega i)$ above gives

$$F(\omega i) = \left(\frac{m(k + c\omega i)}{k - m\omega^2 + c\omega i} \right) \ddot{x}(\omega i) \qquad (6.8)$$

The term in parentheses being the ratio of $F(\omega \mathrm{i})$ to $\ddot{x}(\omega i)$, is called apparent mass.

$$M(\omega i) = \frac{F(\omega i)}{\ddot{x}(\omega i)} = \frac{mk + imc\omega}{k - m\omega^2 + ic\omega} \qquad (6.9)$$

$$|M| = \sqrt{\frac{(mk)^2 + (mc\omega)^2}{\left(k - m\omega^2\right)^2 + (c\omega)^2}} \qquad (6.10)$$

$$\theta = a\tan\frac{mc\omega}{mk} - a\tan\frac{c\omega}{k - m\omega^2} \qquad (6.11)$$

Here *M* is the apparent mass and θ is the phase angle between force and acceleration .

It is difficult to make a real model like that shown in Figure 6.1 as there is no support for the mass other than the spring and damper and therefore no constraint to prevent rotational modes of vibration. An alternative single degree-of-freedom model (model 1b) is shown in Figure 6.2. In this model, the mass of the person is divided into two parts: a support structure, m_1, and a sprung mass, m_2. If a dummy were manufactured according to this model, a

constraint mechanism would be required to ensure that the sprung mass m_2 moved only in the vertical direction.

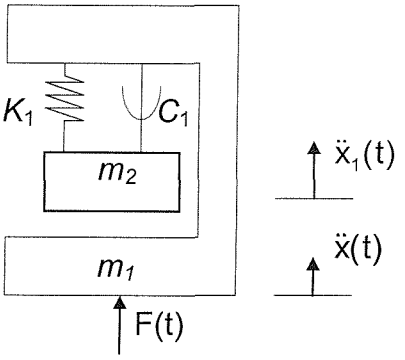

Figure 6.2 Single degree-of-freedom model with rigid support (model 1b)

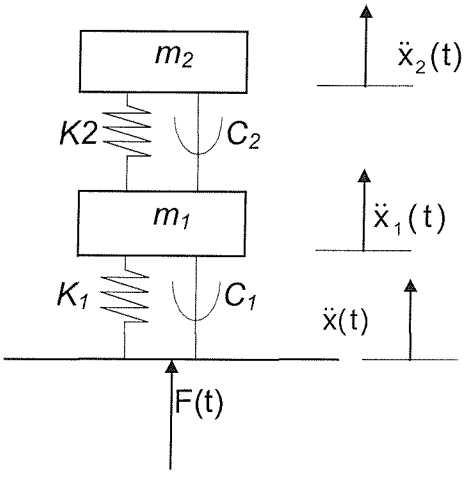

Figure 6.3 Two degree-of-freedom model (model 2a)

The response of this system is given by:

$$F(t) = m_1\ddot{x} + m_2\ddot{x}_1 \tag{6.12}$$

$$m_2\ddot{x}_1 = k_1(x - x_1) + c_1(\dot{x} - \dot{x}_1) \tag{6.13}$$

Based on the same analysis as above, the apparent mass is:

$$M(\omega i) = \left[m_1 + m_2\left(\frac{k_1 + c_1\omega i}{k_1 - m_2\omega^2 + c_1\omega i} \right) \right] \tag{6.14}$$

$$|M| = \sqrt{\frac{D1^2 + E1^2}{A1^2 + B1^2}} \tag{6.15}$$

$$\theta = \text{a}\tan\frac{\text{E1}}{\text{D1}} - \text{a}\tan\frac{\text{B1}}{\text{A1}} \qquad (6.16)$$

Where

$$A1 = k_1 - m_2\omega^2$$
$$B1 = c_1\omega$$
$$D1 = \left((m_1 + m_2)k_1 - m_1 m_2\omega^2\right)$$
$$E1 = (m_1 + m_2)\ \omega\ c_1$$

6.3.2 Two-degree-of-freedom models.

Measurements of the mechanical impedance of the human body usually show evidence of a two-degree-of-freedom response (see e.g., Figure 2.37, Mansfield and Griffin, 1998). For this reason, a two-degree-of-freedom system is also developed here.

Figure 6.3 shows a serial two-degree-of-freedom discrete model (model 2a). The motion equations of this system are:

$$m_2\ddot{x}_2 + k_2(x_2 - x_1) + c_2(\dot{x}_2 - \dot{x}_1) = 0 \qquad (6.17)$$
$$m_1\ddot{x}_1 + k_1(x_1 - x) + c_1(\dot{x}_1 - \dot{x}) + k_2(x_1 - x_2) + c_2(\dot{x}_1 - \dot{x}_2) = 0 \qquad (6.18)$$
$$F(t) = k_1(x - x_1) + c_1(\dot{x} - \dot{x}_1) = m_1\ddot{x}_1 + m_2\ddot{x}_2 \qquad (6.19)$$

The apparent mass is:

$$M(\omega i) = \frac{DD + EEi}{AA + BBi} \qquad (6.20)$$

$$|M| = \sqrt{\frac{DD^2 + EE^2}{AA^2 + BB^2}} \qquad (6.21)$$

$$\theta = \text{a}\tan\frac{\text{EE}}{\text{DD}} - \text{a}\tan\frac{\text{BB}}{\text{AA}} \qquad (6.22)$$

Here

$$AA = m_1 m_2\omega^4 - (m_1k_2 + m_2k_1 + m_2k_2 + c_1c_2)\ \omega^2 + k_1k_2$$
$$BB = (c_1k_2 + c_2k_1)\ \omega - (m_1c_2 + m_2c_1 + m_2c_2)\ \omega^3$$
$$DD = (m_1 + m_2)k_1k_2 - (m_1c_1c_2 + m_2c_1c_2 + m_1m_2k_1)\ \omega^2$$
$$EE = (m_1 + m_2)\ (c_1k_2 + c_2k_1)\ \omega - m_1m_2c_1\omega^3$$

A two-degree-of-freedom system having a support structure is shown in Figure 6.4 (i.e. model 2b). It has two mass-spring systems, m_1 and m_2, supported on the support mass, m. It is tempting to assume that the mass m_2 consists of the masses of the head and the upper torso while the mass m_1 represents the main part of the body and the mass m comprises the skeleton (Suggs *et al.* 1968). However, the models derived in this paper are not intended to represent the locations or mechanisms of body movement: the models show 'equivalent mechanical systems' only in that they have a similar mechanical impedance to the human body.

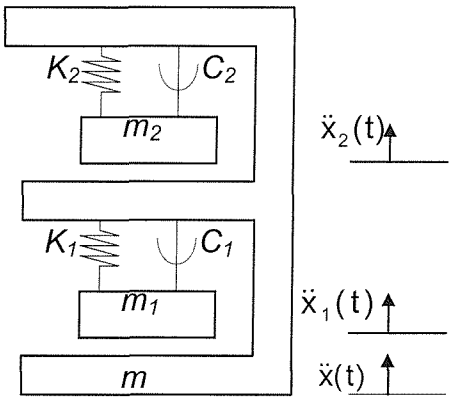

Figure 6.4 Two degree-of-freedom model with rigid support (model 2b)

The equations for vertical axial motion of the model in Figure 6.4 are:

$$F(t) = m\ddot{x} + m_1\ddot{x}_1 + m_2\ddot{x}_2 \tag{6.23}$$

$$m_1\ddot{x}_1 = k_1(x - x_1) + c_1(\dot{x} - \dot{x}_1) \tag{6.24}$$

$$m_2\ddot{x}_2 = k_2(x - x_2) + c_2(\dot{x} - \dot{x}_2) \tag{6.25}$$

The solution of the above equations has the following form:

$$M(\omega i) = \frac{D + E + (F + G)i}{A + Bi} \tag{6.26}$$

$$|M| = \sqrt{\frac{(D+E)^2 + (F+G)^2}{A^2 + B^2}} \tag{6.27}$$

$$\theta = \mathrm{a}\tan\frac{F+G}{D+E} - \mathrm{a}\tan\frac{B}{A} \tag{6.28}$$

Here:

$$A = k_1k_2 - \omega^2(k_1m_2 + k_2m_1) + m_1m_2\omega^4 - c_1c_2\omega^2$$
$$B = (k_1c_2 + k_2c_1)\ \omega - (m_1c_2 + m_2c_1)\ \omega^3$$
$$D = (m + m_1 + m_2)k_1k_2 - (mm_2k_1 + mm_1k_2 + m_1m_2k_1 + m_1m_2k_2)\ \omega^2$$
$$E = mm_1m_2\omega^4 - (mc_1c_2 + m_1c_1c_2 + m_2c_1c_2)\ \omega^2$$
$$F = (m + m_1 + m_2)\ (k_1c_2 + k_2c_1)\ \omega$$
$$G = -(mm_1c_2 + mm_2c_1 + m_1m_2c_2 + m_1m_2c_1)\ \omega^3$$

6.4. Fitting the mathematical models to the experimental data

6.4.1 Fitting to the mean responses

The optimum forms of the models shown in Figures 6.1 to 6.4 were determined by curve fitting to the experimental data obtained by Fairley and Griffin (1989). The least square error method and an optimisation algorithm were utilised again (Dierckx 1995). The parameters in the equations of each model were refined to minimise the function:

$$error = \frac{1}{N}\sum_{i=1}^{N}\left(M_f(i) - M(i)\right)^2 \qquad (6.29)$$

Where $M_f(\iota)$ is the modulus of the apparent mass from the curve fit at the *i*th frequency point and $M(\iota)$ is the modulus of the apparent mass from the measured data. With values of the parameters chosen at random used for starting values, the parameters were varied systematically using an optimisation algorithm (Dierckx 1995). The curves corresponding to the modulus and phase of the normalised apparent mass of each of the models are compared with the corresponding mean of the measured normalised apparent masses of the 60 subjects in Figure 6.5.

By using a similar method of fitting based on the phase of the apparent mass, somewhat different models were obtained with responses as shown in Figure 6.6.

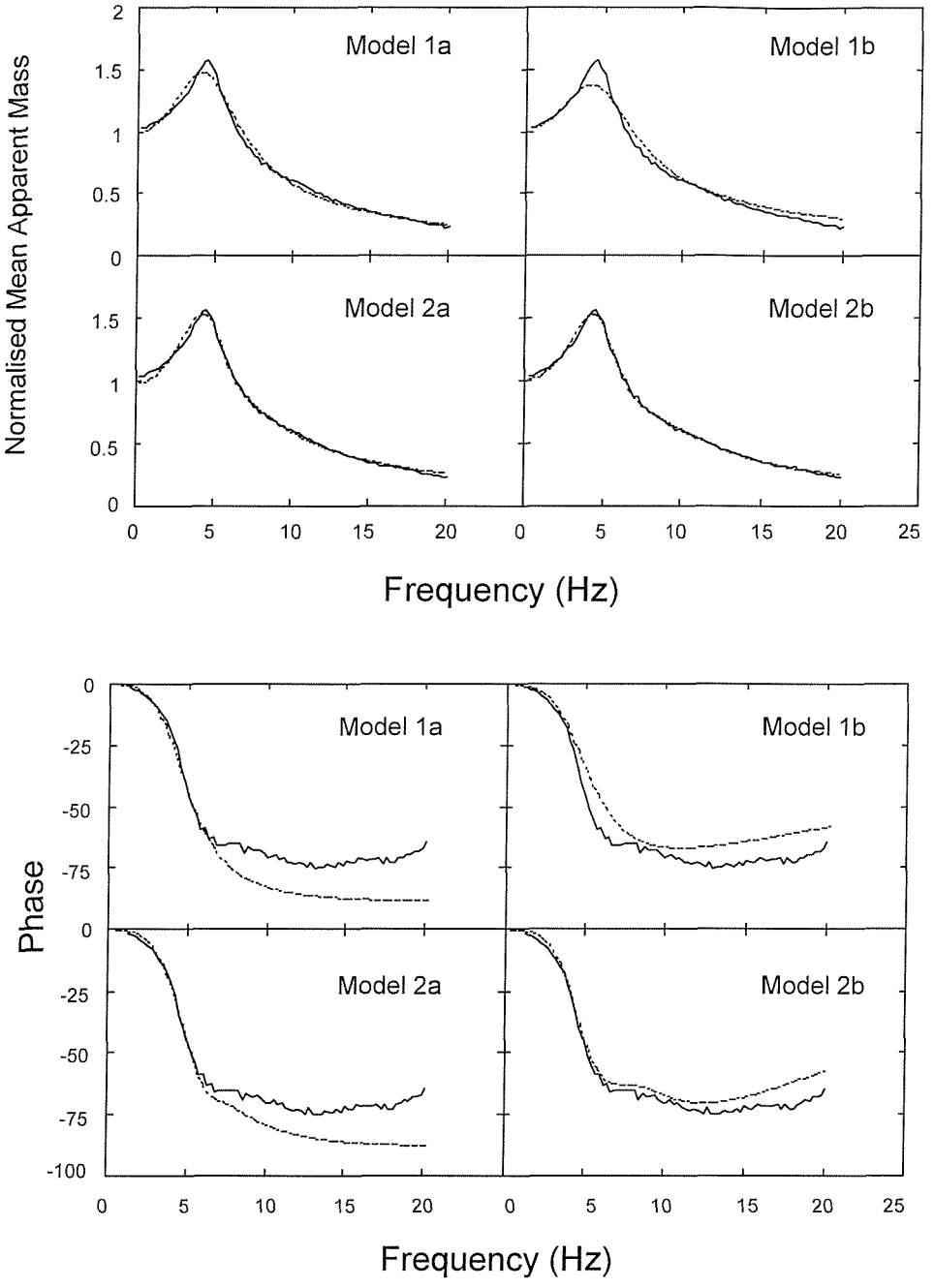

Figure 6.5 Mean modulus and phase of normalised apparent masses of 60 subjects compared with optimised responses of model 1a, 1b, 2a and 2b fitted by minimising the error in the modulus (—— experimental data, - - - - - fitted curves).

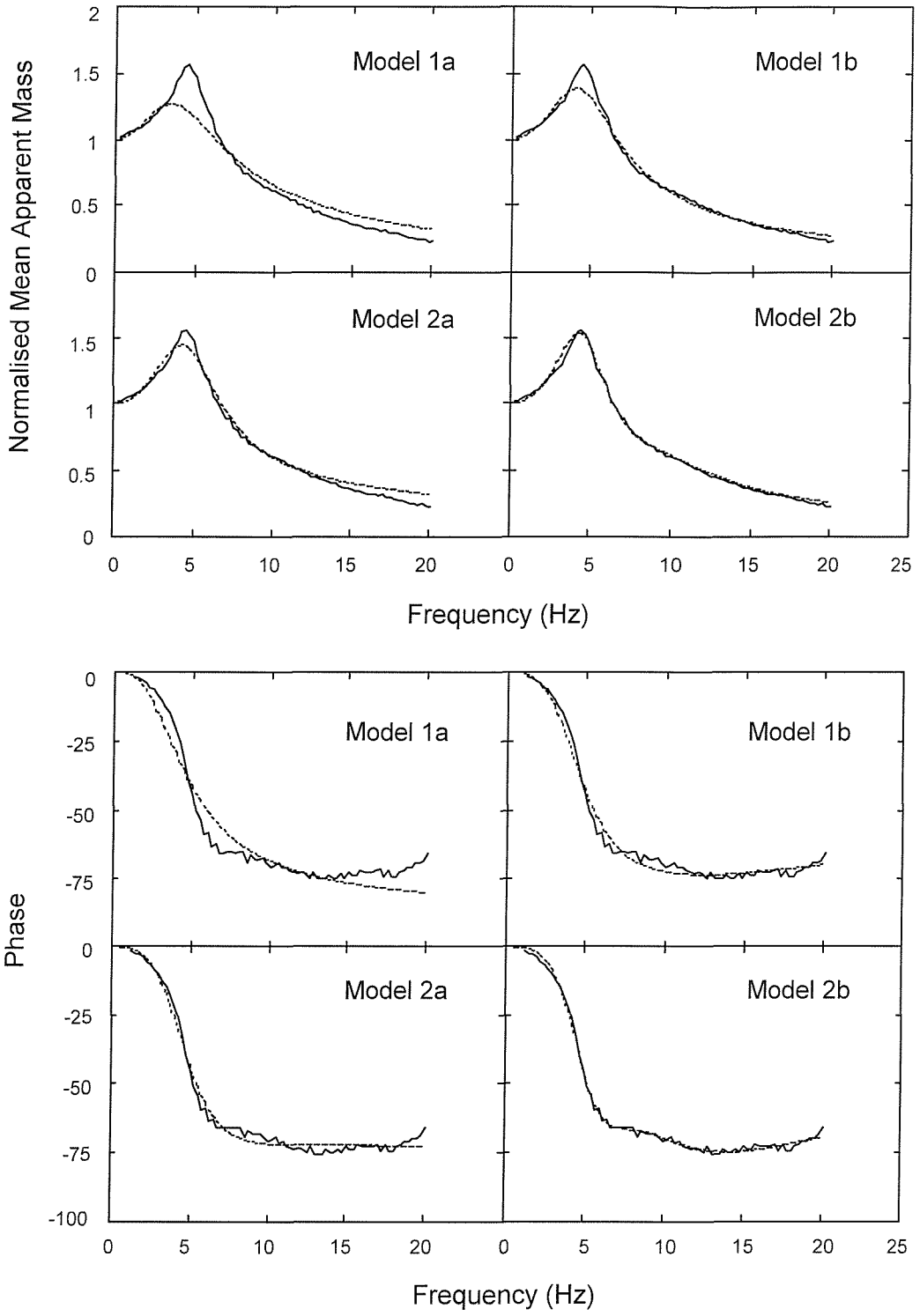

Figure 6.6 Mean modulus and phase of normalised apparent masses of 60 subjects compared with optimised responses of model 1a, 1b, 2a and 2b fitted by minimising the error in the phase (—— experimental data, - - - - - fitted curves).

From Figures 6.5 and 6.6 it was concluded that model 1b and model 2b obtained with phase fitting provided the best fits to the mean of the measured

data. The results in Figure 6.6 suggest that the apparent mass is dominated by a single mode. However, this is really two modes combined together: the two natural frequencies of the two-degree-of-freedom system are very close. Due to the high damping, the two-degree-of-freedom synthesised system shows only one peak. Where a single mode dominates, the response of such a system can be approximated by a single mode with a constant term added to represent the effect of other modes that are above the frequency range of interest. The support mass, m, may represent these higher modes and so the model may not be applied at frequencies higher than those studied here.

6.4.2 Fitting to the individual responses

The form of models 1b and 2b were used to obtain the best fits to the measured apparent masses of each of the 60 subjects who participated in the experiment. The models were fitted by minimising the difference in phase between the measured and predicted responses. The values for each mass, stiffness and damping in both models calculated for each of the subjects are listed in Tables 6.1 and 6.2. For these tables the subjects are separated into the three groups (men, women and children). Within each part of the table, the mean values are the mean values of mass, stiffness and damping within the group of men, women or children. At the foot of the table, the mean values are the mean values of mass, stiffness and damping over the group of 60 subjects. Also shown are the values of mass, stiffness and damping obtained by an optimum fit to the mean curve given by the arithmetic average of the 60 curves from the 24 men, 24 women and 12 children. The damping ratios for model 2b, which can be calculated through parameters in Table 6.2 are very high (in the range 0.24-0.4), so the effects of adjacent modes were combined. This is why increasing the number of modes in the model improved the curve fitting for a system which was dominated by a single mode.

The individual measured normalised apparent masses are compared with the predicted apparent masses in Figure 6.7 for model 1b and in Figure 6.8 for model 2b.

Table 6.1 degree of freedom model 1b fit to the experiment curves

Subjects	Sex	Age	k_1 (N/m)	c_1 (Ns/m)	m_1 (Kg)	m_2 (Kg)	Total mass (Kg)
1	M	26	34142	1187	1.3	44.6	45.9
2	M	16	41151	1122	8.8	35.6	44.4
3	M	39	71772	1845	21.3	86.7	108.0
4	M	38	62976	1631	4.3	52.8	57.1
5	M	34	34653	1312	5.0	47.8	52.8
6	M	33	29409	675	12.9	31.0	43.9
7	M	29	54623	1658	11.7	60.5	72.2
8	M	25	35756	1009	13.0	39.1	52.1
9	M	45	36286	898	15.3	32.7	48.0
10	M	51	66748	1705	0.1	65.8	65.9
11	M	16	38962	985	5.9	35.6	41.5
12	M	27	34822	954	17.2	39.0	56.2
13	M	56	70926	1447	6.8	59.0	65.8
14	M	17	54085	1475	1.4	59.4	60.8
15	M	69	71813	1173	20.9	34.7	55.6
16	M	27	46384	1797	2.1	51.3	53.4
17	M	39	66593	1377	4.7	51.5	56.2
18	M	39	68803	1833	3.4	80.4	83.8
19	M	50	42940	1286	12.2	46.7	58.9
20	M	45	77829	2345	2.1	76.2	78.3
21	M	17	48025	1165	13.6	46.5	60.1
22	M	23	42443	1083	3.1	43.9	47.0
23	M	23	52609	1204	17.3	40.7	58.0
24	M	17	63948	1636	0.9	43.3	44.2
mean 24 men			51987	1366	8.6	50.2	58.8
25	F	24	26951	957	4.8	38.9	43.7
26	F	56	48045	1217	11.7	48.1	59.8
27	F	22	58890	1486	.5	45.3	45.8
28	F	45	40143	1565	3.1	48.6	51.7
29	F	55	58186	1277	1.5	39.7	41.2
30	F	52	37755	1792	0.4	52.8	53.2
31	F	25	36342	1170	12.1	39.9	52.0
32	F	23	38886	1925	1.1	52.2	53.3
33	F	40	32252	621	18.2	33.5	51.7
34	F	23	32174	935	13.8	36.5	50.3
35	F	17	45515	1403	2.2	50.7	52.9
36	F	35	38227	1178	15.4	41.2	56.6
37	F	25	43578	976	16.7	34.5	51.2

Subjects	Sex	Age	k_1 (N/m)	c_1 (Ns/m)	m_1 (Kg)	m_2 (Kg)	Total mass (Kg)
38	F	39	35351	1076	8.2	39.5	47.7
39	F	21	46037	1577	2.6	53.2	55.8
40	F	38	39493	823	11.9	28.8	40.7
41	F	24	50712	1172	9.6	38.4	48.0
42	F	31	30671	880	17.4	47.1	64.5
43	F	59	52524	1319	1.6	58.7	60.3
44	F	21	52151	1003	12.1	31.8	43.9
45	F	41	35154	826	14.9	37.4	52.3
46	F	38	38850	1435	0.1	50.2	50.3
47	F	22	39338	1909	0.8	42.9	43.7
48	F	31	42586	994	18.8	40.8	59.6
mean 24 women			41659	1230	8.3	42.9	51.3
49	F	10	34387	421	12.5	19.4	31.9
50	F	11	32487	762	7.0	26.4	33.4
51	F	7	24887	511	2.1	21.3	23.4
52	F	9	37977	923	2.2	31.1	33.3
53	F	11	36203	992	3.8	30.6	34.4
54	F	14	28960	734	5.5	24.7	30.2
55	M	11	35428	753	3.1	28.2	31.3
56	M	13	47668	1564	0.3	50.9	51.2
57	M	12	25937	820	11.1	34.9	46.0
58	M	13	31973	607	14.2	30.9	45.1
59	M	8	33395	718	3.5	27.5	31.0
60	M	13	31032	1387	0.3	41.4	41.7
mean 12 children			33361	849	5.5	30.6	36.1
mean 60 subjects			44130	1485	7.8	43.4	51.2
fit mean of 60 subjects			44115	1522	4.1	46.7	50.8

Figure 6.9 shows the mean and range of the measured normalised apparent masses of the 60 subjects compared with the fitted curves obtained using the overall mean values of mass, stiffness and damping of the 60 subjects for model 1b and model 2b. The relative values of the various masses and springs affect the frequency response. When K_1 increases and m_1 decreases, the first resonance frequency rises. If m_2 decreases the second peak will appear in the response. The interactions among the masses and springs are

complex, but a useful discussion in the context of human response to vibration requires greater knowledge of the body movements occurring during vibration.

Table 6.2 Two-degree-of-freedom model 2b fit to the experiment curves

Subjects	Sex	Age	k_1 (N/m)	c_1 (Ns/m)	k_2 (N/m)	c_2 (Ns/m)	m (Kg)	m_1 (Kg)	m_2 (Kg)	Total mass (Kg)
1	M	26	19480	379	33076	462	6.5	26.9	14.4	47.8
2	M	16	24769	495	32408	725	6.5	23.3	14.3	44.1
3	M	39	45996	654	74312	1181	15.2	56.3	30.7	102.2
4	M	38	46964	832	42583	433	8.4	38.2	9.4	56.0
5	M	34	28370	773	24781	277	8.2	37.3	6.6	52.1
6	M	33	27466	475	32673	262	6.9	29.1	6.4	42.5
7	M	29	43452	950	42592	521	10.6	48.4	11.5	70.5
8	M	25	32558	702	43856	370	4.7	36.7	8.4	49.8
9	M	45	24075	937	19473	341	10.6	18.4	18.5	47.5
10	M	51	62452	1539	8579	32	5.4	61.0	2.2	68.6
11	M	16	33378	617	26446	179	5.5	30.2	5.1	40.8
12	M	27	27158	444	61480	789	7.3	30.8	15.2	53.2
13	M	56	58555	866	39418	428	8.6	48.1	9.6	66.4
14	M	17	33199	584	38179	589	9.7	36.1	16.1	61.9
15	M	69	69489	1106	10696	1944	1.5	37.3	15.5	54.3
16	M	27	23999	450	57886	925	7.2	27.6	19.5	54.3
17	M	39	51950	774	41713	391	6.0	40.6	10.4	57.0
18	M	39	46763	723	66688	789	10.2	50.0	20.6	80.8
19	M	50	42940	1286	23580	62	12.2	46.7	4.4e-8	58.9
20	M	45	38524	694	63705	1419	10.1	37.3	30.1	77.5
21	M	17	39619	654	56222	639	5.5	39	12.7	57.2
22	M	23	33234	489	48621	465	4.7	33.8	10.8	49.3
23	M	23	44330	713	76006	949	3.4	36.9	15.9	56.1
24	M	17	38983	522	63842	463	8.3	26.8	11.9	47.0
mean 24 men			39071	736	42867	609	7.6	37.4	13.2	58.2
25	F	24	14024	212	32783	671	6.2	19.9	16.6	42.7
26	F	56	58657	1392	21911	236	9.4	30.7	23.1	63.3
27	F	22	57632	801	23411	269	9.3	19.4	18.6	47.4
28	F	45	28143	780	32115	455	6.9	34.6	10.1	51.6
29	F	55	32519	479	38142	348	8.8	23.0	10.4	42.2
30	F	52	29715	762	50028	466	5.5	36.1	10.8	52.5
31	F	25	35293	981	27790	127	7.0	39.1	3.9	50.0
32	F	23	24838	592	54586	625	7.8	30.6	14.3	52.7
33	F	40	27850	427	45774	706	8.6	29.6	10.7	48.9
34	F	23	29510	1201	9738	137	7.2	30.0	11.7	48.8

Subjects	Sex	Age	k_1 (N/m)	c_1 (Ns/m)	k_2 (N/m)	c_2 (Ns/m)	m (Kg)	m_1 (Kg)	m_2 (Kg)	Total mass (Kg)
35	F	17	23768	325	62185	910	9.3	28.2	21.6	59.1
36	F	35	35475	779	52313	402	7.2	37.8	9.0	54.0
37	F	25	42718	791	44800	273	8.4	35.0	6.1	49.5
38	F	39	30298	635	34964	258	5.1	33.7	7.2	45.9
39	F	21	53928	1276	12718	156	5.6	33.7	16.7	56.0
40	F	38	34767	604	32934	357	7.0	26.2	5.7	38.9
41	F	24	50012	1402	9332	76	5.4	33.7	7.5	46.6
42	F	31	27309	618	38489	526	10.0	42.0	10.2	62.2
43	F	59	36931	578	37228	560	9.1	39.2	14.1	62.5
44	F	21	51014	930	40675	494	4.3	33.0	5.4	42.7
45	F	41	23601	350	35771	736	9.6	25.6	14.3	49.5
46	F	38	33723	886	27262	204	5.3	39.7	5.6	50.6
47	F	22	29733	1291	20719	134	4.6	34.8	4.6	44.0
48	F	31	36403	1720	18585	224	6.6	32.4	18.5	57.6
mean 24 women			35328	825	33511	340	7.3	32.0	11.5	50.8
49	F	10	37407	537	37561	199	4.1	23.1	4.1	31.3
50	F	11	31410	617	14398	55	5.0	25.6	1.9	32.5
51	F	7	24672	500	261	8.8	0.9	21.2	1.1	23.2
52	F	9	32118	814	87658	120	2.1	30.8	0.5	33.4
53	F	11	24752	1002	8911	43	2.4	29.8	3.7	35.9
54	F	14	26590	568	19975	159	3.5	22.9	3.2	29.6
55	M	11	35428	754	74657	1271	3.1	28.2	1.1e-8	31.3
56	M	13	36735	744	45494	355	7.3	35.0	9.5	51.8
57	M	12	25934	820	14442	455	4.1	34.9	7.0	46.0
58	M	13	29360	446	45128	653	4.3	29.5	9.9	43.7
59	M	8	33395	718	95584	9.6	3.6	27.5	1.1e-7	31.1
60	M	13	23199	682	25296	168	6.9	28.8	5.8	41.6
mean 12 children			30083	683	39114	291	3.9	28.1	3.9	36.0
mean 60 subjects			35776	761	38374	458	6.7	33.4	10.7	50.8
fit mean of 60 subjects			35007	815	33254	484	5.6	36.2	8.9	50.7

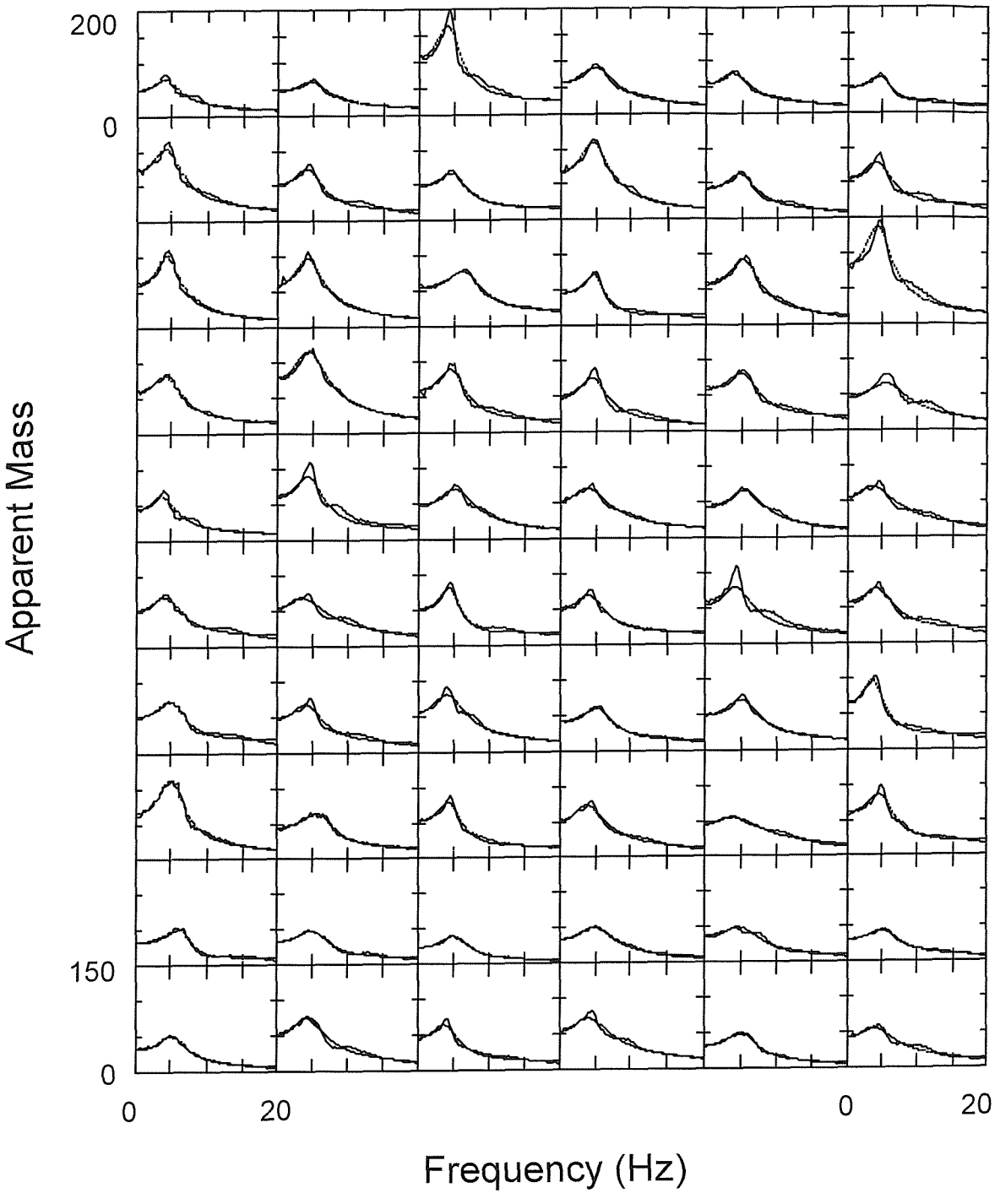
200
0
150
0
0
20
0
20
Apparent Mass
Frequency (Hz)

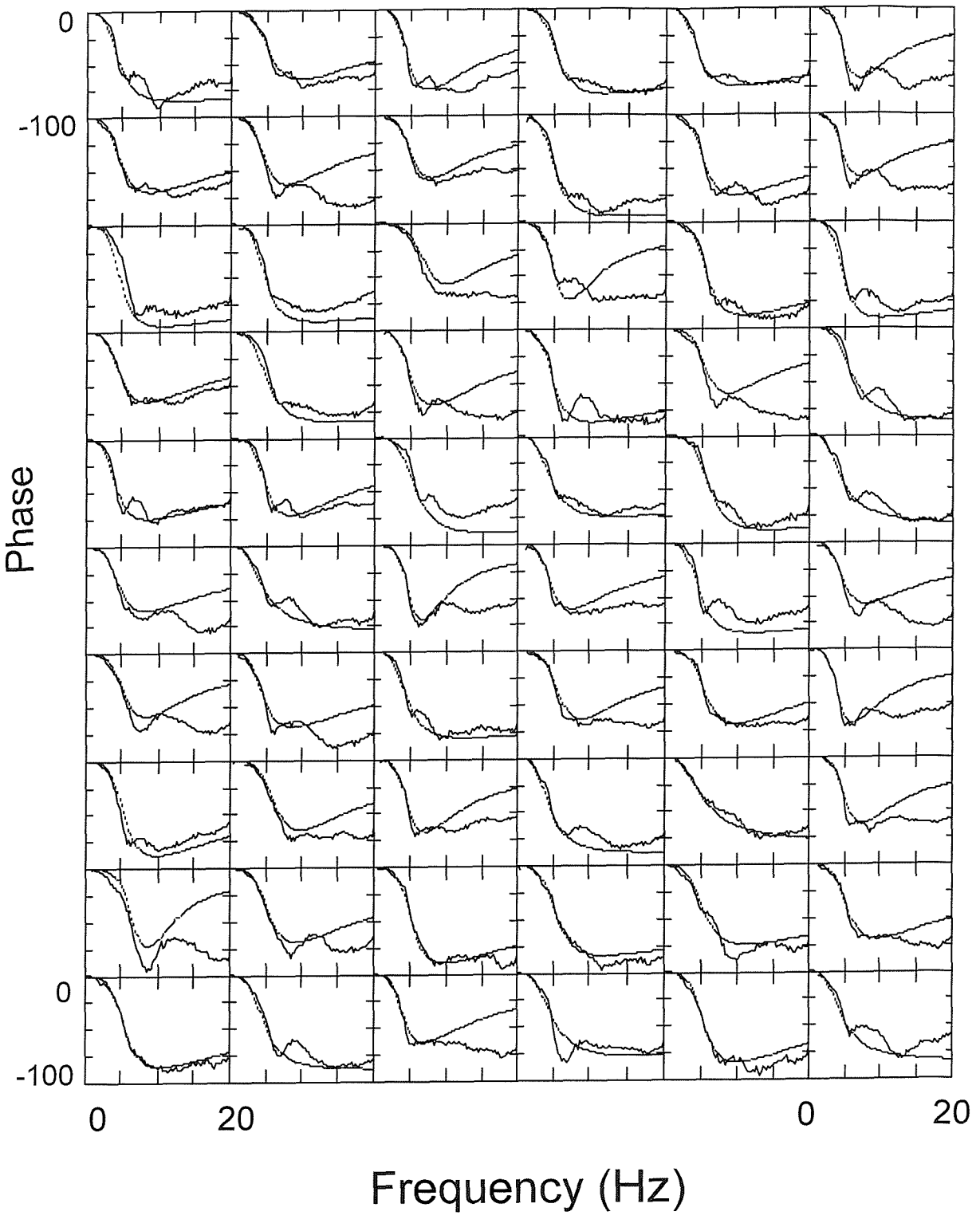

Figure 6.7 Comparison of measured modulus and phase of apparent mass compared with values fitted using model 1b. (— experimental curve, --- fitted curves)

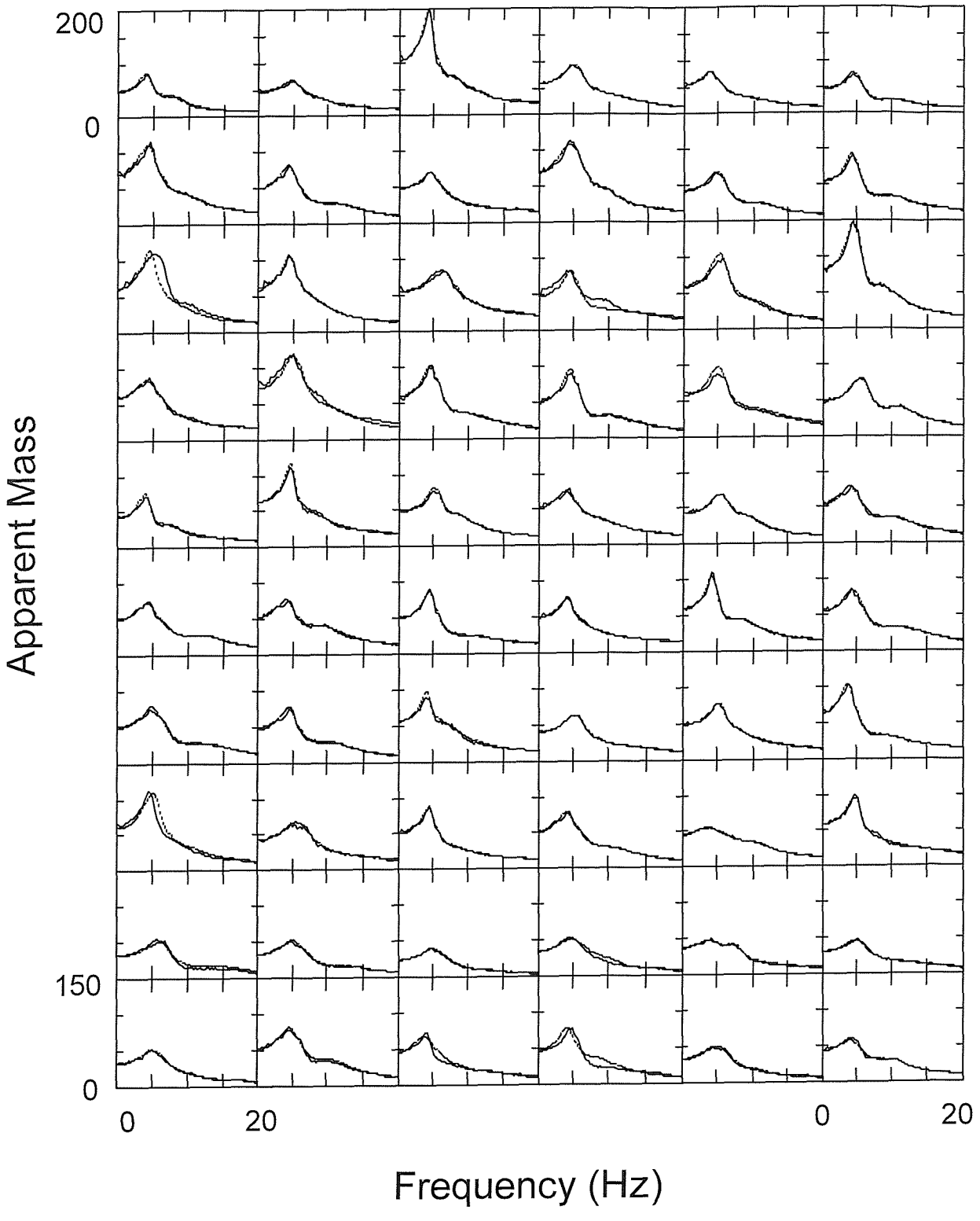
200
0
150
0
0
20
0
20
Apparent Mass
Frequency (Hz)

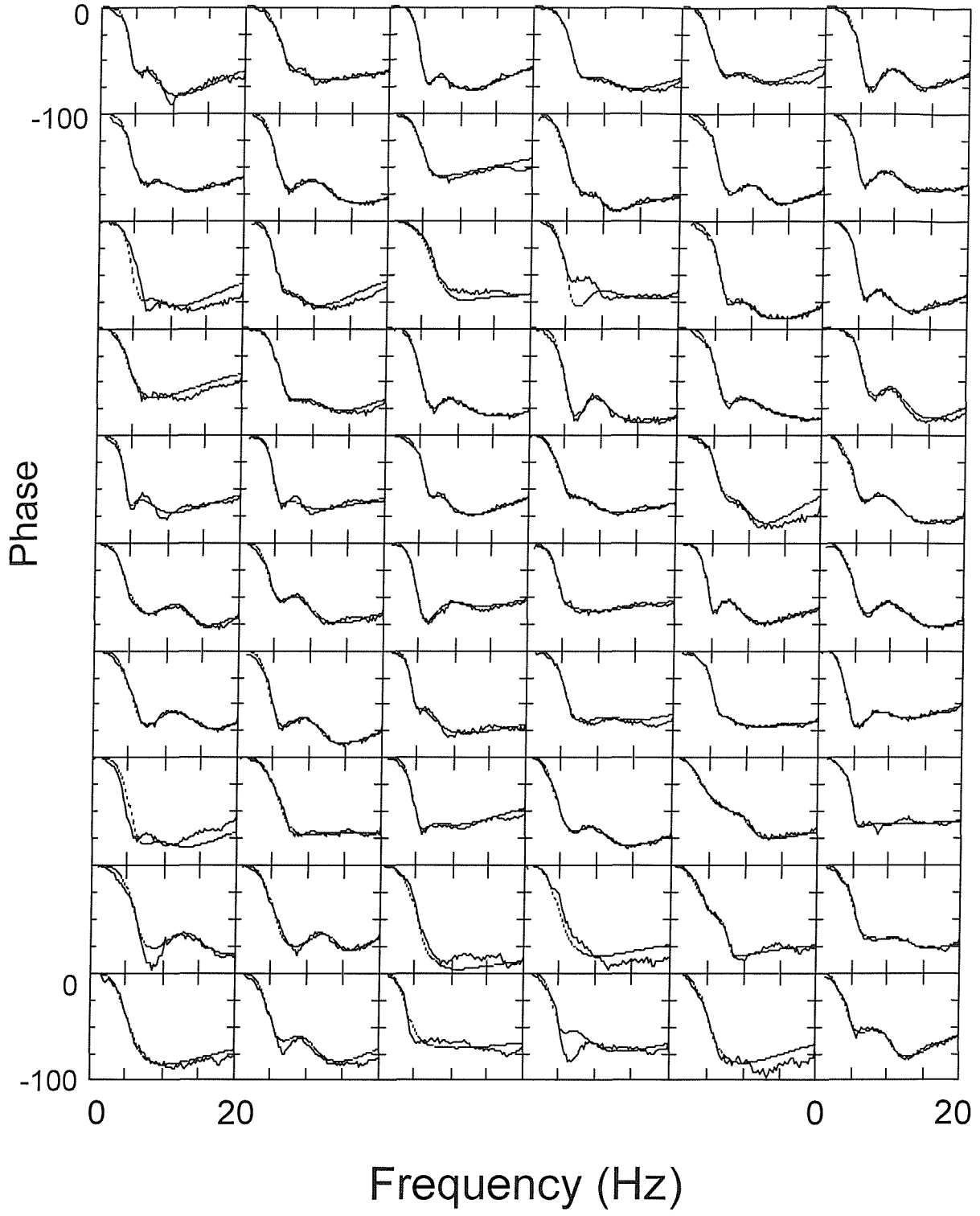

Figure 6.8 Comparison of measured modulus and phase of apparent mass compared with values fitted using model 2b. (— experimental curve, --- fitted curves)

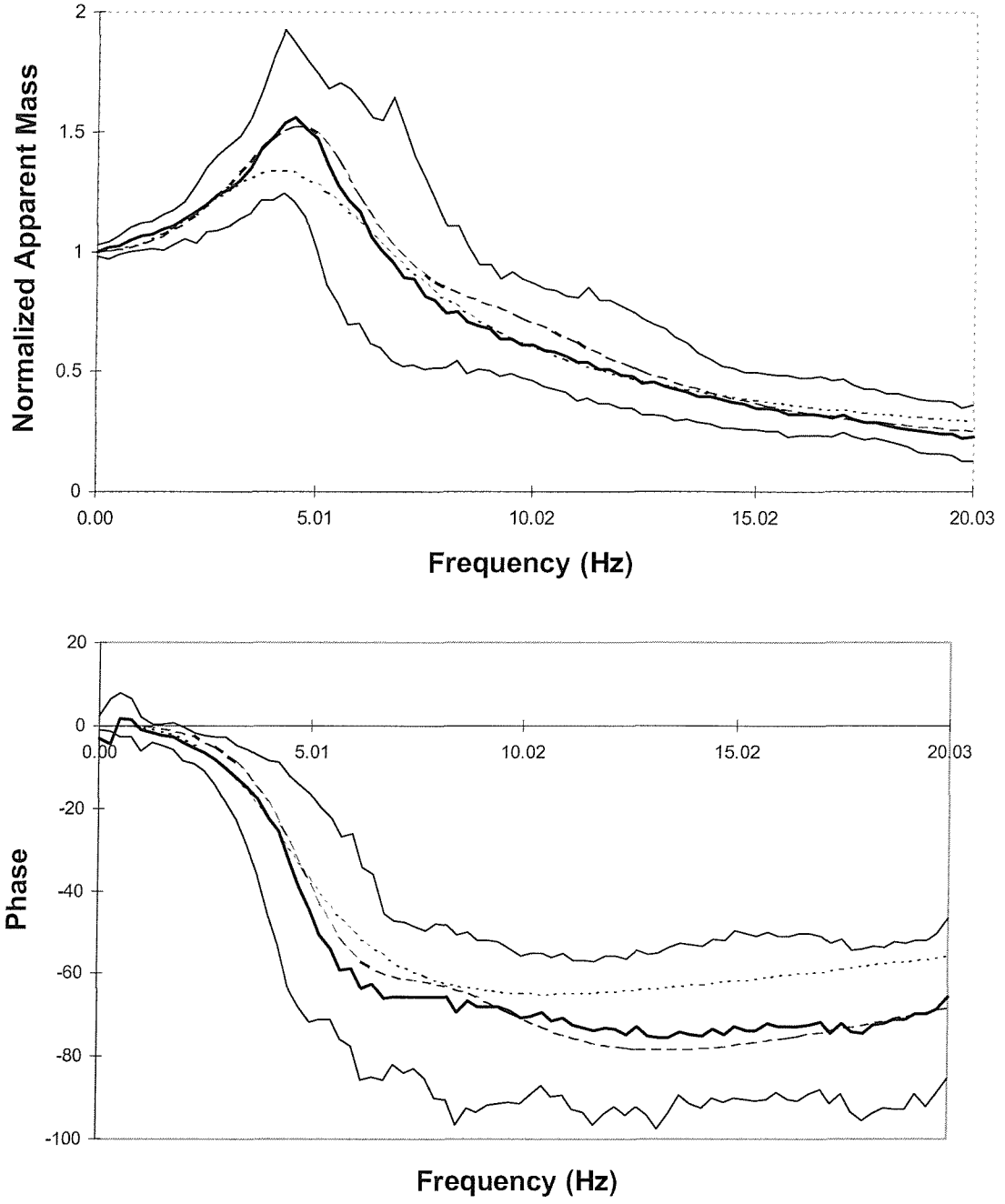

Figure 6.9 Mean and range of the measured normalised apparent masses of the 60 subjects compared with the fitted curves obtained using the mean values of mass, stiffness and damping derived for each of the 60 subjects using model 1b and model 2b. (— the maximum and minimum value curve, ▬ mean experimental data curve, ··· model 1b fitted curve, --- model 2b fitted curve).

6.4.3 Statistical Comparisons

Statistical comparisons have been made to identify the causes of variations in model parameters between and within the three groups of subject.

Between the groups of men, women and children

The male and female group were not significantly different in age ($p>0.1$, Mann-Whitney U-test) although, of course, significantly older than the children. The fitted parameters for the men, women and children have been compared using model 2b. The men had a total mass, a mass m_1, a stiffness k_2 and damping c_2 marginally significantly greater than the females ($p<0.1$, see Table 6.2). There were no statistically significant differences in the values of m_2, m, k_1 or c_1. All measures of mass were significantly less for the group of children than for the men and the women. There was no difference in k_2, but the children had values of k_1 significantly less than the men. The value of c_2 was also significantly lower for the children than for the men ($p<0.01$) and marginally significantly lower than for the women ($p<0.1$).

Within groups of men, women and children

Within each of the three groups of subjects, the correlations between subject age and the masses, stiffnesses and damping of the models fitted to the phase data were investigated using Kendall's correlation coefficient. Except where stated, the significance level is 0.05. For both the single degree-of-freedom (model 1b) and the two-degree-of-freedom model (model 2b) there was a significant positive correlation between age and total mass among the men and among the children, but not among the women. The effect was mainly due to a correlation with the mass m_2 in model 1b and due to a correlation with m_1 in the men ($p<0.01$) and with m and m_2 in the children when using model 2b.

The only other significant correlations with age were both among the men and were also positive: the value of k_1 in both models 1b and model 2b, and the value of c_1 in model 2b ($p<0.001$). These correlations suggest greater mass, stiffness and damping with increased age among the 24 men.

With both model 1b and model 2b, there was a highly significant positive correlation between k_1 and c_1 for the men ($p<0.001$). This correlation was also significant for the women but not for the children. Similarly, in model 2b there was a highly significant positive correlation between k_2 and c_2 for the men and

the women ($p<0.001$) but not for the children. In model 2b there was a positive correlation between values of k_1 and k_2 only among the children. In model 2b there was a highly significant negative correlation between c_1 and c_2 among the women only ($p<0.001$).

For all three groups of subjects in model 1b, there was a negative correlation between mass m_1 and damping c_1: this was highly significant for the women ($p<0.001$) and only marginally significant among the children ($p<0.1$). For the corresponding mass, m, in model 2b there was a significant negative correlation with c_1 and a significant positive correlation with c_2, but only for the women.

In model 1b there were significant positive correlations between m_2 and c_1 for all three groups and the correlation was highly significant for the men and women ($p<0.001$). In model 2b there were significant positive correlations between m_1 and c_1, for the men and children only; for all three groups there were significant positive correlations between m_2 and c_2 which were highly significant for the men ($p<0.001$) and marginally significant for the children ($p<0.1$).

In model 1b there was a highly significant positive correlation between k_1 and m_2 ($p<0.001$), but only for the men. Similarly, in model 2b, there was a highly significant positive correlation between k_1 and m_1 ($p<0.001$), and a significant positive correlation between k_2 and m_2, but again only for the men.

These correlations seem to suggest some differences between the groups of subjects, especially between the men and the women. Heavier men seem to exhibit increased stiffness whereas this is less obvious for the heavier women. However, such conclusions require care since the models are not necessarily representative of the mechanical structure and movements of the body, which is far more complex than a two-degree-of-freedom system.

6.5 DISCUSSION

The driving point impedance differs between subjects and so different model parameters are required to obtain the optimum impedance model for each subject. Other studies show that the driving point dynamic response of the body is non-linear (e.g. Fairley and Griffin 1989 and Mansfield 1998), so different parameters will provide the optimum model at different vibration magnitudes. Alternatively, the parameters in the model should be non-linear.

Comparing the parameters of model 1b with the previous model developed by Fairley and Griffin (1986), reveals no large or systematic differences between the two models. It appears that either model could be used to represent the apparent masses of people over the frequency range 0 to 20 Hz by a single-degree-of-freedom system.

The individual data shown in Figures 6.7 and 6.8, and the mean values shown in Figure 6.9, indicate that a two-degree-of-freedom mechanical model provides a better fit to the measured data than a single degree-of-freedom model. Use of the two-degree-of-freedom model provides a better fit to the phase data at frequencies greater than about 8 Hz and an improved fit to the modulus at frequencies around 5 Hz.

It would be possible to develop mathematical models of the driving point impedance of the body having more than two-degrees-of-freedom, but the results shown here suggest that this is unnecessary when representing the average response of a group of subjects to a specific vibration input. A greater number of degrees-of-freedom may be required to explain the movements of the body responsible for apparent mass or predict the transmission of vibration through the body.

6.6 CONCLUSIONS

Curve fitting has allowed the development of mathematical models which provide a good fit to measured values of the normalised apparent masses of subjects.

There are large differences in the model parameters for different persons (Tables 6.1 and 6.2), but the mean parameters of the two adult groups of subjects (men and women) are similar. This may explain why different seat transmissibilities are obtained with different seats but there are fairly small differences between the mean values given by groups of subjects with the same seat.

Four human body mathematical models have been considered. By comparing the responses of the models with the measured responses, model 1b (single degree-of-freedom with a rigid support) and model 2b (two-degrees-of-freedom with a rigid support) were selected as the most suitable models for representing the effective apparent masses of subjects exposed to vertical vibration.

The single degree-of-freedom model and the two-degree-of-freedom model both provided results close to the measured modulus of apparent mass. However, the two-degree-of-freedom model provided a better fit to the phase and also a better fit near the principal resonance at 5 Hz. For best results a two-degree of freedom model is therefore recommended.

When predicting the transmissibility of seats, it is recommended that the two-degree-of-freedom model using a support mechanism (i.e. model 2b) is used.

CHAPTER 7

FACTORS AFFECTING SEATED BODY APPARENT MASS

7.1 Introduction

It has been mentioned that the aim of this thesis is to develop a seat and a body model so that the prediction of seat transmissibility can be obtained. The body models have been put forward in Chapter 6 based on the measured body apparent mass. Although, it has been shown that these models can well represent the seated body in the vertical axis, there are still some problems to be resolved, such as whether the models can represent the seated body in any vibration environments.

Many studies regarding seated body dynamic response have considered the effect of factors, such as subject posture, vibration spectra, footrest and backrest etc. These studies revealed that the influences of these factors were significant on the measured apparent mass. Therefore, a series study was conducted to investigate how these factors affect the mathematical model and how to develop a model which can be used in different vibration environments. It was known that there was an influence of subject sitting posture on body apparent mass, but the model was only to represent the subject in normal sitting postures hence it was not needed to consider the influence of other sitting postures.

Using mathematical models to represent the dynamic responses of the seated body is not a new idea, many studies have been conducted to investigate its possibility. Various biodynamic mathematical models have been developed (e.g., Vogt 1968, Suggs 1969, International Organization for Standardization 1981). However, as discussed in Section 2.2.3, although these models were developed based on the measured body impedance, the authors had not considered the effect of some factors on these models. Therefore, an

investigation how to develop a good body mathematical model for different vibration conditions is needed.

The main purpose of this chapter is to obtain an improved mathematical model of the apparent mass of the seated person, starting from that developed in Chapter 6, which could be used in procedures for predicting seat transmissibility. In other words, the body mathematical model could be used under any conditions for seat transmissibility prediction, such as with different input vibration magnitudes, different input vibration spectra, hard and soft seat, different seat inclinations and different seat backrest angles.

7.2 Effect of vibration magnitude

Experimental studies have shown that the apparent mass of the seated human body is non-linear with respect to vibration magnitude (e.g. Fairley and Griffin 1989, Hinz and Seidal 1987, Mansfield 1994 and Smith 1994). These studies show that as the magnitude of random vibration increases the mean resonance frequency decreases (Figure 2.15). This implies that when the vibration conditions change, the dynamic responses of the human body change. However, the previously developed model (see Section 6.3.1 and 6.3.2) cannot reflect the change of body dynamic response that happens at different vibration magnitudes. How to develop a body mathematical model to reflect these changes that happen to body apparent mass at varied vibration magnitudes is the target of the research in this section.

7.2.1 Previous experimental results

Mansfield (1994) investigated the influence of vibration magnitudes on the seated body apparent masses. The data that he obtained will be used in this study to observe how the vibration magnitudes influence the mathematical model, which is used to replace the seated body. In his study, the whole-body driving-point apparent masses of twelve persons were obtained with subjects seated on a flat rigid seat. Subjects sat on the top plate of a Kistler 9821B force platform which was 600 mm wide and 400 mm deep and 470 mm above a foot support that moved with the seat. Vertical motion of the platform was

measured using an Entran EGCSY-240D*-10 accelerometer mounted beneath the seat surface. The experiment was conducted using a one-metre stroke electro-hydraulic vertical vibrator in the Human Factors Research Unit at the Institute of Sound and Vibration Research. Subjects sat on the seat in an upright posture without their backs touching a backrest.

Subjects were exposed to 60 seconds of Gaussian random vibration with a flat constant bandwidth acceleration spectrum between 0.2 and 20 Hz. The vibration was presented at six magnitudes: 0.25, 0.5, 1.0, 1.5, 2.0 and 2.5 ms^{-2} r.m.s. Signals from the accelerometer and the force platform were conditioned and acquired at 100 samples per second via 33 Hz anti-aliasing filters. Twelve male subjects participated in the experiment.

7.2.2 Human body mathematical model

A two-degree-of-freedom model, proposed in Chapter 6, was used to fit the experimental data (Figure 6.4). The model has two mass-spring-damper systems, m_1, k_1, c_1 and m_2, k_2, c_2, supported on a mass, m. The model is merely an equivalent mechanical model, which can give the correct body response to vertical vibration in the frequency range from 0.5 to 20 Hz, and not a model that represents how the body moves during vibration.

7.2.3 Model parameters acquired and discussion

The model in Figure 6.4 was fitted separately to the moduli and the phases of the apparent masses measured for each of the twelve subjects. The fitting was performed by curve fitting using MATLAB 'fmins' version 4.0. The least square error method and an optimisation algorithm were utilised (Dierckx 1995) as before.

Figure 7.1 compares the mean measured and mean fitted apparent masses for the 12 subjects at the six magnitudes of vibration. When the mean measured data were fitted the model masses kept fixed (i.e., only model stiffness and damping changed). How to fix the model masses is explained in Section 7.2.5. Different results were obtained by fitting to the modulus and

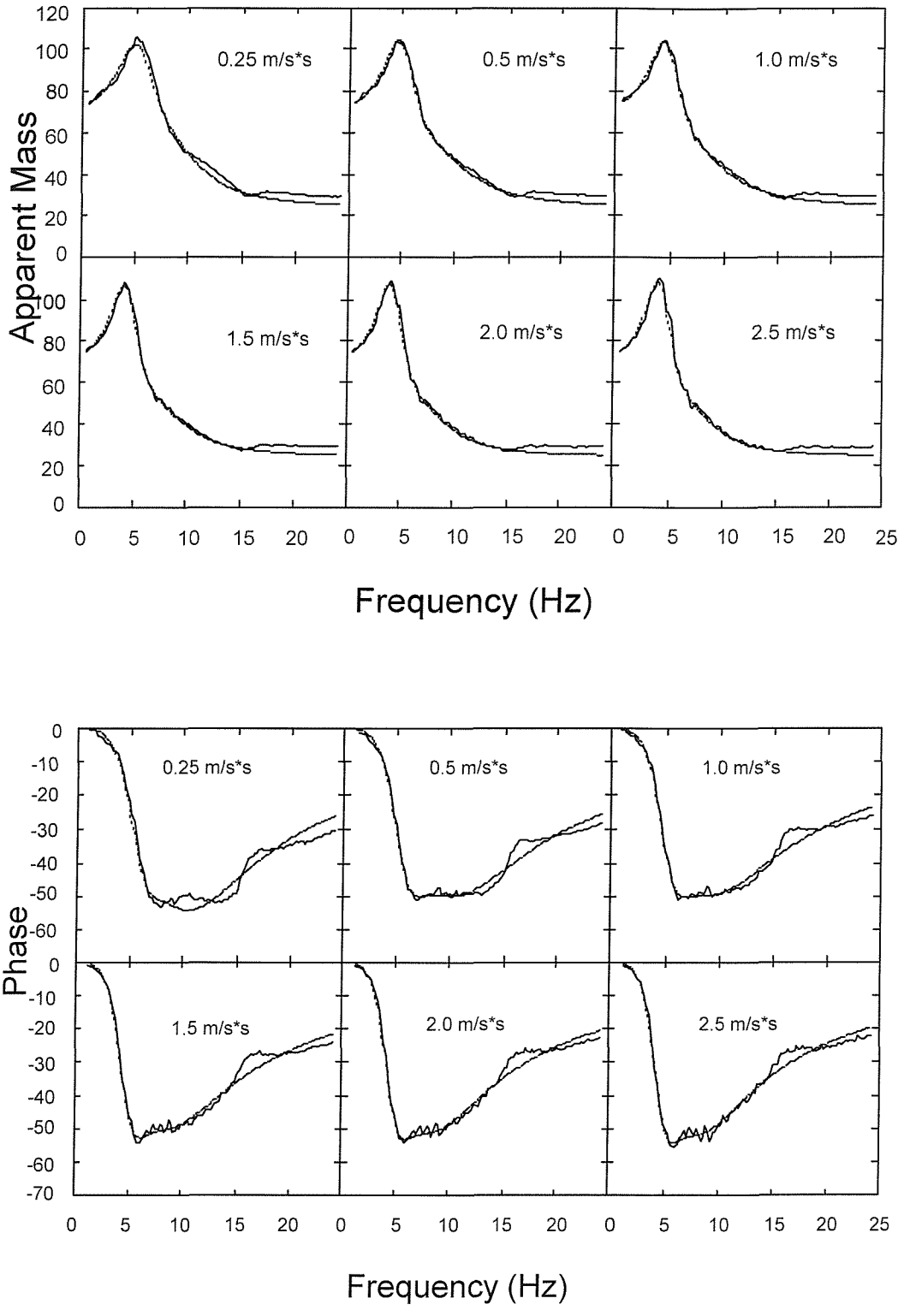

Figure 7.1.Using a two-degree-of -freedom model to fit the mean phase of twelve subjects' apparent mass (——— measured, ---------- fitted).

phase of the apparent mass. It was found that by fitting to the phase, the differences in phase between the measured and predicted responses were

minimised without increasing the differences in the modulus. The phase fitting method was therefore selected. Table 7.1 shows the model parameters obtained for all twelve subjects at the six magnitudes by fitting to the phase of the apparent mass. In the calculation of the mass *m,* the weight of platform (16 kg) was subtracted. Table 7.1 shows also the fitting result from mean measured data. It is a result coming from all model masses fixed condition.

Table 7.1 Twelve subjects' six magnitudes model parameters by fitting phase.

Subject	Magnitude (m/s^2)	k_1 (N/m)	c_1 (Ns/m)	k_2 (N/m)	c_2 (Ns/m)	m (kg)	m_1 (kg)	m_2 (kg)
s1	0.25	60089	703	30641	538	8.7	13.3	33.1
	0.5	40161	433	29138	611	7.0	8.5	34.0
	1.0	31992	344	24925	523	7.3	8.2	33.5
	1.5	29965	357	22182	445	7.4	9.0	32.4
	2.0	29589	431	20159	363	7.3	11.0	30.0
	2.5	24554	371	17971	371	7.2	10.6	31.2
s2	0.25	32243	75	89178	1482	7.2	1.6	50.5
	0.5	26859	57	77110	1494	7.3	1.3	51.1
	1.0	20583	43	65509	1422	7.0	1.0	51.6
	1.5	25850	61	59696	1301	7.2	1.2	51.2
	2.0	19588	48	54731	1249	7.3	0.9	51.3
	2.5	25421	76	53842	1199	7.2	1.2	51.1
s3	0.25	80920	12.6	79097	2142	6.0	1.1	52.3
	0.5	61723	710	54955	1088	8.0	10.9	41.1
	1.0	53219	668	46473	975	8.3	11.2	40.1
	1.5	37092	375	37315	792	9.9	8.5	41.3
	2.0	46799	611	32436	658	9.5	13.3	37.2
	2.5	47216	617	33546	598	9.3	13.3	37.1
s4	0.25	55903	463	48936	668	9.6	11.5	37.6
	0.5	64764	777	33934	412	9.4	17.3	30.6
	1.0	57342	797	26442	315	9.6	19.2	28.6
	1.5	46003	608	26509	412	9.1	15.8	32.5
	2.0	44726	763	21300	275	9.3	20.3	27.8
	2.5	42212	729	20773	296	9.1	19.4	28.9
s5	0.25	45020	155	75401	1531	8.1	2.1	48.5
	0.5	43957	164	65450	1518	7.9	2.1	48.9
	1.0	37296	118	54758	1318	8.5	1.9	48.3
	1.5	43185	175	53459	1259	8.1	2.5	48.0
	2.0	6473	1912	41307	722	3.6	16.1	38.9
	2.5	11379	1551	40975	847	4.9	11.6	42.1

Subject	Magnitude (m/s^2)	k_1 (N/m)	c_1 (Ns/m)	k_2 (N/m)	c_2 (Ns/m)	m (kg)	m_1 (kg)	m_2 (kg)
s6	0.25	33172	380	88525	1916	8.3	28.9	38.3
	0.5	21715	249	84749	1893	8.8	24.3	40.7
	1.0	13659	168	60857	1848	8.1	18.5	47.3
	1.5	12417	140	47454	1768	7.2	16.1	50.7
	2.0	11797	133	52572	1663	8.2	17.0	48.7
	2.5	10999	179	45545	1594	6.5	16.1	51.3
s7	0.25	67046	853	38186	478	8.7	14.9	33.0
	0.5	68134	1002	32283	367	8.4	18.1	30.1
	1.0	57664	891	27259	334	8.7	17.9	30.0
	1.5	46352	743	25594	357	8.9	15.5	32.2
	2.0	41875	688	23203	321	9.3	15.8	31.5
	2.5	39750	789	20971	267	8.7	18.6	29.3
s8	0.25	113320	1422	42770	349	5.5	22.9	23.6
	0.5	103021	1048	39671	382	5.1	19.3	26.0
	1.0	88386	1417	34202	356	4.8	22.4	25.2
	1.5	68486	1139	28576	305	6.0	22.1	24.5
	2.0	61055	1043	26327	291	6.5	21.2	24.8
	2.5	52734	898	28244	339	6.2	19.4	26.9
s9	0.25	84492	1402	51544	559	5.9	20.4	32.9
	0.5	70811	1452	34085	413	6.8	23.8	27.8
	1.0	67279	961	35113	436	8.7	18.5	31.1
	1.5	47299	1052	30514	441	8.2	18.7	31.4
	2.0	48570	715	32779	466	9.0	16.2	33.1
	2.5	41613	924	24551	338	8.5	20.1	29.6
s10	0.25	13420	29	101810	1743	8.7	4.9	52.0
	0.5	8650	25	86373	1548	9.6	3.6	52.3
	1.0	42891	415	38933	1405	8.5	26.1	31.0
	1.5	22998	183	52777	1465	8.4	18.3	38.9
	2.0	24285	200	45429	1276	9.3	20.1	36.1
	2.5	18734	152	45174	1258	9.3	16.9	39.3
s11	0.25	30241	67	53085	1044	9.1	1.2	46.0
	0.5	19782	33	41069	1039	8.7	0.8	46.2
	1.0	9396	17	32535	991	8.2	0.5	46.0
	1.5	13601	28	30863	920	8.3	0.7	45.8
	2.0	12383	24	28442	871	8.5	0.6	45.6
	2.5	15124	34	28749	843	8.0	0.7	46.0
s12	0.25	24752	139	51452	1279	6.0	4.4	39.0
	0.5	34028	372	29666	781	6.5	10.1	32.7
	1.0	41201	737	14304	318	6.8	21.5	21.0

Subject	Magnitude (m/s^2)	k_1 (N/m)	c_1 (Ns/m)	k_2 (N/m)	c_2 (Ns/m)	m (kg)	m_1 (kg)	m_2 (kg)
	1.5	35462	587	16786	385	6.9	17.2	25.4
	2.0	35462	587	16786	385	6.9	17.2	25.4
	2.5	32350	489	20420	448	6.6	14.6	28.2
mean	0.25	38474	596	47150	954	8.1	12.8	37.2
	0.5	42650	666	41331	823	8.1	12.8	37.2
	1.0	35143	642	35413	768	8.1	12.8	37.2
	1.5	31568	607	31720	678	8.1	12.8	37.2
	2.0	29043	571	30078	654	8.1	12.8	37.2
	2.5	27528	548	29005	625	8.1	12.8	37.2

Although Figure 7.1 showed only the mean subjects' curve fitting results at six different magnitudes, individual subject result is similar to this. The results confirm that a two degree-of-freedom model can provide a reasonable prediction of the apparent mass of human body.

7.2.4 Dependence of model parameters on vibration magnitude

Statistical tests were conducted to investigate the correlation between the parameters of the mathematical model and the vibration magnitude. The Spearman rank correlation was used with a significance criterion of $p<0.05$.

Change in model stiffness with vibration magnitude

Table 7.2 shows that there were significant negative correlations between vibration magnitude and stiffness for both k_1 and k_2 ($p<0.05$, except for subjects 10, 11 and 12 in respect of k_1 , and subject 3 in respect of k_2). Subject 10 showed a positive correlation between vibration magnitude and k_1. A negative correlation indicates that the model stiffness decreased with increasing vibration magnitude.

Change in model damping with vibration magnitude

The damping represented by c_2 shows a highly significant negative correlation with vibration magnitude for all subjects ($p<0.05$). Although the damping represented by c_1 also has a negative correlation coefficient for all subjects, the correlation is not statistically significant for subjects 6, 8, 9, 10 and 12.

Table 7.2 The statistical correlation between vibration magnitudes and model stiffness and damping in twelve subjects.

	k_1 & magnitude		c_1 & magnitude		k_2 & magnitude		c_2 & magnitude	
Subject	Correlation coefficient range (-1 to 1)	Significance level	Correlation coefficient range (-1 to 1)	Significance level	Correlation coefficient range (-1 to 1)	Significance level	Correlation coefficient range (-1 to 1)	Significance level
1	-1.000	.000	-1.000	.000	-1.000	.000	-1.000	.000
2	-.9429	.005	-.7714	.072	-1.000	.000	-1.000	.000
3	-.8286	.042	-.9429	.005	-.7714	.072	-.9429	.005
4	-1.000	.000	-.8407	.036	-1.000	.000	-.9429	.005
5	-1.000	.000	-.7714	.072	-1.000	.000	-1.000	.000
6	-.9429	.005	-.1429	.787	-.9429	.005	-1.000	.000
7	-1.000	.000	-.8286	.042	-1.000	.000	-1.000	.000
8	-1.000	.000	-.3143	.544	-1.000	.000	-.9429	.005
9	-1.000	.000	-.3714	.468	-.9429	.005	-.9429	.005
10	.6000	.208	-.7143	.111	-1.000	.000	-1.000	.000
11	-.3714	.408	-.8286	.042	-.9429	.005	-1.000	.000
12	-.4638	.354	-.4638	.354	-.8817	.050	-.9856	.000

7.2.5 Modification of mathematical model

The parameters of the model varied with vibration magnitude. This non-linearity could be represented by a new non-linear model. Alternatively, the phenomenon could be represented by a linear model in which the parameters are fixed at different values appropriate for specific magnitudes of vibration. The second option has been developed here.

It seems reasonable to vary only the stiffness and damping of the model to provide a fit for each of the six magnitudes of vibration. Although an improved fit to the measured data could be obtained by also varying the masses, the data in Figure 7.1 suggest this may be unnecessary.

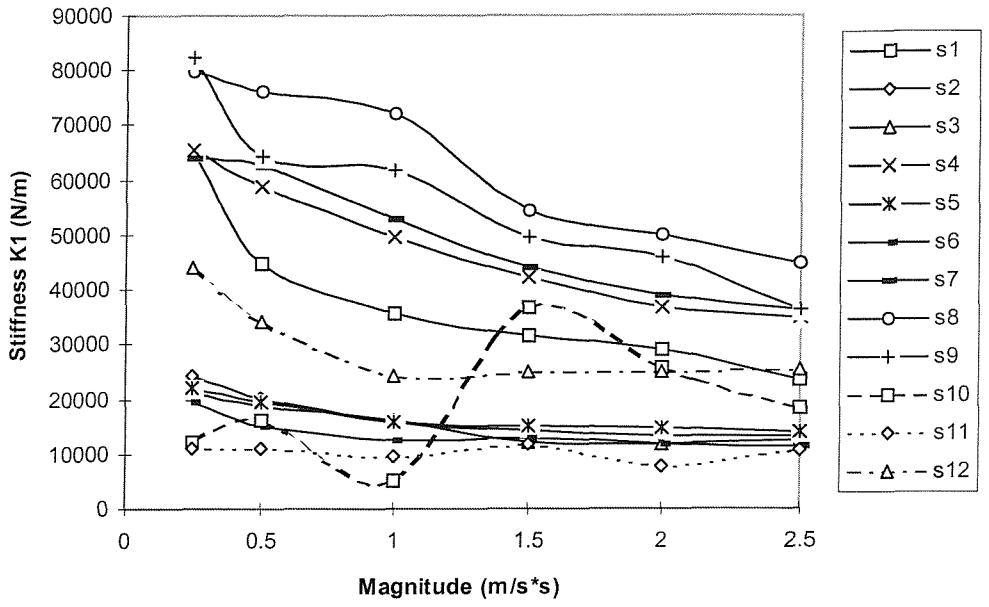

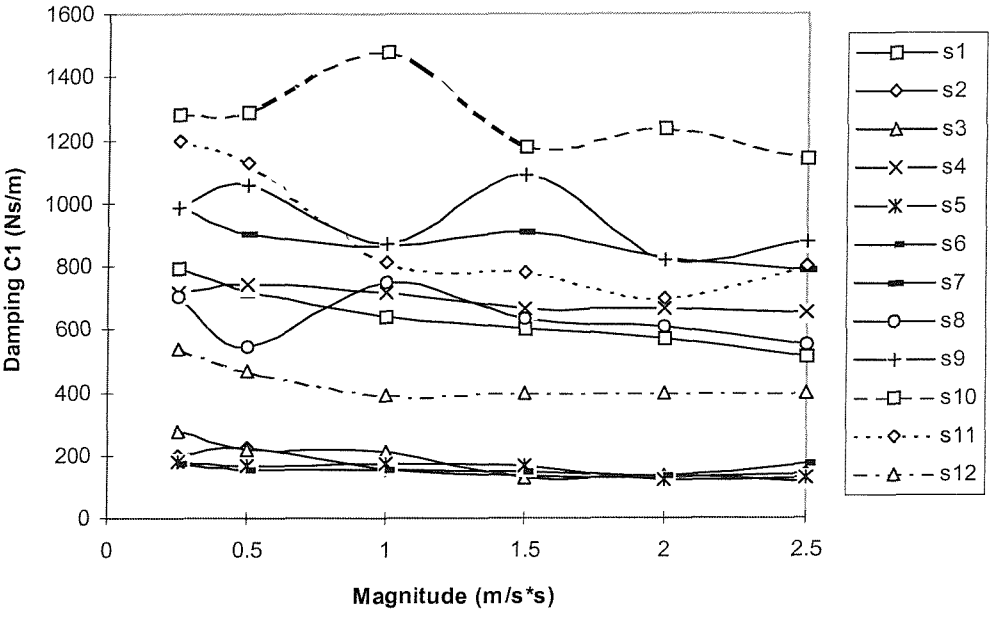

Figure 7.2 Twelve subjects' stiffness k_1 and damping c_1 at different magnitudes (mass fixed).

The masses of the model (m, m_1, and m_2) were fixed according to the mass statistics found in a previous study (Wei and Griffin, 1998):

$$m = 14\% M$$

$$m_1 = 22\% M$$

$$m_2 = 64\% M$$

Where M is the total mass of the subject supported by the seat (i.e. the subject sitting weight).

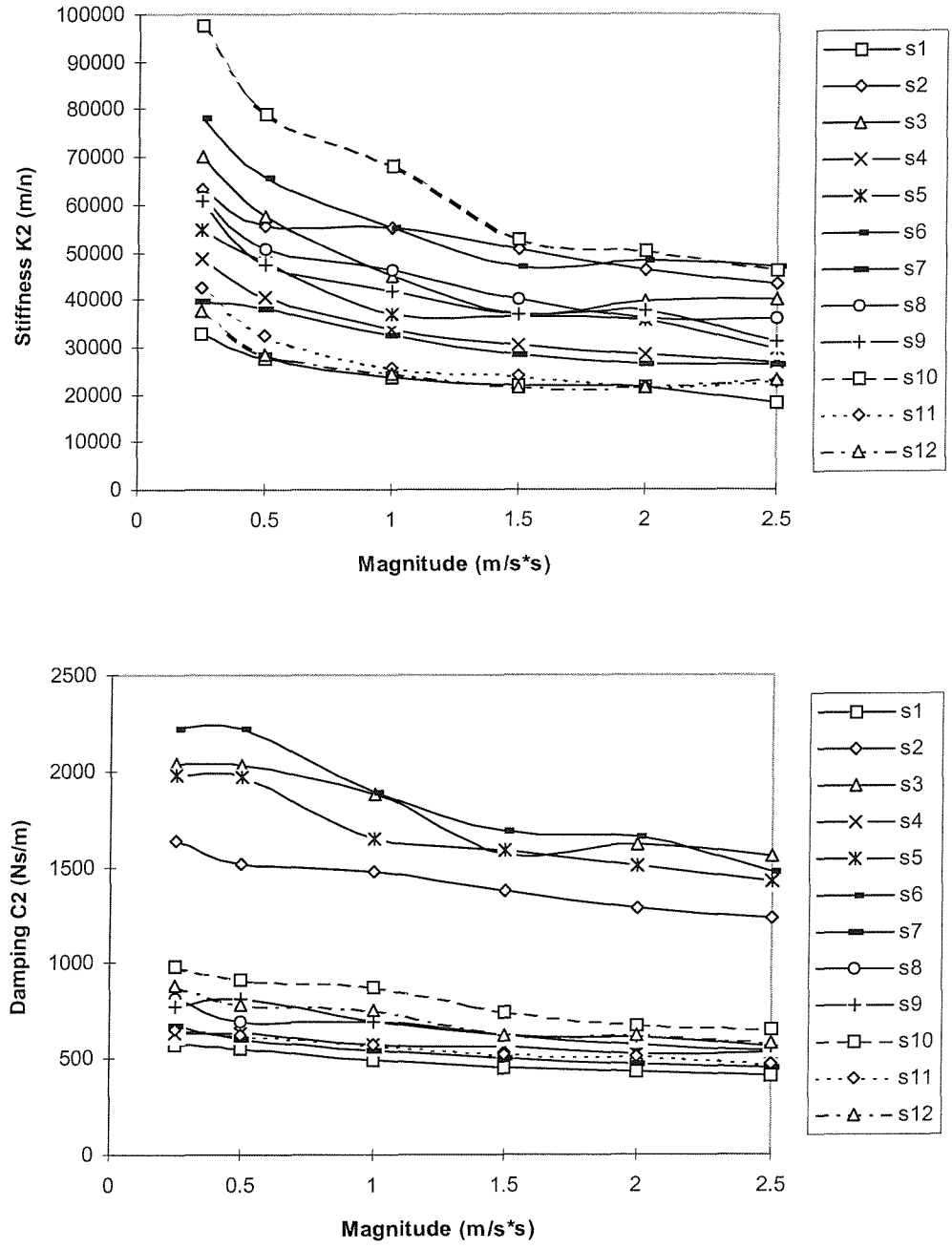

Figure 7.3 Twelve subjects' stiffness k_2 and damping c_2 at different magnitudes (mass fixed).

The same two-degree-of-freedom model in Figure 6.4 was used to fit the experimental data provided by each subject. However, the masses were fixed (as above) according the sitting weight of each subject. The subject mass was

determined from the apparent mass at 0 Hz which means the subject static weight on the force plate. In fact, we can not obtain the apparent mass at 0 Hz, The apparent mass at the lowest frequency can represent approximately weight of the subject.

The damping and stiffness values determined by fitting are shown in Figure 7.2 and 7.3. It can be observed that the model stiffness and damping have distinctive changes with the different vibration magnitudes. The cause of this change can be observed from Figure 7.4. The resonance frequency of the mean measured apparent mass decreased clearly with increase in vibration magnitude.

The mean stiffness and damping values calculated for the twelve subjects at each magnitude were used to determine average model parameters. Figure 7.5 shows the mean stiffness and damping values for the twelve subjects at each magnitude. It is clear that the stiffness and damping decrease with increasing input vibration magnitude. In order to find equations to represent the change of every parameter at different input vibration magnitudes, the simplest equations are proposed here. These equations are:

$$
\begin{aligned}
k_1 &= a_1 - b_1 * \ddot{\bar{x}}^{d_1} \\
k_2 &= a_2 - b_2 * \ddot{\bar{x}}^{d_2} \\
c_1 &= a_3 - b_3 * \ddot{\bar{x}}^{d_3} \\
c_2 &= a_4 - b_4 * \ddot{\bar{x}}^{d_4}
\end{aligned}
\qquad (7.1)
$$

Where: a_1 to a_4, b_1 to b_4 and d_1 to d_4 are unknown coefficients, which are obtained using a curve fitting technique (Figure 7.5). The acquired parameters were found to be following:

$a_1 = 4668$, $b_1 = -30495$, $d_1 = -0.3167$
$a_2 = 12442$, $b_2 = -22653$, $d_2 = -0.3537$
$a_3 = 1166$, $b_3 = 416$, $d_3 = 0.2972$
$a_4 = 696$, $b_4 = 59$, $d_4 = 1.0288$

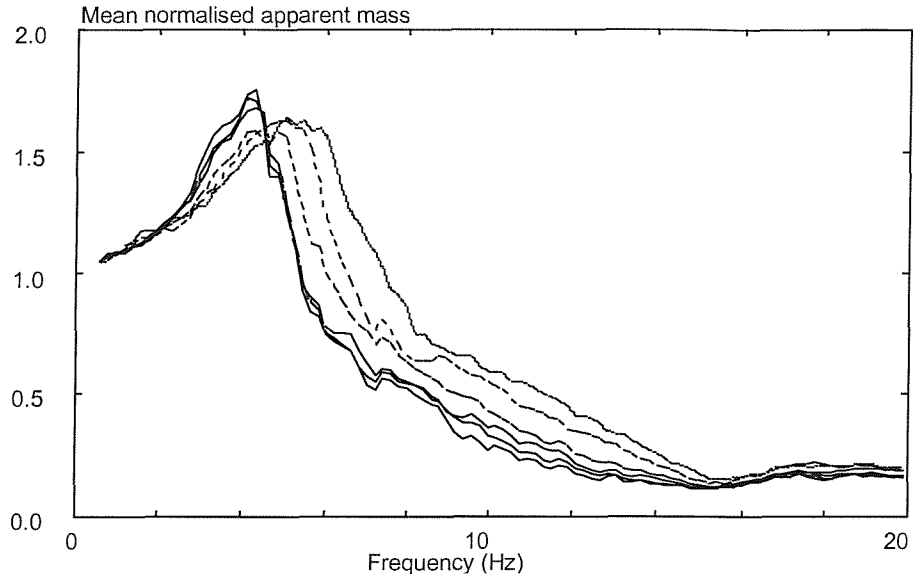

Figure 7.4 Mean measured apparent masses at different vibration magnitude

Substituting for a_1 to a_4, b_1 to b_4 and d_1 to d_4 above gives into equations 7.1, the modification of the stiffness and damping will be expressed as following:

$$k_1 = 4668 + 30495 \times \overline{\ddot{x}}^{-0.3167}$$

$$k_2 = 12442 + 22653 \times \overline{\ddot{x}}^{-0.3537} \qquad (7.2)$$

$$c_1 = 1166 - 416 \times \overline{\ddot{x}}^{0.2972}$$

$$c_2 = 696 - 59 \times \overline{\ddot{x}}^{1.0288}$$

Where $\overline{\ddot{x}}$ (m/s^2 rms) is the acceleration magnitude of the random vibration used in the experiment.

Substituting equations (7.2) into equations (6.27) and (6.28) gives the equations representing a two-degree-of-freedom model which can be used at different vibration magnitudes.

Figure 7.5 compares the mean fitted values of stiffness and damping with those predicted from the above regression equations. The final data are listed in Table 7.3. The predicted values of stiffness and damping are similar to the mean fitted data, so it seems reasonable to use the above expressions for stiffness and damping in a new model of the apparent mass of the human body.

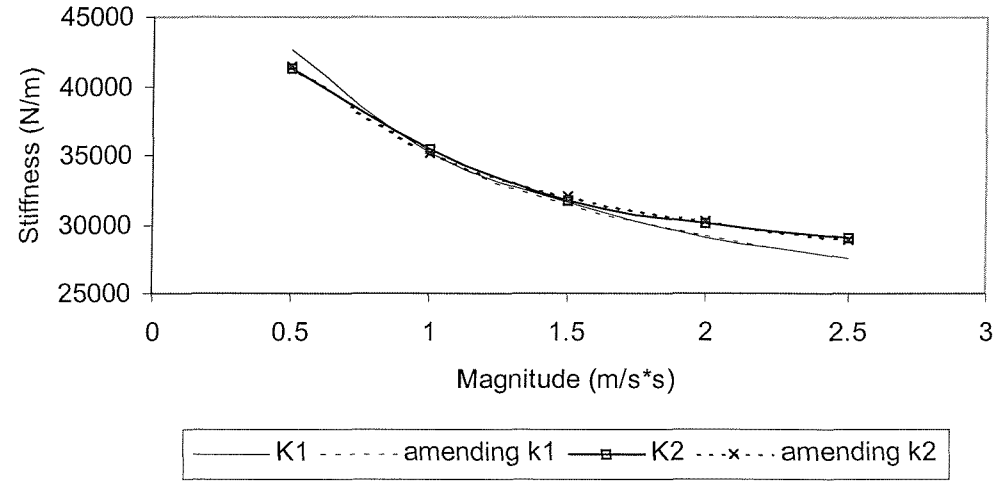

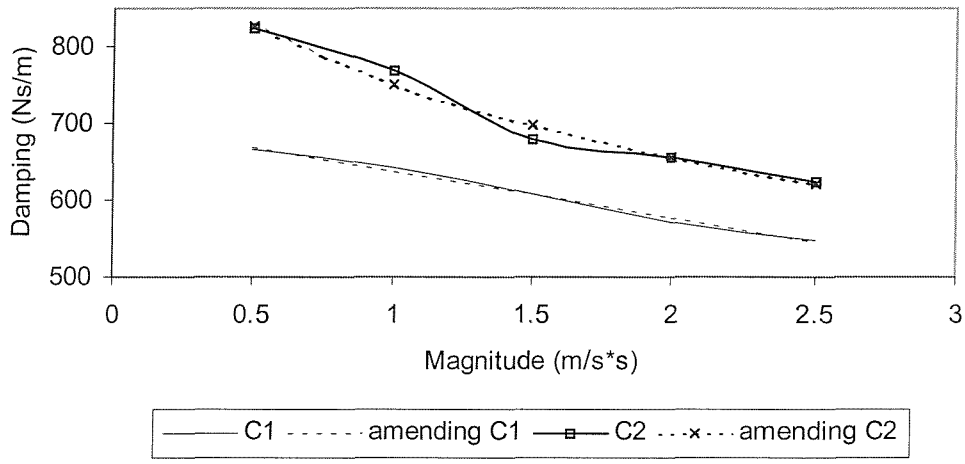

Figure 7.5 Using modified stiffness k_1, k_2 and c_1, c_2 to predict the mean measured stiffness k_1, k_2 and damping c_1, c_1.

Figure 7.6 compares the mean measured apparent mass at each magnitude with that predicted using the modified model equations. The final data are listed in Table 7.3. The predicted values of stiffness and damping are similar to the mean fitted data, so it seems reasonable to use the above expressions for stiffness and damping in a new model of the apparent mass of the human body.

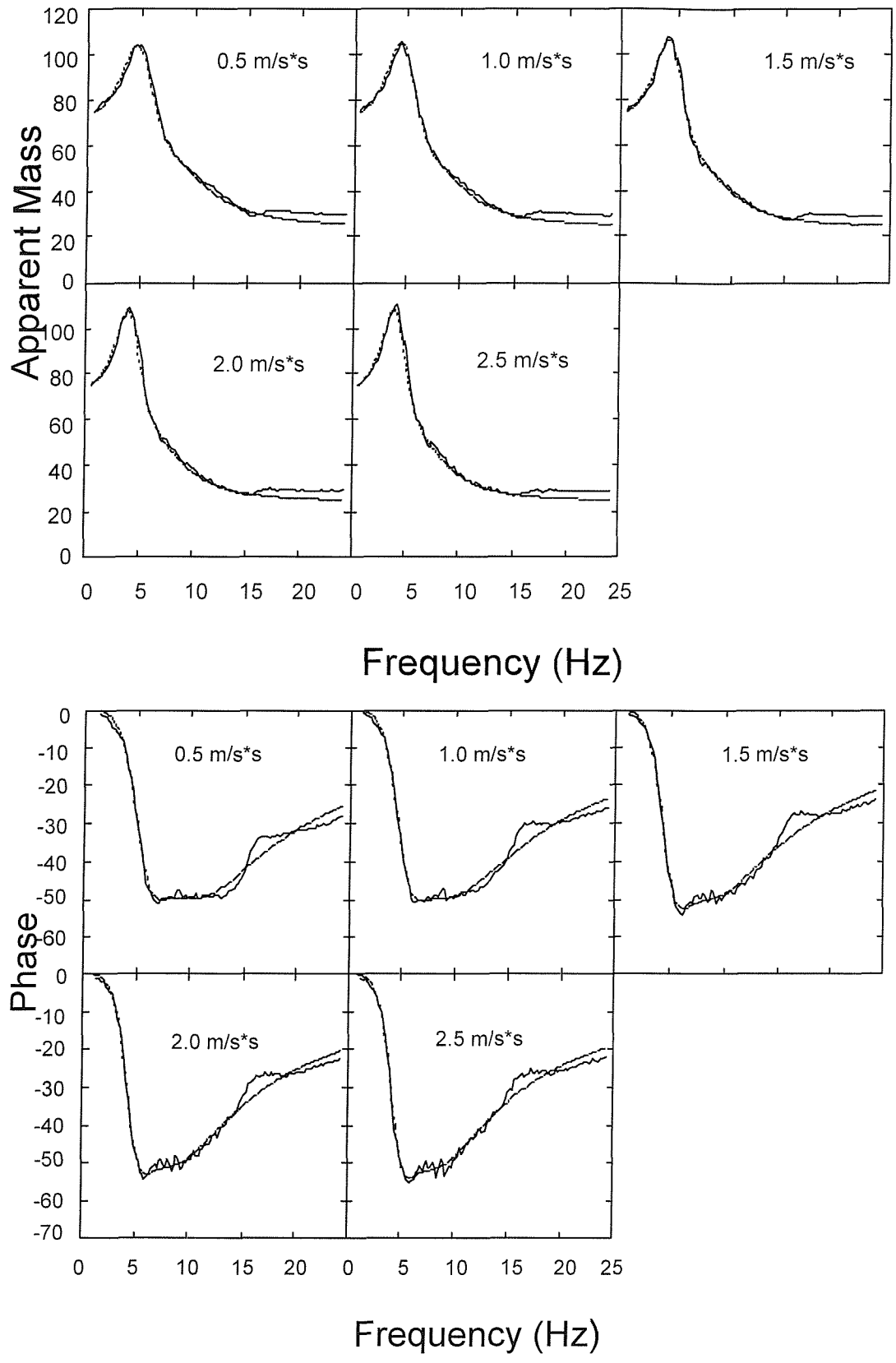

Figure 7.6 Using modified stiffness and damping to predict the mean twelve subjects' apparent mass. (———— measured apparent mass, – – – – – – predicted)

Table 7.3 Modified model stiffness and damping (from equation 7.2).

	k_1	c_1	k_2	c_2
Magnitude	modified value	modified value	modified value	modified value
0.5	42649	677	41590	827
1.0	35163	637	35095	750
1.5	31488	606	31989	697
2.0	29153	576	30047	655
2.5	27482	545	28675	620

7.2.6 Discussion and conclusion

The apparent mass differed between subjects, so different model parameters were obtained while fitting apparent mass for different subjects (Table 7.1). Because large differences exist in model parameters for different subjects, the responses of a large number of subjects should be measured to obtain a universal model to represent the response of subjects to vertical vibration.

The data shown in Figure 7.1 indicate that the two-degree-of-freedom mathematical model can provide a good fit to measured data. A decrease in both stiffness and damping appeared in the model when the vibration magnitude increased.

There are clear and consistent differences in the dynamic response of the body as the magnitude of vibration changes. Although the causes of the non-linearity are not clear, it is obvious that the specification of the mechanical impedance or apparent mass of the body should be specific to a limited range of vibration conditions. In this study, the effect is shown as a function of vibration magnitude, but the application of the findings should recognise that the bandwidth of the vibration spectrum may also have an influence. Hence, the response at a given magnitude shown by this study may be somewhat different from the response at the same magnitude when a different vibration waveform is used.

The two-degree-of-freedom model parameters developed here are different to the model parameters to that in Chapter 6, because they were based on

different measured apparent masses. In Chapter 6, the model stiffness and damping for the mean measured data were fixed. They are k_1=35007 N/m, k_2=33254 N/m, c_1=815 Ns/m and c_2=484 Ns/m. However, in this study, they are expressed in equation 7.2. The stiffness and damping vary with different input vibration magnitudes. When the input vibration magnitude is 1.0 ms^{-2} rms, which is same as in the study in Chapter 6, the corresponding parameters of stiffness and damping of the model derived here are 35095 N/m, 35163 N/m, 750 Ns/m and 637 Ns/m. Little differences exist in parameters of both models. The differences between both models are -88 N/m (k_1), -1909 N/m (k_2), 65 Ns/m (c_1) and –153 Ns/m (c_2). Therefore, the parameters of the model (Chapter 6) at different vibration magnitudes should be the values calculated from equation 7.2 plus the differences shown above.

7.3 Effect of seat cushion inclination

In order to define a standard procedure for predicting seat transmissibility, it is necessary to understand those factors that significantly affect the measured subject apparent mass. These factors include the shape of the indenter head, the seat inclination, the vibration magnitude, the vibration spectrum, the seat backrest, and the subject posture. Therefore, a knowledge of the influence of seat inclination is needed when predicting seat transmissibility from mathematical models of the seat and the human body.

7.3.1 Hypotheses

It was expected that subject apparent mass would vary with different seat inclinations because of postural changes (Fairley and Griffin, 1989; Griffin 1990), even if a subject remained upright in the seat.

7.3.2 Materials and methods

7.3.2.1. Subjects

Ten male subjects participated in the study. They were staff and students of the University of Southampton. Their mean age was 31.9 years, mean height 1.72 m, mean weight 69.6 kg (Table 7.4).

7.3.2.2. Equipment and data collection

The experiment was conducted using an electro-hydraulic vertical vibrator having a maximum stroke of 1 metre. A flat rigid wooden seat with a surface inclination variable between 0° and 23° was used.

Subjects sat on the seat in an upright posture with their backs not touching a backrest and with their hands resting on their knees. The feet of the subjects were supported on a platform that moved with the seat. The footrest height was adjusted by adding height beneath the feet so that all subjects had similar thigh and seat contact areas.

Table 7.4 Subject Characteristics

subject	age (years)	stature (m)	total weight (kg)
1	33	1.82	83
2	24	1.70	65
3	25	1.85	75
4	22	1.68	73
5	35	1.70	62
6	39	1.68	65
7	35	1.68	72
8	40	1.68	70
9	32	1.68	63
10	34	1.74	68

The apparent masses of all ten subjects were measured with the subjects sitting on the seat keeping an upright posture. Motions of the seat were measured using Entran EGCSY-240D*-10 accelerometers mounted both beneath the seat and on the seat surface. The dynamic force was measured at the same point as the accelerometer using a Kistler 9821B force platform. Figure 7.7 shows orientation of the force plate and accelerometer related to the seat surface.

Sixty seconds of Gaussian random vibration with a flat constant bandwidth acceleration power spectrum over the frequency range 0.2 to 25 Hz was presented at 1.5 ms^{-2} r.m.s. The signal was generated, and the acceleration and force signals were collected and analysed, using an *HVLab* system.

The measurements of subject apparent mass were obtained with five inclinations on the supporting surface of the wooden seat: 0^0, 5^0, 10^0, 15^0 and 20^0. The seat was either horizontal or inclined to the rear (i.e., lower at the rear than the front).

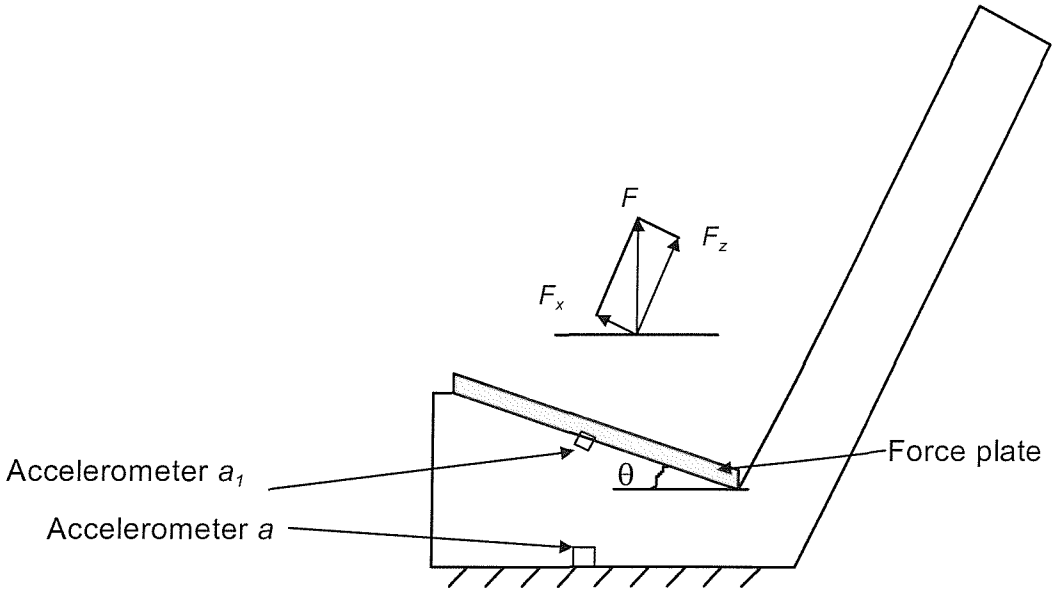

Figure 7.7 Force plate and accelerometers arrangement on the seat surface

7.3.3 Results

Figure 7.8 shows the mean of the ten subjects' apparent masses calculated between the force indicated by the force transducer and the acceleration indicated by the accelerometer on the horizontal base beneath the seat. One reason for a subject's apparent mass changing as the seat inclination increased is that the measured force is less than the true vertical force (see Figure 7.7).

Statistical tests were conducted to determine the significance of the changes in apparent mass with changing seat inclination. The Friedman test was conducted at each 0.25 Hz increment up to 15 Hz using a significance criterion of $p<0.01$.

The apparent masses were significantly influenced by seat inclination between 0 and 1 Hz, between 4.75 and 5.5 Hz, and between 6.75 and 7.5 Hz

(Table 7.5, Friedman test $p<0.01$). At other frequencies the Friedman test indicated that there were no statistically significant changes with seat inclination (i.e. $p>0.01$). Wilcoxon matched-pairs signed ranks tests between the apparent masses measured at pairs of inclinations showed that the differences occurred mainly between the horizontal seat (0 degree inclination) and the other conditions, with the apparent mass decreasing at frequencies below 5.5 Hz and with no significant change at higher frequencies (Table 7.6).

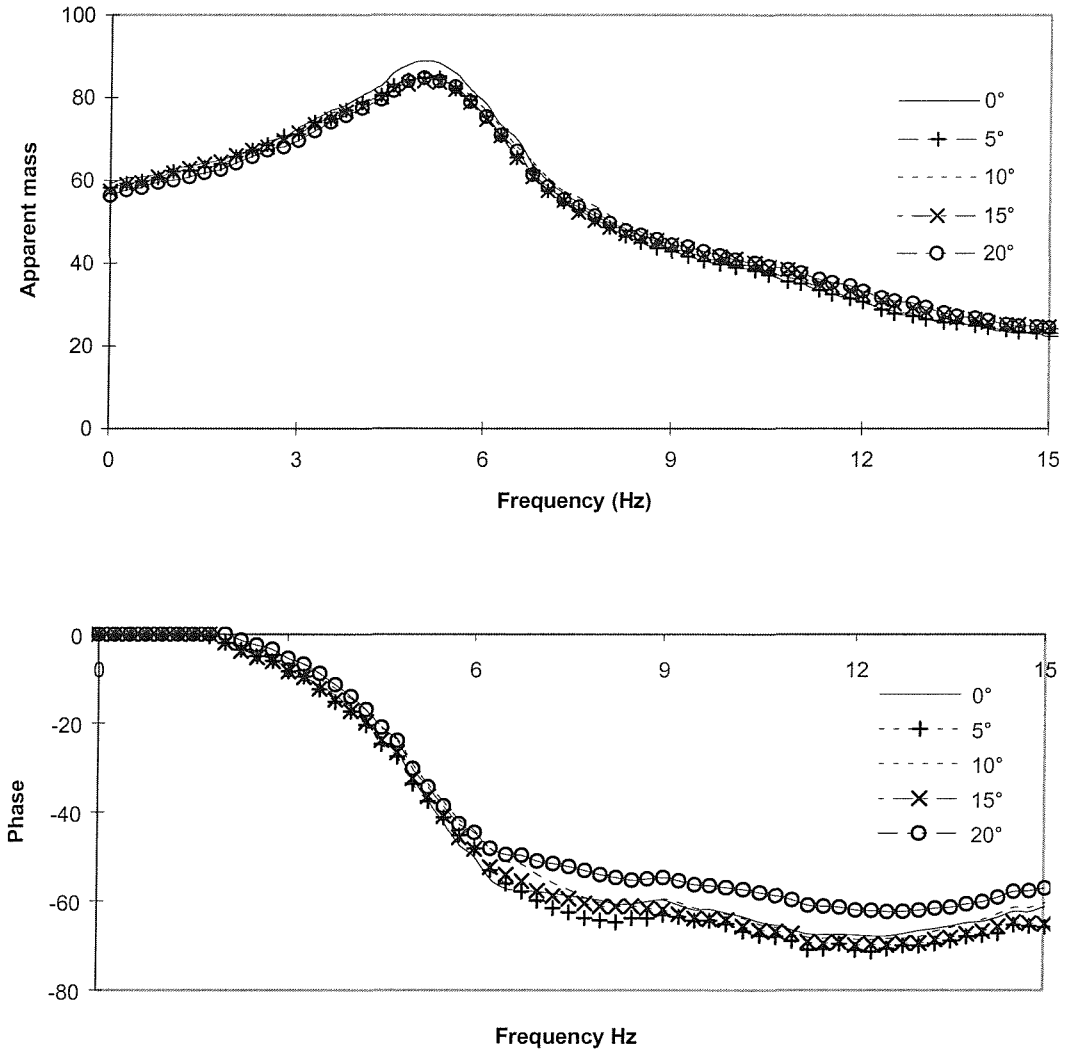

Figure 7.8 Mean apparent mass modulus and phase for 10 subjects at different seat inclinations.

Table 7.5. Comparison of measured apparent masses between five inclinations 0° to 20° (Friedman test).

Frequency (Hz)	Significance level p	Frequency (Hz)	Significance level p	Frequency (Hz)	Significance level p
0.00	0.0013	5.00	0.0006	10.00	0.5853
0.25	0.0009	5.25	0.0023	10.25	0.4834
0.50	0.0013	5.50	0.0079	10.50	0.3540
0.75	0.0127	5.75	0.0248	10.75	0.0263
1.00	0.0005	6.00	0.0553	11.00	0.0149
1.25	0.0210	6.25	0.2042	11.25	0.0860
1.50	0.0174	6.50	0.0588	11.50	0.0639
1.75	0.1618	6.75	0.0065	11.75	0.0264
2.00	0.0463	7.00	0.0174	12.00	0.1093
2.25	0.2799	7.25	0.0094	12.25	0.0097
2.50	0.2471	7.50	0.0081	12.50	0.1771
2.75	0.0109	7.75	0.0109	12.75	0.5690
3.00	0.0614	8.00	0.1172	13.00	0.5842
3.25	0.0298	8.25	0.3386	13.25	0.4834
3.50	0.1018	8.50	0.8879	13.50	0.5541
3.75	0.2311	8.75	0.8372	13.75	0.5394
4.00	0.0496	9.00	0.3600	14.00	0.5842
4.25	0.1353	9.25	0.2250	14.25	0.4306
4.50	0.0131	9.50	0.0852	14.50	0.3653
4.75	0.0007	9.75	0.0632	14.75	0.4873

7.3.4 Discussion

Subject postural changes can result in significant changes in apparent mass (e.g. Kitazaki and Griffin, 1998). When subject posture changes from erect to normal and to slouched, the principal resonance frequency of the normalised apparent mass decreases, and the magnitude of the principal resonance frequency decreased. The effect of subject posture was sufficient to require that subjects keep the same posture in the present experiment as the seat inclination varied.

7.3.5 Conclusion

As expected, the apparent mass changed with change in seat inclination. However the change of the apparent mass was not significant when the subject kept an upright posture at different seat inclinations (Figure 7.8).

Table 7.6 Comparison of measured apparent masses between inclinations 0° and 5°, 0° and 10°, 0° and 15°, 0° and 20° over the significant change frequency range (Wilcoxon matched-pairs signed ranks test).

Frequency (Hz)	Significance level *p* (0°-5°)	Significance level *p* (0°-10°)	Significance level *p* (0°-15°)	Significance level *p* (0°-20°)
0.00	0.3722	0.0111	0.0269	0.0203
0.25	0.0373	0.0076	0.0260	0.0203
0.50	0.3118	0.0076	0.0147	0.0074
0.75	0.3722	0.0502	0.3979	0.0074
1.00	0.2583	0.0076	0.1079	0.0074
4.50	0.0658	0.0076	0.0076	0.0378
4.75	0.0072	0.0072	0.0072	0.0102
5.00	0.0076	0.0076	0.0076	0.0207
5.25	0.0076	0.0107	0.0076	0.0378
5.50	0.0076	0.0281	0.0076	0.1369
6.75	0.3131	0.9526	0.1091	0.1226
7.00	0.1082	0.5933	0.1712	0.3131
7.25	0.2127	0.5933	0.2596	0.2596
7.50	0.3734	0.2596	0.1723	0.4405

Therefore, it is unnecessary to pay attention to seat inclination when subject apparent mass is measured.

7.4 Effect of seat backrest

Experimental studies have shown that a seat backrest and the backrest angle can influence the measured seat transmissibility (Fairley and Griffin, 1989; Lewis & Griffin, 1996). A systematic investigation of the effect of backrests on subject apparent mass is needed to decide how to modify the seat-person model so as to make it suitable. In a seat-person system, the seat backrest may influence the mechanical subsystem representing the human body but will not alter the subsystem representing the seat cushion supporting the body.

The main purpose of this study was to contribute to an improved mathematical model of the apparent mass of the seated person that could be used to predict seat transmissibility. The geometric form of a two-degree-of-freedom model

previously developed by Wei and Griffin (1998a) was used to fit the experimental data.

7.4.1 Experimental method

The whole-body driving-point apparent masses of 10 men were obtained with the subjects seated on a flat rigid seat. Subjects sat on the top plate of a Kistler 9821B force platform that was 600 mm wide, 400 mm deep and 470 mm above the foot support. The foot support moved with the seat but was not supported on the force platform. Vertical motion of the platform was measured using an Entran EGCSY-240D*-10 accelerometer mounted beneath the seat surface. The experiment was conducted using a one-metre stroke electro-hydraulic vertical vibrator in the Human Factors Research Unit at the Institute of Sound and Vibration Research. The input vibration was a random vibration with a flat constant bandwidth acceleration spectrum between 0.5 and 30 Hz at an unweighted acceleration magnitude of 0.5 ms^{-2} r.m.s.

Subjects sat on the seat in six different conditions: (a) no backrest, (b) rigid vertical backrest (i.e. 0^0), (c) soft backrest at 0^0, (d) rigid backrest at 10^0, (e) rigid backrest at 15^0, and (f) rigid backrest at 20^0. The soft backrest consisted of the rigid backrest with an additional square block of foam (60mm thick, 400mm wide, 500mm high). The subjects were supported by the force platform (and the backrest); the backrest was not supported on the force platform.

Subjects were exposed to 60 seconds vibration with a frequency range from 0.5 to 30 Hz. Signals from the accelerometer and the force platform were conditioned and acquired at 400 samples per second via 60 Hz anti-aliasing filters.

Nine male and one female subject participated in the study. They were staff and students of the University of Southampton. Their mean age was 36.7 years, mean height 1.74 m, and mean weight 71.0 kg (Table 7.7).

Table 7.7 Subject characteristics

subject	age (years)	stature (m)	total weight (kg)
1 (male)	36	1.68	75
2 (male)	41	1.70	65
3 (male)	37	1.77	71
4 (male)	41	1.68	72
5 (female)	37	1.65	60
6 (male)	26	1.80	73
7 (male)	42	1.73	68
8 (male)	35	1.80	74
9 (male)	33	1.85	86
10 (male)	39	1.73	66

Measures of apparent mass are reported here after the subtraction of the mass of the platform above the force cells.

7.4.2 Human body mathematical impedance model

The two-degree-of-freedom model from Chapter 6 was used to fit the experimental data (see Section 6.3.2 and Figure 6.4).

7.4.3 Results and model parameters

Figure 7.9 shows the mean measured apparent mass of the 10 subjects for the six sitting conditions when using random vibration. Some individual examples, including coherence, are given in Appendix B. When subjects sat without a backrest, the resonance frequency of the apparent mass was lowest and the apparent mass at resonance was a little higher than in the other conditions. It can also be observed that at frequencies below the resonance frequency the apparent mass was higher than when subjects sat with a backrest. This may be because a part of the sitting mass on the force platform was transferred to the seat backrest when subjects sat in contact with the backrest.

With the 0^0 backrest angle, when the backrest changed from soft to hard, the resonance frequency increased, although there was no change in the apparent mass at resonance. At frequencies above resonance, the apparent mass was greater with the rigid backrest than with the soft backrest.

As the backrest angle increased with the rigid backrest, the resonance frequency of the apparent mass increased but the apparent mass at resonance remained unchanged. At frequencies less than the resonance, the apparent mass decreased with increasing backrest angle. These changes may have been caused by the mass transferring from the seat surface to the backrest.

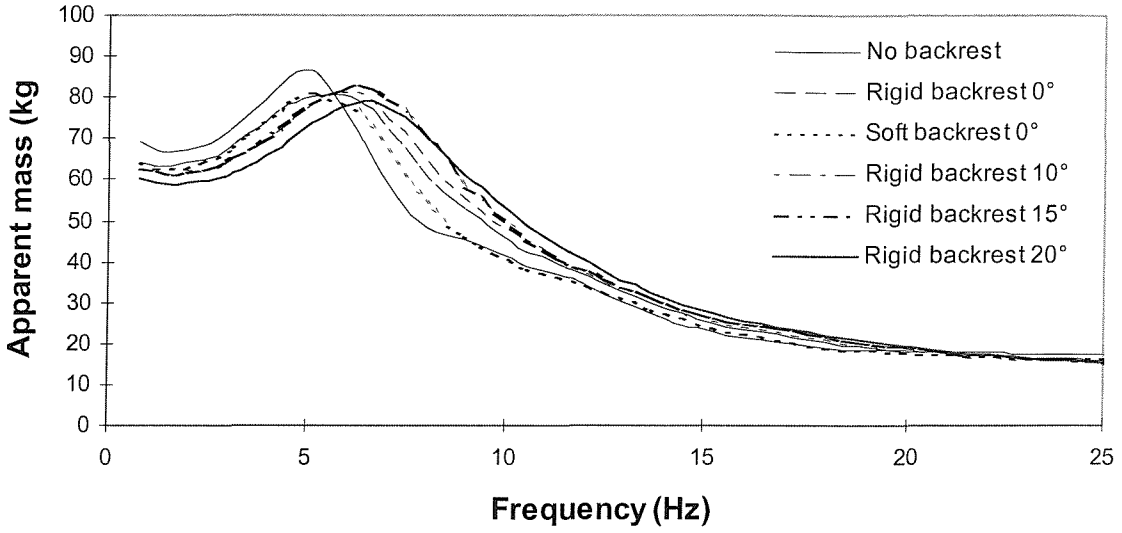

Figure 7.9 Mean apparent masses of ten subjects with different sitting conditions.

The mean measured apparent masses in the different seating conditions can be compared in Figure 7.9. It is clear that there were significant differences in the measured apparent mass with different backrest conditions, and hence a new model, or a modified model might be developed to represent the new data. Because a useful two degree-of-freedom model has been previously defined (Wei and Griffin 1998a), and its application gives useful predictions of seat transmissibility when there is no backrest, modifications to this model for different backrest conditions might be more appropriate than the development of a new model.

The two-degree-of-freedom model in Figure 6.4 was used to fit the measured apparent masses and obtain all model parameters. However, it seemed

unnecessary to change all model parameters when the sitting condition varied.

Figures 7.10 to 7.16 show the sensitivity of the apparent mass to each of the seven parameters in the two degree-of-freedom model shown in Figure 6.4. In these figures, the first model parameter (i.e. the first value of each parameters expressed in every Figure) comes from the values found by Wei and Griffin (1998a) for a group of 60 subjects (24 men, 24 women and 12 children) as measured by Fairley and Griffin (1989). It can be observed that changes to the masses m, m_1 and m_2 have a similar effect on apparent mass at frequencies below resonance. However, when mass m increases, the apparent mass rises at all frequencies, which is not consistent with the measured apparent mass in Figure 7.9, so it was not selected as a useful model parameter to vary. When m_1 decreases, the resonance frequency increases and the apparent mass at resonance decreases. However, when m_2 decreases the resonance frequency is unchanged but the apparent mass decreases. It seems that parameter m_1 is a critical parameter for fitting the changes in apparent mass measured here, although it causes an unobserved change in the apparent mass at resonance.

Figures 7.13 and 7.14 show the effect of the subsystem stiffness k_1 and subsystem damping c_1. As the stiffness k_1 increases, the resonance frequency and the apparent mass at resonance both increase. Changes in the stiffness k_1 may therefore offset the undesired changes arising from changes in m_1. The influence of parameter c_1 is the same as that of damping in a simple one degree-of-freedom system.

Figures 7.15 and 7.16 show the function of subsystem stiffness k_2 and subsystem damping c_2. These two parameters have only a small effect on model predictions and mainly affect apparent mass at frequencies above resonance. Consequently, only the parameters of one subsystem were selected for optimisation when fitting the measured data: m_1, k_1 and c_1.

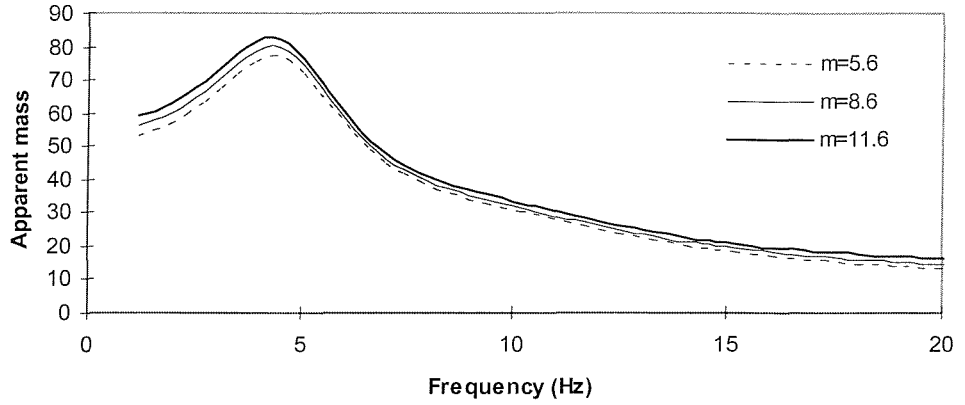

Figure 7.10 The sensitivity of model parameter m in the prediction of apparent mass

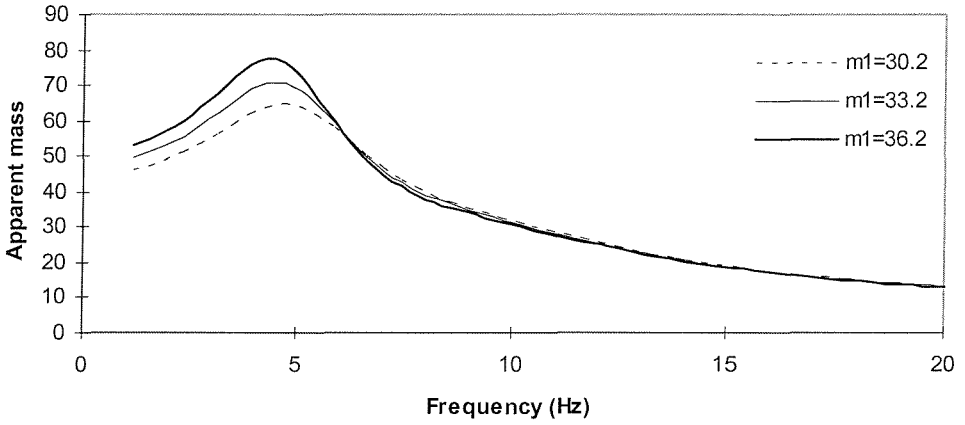

Figure 7.11 The sensitivity of model parameter m_1 in the prediction of apparent mass

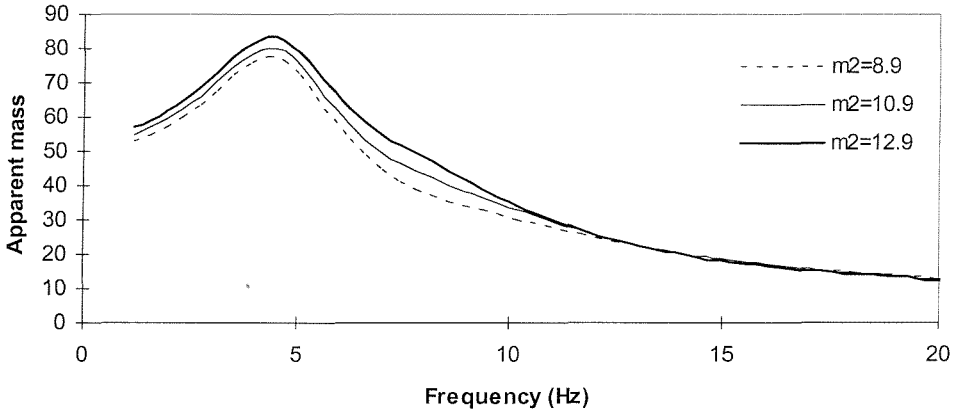

Figure 7.12 The sensitivity of model parameter m_2 in the prediction of apparent mass

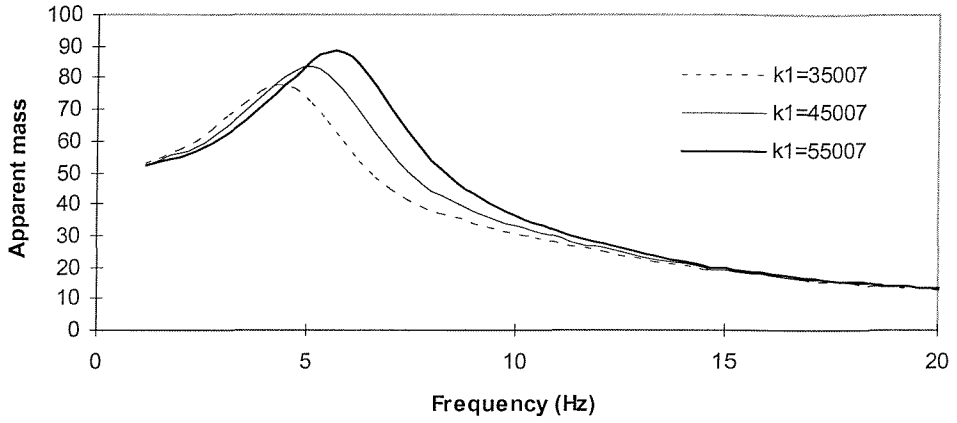

Figure 7.13 The sensitivity of model parameter k_1 in the prediction of apparent mass

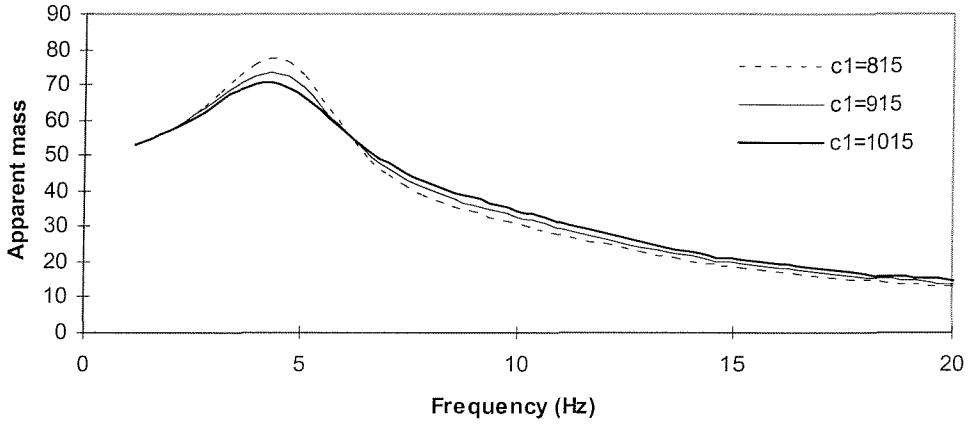

Figure 7.14 The sensitivity of model parameter c_1 in the prediction of apparent mass

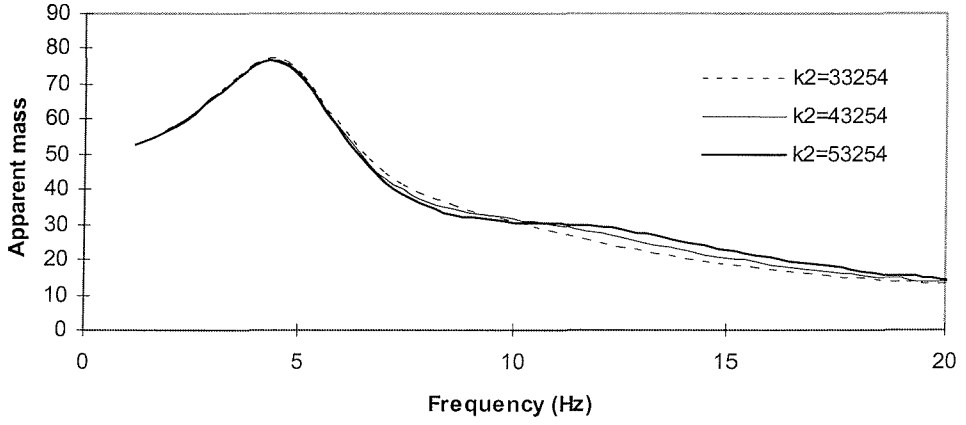

Figure 7.15 The sensitivity of model parameter k_2 in the prediction of apparent mass

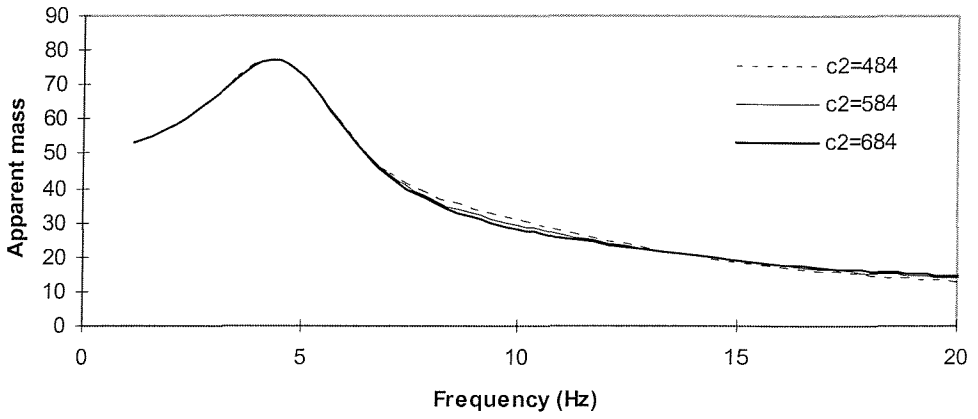

Figure 7.16 The sensitivity of model parameter c_2 in the prediction of apparent mass

For each of the five sitting conditions without the soft backrest, the model in Figure 6.4 was fitted separately to the mean of ten subjects' apparent masses. The fitting was performed using MATLAB (version 4.2).

Figure 7.17 shows the results using the two degree-of-freedom model to fit the mean of the ten subjects' experimental data in the five sitting conditions. When subjects sat without a backrest, all of the model parameters (i.e. m, m_1, m_2, k_1, c_1, k_2 and c_2) were obtained through the MATLAB fitting software using as the starting values the parameters previously found by Wei and Griffin (1998a). When the sitting conditions changed, the model parameters m, m_2, k_2 and c_2 were unchanged and only three parameters (m_1, k_1 and c_1) were varied. All model parameters optimised for the different sitting conditions are listed in Table 7.8. It appears that the mass m_1 decreased while the stiffness k_1 and the damping c_1 increased as the sitting condition changed from without backrest to a backrest angle of 20^0.

7.4.4 Modification of mathematical model

The parameters of the model varied with different backrest conditions. This change could be represented by a new model in which parameters vary as a function of backrest angle. Alternatively, the phenomenon can be represented by a model in which the parameters are fixed at values appropriate for specific

backrest conditions. The second option has been developed here (see Table 7.8 and Figure 7.17).

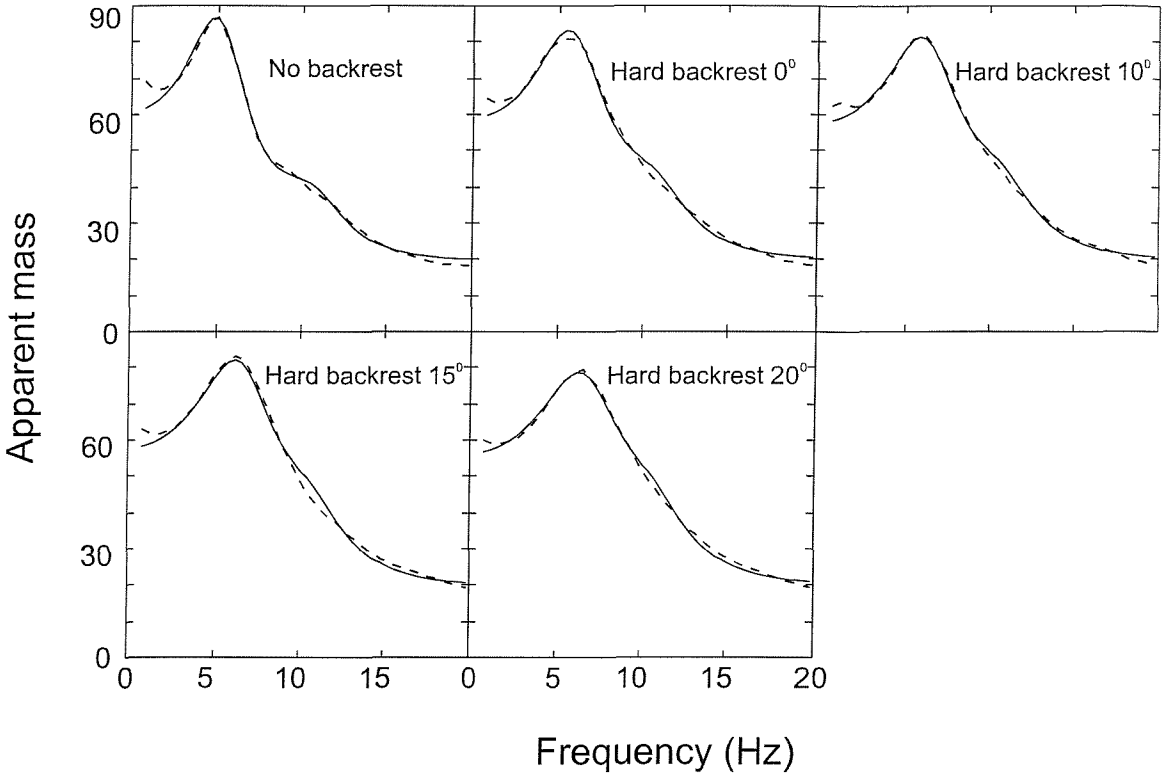

Figure 7.17 Comparison of mean measured apparent mass and response of two degree-of-freedom model (– – – – – measured data, ——— model prediction).

The transmissibility of a seat predicted with a seat-person model having the different parameters is shown in Figure 7.18. The seat model and seat parameters come from Chapter 5. It can be seen that when using the different parameters of the human body model, the predicted seat transmissibilities also varied. With the subject against the backrest and with the backrest angle increasing, the predicted resonance frequency and the transmissibility at resonance increased, but at frequencies higher than 10 Hz, the changes are small.

The values in Figure 7.18 were predicted using apparent mass data for the conditions when there was either no backrest or a rigid backrest; but vehicle seats usually have soft backrests. The coupling between the back and a soft backrest merits further investigation and it should not be assumed that the model in Figure 6.4 or the values in Table 7.8 are optimal. Consequently, the

values in Figure 7.18 may not be found in practice. The primary interest in Figure 7.18 is the illustration that changes in body apparent mass of the type shown in Figure 7.9 affect seat transmissibility.

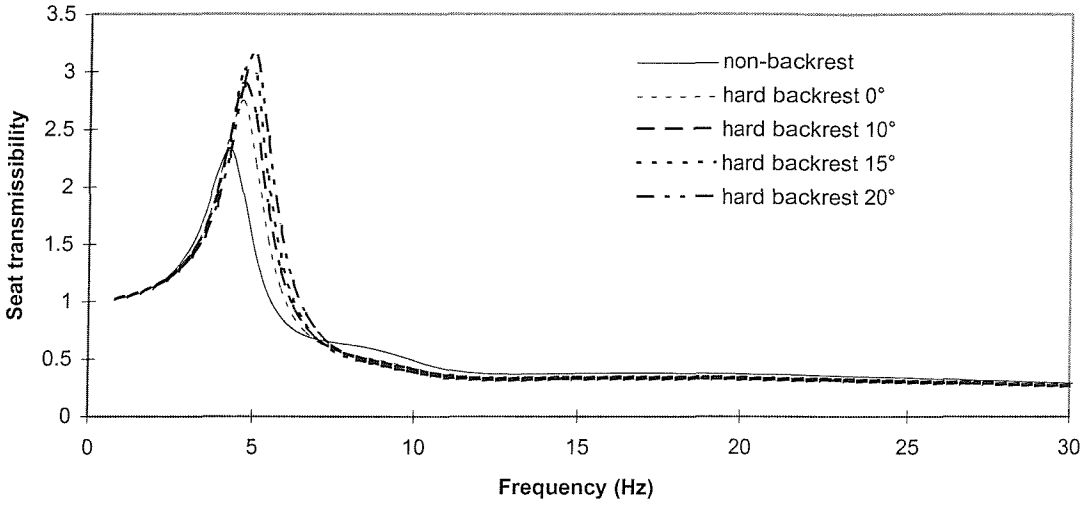

Figure 7.18 Prediction of seat transmissibility using model parameters for different backrest angles.

Table 7.8 Model parameters for each backrest condition.

random vibration							
condition	m	m_1	m_2	k_1	c_1	k_2	c_2
non-backrest	5.05	34.4	6.4	43605	835	30472	208
Rigid backrest 0^0	5.05	32.6	6.4	54326	932	30472	208
Rigid backrest 10^0	5.05	31.3	6.4	58136	941	30472	208
Rigid backrest 15^0	5.05	31.2	6.4	63119	962	30472	208
Rigid backrest 20^0	5.05	29.8	6.4	64324	988	30472	208

7.4.5 Discussion and conclusion

The apparent mass of the body differs between subjects and different model parameters can be obtained for each subject. However, fitting to the mean subjects data can provide a model that represents the average response of subjects (see Chapter 6). Figure 7.17 suggests that the two degree-of-

freedom mathematical model used here can provide a good fit to measured mean data with different backrest conditions.

This study shows that there are clear and consistent differences in the dynamic response of the body as the backrest condition changes. Although the causes of the changes are not clear, it is obvious that the specification of the apparent mass of the body should depend on the backrest conditions.

It is concluded that a two-degree-of-freedom mathematical model can provide a good fit to the apparent mass of the seated human body in the vertical direction. A decrease in the mass m_1, and an increase in both the stiffness k_1 and the damping c_1 might be used to represent changes that occur when there is increased contact with a backrest. However, further investigation of the interaction between the seated body and backrests is required.

7.5 Effect of hard seat and soft seat as well as vibration spectra

It has been shown that the sitting posture, footrest, backrest, vibration magnitude all cause the changes of body apparent mass and mechanical impedance. However, there has been little investigation of the effect of a soft seat on body apparent mass. A systematic investigation of the effect of a soft seat on subject apparent mass is needed to decide how to modify the seat-person model so as to make it suitable. In a seat-person system, a hard seat may result in a different mechanical response of the human body from a soft seat.

The main purpose of this study is to contribute to an improved mathematical model of the apparent mass of the seated person that could be used to predict seat transmissibility. The effect of the input vibration spectrum on the apparent mass was also investigated because the vibration waveform from the surface of a hard seat and a soft seat are different. Again, the geometric form of a two-degree-of-freedom model previously developed in Chapter 6 was used to fit the experimental data.

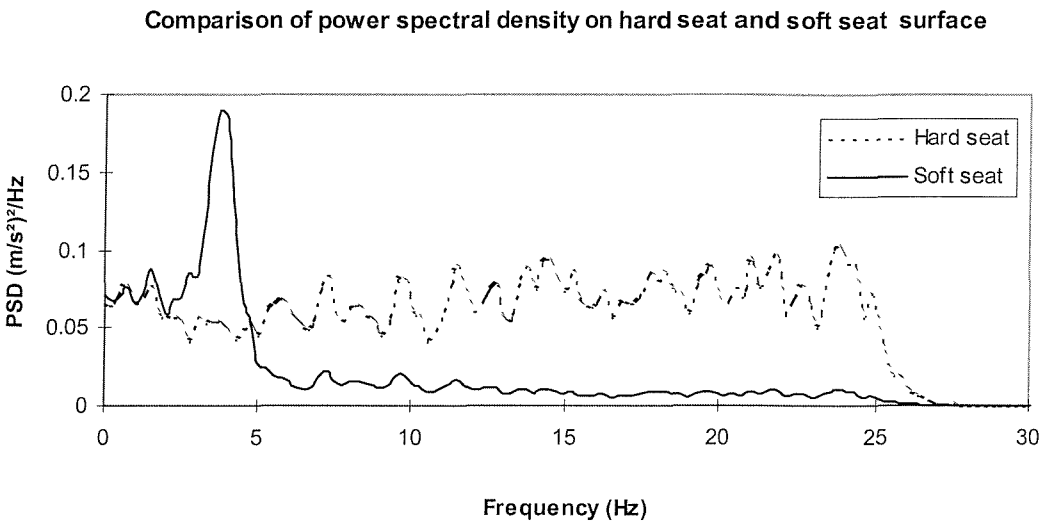

Figure 7.19. Power spectrum on a hard seat (1.47 m/s^2 rms magnitude) and a soft seat (0.86 m/s^2 rms magnitude)

7.5.1 Hypothesis

There are differences in human body dynamic response between a hard seat and soft seat for the follow reasons:

- Vibration magnitude on the seat surface is different from the magnitude beneath the seat (Figure 7.19) so the body response may be different due to non-linearity (see Section 7.2).
- The vibration spectrum is changed. Gaussian random vibration with equal energy at each frequency was used in the hard seat driving point apparent mass experiment. The same vibration spectrum used in the soft seat test but the vibration energy distribution on the soft seat surface varied (Figure 7.19).

7.5.2 Materials and methods

Due to the difference of the input vibration on the seated subject (Figure 7.19), an investigation of the effect of input spectrum is needed to confirm whether the change of subject apparent mass is caused by different input spectrum rather than the difference of seats. In other words, the soft seat itself may not be the cause of any change in body response.

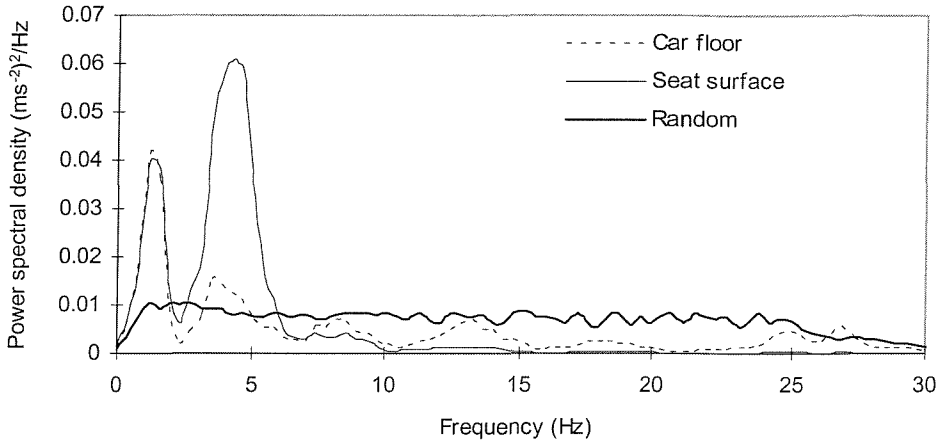

Figure 7.20 Three vibration input spectra with 0.5 ms^{-2} r.m.s. magnitude

The same hard seat, shaker and instruments (Section 7.4.1) were used to conduct experiments. The soft seat was a hard seat modified by adding a block of square foam. The foam was TDI foam, which had a density of 50 $kg.m^3$ and a size 500mm wide by 420mm deep and 110 mm thick. Three different input vibration spectra were used: (i) random vibration with a flat constant bandwidth acceleration spectrum between 0.5 and 30 Hz at an unweighted acceleration magnitude of 0.5 ms^{-2} r.m.s., (ii) vertical floor vibration measured in a car and presented at a magnitude of 0.5 ms^{-2} r.m.s. (unweighted), and (iii) vertical seat surface vibration measured in the same car at the same time and presented with the same unweighted vibration magnitude of 0.5 ms^{-2} r.m.s. (see Figure 7.20). The three input signals had the same sixty-second duration, the first signal, the random vibration, was used in a first experiment to investigate the effect of hard and soft seat on body apparent mass. The second experiment used all three input signals to investigate the effect of the input spectrum on body apparent mass.

Again, the two-degree-of-freedom model proposed in Chapter 6 was used to fit the first experimental data (Figure 6.4), but the model for the second experiment was different. Figure 7.21 shows the model used to fit the data from the second experiment. This is a human body and seat model. The stiffness k and c represent the seat dynamic characteristics. They have been obtained through an indenter test and measured data curve fitting.

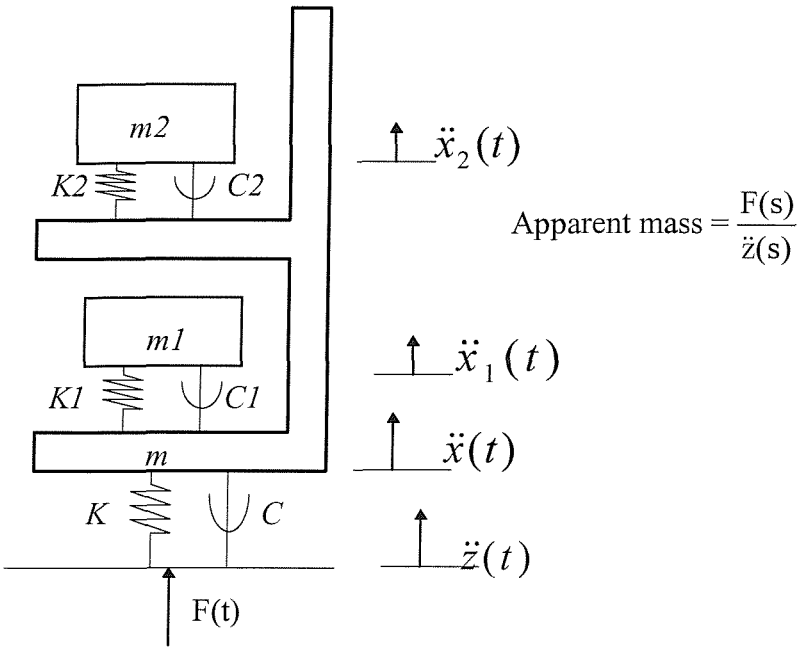

Figure 7.21 The model for seated subject on soft seat.

7.5.3 Results

Ten subjects participated in this study. Figure 7.22 shows the mean of the ten subject apparent masses measured on the hard and soft seat. The mean of the fitted curves for hard and soft seats are also shown in Figure 7.22. The individual measured and fitted curves are similar to the curves shown in Figure 7.22, so they are not presented in here.

All parameters acquired by curve fitting shown in Table 7.9. When using the two-degree-of-freedom model fitted the measured data, the model frame mass, m, was consistent. Figure 7.23 shows the differences of the two-degree-of-freedom body model parameters between the two test conditions. The stiffness, k_1 and k_2, the damping, c_1 and c_2, and the mass, m_2, decreased but the mass, m_1, increased using the soft seat to replace the hard seat. Taking vibration magnitude into account, it means that the stiffness, the damping and the mass, m_2, decreased but the mass, m_1, increased as the vibration magnitude decreased. This result is different from previous conclusions, in which the stiffness and the damping of the model decreased as the vibration magnitude increased. The reason for this phenomenon

presumably is: ① the change of the model mass, ② the change of input vibration magnitude and ③ the change of the input vibration waveform.

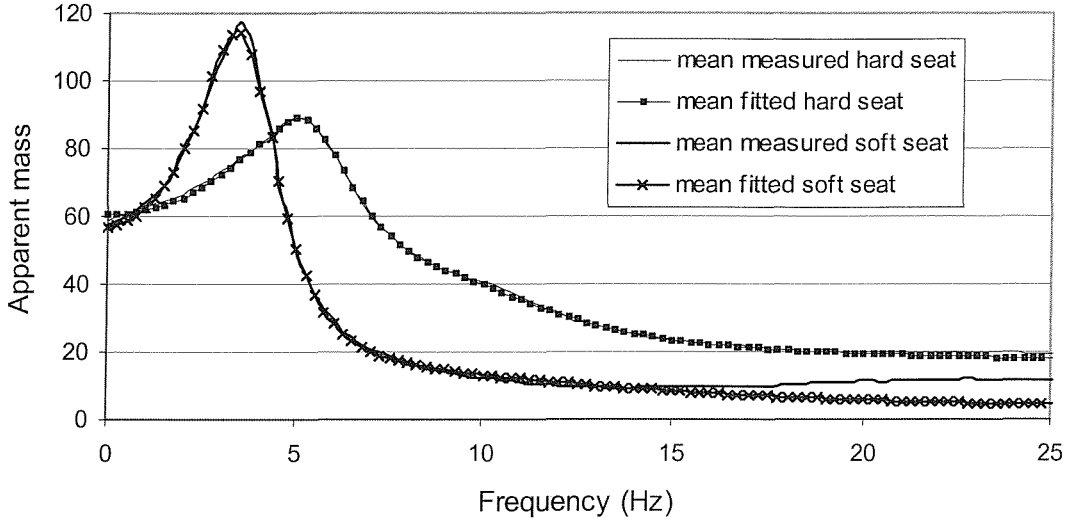

Figure 7.22 Mean measured apparent mass on soft and hard seat as well as the curve fitting results.

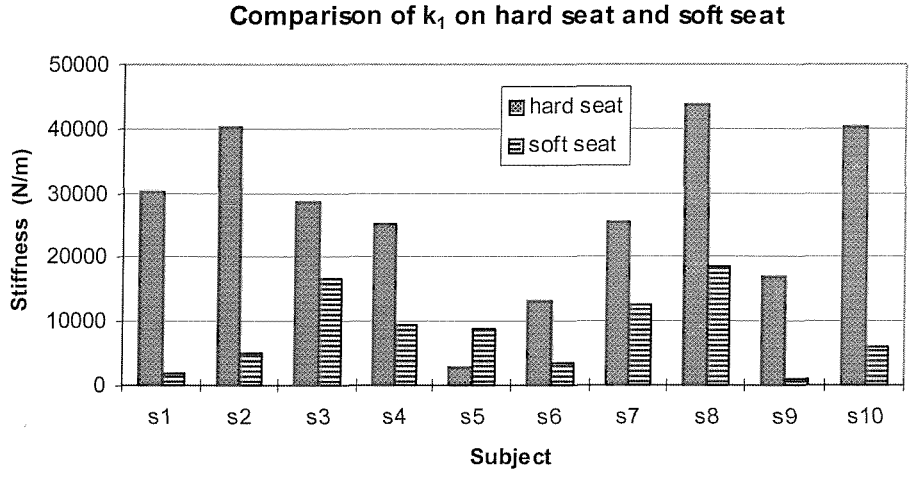

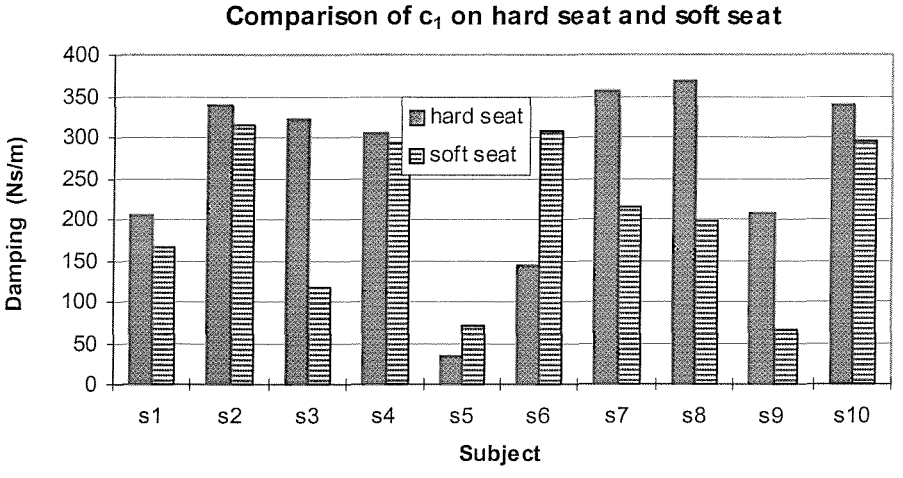

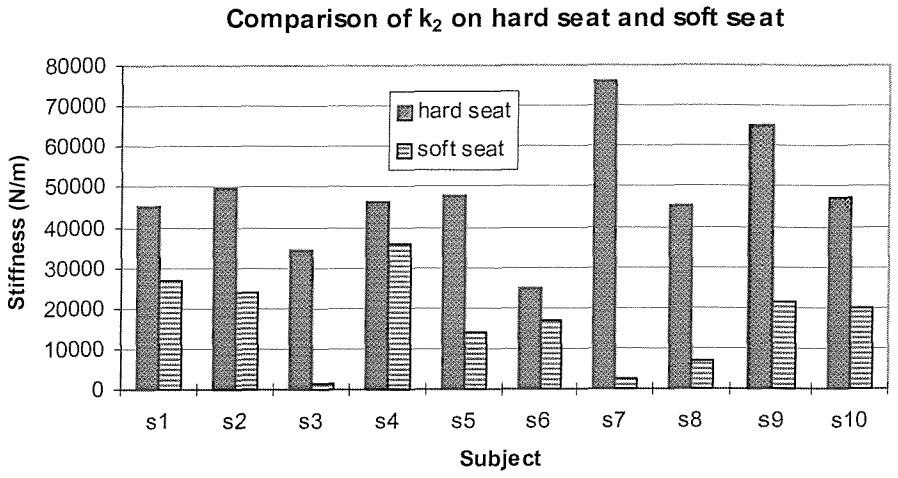
Comparison of k_2 on hard seat and soft seat
Stiffness (N/m)
80000
70000
60000
50000
40000
30000
20000
10000
0
hard seat
soft seat
s1
s2
s3
s4
s5
s6
s7
s8
s9
s10
Subject

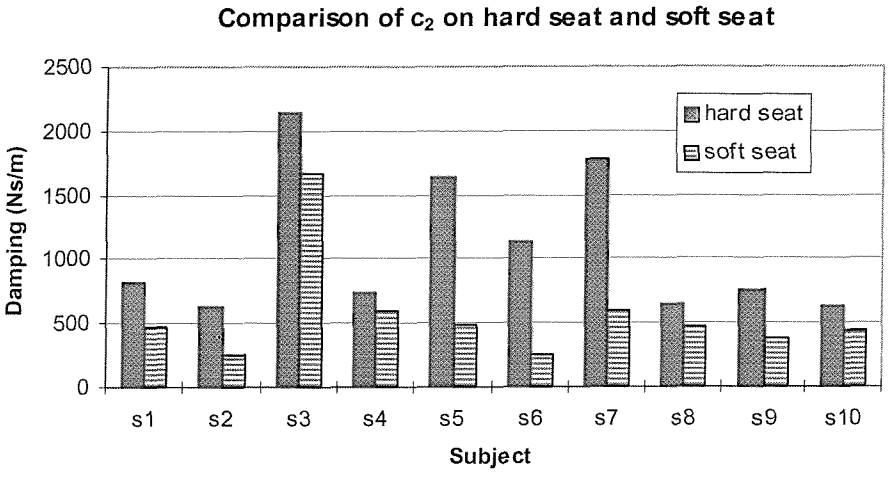
Comparison of c_2 on hard seat and soft seat
Damping (Ns/m)
2500
2000
1500
1000
500
0
hard seat
soft seat
s1
s2
s3
s4
s5
s6
s7
s8
s9
s10
Subject

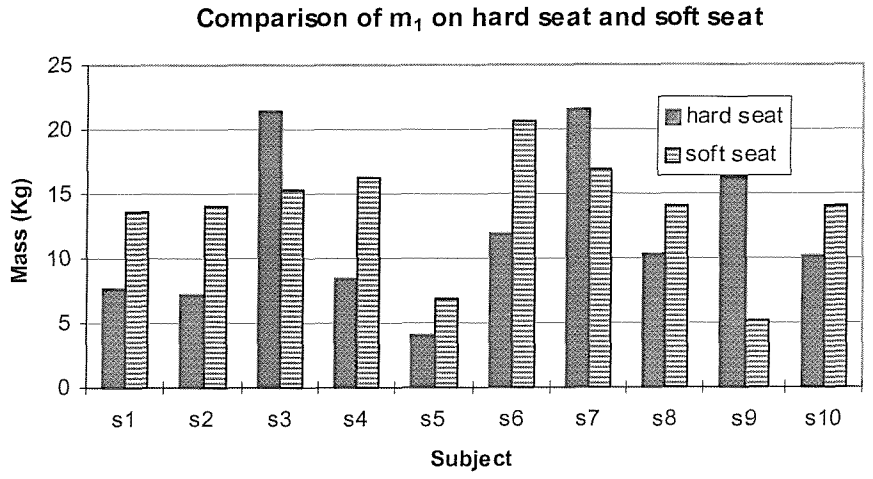
Comparison of m_1 on hard seat and soft seat
Mass (Kg)
25
20
15
10
5
0
hard seat
soft seat
s1
s2
s3
s4
s5
s6
s7
s8
s9
s10
Subject

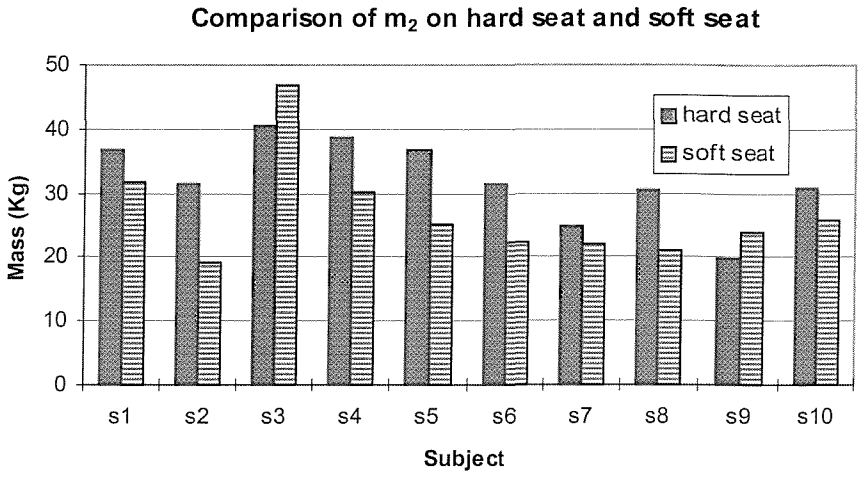

Figure 7.23 The comparison of model parameters between hard seat and soft seat

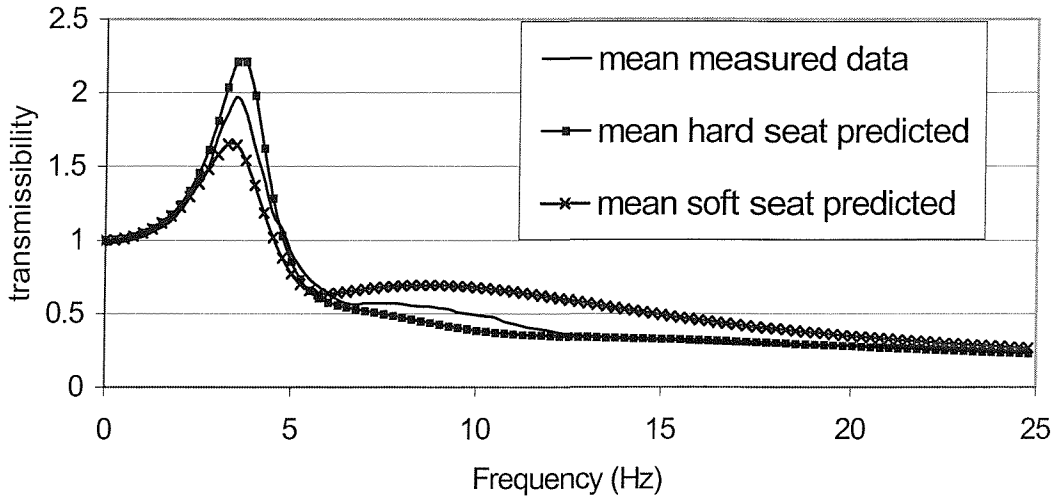

Figure 7.24 Seat transmissibility prediction by using hard seat and soft seat acquired model parameters

Figure 7.24 shows the seat transmissibility predicted by using the two-degree-of-freedom model. The model parameters come from fitting the measured apparent mass from the hard seat and the soft seat data. It is clear that the model parameters for apparent mass coming from the hard seat can produce a better prediction result, especially at frequency above 6 Hz. It can also be observed that the real seat transmissibility is always between the two prediction curves for frequency below 6 Hz.

Table 7.9 Two-degree-of-freedom-model parameters

Subjects	Seat	k_1 (N/m)	c_1 (Ns/m)	k_2 (N/m)	c_2 (Ns/m)	m (kg)	m_1 (kg)	m_2 (kg)	Total mass (kg)
1	Hard	30192	204	45183	821	19.6	7.6	36.8	64
	Soft	1757	167	26764	478	19.6	13.6	31.9	
2	Hard	40162	340	49490	632	16.7	7.2	31.3	55.2
	Soft	4896	314	23723	252	16.7	14.1	19.3	
3	Hard	28715	323	34534	2131	15.8	21.4	40.7	78.7
	Soft	16773	117	1654	1663	15.8	15.3	47.0	
4	Hard	25192	304	46453	735	16.6	8.4	38.8	63.8
	Soft	9342	293	35764	598	16.6	16.2	30.2	
5	Hard	2875	33	47497	1635	15.8	4.0	36.9	57.1
	Soft	8716	70	13933	494	15.8	6.8	25.2	
6	Hard	13198	143	24979	1137	9.3	11.9	31.6	52.8
	Soft	3310	308	16805	244	9.3	20.6	22.2	
7	Hard	2545	357	75827	1783	15.8	21.6	24.8	63.3
	Soft	12714	215	2274	603	15.8	16.8	22.1	
8	Hard	43783	368	45157	638	19.7	10.3	30.5	60.5
	Soft	18517	197	7156	474	19.7	14.0	21.1	
9	Hard	17134	208	65195	752	16.5	16.2	19.8	53.5
	Soft	994	65	21208	370	16.5	5.2	23.9	
10	Hard	40162	340	47320	632	16.5	10.2	30.9	57.6
	Soft	5896	294	19723	433	16.5	14.1	25.8	

For the second experiment, the mean measured apparent masses for the 10 subjects with the three different input spectra (Figure 7.20) for each of the six different sitting conditions are shown in Figure 7.25. Statistical tests were conducted to determine the significance of the changes in apparent mass with changing input spectra. The Friedman test was conducted at each 0.391 Hz increment up to 23 Hz using a significance criterion of $p<0.01$.

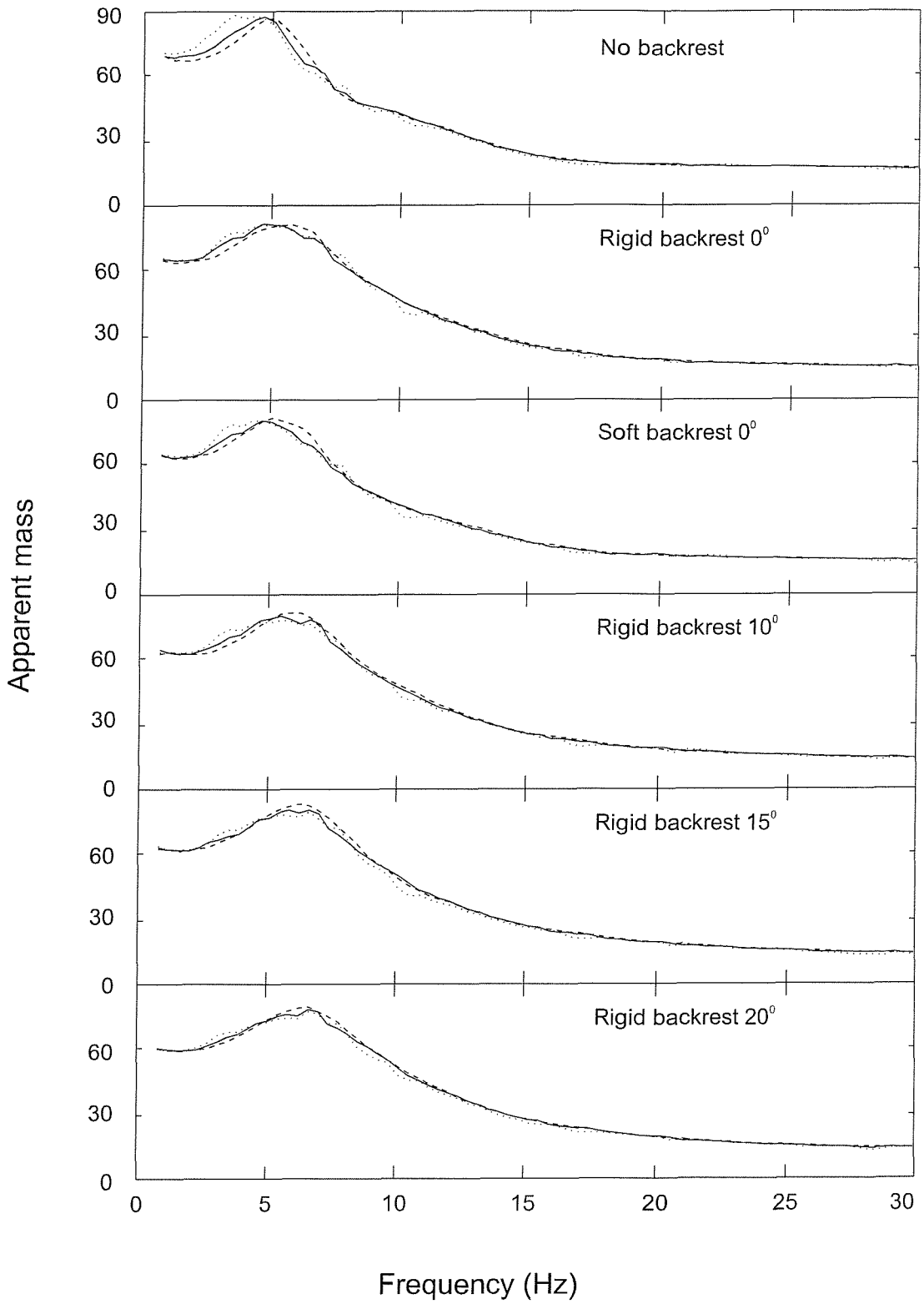

Figure 7.25 The mean apparent masses of ten subjects with different backrest conditions (····· car seat surface spectrum, – – – – random spectrum, ——— car floor spectrum)

Table 7.10 shows the statistical results. With no backrest, the body apparent mass was significantly influenced by the input spectra between 1.56 and 4.3 Hz, between 5.47 and 6.25 Hz, and between 15.2 and 16.4 Hz, as well as 7.03 Hz, 10.5 Hz, 13.7 Hz, 17.6 Hz, 20.3 and 22.7 Hz ($p<0.01$). At other frequencies there was no significant difference in apparent mass between the input spectra. With other conditions having hard and soft backrests, there were similar differences in apparent mass between the three input vibration spectra.

Table 7.10. Comparison of measured apparent masses between three input spectra (Friedman test).

Frequency (Hz)	Significance level p	Frequency (Hz)	Significance level p	Frequency (Hz)	Significance level p
0.0000	0.0247	7.8100	0.0017	15.6000	0.0055
0.3910	0.6703	8.2000	0.6703	16.0000	0.0033
0.7810	0.7408	8.5900	0.3012	16.4000	0.0071
1.1700	0.0136	8.9800	0.0611	16.8000	0.0247
1.5600	0.0033	9.3800	0.4966	17.2000	0.2319
1.9500	0.0007	9.7700	0.0330	17.6000	0.0074
2.3400	0.0002	10.2000	0.4966	18.0000	0.1538
2.7300	0.0001	10.5000	0.0022	18.4000	0.3872
3.1300	0.0001	10.9000	0.0208	18.8000	0.4966
3.5200	0.0002	11.3000	0.0608	19.1000	0.0383
3.9100	0.0002	11.7000	0.4966	19.5000	0.0330
4.3000	0.0079	12.1000	0.0383	19.9000	0.0125
4.6900	0.6703	12.5000	0.5836	20.3000	0.0055
5.0800	0.1225	12.9000	0.2725	20.7000	0.0045
5.4700	0.0074	13.3000	0.5004	21.1000	0.0921
5.8600	0.0007	13.7000	0.0055	21.5000	0.9048
6.2500	0.0012	14.1000	0.0608	21.9000	0.9048
6.6400	0.0247	14.5000	0.0247	22.3000	0.2725
7.0300	0.0055	14.8000	0.0022	22.7000	0.0022
7.4200	0.4966	15.2000	0.0055	23.0000	0.1096

7.5.4 Discussion

There were significant differences of vibration magnitudes between the surface of a hard seat and a soft seat and these changes resulted in variation of human body dynamic response.

It is reasonable to use a two degree-of-freedom model to represent the human body dynamic response in the vertical vibration. Using this model, a good product of apparent mass on a hard seat can be obtained. In fact, a good product of apparent mass on a soft seat can also be obtained.

The parameters of the human body two degree-of-freedom model coming from a hard seat and a soft seat were different. This means that the dynamic responses of the seated body might be different between sitting on a hard seat and a soft seat. However, the cause of this change was not clear. The changes of subject posture, vibration magnitude and vibration spectra all could cause this difference. The seat transmissibility predictions showed that the model parameters from the hard seat seemed more reasonable than the model parameters from the soft seat.

The differences between the vibration on the hard seat and the soft seat were vibration magnitude and vibration spectrum. Further study using the vibration spectrum coming from a soft surface to vibrate a subject sitting on a hard seat should be considered. This will be helpful for building standard human body mathematical models.

7.5.5 Conclusions

There were significant differences in vibration on the hard seat and on the soft seat and these changes resulted in difference in the human body dynamic responses.

The parameters of the two-degree-of-freedom model derived from the hard seat and the soft seat were different. Although these parameters gave good predictions for human body apparent masses, the data from the soft seat did not give such a good prediction of seat transmissibility. The parameters from the soft seat may not be suitable for predicting seat transmissibility.

When subjects changed their sitting condition from hard seat to soft seat, the model stiffness, k_1 and k_2, model damping, c_1 and c_2, and mass, m_2, decreased, but model mass, m_1, increased, except for some subjects.

Using three very different spectra with the same unweighted r.m.s. acceleration, there was a statistically significant effect of the spectra on apparent mass, but the magnitude of the effect was small. This is reasonably consistent with the study conducted by Sandover (1978) who found no difference in apparent mass when using two input vibration spectra of the same vibration magnitude, with one spectrum having more energy at high frequencies and the other having more energy at low frequencies. The differences in apparent mass between the spectra were small compared to differences previously seen with a fixed spectrum of vibration at different magnitudes. It seems that when different input spectra have the same energy (e.g. the same unweighted r.m.s. magnitude) over a range of low frequencies but a different energy distribution, the measured apparent masses may be similar.

7.6 Conclusions

The dynamic response of the body varies when the magnitude of vibration changes. The response of the sitting body to vertical vibration is non-linear. Although the causes of the non-linearity are not clear, it is obvious that the specification of the apparent mass of the body should be specific to a limited range of vibration conditions.

Using a two-degree-of-freedom mathematical model to fit the measured data, a decrease in both stiffness and damping appeared in the model when the vibration magnitude increased. This implies that a non-linear model should be developed to represent the apparent mass at various vibration magnitudes. However, the phenomenon could be represented by a linear model in which the parameters are fixed at different values appropriate for specific magnitudes of vibration. The corresponding model has been proposed here,

and found suitable for different vibration magnitudes, but it is still a linear model.

The new model parameters derived here are different from the model parameters derived in Chapter 6, because different human subjects have been measured. However, the model stiffness and damping are similar to the previously developed model (Chapter 6) at the same vibration magnitude.

The vertical apparent mass varied with variations in seat inclination. However, the change of the apparent mass was not significant when subjects kept upright postures at different seat inclinations. Therefore, if subject apparent mass is measured with an upright posture, it is unnecessary to pay attention to seat inclination.

There are clear and consistent differences in the dynamic response of the body as the backrest condition changes. Although the causes of the changes are not clear, it is obvious that the specification of the apparent mass of the body should depend on the backrest condition.

Using a two-degree-of-freedom mathematical model to fit the measured data, different model parameters appeared when the seat backrest angle changed. A decrease in the mass m_1, and an increase in both the stiffness k_1 and the damping c_1 could be used to represent changes that occur when there is increased contact with a backrest. This suggests that a modification of the model proposed in Chapter 6 might give satisfactory predictions of body apparent mass at different backrest conditions. However, further investigation of the interaction between the seated body and backrests is required.

The apparent mass of the seated human body was influenced by the input spectrum even if the spectrum has the same overall r.m.s. magnitude. However, the influence of the vibration spectrum is not large. The differences in apparent mass between the spectra were small compared to differences previously seen with a fixed spectrum of vibration at different magnitudes.

The parameters of the two-degree-of-freedom model derived from a hard seat and a soft seat were different. The model parameters from the soft seat did not give such a good prediction of seat transmissibility. The model parameters from the hard seat will be preferred in predicting seat transmissibility.

When subjects changed their sitting condition from hard seat to soft seat, the model stiffness, k_1 and k_2, model damping, c_1 and c_2, and mass, m_2, decreased, but model mass, m_1, increased, except for some subjects. Considering the effect of vibration magnitude, this phenomena is opposite to the previous study (see Section 7.2) because the vibration magnitude on the soft seat surface was less than that on the hard seat surface.

CHAPTER 8

PREDICTING SEAT TRANSMISSIBILITY

8.1 Introduction

As discussed in the literature review, there were many methods to obtain seat transmissibility, but the prediction method was a new one and it was hoped to be developed into a standard method. This chapter deals with the prediction of seat dynamic performance without using human subjects. The method is based on separate measurements of the impedance of the seat and the impedance of the human body. A preliminary study (see Chapter 4) showed that the method could give useful predictions in limited conditions. The study here will investigate the possibility of using the method in normal conditions, such as predicting seat transmissibility as measured in the laboratory and in the field and for subjects sitting with and without backrest.

An advantage of the mathematical method of prediction is that it encourages the development of a better understanding of the dynamic performance of seat components (e.g. suspensions, foams, covers). Eventually, with a full understanding of the role and dynamic performance of each seat component it may be possible to predict seat dynamic performance from the physical and chemical construction of the various seat parts. By these means a mathematical model could be used to identify the desired dynamic properties of a seat and the method of achieving this performance could also be predicted. For example the required mix of foam ingredients might be predicted.

The prediction of seat transmissibility requires knowledge of the mechanical impedance of the seated human body. The study in Chapter 6 has developed two optimum models of the impedance of the seated body: a single-degree-of-freedom model and a two-degree-of-freedom model. The two-degree-of-freedom model has been further developed in Chapter 7 so that it could be

used in different test environments, such as different vibration magnitudes and different backrest inclinations. The seat impedance has been studied in Chapter 5. A seat model has been put forward based on the measurement of seat impedance, which were obtained by a defined seat test method – the indenter method. The prediction of seat transmissibility from two seat-person models, which were two degree-of-freedom and three degree-of-freedom models, will be compared in this study.

The purpose of the study in this chapter is to assess the accuracy of the prediction method through a comparison between measured and predicted seat transmissibility. The seat transmissibility will be measured in two conditions, in the laboratory and in the field. Factors affecting seat transmissibility will also be investigated so that reliable seat transmissibility can be obtained.

8.2 Seat transmissibility measurement

The transmissibility of a seat is the ratio of the vibration at the seat surface to the vibration at the base of the seat. An accelerometer placed on the surface of the seat may cause discomfort to the subject, thereby inducing a different posture and causing a change of the seat transmissibility. Therefore, a suitable measurement device is needed to measure seat transmissibility. The Society of Automotive Engineers (SAE 1974) recommended a semi-rigid disc containing accelerometers to measure the vibration on a seat surface. It is called the "SAE-pad".

In vehicles, there are different vibrations at the different floor parts. Hence, selecting a correct place to measure seat base vibration is important. Messenger *et al.* (1992) suggested that the accelerometer placed on the vehicle chassis should be located within a circle of 200 mm diameter centred directly beneath the seat.

The aim of this study is to predict seat transmissibility. The method to assess the prediction method is comparing the predicted result with the measured

seat transmissibility. Therefore, obtaining good measured seat transmissibility is important. This study was designed to investigate the effect of some factors on measured seat transmissibility.

8.2.1 Factors affecting seat transmissibility

Laboratory measurements of the transmissibilities of seats and cushions have often employed horizontal seats. In practice, car seats are usually inclined because seat comfort is increased in static conditions when a rearward inclination forces the back against the backrest. Therefore, a knowledge of the influence of seat inclination is needed when measuring seat transmissibility or predicting seat transmissibility from mathematical models of the seat and the human body.

8.2.1.1 Hypothesis

It was hypothesised that seat transmissibility will decrease with increasing seat inclination because the measured 'vertical' acceleration, a_{2z}, is less than the true vertical acceleration, a_3, (Figure 8.1).

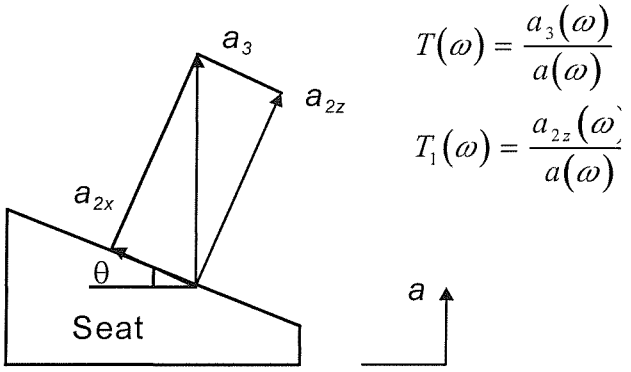

Figure 8.1 Transmissibility measures for an inclined seat.

8.2.2 Experimental method

Ten male subjects participated in the study. A one metre electro-hydraulic vertical shaker was used. A wooden seat was used (see Section 7.3.2.2) with a square block of foam (109mm thick, 500mm wide, 500mm deep) placed on the seat surface as a cushion on which subjects sat (Figure 8.2). The wooden seat inclination could be adjusted according to requirement.

The cushion transmissibility was measured with each of the ten subjects. Motions of the seat were measured using Entran EGCSY-240D*-10 accelerometers mounted beneath the seat and on the seat surface. The motion at the interface between the subject and the cushion was measured using a SAE pad (Figure 8.2).

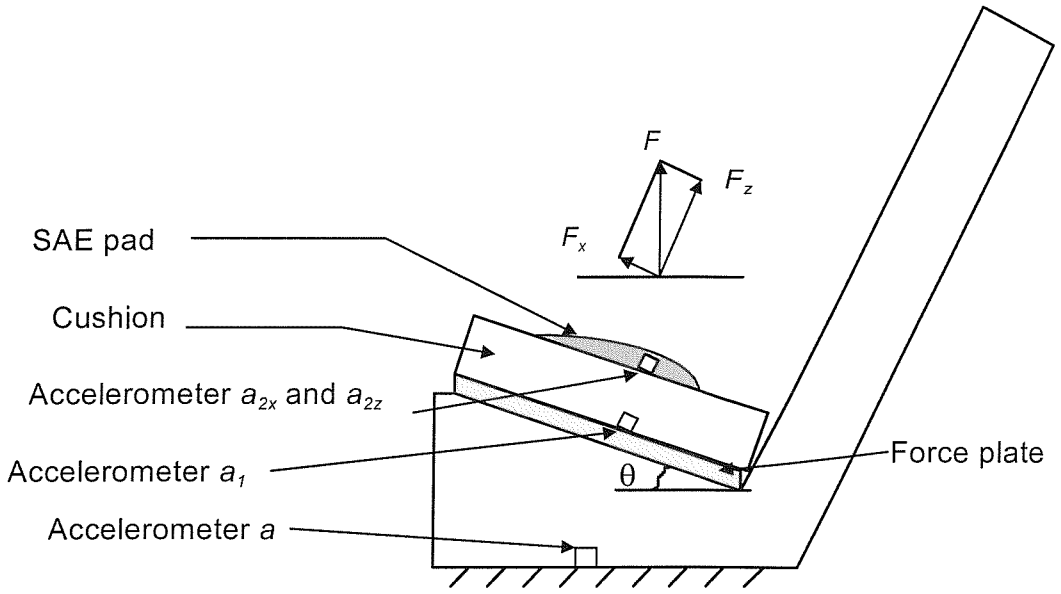

Figure 8.2. Seat and accelerometers arrangement

Subjects kept an upright posture with their backs not touching the backrest during the experiment. The subject was exposed to vertical random vibration in the frequency range from 0.2 to 25 Hz with a magnitude of 1.5 ms^{-2} r.m.s. The measurements of seat transmissibility were obtained with five inclinations: 0°, 5°, 10°, 15° and 20°.

8.2.3 Data analysis

The following frequency response functions can be defined:

Three seat transmissibilities, $T(\omega)$:

$$T_1(\omega) = \frac{a_{2z}(\omega)}{a(\omega)} \qquad (8.1)$$

$$T_2(\omega) = \frac{a_{2z}(\omega)}{a_1(\omega)} \quad (8.2)$$

$$T_3(\omega) = \frac{a_3(\omega)}{a(\omega)} \quad (8.3)$$

Where:

$$a_3 = \frac{a_{2z}}{\cos(\theta)}$$

$$\theta = \arctan\frac{a_{2x}}{a_{2z}}$$

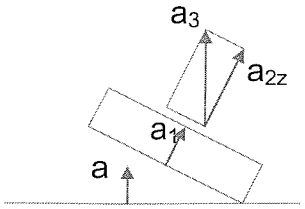

Figure 8.2 illustrates the measurement orientations for the three seat transmissibilities with a seat inclination, θ. The acceleration a_{2z}, measured on the seat surface within the SAE pad, was not in the true vertical vibration, a_3, except when the seat inclination was 0 degrees (Figure 8.1). The acceleration, a_{2x}, was measured at the same location on the seat surface and might be described as the fore-and-aft acceleration, but it was only in a horizontal direction when the seat inclination was 0 degrees. Figure 8.2 shows that the acceleration a_1 was measured in the same direction as a_{2z} but was measured on the force plate. The vertical acceleration, a, of the vibrator was measured at the seat base.

8.2.4 Results

8.2.4.1 Effect of seat inclination

Figure 8.3 shows for one subject the changes in cushion transmissibility, measured between the accelerometer a_{2z} (in the SAE pad) and the vertical accelerometer a (on the horizontal surface beneath the seat) as the seat inclination increased from 0° to 20°. Figure 8.4 shows similar data when the transmissibility was calculated between the accelerometer a_{2z} (in the SAE pad) and the accelerometer a_1 (on the inclined surface beneath the seat). Figure 8.5 shows similar data when the transmissibility was calculated between accelerometer a_{2z} (in the SAE pad after correction for the assumed inclination of the pad) and accelerometer a (on the horizontal surface beneath

the seat). Data from the other subjects were generally similar to those illustrated.

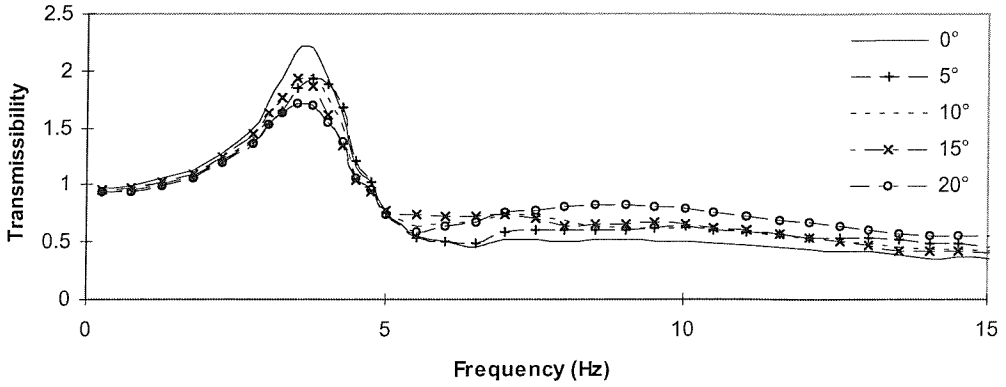

Figure 8.3 Seat transmissibility, $T_1(\omega)$, for one subject.

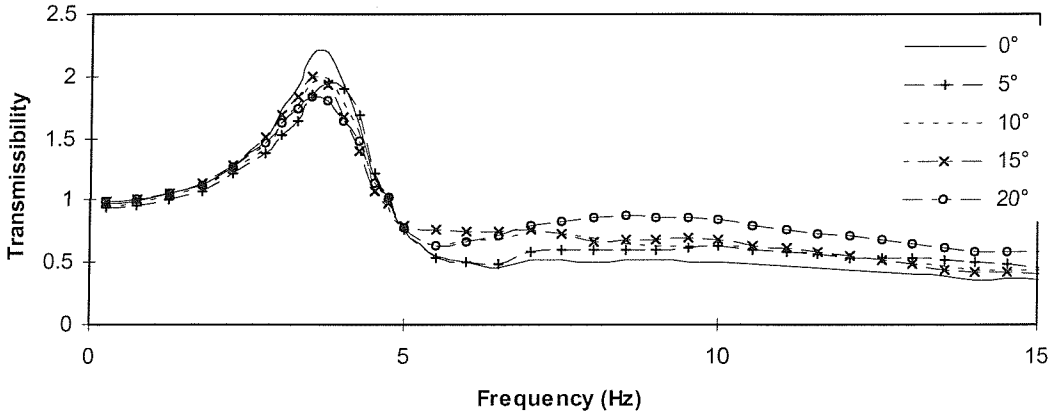

Figure 8.4. Seat transmissibility, $T_2(\omega)$, for one subject.

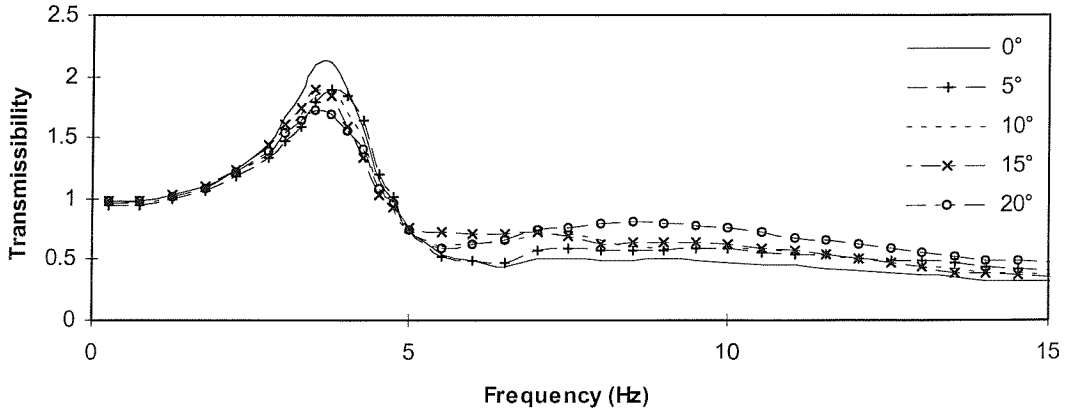

Figure 8.5. Seat transmissibility, $T_3(\omega)$ for one subject.

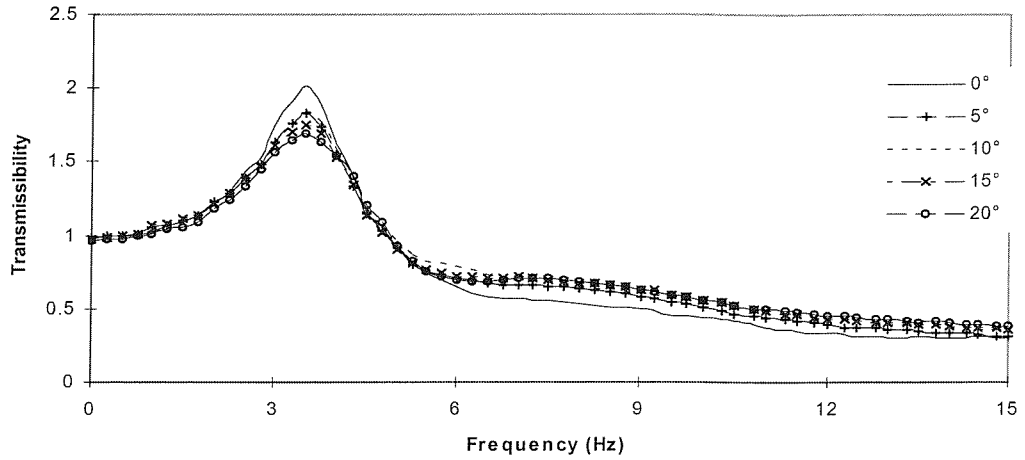

Figure 8.6 Mean seat transmissibility, T_1, for 10 subjects at different seat inclinations.

Figure 8.6 shows the means of the cushion transmissibilities, T_1, obtained with the 10 subjects when sitting with the different inclinations. Although with every subject the seat transmissibility varied with changes in seat inclination, the mean change was small.

From Figure 8.6 it is seen that the cushion transmissibility tended to decrease at frequencies close to, and below, the resonance frequency as the seat inclination increased. This might be partially explained by the angle of inclination causing the acceleration a_{2z} to be less that the acceleration a_3 (Figure 8.1).

Statistical tests were conducted to determine the significance of the changes in transmissibility and apparent mass with changing seat inclination. The Friedman test was conducted at each 0.25 Hz increment up to 15 Hz using a significance criterion of $p<0.01$.

Table 8.1 shows that the transmissibilities were significantly influenced by seat inclination between 1 and 3.75 Hz, between 8 and 9.75 Hz, and between 12 and 14.75 (Table 8.1, $p<0.01$). At other frequencies there was no significant change with seat inclination. Wilcoxon matched-pairs signed ranks

Table 8.1. Comparison of measured cushion transmissibilities between five inclinations 0° to 20° (Friedman test).

Frequency (Hz)	Significance level *p*	Frequency (Hz)	Significance level *p*	Frequency (Hz)	Significance level *p*
0.00	0.3183	5.00	0.7358	10.00	0.0114
0.25	0.1126	5.25	0.1765	10.25	0.0261
0.50	0.0174	5.50	0.2270	10.50	0.0301
0.75	0.0191	5.75	0.2270	10.75	0.0186
1.00	0.0030	6.00	0.1933	11.00	0.0125
1.25	0.0007	6.25	0.1933	11.25	0.0168
1.50	0.0015	6.50	0.1661	11.50	0.0093
1.75	0.0018	6.75	0.1351	11.75	0.0159
2.00	0.0012	7.00	0.2523	12.00	0.0031
2.25	0.0033	7.25	0.1712	12.25	0.0019
2.50	0.0007	7.50	0.0708	12.50	0.0031
2.75	0.0016	7.75	0.0432	12.75	0.0011
3.00	0.0002	8.00	0.0070	13.00	0.0008
3.25	0.0000	8.25	0.0068	13.25	0.0028
3.50	0.0000	8.50	0.0033	13.50	0.0034
3.75	0.0019	8.75	0.0026	13.75	0.0016
4.00	0.0316	9.00	0.0021	14.00	0.0007
4.25	0.5859	9.25	0.0040	14.25	0.0031
4.50	0.8043	9.50	0.0042	14.50	0.0090
4.75	0.3848	9.75	0.0030	14.75	0.0063

tests between transmissibilities measured at pairs of inclinations showed that the differences occurred mainly between the horizontal seat (0 degree inclination) and the other conditions (Table 8.2). As the seat inclination increased, the transmissibility decreased between 1 and 3.75 Hz and increased at frequencies between 8 and 9.75 Hz and between 12 and 14.75 Hz.

The frequency regions over which the seat inclination had a significant influence on cushion transmissibility are different from those where there was a significant change in apparent mass (see Section 7.3). However, it is known that cushion transmissibility is partially determined by subject apparent mass. At some frequencies both the apparent mass and the transmissibility changed, and the two changes may be associated. However, in general, even when both the subject apparent mass and the cushion transmissibility both changed, the change in apparent mass seems insufficient to explain the change in cushion transmissibility. This could be observed from the

Table 8.2. Comparison of measured cushion transmissibilities between inclinations 0° and 5°, 0° and 10°, 0° and 15°, 0° and 20° over the significant change frequency range (Wilcoxon matched-pairs signed ranks test).

Frequency (Hz)	Significance level p (0°-5°)	Significance level p (0°-10°))	Significance level p (0°-15°)	Significance level p (0°-20°)
1.00	0.5907	0.3097	0.8658	0.0189
1.25	0.2059	0.1082	0.4418	0.0592
1.50	0.3105	0.1091	0.3734	0.0069
1.75	0.4416	0.1122	0.2855	0.0050
2.00	0.3118	0.1094	0.1917	0.0189
2.25	0.0741	0.0733	0.0277	0.0077
2.50	0.0279	0.0109	0.0125	0.0050
2.75	0.0378	0.0189	0.0209	0.0050
3.00	0.0093	0.0050	0.0049	0.0049
3.25	0.0050	0.0050	0.0050	0.0050
3.50	0.0069	0.0050	0.0050	0.0050
3.75	0.0068	0.0123	0.0069	0.0093
8.00	0.0069	0.0108	0.0093	0.0218
8.25	0.0069	0.0069	0.0069	0.0218
8.50	0.0069	0.0069	0.0069	0.0166
8.75	0.0069	0.0051	0.0069	0.0166
9.00	0.0093	0.0093	0.0051	0.0166
9.25	0.0125	0.0125	0.0051	0.0281
9.50	0.0093	0.0069	0.0051	0.0218
9.75	0.0051	0.0093	0.0051	0.0367
12.00	0.0367	0.0125	0.0069	0.0051
12.25	0.0469	0.0125	0.0051	0.0051
12.50	0.0593	0.0125	0.0069	0.0051
12.75	0.0469	0.0125	0.0051	0.0050
13.00	0.0829	0.0125	0.0051	0.0051
13.25	0.0928	0.0218	0.0069	0.0051
13.50	0.1141	0.0218	0.0069	0.0051
13.75	0.1394	0.0218	0.0069	0.0050
14.00	0.1394	0.0218	0.0051	0.0051
14.25	0.1688	0.0284	0.0069	0.0069
14.50	0.3329	0.0469	0.0165	0.0093
14.75	0.2845	0.0506	0.0125	0.0069

comparison between the change in apparent mass (Figure 7.8) and the change in cushion transmissibility (Figure 8.6).

8.2.4.2 Seat transmissibilities at different measured positions

The seat transmissibilities $T_1(\omega)$, $T_2(\omega)$ and $T_3(\omega)$ were calculated from the acceleration measured at different acceleration measured positions. Figure 8.7 compares the three cushion transmissibilities at each of the five inclinations for one typical subject. Other subjects gave similar results and showed that at angles up to 20 degrees the accelerometer orientation had little affect on the measured vertical seat transmissibility.

8.2.5 Discussion

Figure 8.6 shows that with increased seat inclination the cushion transmissibility decreased at low frequencies (below about 6 Hz) and increased at higher frequencies. This means that increased seat inclination will tend to improve dynamic cushion comfort at the resonance frequency but degrade dynamic comfort at higher frequencies, assuming other aspects of comfort are not changed by the seat inclination (e.g. an effect of increased contact with the seat backrest). However, the changes appear to be small.

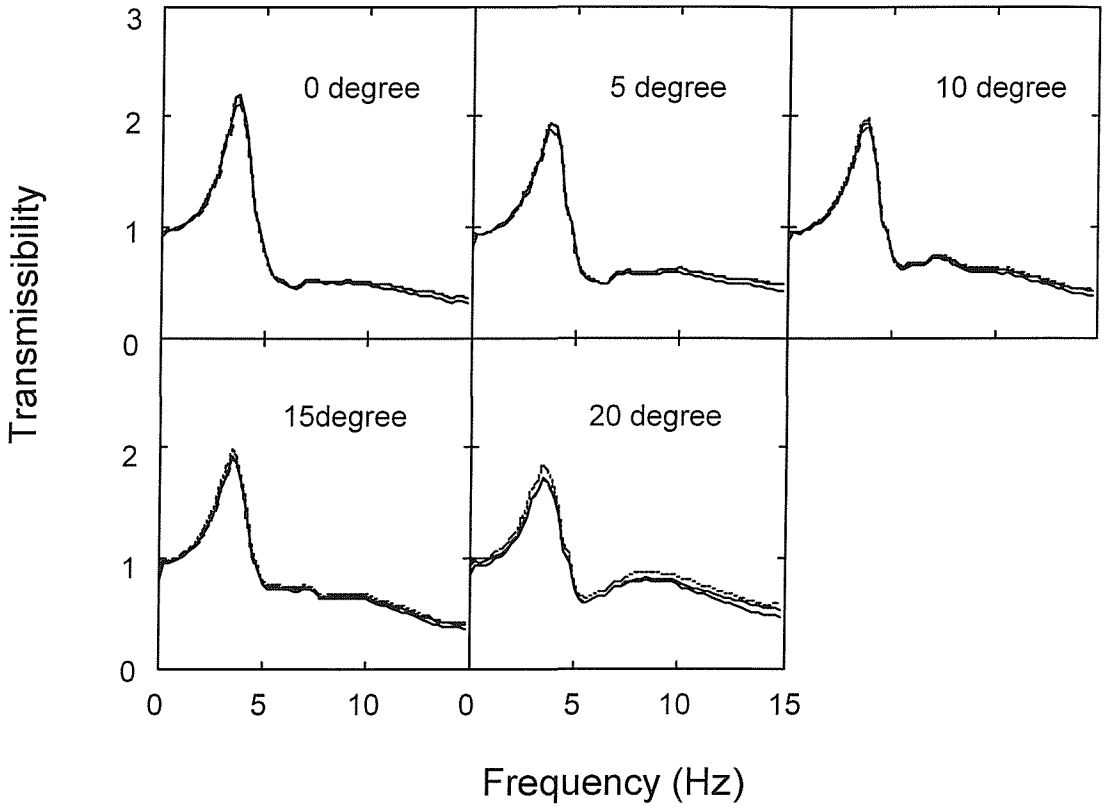

Figure 8.7. Seat transmissibilities $T_1(\omega)$, $T_2(\omega)$ and $T_3(\omega)$ at different seat inclinations for one subject. ($T_1(\omega)$ ———, $T_2(\omega)$ ----------, $T_3(\omega)$ ·····).

The seat transmissibility may have changed with seat inclination because either the subject apparent mass changed or the cushion dynamic properties changed. The cushion thickness in the true vertical direction increased as the seat inclination increased, so the cushion stiffness will have slightly decreased and the cushion damping will have varied for similar reasons. The change of subject apparent mass may have affected cushion transmissibility at low

frequencies (see Section 7.3), but it seems insufficient to explain the change in transmissibility at high frequencies.

Figure 8.7 shows that similar seat transmissibilities were obtained for $T_1(\omega)$ and $T_2(\omega)$. This suggests that the orientation of the accelerometers is not of prime importance when measuring seat transmissibility on surfaces inclined by up to 20 degrees. The hypothesis 8.2.1.1 is therefore false.

8.2.6 Conclusion

As expected, the study here revealed that the transmissibility of a cushion changed as the seat inclination varied. Compared with previous studies – the influence of seat inclination on apparent mass (see Section 7.3) and the influence of seat inclination on seat impedance (see Section 5.3), it could be observed that the influence of the seat inclination on seat transmissibility was greater than on apparent mass and on seat impedance. The change of the seat transmissibility may be caused by both the change of apparent mass and the change of the seat impedance as the seat inclination changed.

The accelerometers placed at different positions (see Figure 8.2, a_1 and a) and the orientation of the accelerometers had no significant influence on the measured seat transmissibility. Therefore, we do not need to pay more attention on them when we measure seat transmissibility.

8.3 Predicting seat transmissibility from seat-person model

A seat model has been developed in Chapter 5. The indenter test rig has been defined to measure seat impedance, which can be used to obtain the parameters of the seat model. The seat model combines with the seated body model that was proposed in Chapter 6 to compose a seat-person model, which will be used to predict the seat transmissibility in various vibration environments (see Chapter 7).

The purpose of the study in this section is to assess the accuracy with which seat transmissibility can be predicted from the proposed models of human

mechanical impedance and alternative measurements of seat mechanical impedance. The seat transmissibility predictions will be performed for two environments: the laboratory and the field (in cars).

8.3.1 Predicting seat transmissibility measured in the laboratory.

Seat transmissibilities measured in the laboratory have high repeatability and high coherency because of the controlled single input vibration. So, the prediction method will be assessed first using laboratory measurements.

8.3.1.1 Experimental measurements

The experiments were conducted separately with a car seat and with a rectangular sample of foam. The car seat was the driving seat from a modern small family car. It was constructed from a steel frame with moulded foam supported from beneath by a contoured steel seat pan and fully encased within a cover. The TDI foam in the seat had a density of 50 $kg.m^3$. The rectangular sample of foam was 500mm wide by 420mm deep and 120mm thick. It is described as a 'soft feeling type' polyurethane foam used for car seating. It had a density of approximately 40 $kg.m^3$ and a hardness of about 7.0 kPa.

8.3.1.1.1 Measurement of seat mechanical impedance with an indenter

The indenter test rig and instruments are described in Chapter 5 and Appendix A. A SIT-BAR was used as the indenter. The force on the indenter and the acceleration at the base of the seat were measured during a 100 s period of random vibration (0.5 ms^{-2} r.m.s.) produced by the electrodynamic vibrator. The vibration had a flat acceleration power spectral density over the range 1.0 to 30 Hz (± 10%).

The measurements were obtained with each of 6 pre-loads (300N to 800N) applied to the surface of the seat and the foam sample. Signals from the force transducer and the accelerometer were signal conditioned and were acquired at 100 samples per second into an *HVLab* system via 50Hz anti-aliasing filter.

8.3.1.1.2 Measurement of seat transmissibility using human subjects

The transmissibilities of the seat and the foam were measured while they supported 8 male subjects (mean age 35 years; mean mass 64 kg). Again, the base of the seat was excited by a 100 s period of random vibration at 0.5 ms^{-2} r.m.s. (see Figure 8.8). The vibration at the subject-seat interface was measured using an Entran piezo-resistive accelerometer (type EGCSY-240*-10) in an SAE pad (see ISO 10326-1, 1992). All subjects kept upright postures with their backs not touching the seat backrest and with their hands resting on their knees. The feet of the subjects were supported on a stationary footrest with a height was adjusted according to subject height so that the same contact area between the subject thighs and the seat was kept.

8.3.1.2 Theory and results

8.3.1.2.1 Indenter

A simple model which includes only stiffness, k, and damping, c, was used to represent the foam and the seat. The model parameters were obtained by curve fitting. The calculated values of stiffness and damping are tabulated in Table 8.3.

Table 8.3 The stiffness and damping coefficients of the seat and foam with different pre-loads.

	seat		foam	
Pre-load	k	c	k	c
300N	42300	260	21167	354
400N	44121	270	23904	457
500N	50210	276	25082	515
600N	59300	280	34903	570
700N	68000	285	42340	740
800N	73000	293	54363	831

8.3.1.2.2 Human subjects

The prediction of seat transmissibility with human subjects was based on the one degree-of-freedom and two degree-of-freedom models developed by Wei and Griffin 1998a (from measurements of the apparent masses of 60 subjects obtained by Fairley and Griffin 1989). The two degree-of-freedom model has the same form as the model in ISO 5982 (see ISO 5982 1981) but different masses, stiffness and damping. The model parameters were determined from

the measured apparent masses by curve fitting (Table 8.4). The two seat-person mathematical models are shown in Figures 8.9 and 8.10, where *k* and *c* represent the seat or foam dynamic characteristics selected from the indenter results in Table 8.3 according to the subject's weight. The parameters of the two models of the human body are listed in Table 8.4.

Table 8.4 Parameters of one degree and two degree of freedom models.

	k_1	c_1	k_2	c_2	m	m_1	m_2
*Model 1	44130	1485			7.8	43.4	
*Model 2	35776	761	38374	458	6.7	33.4	10.7

*: Model 1 is one degree-of-freedom model and model 2 is two degree-of-freedom model (see Table 6.1 and 6.2).

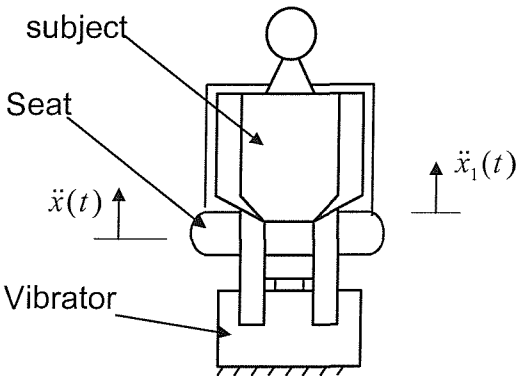

Figure 8.8 Seat loaded with a person.

One degree-of-freedom model:

The response of the one degree-of-freedom model (i.e. Figure 8.9) is given by:

$$m_1\ddot{x}_1 + k_1(x_1 - x) + c_1(\dot{x}_1 - \dot{x}) = 0 \qquad (8.4)$$

$$m_1\ddot{x}_1 + m\ddot{x} = k(z - x) + c(\dot{z} - \dot{x}) \qquad (8.5)$$

The seat (or foam) transfer function is:

$$T(\omega) = \frac{\ddot{x}(\omega)}{\ddot{z}(\omega)} = \frac{A + Bi}{D + Ei} \qquad (8.6)$$

The transmissibility and phase of the seat response are given by:

$$|T| = \sqrt{\frac{A^2 + B^2}{D^2 + E^2}} \qquad (8.7)$$

$$\theta = a\tan\frac{B}{A} - a\tan\frac{E}{D} \qquad (8.8)$$

where:

$$A = kk_1 - (m_1 k + cc_1)\ \omega^2$$

$$B = (c_1 k + ck_1)\ \omega - m_1 c\omega^3$$

$$D = \left(k - (m + m_1)\ \omega^2\right)k_1 + (mm_1\omega^2 - km_1 - cc_1)\ \omega^2$$

$$E = \left(kc_1 + k_1 c - (m_1 c + mc_1 + m_1 c_1)\ \omega^2\right)\omega$$

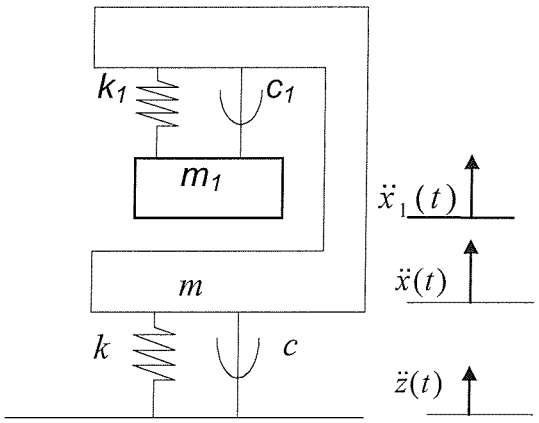

Figure 8.9 First seat/person system model.

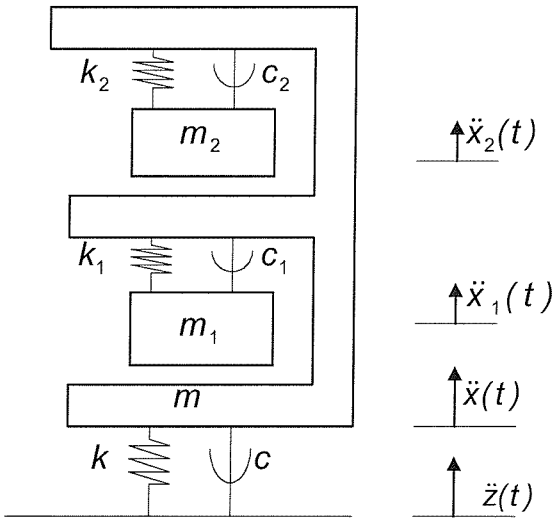

Figure 8.10 Second seat/person system model.

The parameters describing the mechanical impedance of the human body and the seat or foam were previously obtained from experimental data by curve

fitting, as described in Section 6.3. However, for this single degree-of-freedom model, the mass was changed according the real weight of each subject: the value of (m + m_1) was made equal to the assumed sitting weight of each subject (i.e. 75% of the subject's total weight). The values of k_1 and c_1 were not changed as there was no basis for deciding how these depend on subject mass. Equations (8.7) and (8.8) were then employed to predict the seat and foam transmissibility for each subject. The predicted transmissibilities are compared with the transmissibilities measured with the eight subjects sitting on the seat and on the foam as in Figures 8.11 and 8.12. It can be seen that the transmissibility at resonance and at higher frequencies is generally well predicted by the model. However, the single degree-of-freedom model fails to predict the second seat resonance apparent at about 7 or 8 Hz for most subjects.

Two degree-of-freedom model:

The response of the two degree-of-freedom model of the person combined with the seat is given by:

$$m_1\ddot{x}_1 + k_1(x_1 - x) + c_1(\dot{x}_1 - \dot{x}) = 0 \qquad (8.9)$$

$$m_2\ddot{x}_2 + k_2(x_2 - x) + c_2(\dot{x}_2 - \dot{x}) = 0 \qquad (8.10)$$

$$m\ddot{x} + m_1\ddot{x}_1 + m_2\ddot{x}_2 = k(z - x) + c(\dot{z} - \dot{x}) \qquad (8.11)$$

The seat transfer function is given by:

$$T(\omega) = \frac{F + Gi}{(H+L) + (M+N)i} \qquad (8.12)$$

and the seat transmissibility and phase are given by:

$$|T| = \sqrt{\frac{F^2 + G^2}{(H+L)^2 + (M+N)^2}} \qquad (8.13)$$

and $$\theta = \text{a}\tan\frac{G}{F} - \text{a}\tan\frac{M+N}{H+L} \qquad (8.14)$$

where:

$$F = kP_1 - cP_2\omega$$
$$G = kP_2 - cP_1\omega$$
$$H = P_1P_5 - P_2c\omega - m_1k_1P_3\omega^2$$
$$L = m_1c_1c_2\omega^4 + \left(m_2k_2P_4\omega^2 - m_2c_1c_2\omega^4\right)$$
$$M = P_2P_5 - cP_1\omega - \left(m_1c_1P_3 - m_1c_2k_1\right)\ \omega^3$$
$$N = m_2c_2P_4\omega^3 + m_2k_2c_1\omega^3$$
$$P_1 = m_1m_2\omega^4 + k_1k_2 - \left(m_1k_2 + m_2k_1 + c_1c_2\right)\ \omega^2$$
$$P_2 = \left(c_1k_2 + c_2k_1\right)\ \omega - \left(m_1c_2 + m_2c_1\right)\ \omega^3$$
$$P_3 = k_2 - m_2\omega^2$$
$$P_4 = k_1 - m_1\omega^2$$
$$P_5 = k - m\omega^2$$

With this model, the mass was not adjusted to the weight of each subject: the masses of m, m_1 and m_2 were those derived from the previous study (see Table 8.4 and Wei and Griffin 1998a). The predicted gains and phases of the transmissibilities are compared with the measured transmissibilities using human subjects in Figures 8.13 and 8.14. It can be seen that the two degree-of-freedom model of the human body predicted a second resonance in the seat transmissibility and that in many cases this provided a better fit to the measured seat transmissibility than was obtained with the one degree-of-freedom model. Although the predicted phase is closer to the measured phase with the two degree-of-freedom model than with the single degree-of-freedom model, the prediction is less good than for the prediction of the modulus.

Over the group of subjects as a whole, there was an encouraging correspondence between the measured and predicted values (Figures 8.15 and 8.16). When using the two degree-of-freedom model for the foam, the mean predicted values fell within the range of the gain and almost within the range of the phase values measured for the eight subjects over the frequency range 1.25 to 25 Hz. With the seat, the predictions were not so accurate but they still fell within the range of measured values of gain and phase over much of the frequency range.

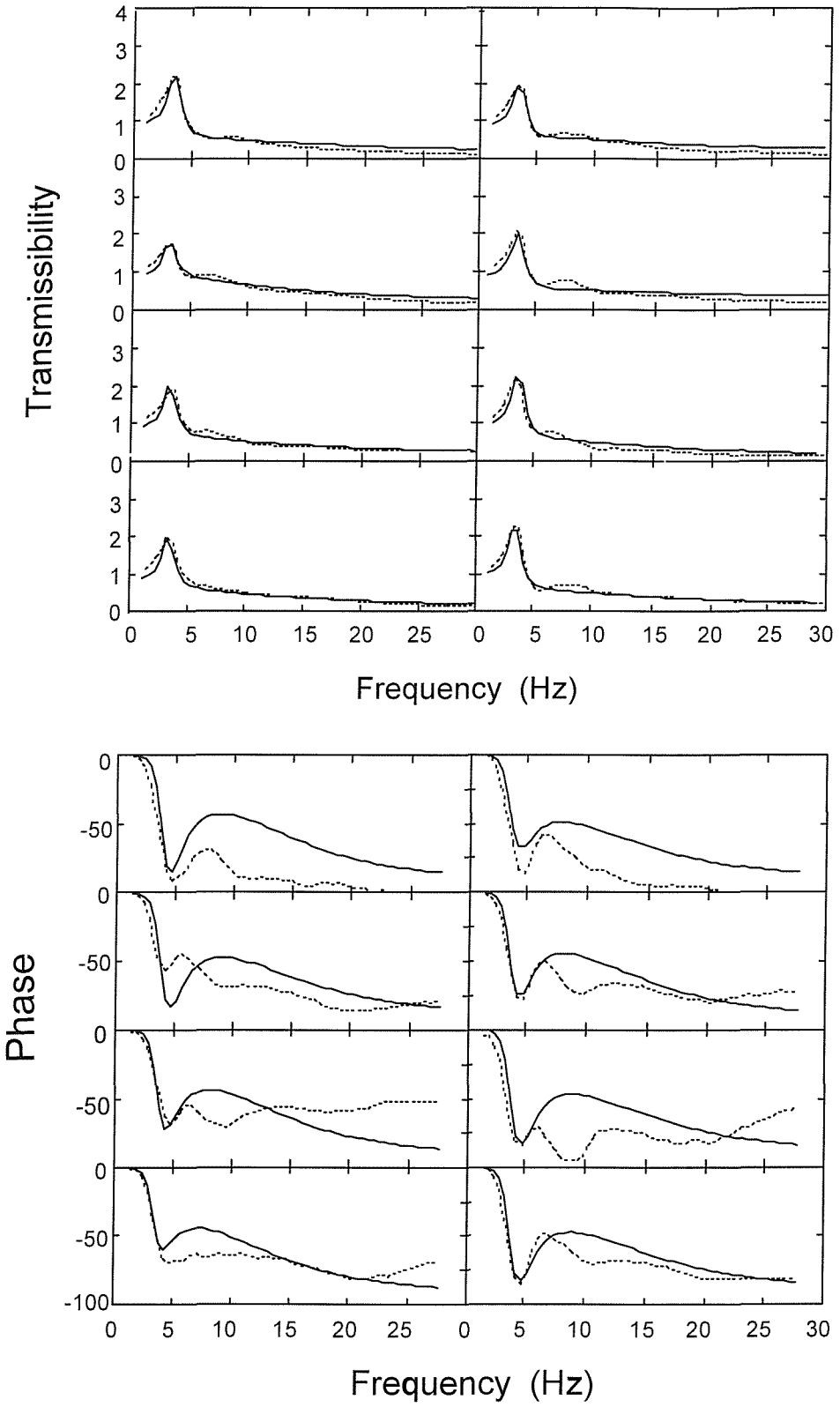

Figure 8.11. Comparison of measured and predicted foam transmissibility and phase when using single degree-of-freedom model for eight different male subjects (------measured transmissibility; ——predicted transmissibility, and ------ measured phase; ——predicted phase).

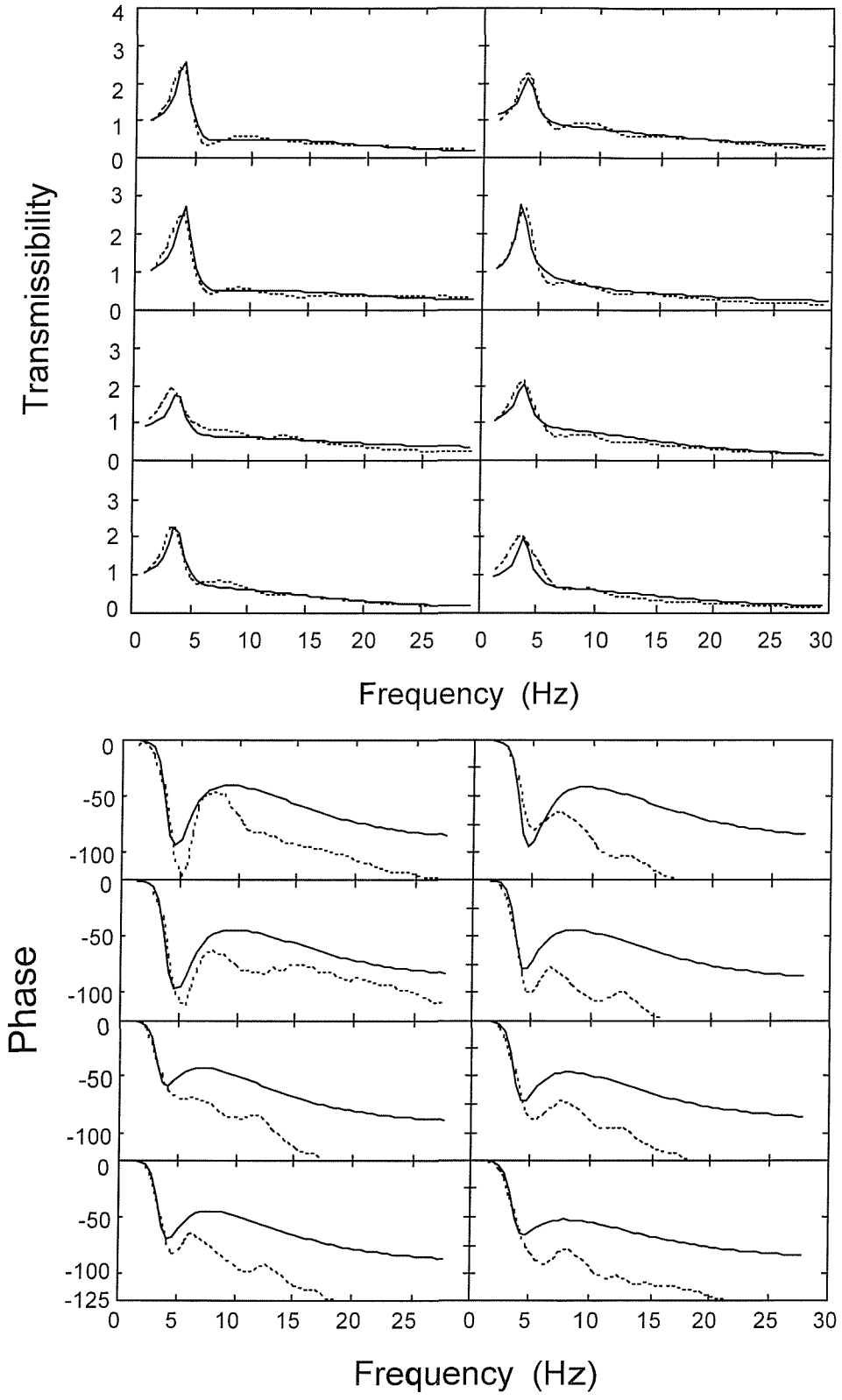

Figure 8.12. Comparison of measured and predicted seat transmissibility and phase when using single degree-of-freedom model for eight different male subjects (------measured transmissibility; ——predicted transmissibility, and ------ measured phase; ——predicted phase).

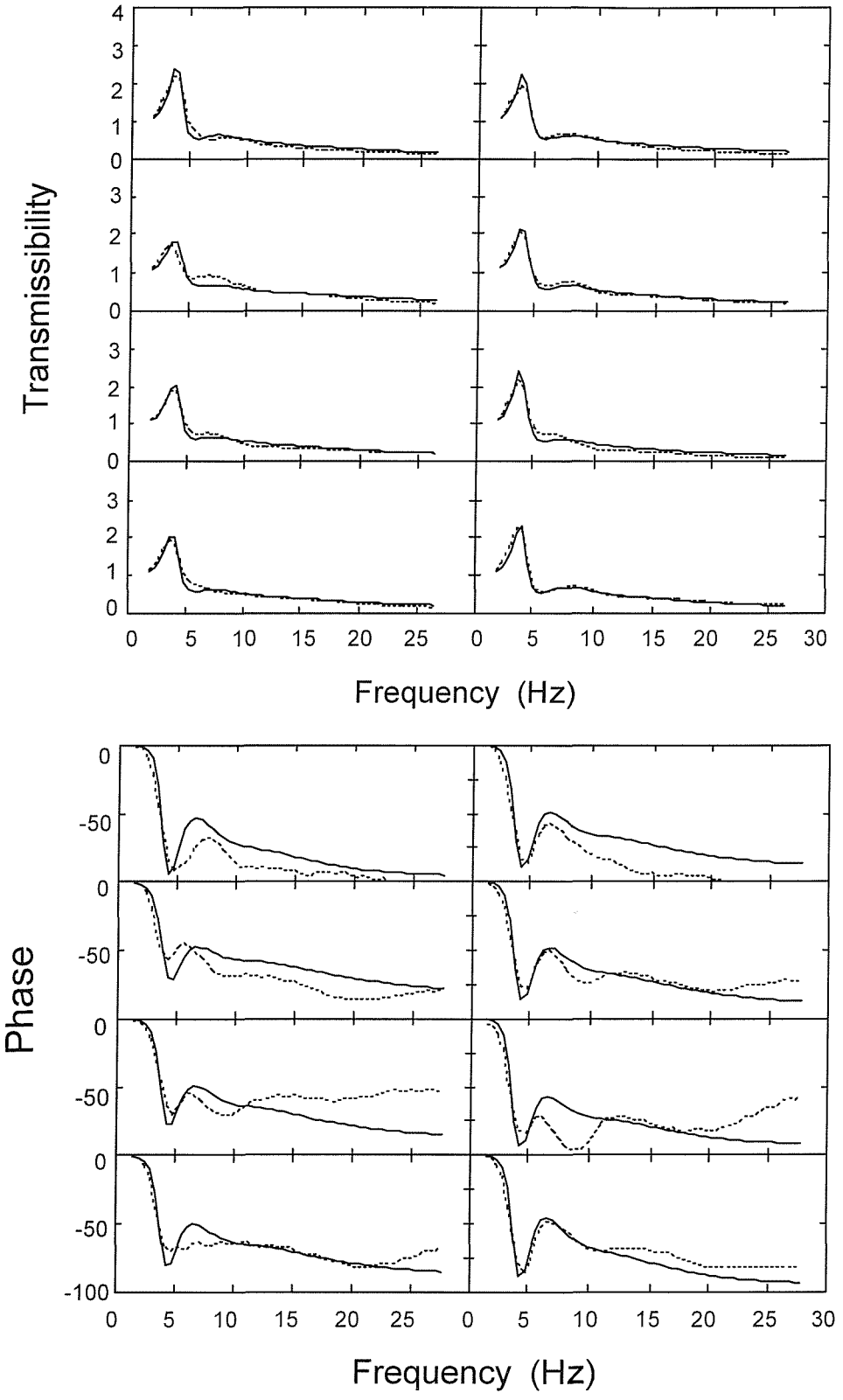

Figure 8.13. Comparison of measured and predicted foam transmissibility and phase when using two degree-of-freedom model for eight different male subjects (------measured transmissibility; ——predicted transmissibility, and ------measured phase; ——predicted phase).

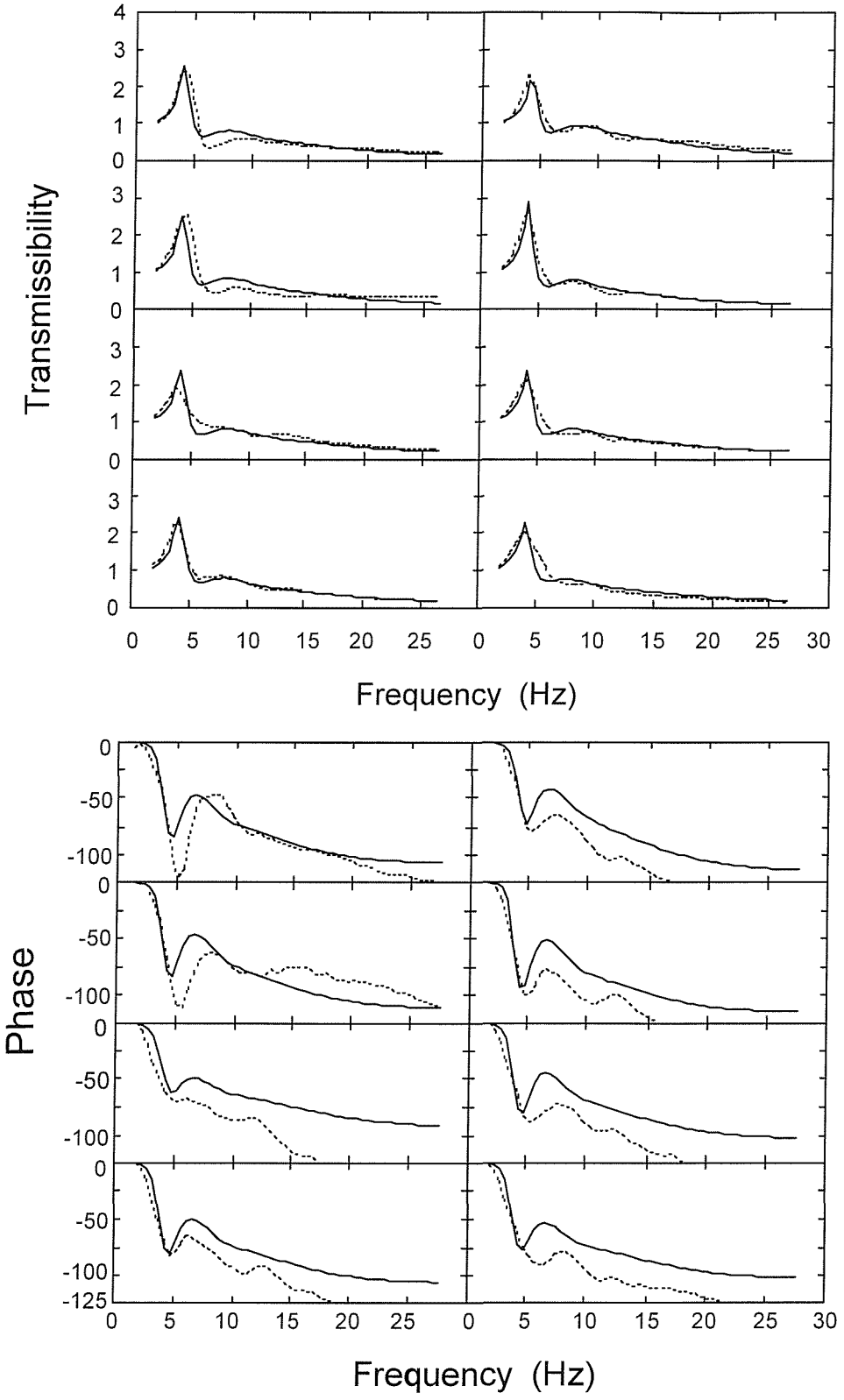

Figure 8.14. Comparison of measured and predicted seat transmissibility and phase when using two degree-of-freedom model for eight different male subjects (------measured transmissibility; ——predicted transmissibility, and ------measured phase; ——predicted phase).

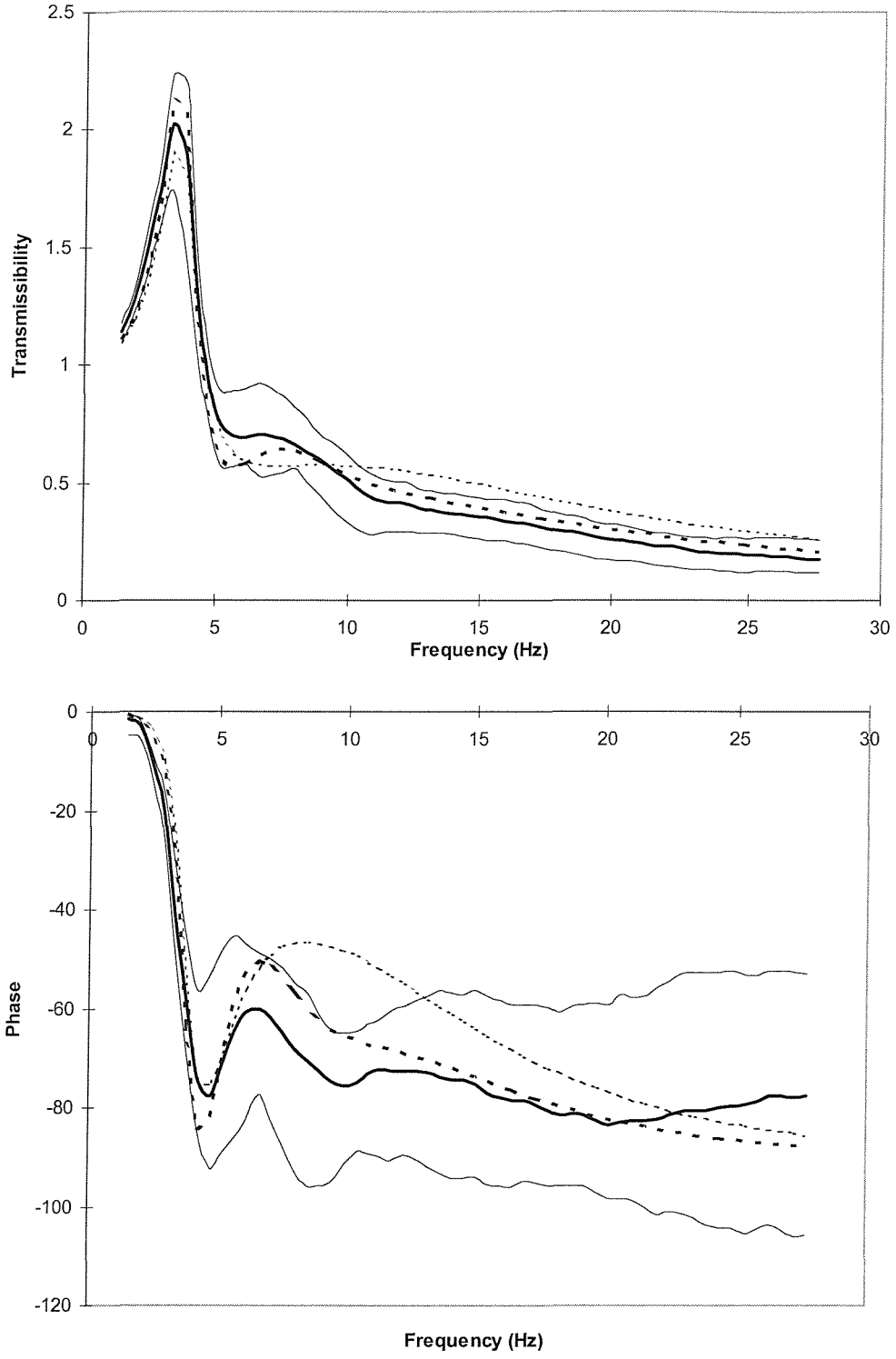

Figure 8.15 Comparison of measured and predicted foam transmissibility and phase (——— mean experimental data, ——— maximum experimental data, ——— minimum experimental data, ····· single degree-of-freedom model mean data, _ _ _ _ _ two degree-of-freedom model mean data).

8.3.1.3 Discussion and conclusion

From the measurements of the seat and foam stiffness at different pre-loads (Table 8.3) it was seen that the stiffness increased appreciably with increases in the load. This may partially explain why measurements of seat transmissibility show only small changes in resonance frequency with subjects of different mass (e.g. Corbridge and Griffin 1989).

The methods shown here appear to allow useful predictions of seat transmissibility from measurements of the dynamic properties of the seat material. This should allow the selection of optimum materials, and the generation of optimum shapes of materials, so as to maximise the attenuation of vibration to seat occupants. It should be possible to devise a test rig in which the SEAT value is produced from measurements of the dynamic properties of a material and the known spectrum of vibration in a vehicle (see Griffin 1990).

The SIT-BAR used here gave good results and can be assumed to be a reasonable shape for determining the seat dynamic properties (see Section 5.3).

Two alternative models of the seat-person system have been investigated. A single degree-of-freedom model can adequately reflect the dynamic characteristics of the human body at low frequencies and can be used to predict seat transmissibility at the seat resonance, usually seen around 3 to 5 Hz. However a two degree-of-freedom model provides better predictions of seat transmissibility: it predicts the second resonance, often seen in measurements of seat transmissibility around 8 Hz, and may give useful predictions of seat transmissibility at frequencies up to 25 Hz.

The encouraging results obtained from the prediction method suggest that it should allow the prediction of SEAT values for seats used in specific vibration environments.

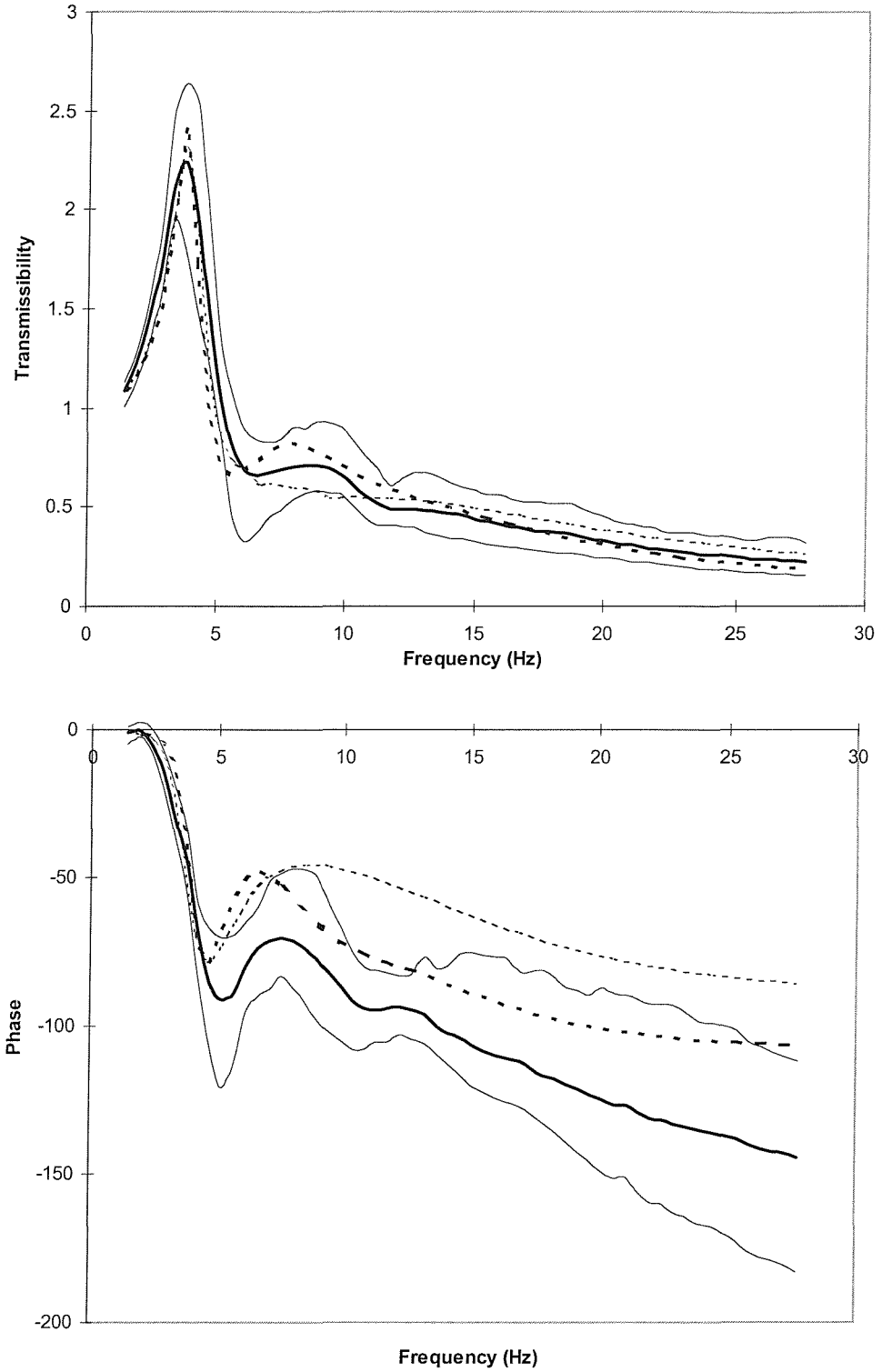

Figure 8.16. Comparison of measured and predicted foam transmissibility and phased (——— mean experimental data, ——— maximum experimental data, ——— minimum experimental data, ····· single degree-of-freedom model mean data, _ _ _ _ _ two degree-of-freedom model mean data).

However, these encouraging results were obtained in conditions where the subject kept an upright posture with no backrest included and the seat transmissibility was measured in the laboratory. Further assessment in field conditions is needed.

8.3.2 Predicting seat transmissibility measured in the field.

The seat transmissibility measured in the field could differ from that measured in the laboratory for several reasons. Seat transmissibility is sometimes measured in the laboratory using random vibration with equal energy at each frequency while subjects keep an upright posture. In a vehicle a driver leans against the seat backrest and the input vibration has a spectrum that is characteristic of the car and the road. In addition, any cross-axis coupling in the dynamic response of a seat-person system may have important implications in field measurements where vibration occurs in many axes. Predicting seat transmissibility in the field is therefore far more difficult than predicting seat transmissibility in the laboratory. The overall aim of the research is to make it possible to predict seat transmissibilities in practical situations.

8.3.2.1 Experimental measurements

Seat transmissibility measurement

Measurements were conducted separately in the passenger seats of three cars: Mondeo, Fiesta and Jaguar. The transmissibilities of the seats were measured while they supported 6 subjects driving over 4 different roads at three different speeds: 70, 40 and 30 miles per hour. The four roads were a concrete motorway, a tarmac motorway, a tarmac A class road, and tarmac rural road. The vibration at the subject-seat interface was measured using an Entran piezo-resistive accelerometer (type EGCSY-240*-10) in an SAE pad (see ISO 10326-1, 1992). The vibrations at the seat base were measured using four Entran piezoresistive accelerometers at the four seat supporting corners so that the seat input vibration could be obtained. All subjects maintained a normal posture with their backs touching the seat backrest, which had a 20° inclination, and with their hands resting on their knees.

Measurement of seat mechanical impedance with an indenter

The indenter test rig was utilized to acquire the seat dynamic properties (see Section 8.3.1.1.1). Four input spectra were adopted to represent the four different roads. The four input spectra were not the spectra measured on car floor, they were spectra calculated from the displacement on the floor subtracted from the displacement on the seat. Three random flat vibration spectra (0.4, 0.8 and 1.2 m/s^2 r.m.s.) were also used over a frequency range from 0 to 50 Hz.

The measurements were obtained with a 500N pre-load applied to the surfaces of the three seats. Signals from the force transducer and the accelerometer were acquired at 400 samples per second into an *HVLab* system via 100 Hz anti-aliasing filter. Example results are given in Appendix B.

8.3.2.2 Prediction results

Table 8.5 shows seat model parameters calculated from the indenter test. Table 8.4 shows body model parameters at 1.0 m/s^2 r.m.s. input magnitude. The parameters of the body model for different magnitudes was calculated from equation 8.15, which was derived in Chapter 7.2.5.

$$
\begin{aligned}
k_1 &= -88 + (12442 + 22653 \times \ddot{\bar{x}}^{-0.3537}) \\
k_2 &= -1909 + (4668 + 30495 \times \ddot{\bar{x}}^{-0.3167}) \\
c_1 &= -153 + (696 - 59 \times \ddot{\bar{x}}^{1.0288}) \\
c_2 &= 65 + (1166 - 416 \times \ddot{\bar{x}}^{0.2972})
\end{aligned}
\qquad (8.15)
$$

where $\ddot{\bar{x}}$ is the input vibration magnitude measured at the seat surface (m/s^2, r.m.s.)

The mean input vibration magnitudes for three seats were separately: 0.54 m/s^2 r.m.s. (Fiesta), 0.67 m/s^2 r.m.s. (Mondeo) and 0.53 (Jaguar) m/s^2 r.m.s. Using the seat-person model (Figure 8.10) the seat transmissibility for the A road at 30 mile/h speed was predicted as in Figure 8.17.

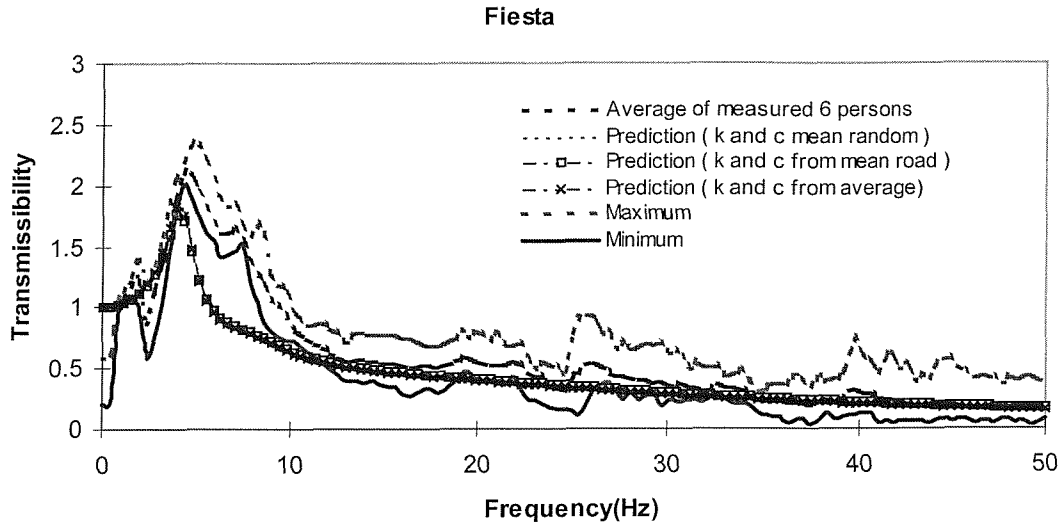

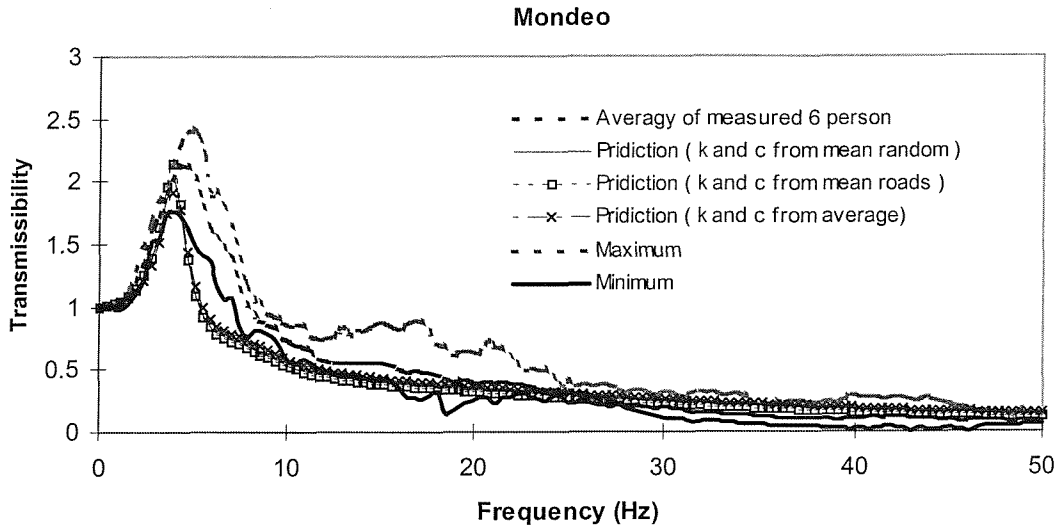

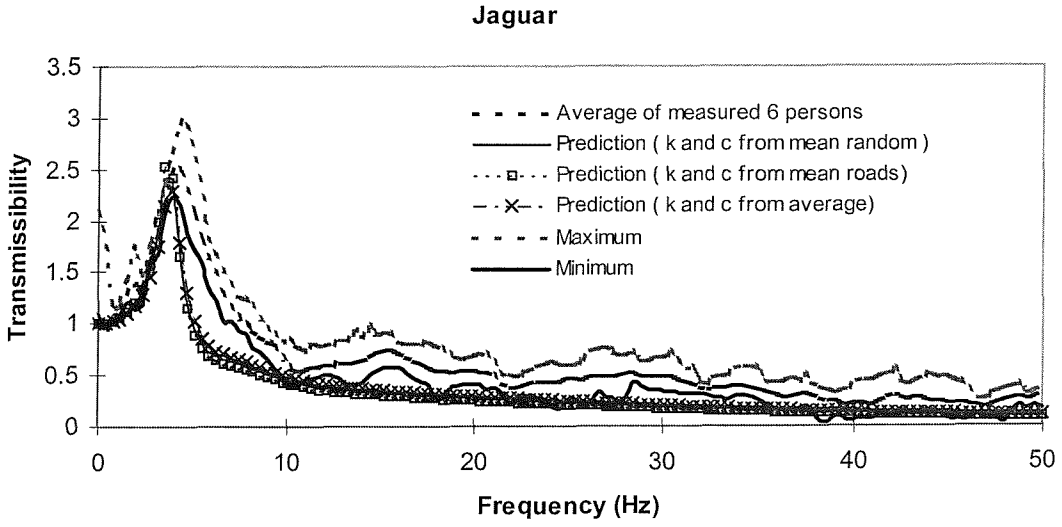

Figure 8.17 Prediction of the three seat transmissibilities

Table 8.5 Model parameters for the three seats

	500 N					
Input vibration	Mondeo		Fiesta		Jaguar	
	K (N/m)	C (Ns/m)	K(N/m)	C(Ns/m)	K(N/m)	C(Ns/m)
Mean roads	71059	192	85229	203	61234	126
Mean random	57337	121	78620	181	56392	109
average	67317	172	81924	192	58813	118

It can be seen that the correspondence between the measured and predicted values (Figure 8.17) is not as good as was obtained in the laboratory (although still far better than would have been obtained using a rigid mass to measure seat transmissibility). The predicted values and measured values are similar only below 4 Hz. In the frequency range from 4 to 10 Hz, the predicted values are significantly lower than the measured values, at frequencies above 10 Hz, the difference between them is small. The difference may be caused by the seat backrest. It has been shown that the seat backrest has a large effect on body apparent mass (see Section 7.4). Hence, a modified model should be used to predict the seat transmissibility.

In the above the body model has been adjusted according to the input vibration magnitudes. The model parameters were calculated from equation 8.15. The modification of the model for different seat backrest inclinations should be made according to the study in Section 7.4. A decrease in the model mass m_1, and an increase in both the model stiffness k_1 and the model damping c_1 can represent the changes that occur when there is increased backrest inclination. The ratios for these three parameters were calculated between no backrest and backrest at 20^0 (Table 7.8). The same ratios were used here between the parameters shown in Table 8.4 and the modified parameters that will be used to predict seat transmissibility.

Figure 8.18 shows the results of using the modified seat-person model for predicting seat transmissibility. Although this model provides improved predictions, the differences between the measured and predicted values are still large, especially over the frequency range from 5 to 20 Hz. This suggests that the effect of the seat backrest on seat transmissibility is not only caused by the response of the seated person, the seat has also an influence.

The seat-person model developed in Section 8.3.1.2 is based on a seat and human body model derived, respectively, from measured seat and measured human body dynamic responses. The role of the seat backrest has not been fully considered. Although, a modified model has been developed representing the human body that leans against a seat backrest, a seat-person model derived from it does not reflect the interaction between the seat and the body.

A sensitivity analysis of the seat-person model parameters was required to guide the study towards developing an improved model.

8.3.2.3 Sensitivity of seat-person model parameters

Figures 8.19 shows the sensitivity analysis of seat-person model parameters. The original model parameters come from measurements of the Mondeo seat (Table 8.5) and the proposed body model (Table 8.4). The comparison shows the predictions of the seat transmissibility between the original model parameters, a 10% increase in parameters and a 20% increase in parameters.

It can be observed that a change to the mass, m, had the smallest effect on seat transmissibility predictions. An increase in mass, m_1 caused the resonance frequency to decrease but with no change in transmissibility at frequencies above 7 Hz. The effect of changes to m_2 was very small. An increase in mass, m_2 caused the first and second resonance peak to decrease but it had no influence at other frequencies. It seems that parameter m_1 is a critical parameter for predicting the measured seat transmissibility if there is a change in resonance. The second mass, m_2, controls the second peak in the seat transmissibility prediction.

The effect of the subsystem stiffness, k_1, and subsystem damping, c_1, was significant. As the stiffness k_1 increased, the resonance frequency and the transmissibility at resonance both increased but at frequency above resonance the transmissibility decreased from 5 to 12 Hz. The influence of parameter, c_1, was different tom the stiffness, k_1; when c_1 increased, the transmissibility increased over the frequency range from 4 Hz to 7 Hz and then decreased at frequencies above 7 Hz.

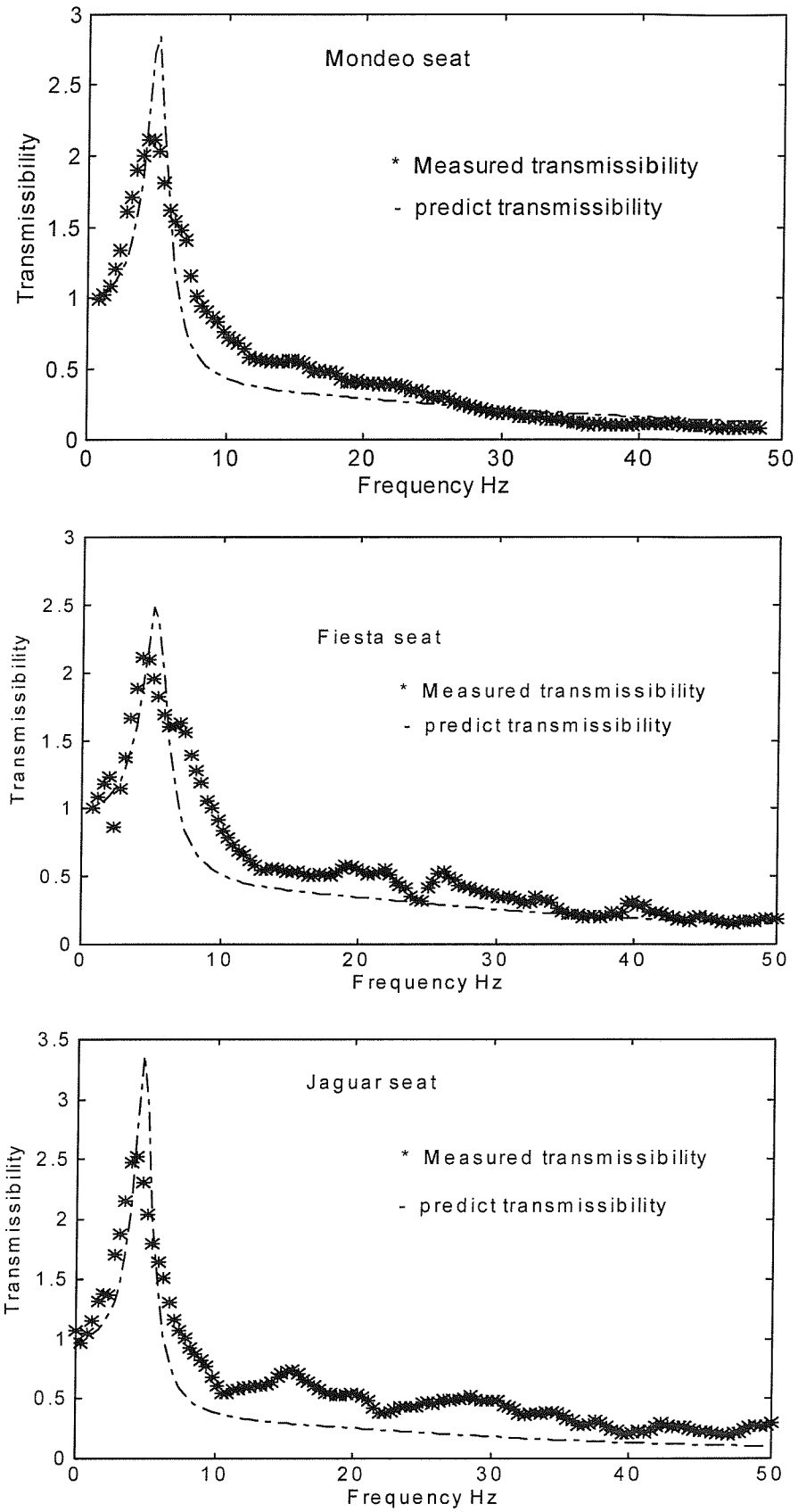

Figure 8.18 Comprison between predicted and measured transmissibilities for three seats (using modified model)

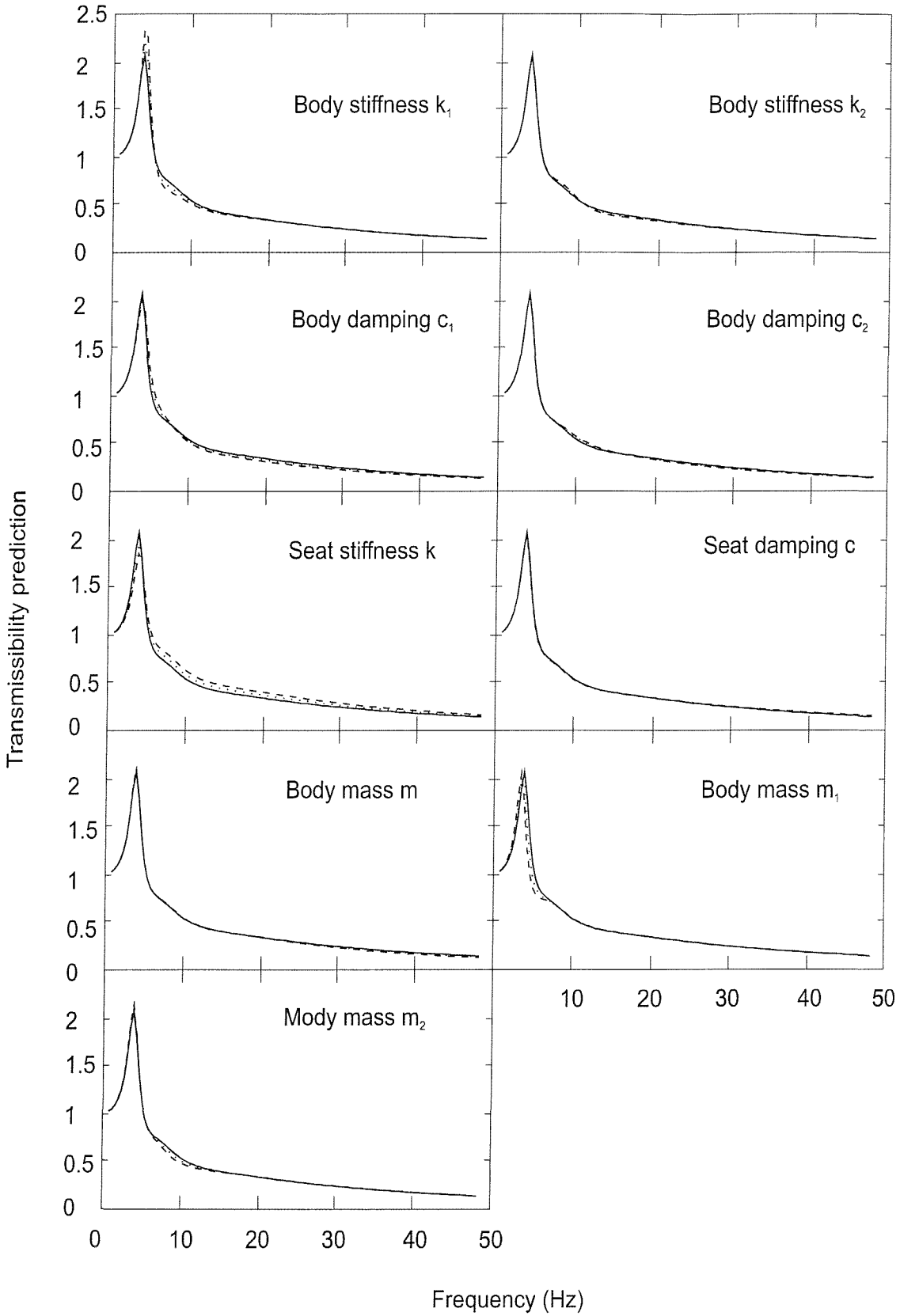

Figure 8.19 Sensitivity of predicted seat transmissibility to seat-person model parameters (——— original parameters, ... 10% increase in parameters, – – – – 20% increase in parameters

The function of the subsystem stiffness, k_2, and the subsystem damping, c_2, are also shown in Figure 8.19. These two parameters had only a small effect on the seat transmissibility predictions compared with the same change in the stiffness, k_1, and damping, c_1. The effect of c_2 on seat transmissibility predictions is similar to parameter c_1,

The effect of the seat parameters, k, and, c, on the seat transmissibility predictions is different from corresponding body parameters. As the stiffness, k, increased, the resonance frequency increased and the seat transmissibility at resonance decreased. Changes in the stiffness, k, may therefore offset the undesired increase arising from changes in m_1 at the resonance frequency. However, an increase of stiffness, k, will cause the seat transmissibility to increase at frequencies above the resonance frequency. The influence of parameter c was very small. Consequently, only changes to parameters m_1, k_1, c_1 and k can move the predicted seat transmissibility towards the seat transmissibility measured in the field.

The seat stiffness was measured by the indenter test and was therefore fixed. Hence, changes to parameters m_1, k_1 and c_1 are the only way to obtain improved prediction of seat transmissibility measured in the field. An increase of the backrest inclination and a decrease of the input magnitude both produced an increase in the model stiffness, k_1, and damping, c_1. The increases of the backrest inclination also caused a decrease in mass, m_1, (see Section 7.2 and 7.4). The seat transmissibility measured in the field had a large backrest inclination and small vibration magnitude (see Section 8.3.2.1) so that the modified model used in Figure 8.18 had a greater stiffness, k_1, and damping, c_1, and a lower mass, m_1, than the original model. Sensitivity analysis here showed that the previous study of the effect of backrest and input magnitude on apparent mass provided a useful method to obtain model parameters. Although the final results are not satisfactory, all the trends are in the correct direction.

It appears that the differences between the measured and the predicted seat transmissibilities were caused by the seat backrest. Although the effect of

backrest has been considered in the body model, the interaction between the seat backrest and the body has not been reflected correctly. Therefore, a new model is necessary for this condition.

8.3.2.4 New seat-person model and its function

Figure 8.20 shows a seated person with backrest. There are two forces applied to the seated person. The forces are: force, F_v, from the seat cushion and force, F_b, from the seat backrest. The force from the backrest is composed of a vertical force, F_1, and a horizontal force, F_2. Because only vertical vibration is concerned here, the total forces applied to the subject will be assumed to be the forces, F_1 and F_v, which might be transmitted by the seat cushion and the seat backrest stiffness and damping.

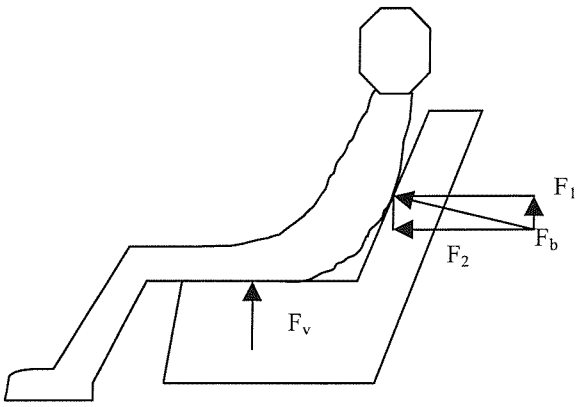

Figure 8.20 Seated person with backrest

Based on the above assumption, a new model (Figure 8.21) is devised. The model includes additional parameters, backrest stiffness, k_b, and backrest damping, c_b. Because the mass supported by the seat backrest is only part of the body mass, only mass, m_1, is connected to the seat base through the backrest stiffness and damping in the whole seat-person system.

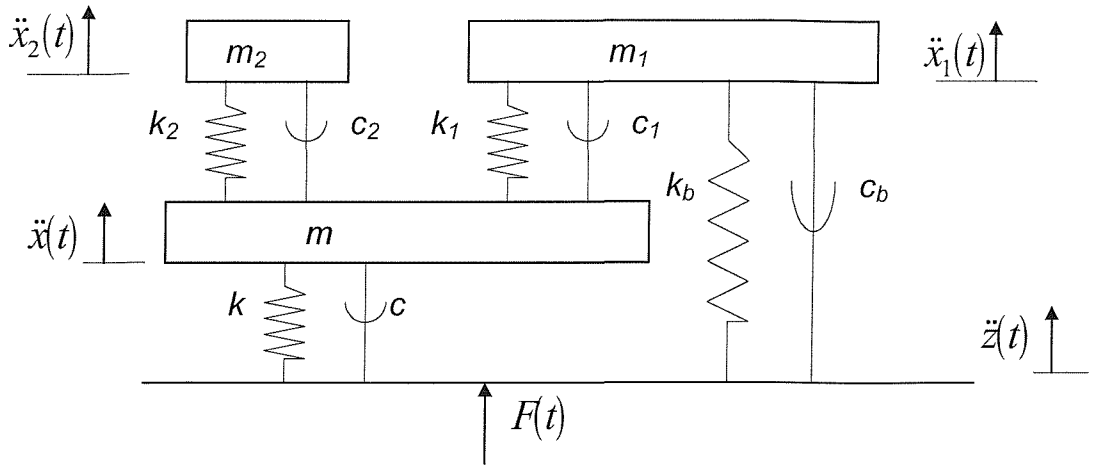

Figure 8.21 Model for seat-person system with seat backrest

The equations of motion of this model (Figure 8.21) are given by:

$$m_1\ddot{x}_1 + k_1(x_1 - x) + c_1(\dot{x}_1 - \dot{x}) + k_b(x_1 - z) + c_b(\dot{x}_1 - \dot{z}) = 0 \qquad (8.16)$$

$$m_2\ddot{x}_2 + k_2(x_2 - x) + c_2(\dot{x}_2 - \dot{x}) = 0 \qquad (8.17)$$

$$m\ddot{x} + k(x - z) + c(\dot{x} - \dot{z}) + k_1(x - x_1) + c_1(\dot{x} - \dot{x}_1) + k_2(x - x_2) + c_2(\dot{x} - \dot{x}_2) = 0 \qquad (8.18)$$

$$F(t) = m\ddot{x} + m_1\ddot{x}_1 + m_2\ddot{x}_2$$

$$F(t) = k(z - x) + c(\dot{z} - \dot{x}) + k_b(z - x_1) + c_b(\dot{z} - \dot{x})$$

Upon taking the Laplace transforms and substituting ωi for s, the model in the frequency domain becomes:

$$x_1(\omega) = \frac{k_1 + c_1 i\omega}{(k_1 + k_b) - m_1\omega^2 + (c_1 + c_b)i\omega}x(\omega) + \frac{k_b + c_b i\omega}{(k_1 + k_b) - m_1\omega^2 + (c_1 + c_b)i\omega}z(\omega)$$

$$x_2(\omega) = \frac{k_2 + c_2 i(\omega)}{k_2 - m_2\omega^2 + c_2 i\omega}x(\omega)$$

$$\left[-m\omega^2 + k + k_1 + k_2 + (c + c_1 + c_2)i\omega\right]x(\omega) - (k_1 + c_1 i\omega)x_1(\omega)$$
$$-(k_2 + c_2 i\omega)x_2(\omega) - (k + ci\omega)z(\omega) = 0$$

Substituting for $x_1(\omega j)$ and $x_2(\omega j)$ above gives:

$$(a_1 + a_3 + a_6 - m\omega^2 - \frac{2a_3a_6}{a_2})x(\omega) = \left(a_1 + \frac{a_3a_5}{a_4}\right)z(\omega)$$

Where:

$$a_1 = k + ci\omega$$
$$a_2 = k_2 + c_2 i\omega - m_2\omega^2$$
$$a_3 = k_2 + c_2 i\omega$$
$$a_4 = k_1 + k_b + (c_1 + c_b)i\omega - m_1\omega^2$$
$$a_5 = k_b + c_b i\omega$$
$$a_6 = k_1 + c_1 i\omega$$

The seat transmissibility is ratio of $x(\omega)$ to $z(\omega)$.

Comparing this model with the previously developed model, it can be seen that the stiffness and damping of the interaction between the back and the seat backrest are included (the interaction may include the action of the seat backrest and the body back tissue). However, the values of these two parameters (stiffness, k_b, and damping, c_b) are unknown. A new test is needed to measure the physical values of these two parameters.

Model parameters, k_b, and c_b, are used here to investigate the new model. The other model parameters come from Table 8.4 and 8.5. Figure 8.22 shows a comparison between predicted and measured transmissibilities of the three seats. It can be seen that the new model provides a better prediction of the seat transmissibilities measured in the field than the original and the modified model through a comparison between Figures 8.17, 8.18 and 8.22. The encouraging results obtained from the new model suggest that the form of the new model may be suitable for predicting field measurements of seat transmissibility.

Figures 8.23 and 8.24 show the effect of variation in stiffness, k_b, and damping, c_b. When the stiffness, k_b, increases, the resonance frequency and the transmissibility at resonance both increase. An increase in the damping, c_b, causes a decrease of seat transmissibility at resonance. The functions of the stiffness, k_b, and damping, c_b, are similar to those of a simple system. The correct increase of stiffness, k_b, and damping, c_b, will increase the resonance frequency and at same time keep the transmissibility at resonance

unchanged. This confirms that the effect of contact with the seat backrest on seat transmissibility is important. Any seat-person system model representing a person sitting on a seat with a backrest should include the effect of backrest contact, even though only vertical vibration is concerned.

8.3.3 Conclusion

Many models have been developed to predict seat transmissibility. Among them, a single degree-of-freedom model (see Section 6.3.1) and two degree-of-freedom model (see Section 6.3.2) both can provide good predictions for laboratory measurements of seat transmissibility, but the latter is better. A two degree-of-freedom model can predict the second resonance which is often seen in measurements of seat transmissibility around 8 Hz.

Although single degree-of-freedom and two degree-of-freedom models can give useful seat transmissibility predictions, the predictions were produced in limited conditions, with subjects in upright postures (not touching backrest) and with pure vertical input vibration.

A modified model, based on different vibration magnitudes and backrest inclinations, can give improved seat transmissibility predictions.

A new model that represents a seat-person system in a car has been developed and encouraging results have been obtained. However, physical parameter values are required for the backrest stiffness and damping.

8.4 Conclusion

The transmissibility of a cushion is affected by the inclination of the cushion, but the effect of the cushion inclination is small. It seems unnecessary to pay attention to the seat inclination when measuring seat transmissibility. The use of alternative orientations of the accelerometers to measure the cushion transmissibility showed similar small differences.

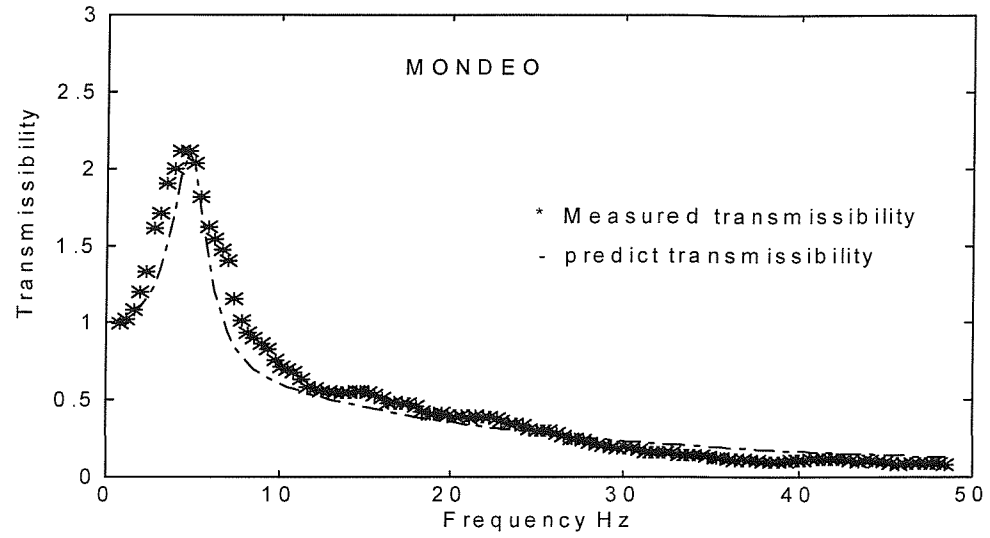

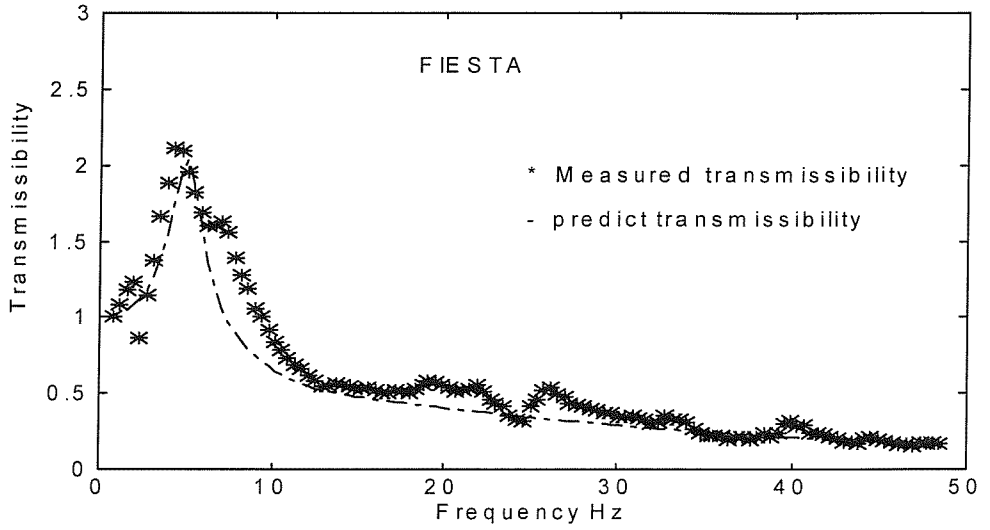

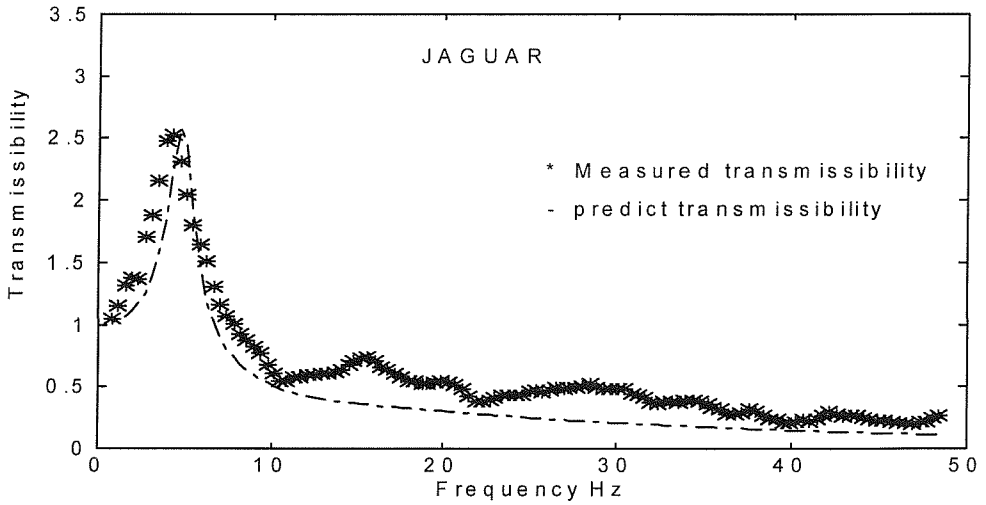

Figure 8.22 Comparison between predicted and measured transmissibilities of three seats (using new model with stiffness k_b=13000 N/m and damping c_b=100 Ns/m)

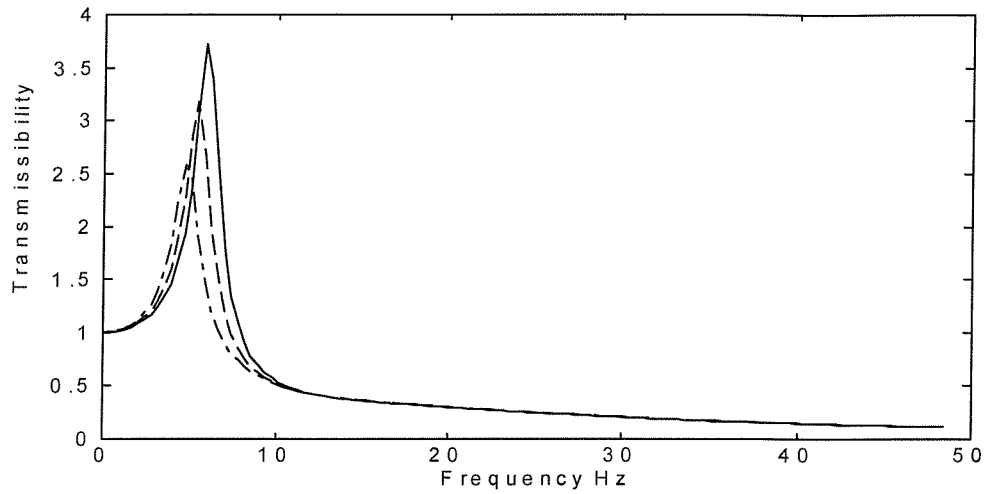

Figure 8.23 The effect of the model stiffness, k_b, on prediction of seat transmissibility (–·–·–· k_b=13000 N/m, – – – – k_b=23000 N/m, ——— k_b=33000 N/m, c_b=100Ns/m)

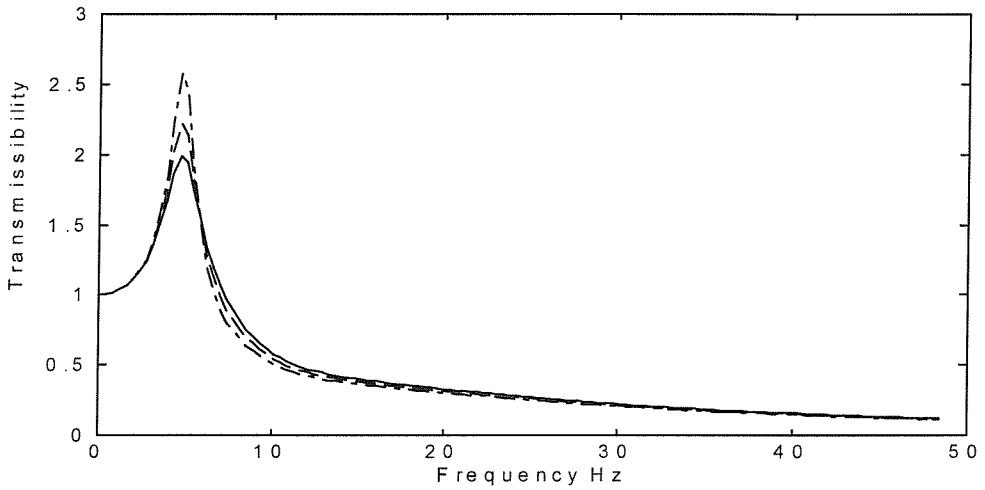

Figure 8.24 The effect of the model damping, c_b, on prediction of seat transmissibility (–·–·–· c_b=100 Ns/m, – – – – c_b=200 N/m, ——— c_b=300 N/m, k_b=13000 N/m)

A single degree-of-freedom model can adequately reflect the dynamic characteristics of a seat at low frequencies but it cannot give good predictions of the second resonance. A two degree-of-freedom model can provide good predictions of seat transmissibility over the frequency range from 0.5 to 25 Hz.

For field measurements of seat transmissibility, use of the above models cannot give good predictions. A modified model, appropriate to different vibration magnitudes and different backrest inclinations, can improve

predictions of the measured data, but it was still not satisfactory. A new model reflecting the interaction between the seat backrest and the seated body is better.

CHAPTER 9

CONCLUSIONS AND RECOMMENDATIONS

9.1 Introduction

The main conclusions and recommendations from the research are summarised in this Chapter. The main findings, the contributions to knowledge, are divided into three parts in Sections 9.2, 9,3 and 9.4. Section 9.2 provides a summary of the main findings when using an indenter to test seats. The human body mathematical model developments are included in Section 9.3. The standard seat test procedure, the main objective of this research, is included in Section 9.4. Finally, general recommendations for future research are produced in Section 9.5.

9.2 Indenter test method development

As implied in the thesis title, predictions of seat transmissibility can be made from the measured seat impedance. Therefore, how to obtain good seat impedance data is important for predicting seat transmissibility. Many methods have been used to obtain seat impedance, but no previous studies have compared these methods, and so no standard method has been developed to measure seat impedance. Fairley and Griffin (1986) proposed an indenter method to measure seat impedance. A study in Section 5.2.2.1 was conducted to investigate which method can give good seat impedance measurements. As discussed in Section 5.2.2.1.4, using an indenter to measure seat impedance was found to be better than other methods (i.e., using sand-bag or mass).

Although using an indenter to measure seat impedance is not a new method (Fairley and Griffin, 1986), there were no previous investigations of the effects of various factors on the measured results. However, when using an indenter to measure seat impedance the results are affected by many factors, such as

indenter head area, vibration magnitude, seat inclination angle and pre-load. Therefore, studies were needed and conducted here to investigate the influence of these factors on measured seat impedance using an indenter. The findings were as follows.

9.2.1 Effect of contact area on indenter test

The effect of contact area between an indenter and the foam, or seat, was investigated. Five different contact areas were used. As expected, the contact area is important in the indenter test. Using different contact areas, different foam, or seat, impedance was obtained. However, there was no correlation between the contact area and the seat stiffness and damping.

A shaped buttocks with approximately the same shape as the seated human body might be reasonable for foam testing. However, it does not provide good foam impedance and the data obtained from a buttock did not give good predictions of foam transmissibility. The study in Section 5.2.2.2 showed an additional problems when using a buttocks to measure seat impedance, so it cannot currently be recommended for obtaining a good prediction of foam transmissibility.

Using a SIT-BAR to measure seat properties is better than using other contact areas, because a SIT-BAR has a small size in the fore-and-aft direction so a small twist force is produced in measurements. The data from measured seat, or foam, impedance using a SIT-BAR produced a good prediction of seat, or foam, transmissibility (see Sections 4.3 and 8.3.1.2). A SIT-BAR, therefore, is recommended as an indenter to measure seat impedance.

9.2.2 Effect of static forces on indenter test

Many studies have been concerned with the effect of subject weight, or static forces, on measures of seat dynamic response. Some studies showed that a subject's weight affected suspension seat transmissibilities, such as Matthews (1967), Stayner (1971) and Burdorf and Swuste (1993), but other researchers, such as Corbridge (1981), Fairley (1986) and Corbridge *et al.* (1989), showed that the influence of subject mass was small on seat transmissibilities.

Varterasian and Thompson (1977) investigated the effect of subject weight on the transmissibilities of conventional seats. They found that there were only small differences in the resonance frequency and transmissibility at resonance when subject weight varied from 31 kg to 72 kg. No matter what happened in previous studies, it was clear that an investigation of the effect of static force on an indenter test was needed.

The investigation found that seat, or foam, impedance was affected by varying the pre-load. The measured data showed that the stiffness and the damping of a block of foam, or a seat, increased with increased static load. It is therefore recommended that an appropriate static force is needed when determining foam, or seat, dynamic stiffness.

9.2.3 Effect of inclination angle on indenter test

There were no previous studies concerned with the effect of seat, or foam, inclination angles on seat dynamic responses, so it was necessary to obtain knowledge in this field. An experiment was conducted to investigate the influence of foam inclination angle on foam impedance. It was found that foam impedance varied only slightly when foam inclination angles increased. So it was concluded that foam inclination was not important when determining foam impedance using an indenter. However, it was still recommended that the seat mount for an indenter test should be in accordance with the requirements of the seat manufacturer.

The horizontal motion caused by a seat, or foam, inclination in an indenter test must be avoided so that the correct vertical seat dynamic property can be achieved. This means that a strong frame is needed in an indenter rig (see Figure 5.15).

9.2.4 Effect of vibration magnitudes on indenter test

It is well known that the input vibration magnitude affects seat, or foam, transmissibility when measured using human subjects. Stayner (1972), Leatherwood (1975), Ashley (1976), Fairley (1983, 1986), Corbridge (1987) and Fairley (1990) revealed that the effect of vibration magnitude on seat

transfer functions was significant. The effect of vibration magnitude on seat transmissibility includes two parts, one is the effect of vibration magnitude on seat impedance and the other is the effect of vibration magnitude on the response of the human body. It was clear that an investigation of the effect of vibration magnitude on seat impedance was needed. However, no previous research had been conducted in this field.

An experiment was performed to investigate the effect of vibration magnitude on seat impedance. It was found that there were no large differences in seat impedance over the vibration magnitude range from 0.25 to 2.5 ms^{-2} rms, but if the vibration magnitude was changed too much, such as when the sinusoidal input vibration amplitude changed from 0.25 mm to 5 mm, the differences of seat impedance caused by variations in vibration magnitude become clear (see Section 5.2.2.2). It was recommended that seat impedance should be measured with any reasonable magnitude of vibration, such as 1.0 or 1.5 m/s^2 rms.

It was found that seat stiffness decreased when sinusoidal vibration amplitudes increased from 0.25 mm to 5 mm. Although seat damping also changed as sinusoidal vibration amplitudes varied, the change did not vary systematically.

9.3 Seated body model development

Many researchers have investigated the dynamic response of the seated body. Various experiments have been conducted to obtain the impedance of the seated body. It was found that the mechanical impedance of the seated body had the features of a one, or two, degree-of-freedom system. Most measurements of sitting body impedance, or apparent mass, have one, or two, resonance frequencies. Therefore, Payne (1965), Vogt *et al.* (1968), International Standard ISO 5982 (1981) and Fairley and Griffin (1989) developed one, or two, degree-of-freedom models to represent the seated body. Although, Smith (1994) showed four resonance frequencies on measured body mechanical impedance this finding has not been verified by other researchers.

Two single degree-of-freedom and two two degree-of-freedom lumped parameter models were developed to represent the seated body in the vertical direction using previous measured data. The analysis showed that a single degree-of-freedom and the two degree-of-freedom models with support mass were both suitable to represent the apparent mass for the seated body. However, the latter can provide better predictions of the measured apparent mass even when the measured apparent mass showed only one clear resonance.

A curve fitting technique based on MATLAB was used to obtain model parameters. A comparison was made between two curve fitting methods, fitting the measured apparent mass modulus and fitting the measured phase. It was found that the latter provided more reasonable parameters for the proposed models. The study showed that the model parameters could be decided by the measured apparent masses. This means that good model parameters could be achieved through good measurements of sitting body impedance, or apparent mass.

It has been shown by many researchers that the apparent mass of the sitting body is affected by many factors, but no studies have previously investigated the correlation between the mathematical model and the varied apparent mass caused by these factors, such as vibration magnitude, hard or soft seat, seat inclination, seat backrest and vibration spectra. Therefore, a series studies was conducted to investigate how these factors influence a body mathematical model based on the measured apparent mass. The findings contribute to the body model development.

9.3.1 Effect of vibration magnitude on body apparent mass

Miwa (1975), Vogt (1968), Mertens (1978), Hinz and Seidel (1987), Fairley and Griffin (1989), Smith (1994), Mansfield (1998) and Kitazaki (1998) revealed that vibration magnitude influenced the measured sitting body impedance, or apparent mass. However, Coermann (1962), Prodko *et al.* (1966) and Sandover (1978) obtained a contrary conclusion. The differences between the conclusions may be caused by the different experimental

conditions, for example the experiment conducted by Sandover (1978) used a seat backrest. The movement restriction by a seat backrest may reduce the change of the sitting body impedance at different vibration magnitudes. The experiments conducted by Fairley and Griffin (1989), Mansfield (1998) and Kitazaki (1998) had the same experimental conditions, so the conclusions produced by them were similar and showed the sitting body having a non-linear response at different vibration magnitudes.

Because the sitting body response is non-linear, the linear model produced in Section 6.3 could not be used at different magnitudes. A non-linear model, or modified linear model, which can be used at different magnitudes, was needed. The latter approach was selected in this study. Previously obtained experimental data (Mansfield, 1998) were used. It could be observed that there were clear and consistent differences in the dynamic responses of the body as the magnitude of the vibration changed. Although the causes of the non-linearity are not clear, the specification of the mechanical impedance, or apparent mass, of the body should be specific to a limited range of vibration conditions.

There are two ways to modify a linear two-degree-of-freedom model to make it suitable for different vibration magnitudes. One is to change the model masses and the other is to change model stiffness and damping. Although changing all model parameters can provide good body apparent mass prediction, it makes the problem more complex. Changing model stiffness and damping were used here to modify the model. The varied mean model stiffness and damping were obtained by using a previously developed two degree-of-freedom model (see Section 6.3) to fit the measured apparent mass at different vibration magnitudes. It was found that the model stiffnesses, k_1 and k_2, and model damping, c_1 and c_2, decreased with increases in the vibration magnitude when all model masses, m, m_1 and m_2, were kept constant. Equations were therefore developed to represent the change of model stiffness, k_1 and k_2, and model damping, c_1 and c_2, at different vibration magnitudes.

The previously developed model (see Section 6.3) represents only one vibration magnitude (1.0 m/s^2 rms), so it cannot be used at other vibration magnitudes due to the influence of vibration magnitude on the measured apparent mass. The equations derived from curve fitting were used to modify the model stiffnesses, k_1 and k_2, and the damping, c_1 and c_2, so that the model would be useful with varied vibration magnitudes. A good prediction of the measured apparent masses was produced using the modified model at different magnitudes.

9.3.2 Effect of seat cushion inclination on body apparent mass

A car seat is generally inclined from the horizontal to improve seat static comfort. No previous studies had been conducted to investigate the influence of seat inclination on either seat transmissibility or seated body apparent mass. A study was therefore conducted to investigate the effect of seat inclination on sitting body apparent mass, because it was assumed that the inclination of a seat cushion might cause a change of a subject posture, even when a subject keeps an upright posture.

As expected, the apparent mass changed with seat inclination. However the change of the apparent mass was small. Therefore, it seems unnecessary to pay attention to seat inclination when measuring subject apparent mass. In other words, there was no influence of seat inclination on the seated body mathematical model.

9.3.3 Effect of seat backrest on body apparent mass

There are a few investigations concerning the effect of a seat backrest on the measured apparent mass of the body. Coermann and Okada (1964) found that there was no consistent change in the mechanical impedance of the body between with and without a seat backrest. However, Fairley and Griffin (1989) obtained an opposite conclusion and reported significant differences between the two conditions. They showed that there were clear and consistent differences in the dynamic response of the body as the backrest condition changed. This means that the specification of the apparent mass of the body should depend on the backrest conditions.

An experiment was conducted to investigate the influence of backrest angle on measured apparent mass. It was found that the measured body apparent mass changed as the backrest condition changed. This means that the previously developed model based on the no backrest condition (see Section 6.3) could not be used to represent the sitting body with a backrest. So a modification of the model was needed so that it can be used to represent a seated body with varied backrest conditions. A sensitivity analysis of the parameters of the body model was conducted.

It was found that a decrease in the model mass, m_1, and an increase in both the model stiffness, k_1, and the damping, c_1, can represent changes of the measured apparent mass with changed backrest conditions. The changes of these parameters have been tabulated. A comparison was performed between the measured apparent mass and that predicted by the modified model with different backrest conditions. It was concluded that the modified model represented the sitting body with different backrest conditions.

9.3.4 Effect of hard and soft seat as well as vibration spectra on body apparent mass

It was assumed that the response of the sitting body would change between sitting on a hard seat and sitting on a soft seat. The reason for a change may be the change of input vibration spectra. However, no previous studies had been conducted to investigate the effect of a hard seat and a soft seat on the measured apparent mass of the body. Two experiments were conducted. One investigated the influence of the hard seat and the soft seat on apparent mass and one investigated the effect of vibration spectra on apparent mass. Sandover (1978) revealed that the effect of vibration spectra on apparent mass was small, but Fairley (1986) showed a different conclusion.

The experimental results suggested that there were differences between body apparent masses obtained on hard and soft seats. The model parameters, derived from a hard seat and a soft seat, were also different. Although these parameters may give good predictions for the measured body apparent masses, the data from the soft seat did not give good predictions of seat

transmissibility. So, the parameters derived from the soft seat may not be suitable for seat transmissibility prediction models.

The investigation showed that the model stiffnesses, k_1 and k_2, model damping, c_1 and c_2, and mass, m_2, decreased, but the model mass, m_1, increased when subjects changed from a hard seat to a soft seat,

The study of the effect of the vibration spectrum showed that there was a statistically significant effect of the spectrum on apparent mass, but the magnitude of the effect was small.

9.4 Predicting seat transmissibility

A seat-person model was set up from the above studies. A good prediction of seat transmissibility measured without a seat backrest was obtained. However the model could not give a good prediction of seat transmissibility measured with a backrest.

A new model was then developed based on the assumed interaction between the body back and the backrest. The model included a new part, which reflected the interaction between the seat backrest and the seated body. The model gave improved predictions of seat transmissibilities measured in the field.

Therefore, the aim of this study was realized. A standard seat test procedure was then developed to predict seat transmissibility.

9.5 Recommendations

The study in this thesis has only considered the vibration in vertical direction. Vibration in other axes also plays an important role in seat dynamic properties. So a logical extension of this work is to identify the response of the body to vibration in other axes, such as the fore-and-aft axis.

The non-linearity of the body response at different vibration magnitudes revealed in Chapter 7 suggests that a non-linear body model is needed to represent the non-linear body response.

Some researchers consider that the dynamic response of the viscera make a major contribution to the principal resonance of the apparent mass for a seated body. However, the mechanism of the visceral response has not been well understood. The single degree-of-freedom and the two degree-of-freedom model developed here were based on the feature of the measured apparent mass and not knowledge of the internal body response. The models cannot be used to explain any internal dynamic behaviour of the body in a vibration environment. Knowledge of the body response is important, so a model based on such knowledge is needed and may produce a better prediction of seat transmissibility.

Although a preliminary model representing a seated body with the backrest has been developed, the model can only be used in vertical direction. However, the effect of the backrest on apparent mass, or the effect of the backrest on seat transmissibility, is not only in the vertical direction. The backrest of a seat has more influence on motion in the fore-and-aft, or rotational axes. A further study of the effect of the backrest on seat transmissibility, or the effect of the backrest on apparent mass of the body, in the fore-and-aft axis is needed so that a new model can be developed to predict seat transmissibility in the fore-and-aft axis. An extension to such a research program could investigate combinations of all directions of translational and rotational motion.

APPENDIX A LABORATORY METHOD FOR PREDICTING SEAT TRANSMISSIBILITY

1. Introduction

The transmission of vibration to the body can cause discomfort, impaired performance and health problems. Seats influence the transmission of vibration to the body, either increasing the overall severity of vibration or reducing the overall severity of vibration. The dynamic response of a seat can therefore have a large influence on human responses to vibration.

The transmissibility of a seat depends on many factors, including the seat characteristics and the mechanical impedance of the load on the seat (e.g. the human body). It is not, in general, possible to measure or predict the transmission of vibration without considering the effect of the seat loading. Seats do not normally have the same transmissibility when measured with a subject and a rigid mass.

The transmissibility of a seat can be measured in vehicles or in the laboratory with suitable subjects sitting on the seat. However, this is time-consuming and may impose some risks to the subject. The measurements will also depend on the subject chosen for the studies. Transmissibility may alternatively be measured with a suitable anthropodynamic dummy replacing the human subject.

Seat transmissibility can also be estimated without either a human subject or a dummy. From a knowledge of the mechanical impedance of the human body and suitable measurements of the mechanical impedance of the seat, the seat transmissibility can be predicted. This has the advantage that human subjects are not required, and the likely effect of physical changes to the seat (e.g. damping, stiffness, geometry) may be more easily determined.

2. Scope

This document specifies the instrumentation requirements, the measurement method and the calculation procedure required to predict seat transmissibility. A standardised means of reporting results is also presented.

The use of the recommended method for measurement and analysis should make it possible to compare test results from different laboratories.

3. NORMATIVE REFERENCES

The following normative documents contain provisions of this test method.

ISO 2631:1997

Mechanical vibration and shock - evaluation of human exposure to whole-body vibration. Part 1: General requirements. International Standard, ISO 2631-1.

ISO 5347-0:1987

Methods for the calibration of vibration and shock pick-ups - Part 0: Basic concepts.

ISO 2041:1975

Vibration and shock - Vocabulary.

4. Symbols and indices

For the purposes of this test procedure, the following symbols and indices apply.

4.1 Symbols

c	Viscous damping of seat, Ns/m
c_1	Viscous damping of body first subsystem, Ns/m
c_2	Viscous damping of body second subsystem, Ns/m
c_b	Viscous damping for seat-person model with backrest, Ns/m
F	Force, Newton
f	Frequency, in hertz (Hz).
i	Assumed unit ($i^2 = -1$).
k	Stiffness of seat, N/m
k_1	Stiffness of body first subsystem, N/m
k_2	Stiffness of body second subsystem, N/m
k_b	Stiffness for seat-person model with backrest, N/m
m	Model frame mass, kg
m_1	Mass of body first subsystem, kg
m_2	Mass of body second subsystem, kg
PSD	power spectral density expressed as mean square acceleration per unit bandwidth $(m/s^2)^2/Hz$
PDF	probability density function of acceleration amplitudes
r.m.s.	root mean square
$s(\omega)$	Dynamic stiffness
|T|	Modulus of seat transmissibility
θ	Phase of seat transmissibility

x Displacement, in metres *(m)*

$\dot{x}$ Instantaneous velocity, in metres per second (ms^{-1}).

$\ddot{x}$ Instantaneous acceleration, in metres per second squared (ms^{-2}).

5. Instrumentation

5.1 Acceleration, displacement and force transducers

Vibration at the seat base and vibration transmitted to the subject shall be sensed by accelerometers or displacement transducers.

The accelerometers, together with their amplifiers, shall be capable of measuring r.m.s. acceleration levels ranging from 0.05 to 20 m/s^2 with a crest factor of up to 6. The accelerometers and amplifiers shall be capable of an accuracy of ±2.5% of the actual r.m.s. vibration level in the frequency range 0.5 to 100 Hz. The resonance frequency of the accelerometers shall be greater than 300 Hz.

One accelerometer or displacement transducer and one force transducer are used on a seat indenter test rig (see Figure 1).

Motion of the vibrator platform is measured using an accelerometer.

> *Note:* A suitable accelerometer is an Entran EGCSY-240D*-10 having a sensitivity of approximately 13 mV/g with an operating range of ±10 g.

Displacement of the vibrator platform may be measured using a displacement transducer.

> *Note:* A suitable displacement transducer is a DC-LVDV D2/200A having a sensitivity of approximately 0.16 v/mm with an operating range of ±10 mm.

The driving force whilst testing the seat is measured using a force transducer.

> *Note:* A suitable force transducer is a Kistler 9321A force cell with a sensitivity of approximately ±3.97 pC/N.

The characteristics of the vibration measuring system, signal conditioning and data acquisition equipment, including recording devices shall be specified for the relevant tests, especially the dynamic range, sensitivity, accuracy, linearity and overload capacity.

> *Note:* Suitable signal conditioning for the force cell is a Kistler KIAG5001 or a B&K 2635 charge amplifier.

5.2 Indenter

An indenter is used to apply a pre-load to the seat surface. Figures 1 and 3 show a suitable indenter arrangement. The indenter head consists of a SIT-BAR (Figure 2), attached to a rigid steel frame.

The indenter is moved up and down on to the top surface of the test seat so as to vary the applied static force between indenter and the seat. The indenter is mounted on a bearing which allows it to rotate as the indenter is moved up and down.

5.3 Seat mounting

The test seat shall be mounted on the platform with the same method of attachment and at the same angle as it is mounted on the floor of the test vehicle. The platform shall be mounted on a vibrator that is capable of generating vibration along the vertical (z-axis).

The seat shall be adjusted to enable the indenter to apply force to the centre of the seat surface.

When the inclination of the seat surface is adjustable, the angle during testing shall be specified.

> *Note:* The seat backrest may influence the seat impedance measured by an indenter. In order to minimise the effect of the seat backrest, it should be adjusted to the upright position. If the seat backrest cannot be adjusted to the upright position, an additional device is needed to fix the seat backrest to prevent horizontal movement during vertical motion of the seat base.

5.4 Transducer mounting

An accelerometer shall be located on the platform at the support for the seat. If using a displacement transducer, one end of the displacement transducer shall be located at the same location as the accelerometer and the other end shall be located at a still base.

A force transducer shall be located above the indenter over the seat surface (Figures 1 and 3). One side of the force transducer shall be connected to the indenter and the other side connected to the bearing (Figure 3).

5.5 Data acquisition and signal generation

An input signal can be either a sinusoidal or a random signal produced by computer or a signal obtained from the floor of a vehicle. A digital-to-analogue (D/A) conversion card and a filter are needed to produce the required vibration.

Data recording can be achieved using digital recording techniques. In all cases the data recording shall have sufficient dynamic range to ensure that vibration signals over the full frequency range can be reliably recorded.

Note: A suitable data acquisition and signal generation system is *HVLab* developed by the Human Factors Research Unit, Institute of Sound and Vibration Research, University of Southampton. It can acquire and analyse up 16 channels of time varying analogue signals whilst simultaneously outputting 2 channels. The number of channels, sampling rate and duration are controlled by *HVLab* software. An analogue-to-digital and a digital-to analogue computer interface card and a *Techfilter* TF-16 anti-aliasing card are included in the system.

5.6 Calibrate

The instrumentation shall be calibrated in accordance with ISO 5347 and, depending on the type of measuring system used, to the relevant part of ISO 5347. The force transducer should be calibrated in two conditions: static and dynamic. In particular, the calibration procedures should ensure that the acceleration sensitivity varies less than $\pm 0.5\%$ of a mean value over the interesting frequency range and less than $\pm 6\%$ of the mean value over the full measured frequency range from 0 to 30 Hz.

The effect of ambient temperature on the performance of all instruments shall be known. Instruments shall be operated within the temperature limits to which the required accuracy can be expected.

Calibration shall be made before and after each test series.

6. Vibration equipment

6.1 Vibrator

The minimum required is a vibrator capable of driving a platform in the vertical direction. The dynamic response of the exciter shall be capable of exciting the seat with the indenter and additional equipment, in accordance with the specified test input vibration.

Note: A suitable vibrator is a Derritron VP85 powered by a 1000W Derritron amplifier. A maximum displacement of 25.4 mm is possible and the vibrator is capable of producing a force of 3.3 kN. Mechanical and electrical stops are fitted to the vibrator. Emergency stop buttons shall also be accessible to the experimenter.

6.2 Indenter rig

The indenter rig is shown in Figure 1 and 3. It should be rigid and strong enough to resist motion in the horizontal direction caused by seat surface inclination.

6.3 Control system

The frequency response characteristics of the vibration system shall be compensated to ensure that the power spectral density (PSD) and the probability density function (PDF) of the acceleration amplitudes of the vibration at the seat mounting base comply

with the requirements of the specified test input. This means that all input signals must be equalised for the response of the system before they are used in a seat test.

7. Vibration testing of a seat

7.1 Test ambient conditions

The tests are to be performed in controlled climatic conditions:

Temperature: 23 ^{0}C ± 2 ^{0}C (or as specified in the test schedule)

Relative humidity: the maximum acceptable variation is ±15% RH

The seat should be allowed to acclimate to these conditions for a minimum of 12 hours period.

7.2 Static test

Three repeated compression cycles are performed for each test condition at a compression speed not greater than 100mm/min. The force and displacement measurements during the three cycles shall be recorded.

(1) Pre-conditioning

Three initial compression cycles between 50N (pre-load) and 750N.

(2) Test conditions

400 to 600 N three cycles

300 to 700 N three cycles

200 to 800 N three cycles

7.2.1 Accuracy

The compression axial force shall be measured to an accuracy of ±2.5% of the true value.

The compression displacement shall be measured to an accuracy of ±2.5% of the true value.

7.3 Dynamic test

7.3.1 Random excitation with given spectrum

7.3.1.1 Excitation signal

Three different magnitudes of random excitation, each having a nominally flat constant bandwidth acceleration spectrum, or three excitation signals from a vehicle are applied

with the vibrator. The duration of each of the three random signals shall be 2 minutes in a frequency range from 0.5 to 50 Hz (or as specified).

In some applications, a test may be conducted with additional inputs so as to test for non-linearities in the seat response. The additional inputs may be the standard spectrum presented at different magnitudes or a defined spectrum for a specific vehicle.

When using spectra from a vehicle, care is required to ensure that coherent data are obtained at all frequencies.

> *Note:* The spectrum of the test input from a vehicle shall be determined from the expected seat deflection, not the expected spectrum on the vehicle floor.

The root-mean-square value of the test acceleration shall be within ±10% of the required value. Tests shall be conducted at three magnitudes: 0.5, 1.0 and 1.5 ms^{-2} (or as specified).

7.3.1.2 Preload

The indenter head shall be applied to the seat surface with a specified required pre-load.

> *Note:* When testing seats for normal adults, a pre-load of 550N applied to seat surface is normally appropriate.

After applying the pre-load, there should be a pause of 5 minutes to allow the seat to settle. The pre-load should then be checked and corrected, if necessary, before commencing the tests.

7.3.1.3 Accuracy

The compression axial force time history shall be measured with an accuracy of ±2.5% of the true value.

The displacement time history shall be measured with an accuracy of ±2.5% of the true value.

7.3.2 Sinusoidal excitation

If required, a sinusoidal displacement signal is to be applied with three different preload forces. Unless otherwise specified, the forces shall be 500N, 600N and 700N.

7.3.2.1 Excitation signal

The displacement excitation must be within the frequency range 1 Hz to 30 Hz. The sinusoidal displacement can be either swept sine, with a sweep rate less than 0.5 Hz/s, or stepped sine with a step 1 Hz.

The test should be repeated for a series of displacement amplitudes: 1, 2 and 5mm. The swept sine (or stepped sine) may be truncated at the upper frequency when the acceleration reaches 10 ms^{-2} r.m.s.

7.3.2.2 Accuracy

The sinusoidal compression force time history shall be measured with an accuracy of ±2.5% of the true value at each frequency.

The sinusoidal displacement time history shall be measured with an accuracy of ±2.5% of the true value at each frequency.

8. Analysis

8.1 Spectral analysis

Spectra of the force and displacement shall be calculated with a frequency resolution not greater than 0.25 Hz (corresponding to not less than 96 degrees of freedom).

8.2 Coherency

The coherency between the force and acceleration signals shall be determined over the frequency range 0.5 to 30 Hz. The prediction of seat transmissibility in Section 9 shall be assumed to be inaccurate at any frequency where the coherency falls below 0.8.

9. Calculation of equivalent seat stiffness and damping

If using an accelerometer to measure the motion of the seat base, the acceleration at the seat base shall be integrated twice to obtain the displacement at the seat base.

9.1 Seat dynamic stiffness

The seat dynamic stiffness, $s(\omega)$, is the complex ratio of force to displacement and is assumed to have the form:

$$s(\omega) = \frac{F(\omega)}{x(\omega)} = k + c\omega i$$

In $s(\omega)$, the real part, k, is the equivalent seat stiffness, and the imaginary part, c, is the equivalent viscous damping.

Note: A curve fitting method can be used to obtain seat parameters k and c (i.e. the effective stiffness and damping) from the real and imaginary components of $s(\omega)$. The least square error method with an optimisation algorithm may be utilised. The parameters in the above equation were refined to minimise the function:

$$error = \frac{1}{N}\sum_{i=1}^{N}\left(k_f(i) - k(i)\right)^2$$

$$error = \frac{1}{N}\sum_{i=1}^{N}\left(c_f\omega(i) - c\omega(i)\right)^2$$

where $k_f(i)$ is the corresponding dynamic stiffness from the curve fit at the ith frequency point and $k(i)$ is the dynamic stiffness in the measured data and $c_f\,\omega(i)$ is the corresponding damping from the curve fit at the ith frequency point and $c\omega\,(i)$ is the damping in the measured data. Using values for the parameters chosen at random as starting values, the parameters may be varied systematically using the optimisation algorithm.

Note: The measured data may be first converted from *HVLab* data files to ASCII data, and then imported to MATLAB for curve fitting (see Annex A).

10. Calculation of predicted seat transmissibility

10.1 Human body mathematical model

The apparent mass of the human body shall be assumed to be represented by the model in Figure 4 and 5 with values of stiffness, viscous damping and mass as defined in Table 1.

Note: The human body has a non-linear response to vibration. Although the parameters given in Table 1 will often be sufficient, some deviation may be necessary with stimuli having high or low magnitudes.

Note: The model shown in Table 1 adequately represents the input impedance of the seated human body. However, it should not be assumed to represent how vibration is transmitted through the body or give any indication of the discomfort or risk of injury produced by vibration. The discomfort and injury potential of vibration should be estimated from the vibration on the seat surface using the appropriate standard.

Table 1 Parameters of single degree-of-freedom model, model A, and two degree-of-freedom model, model B.

	k_1	c_1	k_2	c_2	m	m_1	m_2
Model A	44943	1390			6.0	45.6	
Model B	35776	761	38374	458	6.7	33.4	10.7

10.2 Prediction of seat transmissibility

10.2.1 Model of seat-person system without backrest

Figures 6 and 7 shows the assumed model that combines the seat stiffness and damping with the model of the apparent mass of the human body. The models can be used to predict the transmissibility of a seat without seat backrest.

> *Note:* The MATLAB program for calculating seat transmissibility is given in Appendix B.

Prediction of seat transmissibility using two degree-of-freedom model (Figure 6)

The transmissibility and phase of the seat response are given by:

$$|T| = \sqrt{\frac{A^2 + B^2}{D^2 + E^2}}$$

$$\theta = a\tan\frac{B}{A} - a\tan\frac{E}{D}$$

where:

$$A = KK_1 - (m_1K + CC_1)\ \omega^2$$

$$B = (C_1K + CK_1)\ \omega - m_1C\omega^3$$

$$D = \left(K - (m + m_1)\ \omega^2\right)K_1 + \left(mm_1\omega^2 - Km_1 - CC_1\right)\ \omega^2$$

$$E = \left(KC_1 + K_1C - (m_1C + mC_1 + m_1C_1)\ \omega^2\right)\ \omega$$

Prediction of seat transmissibility using three degree-of-freedom model (Figure 7)

The seat transmissibility and phase are given by:

$$|T| = \sqrt{\frac{F^2 + G^2}{(H + L)^2 + (M + N)^2}} \qquad (1)$$

$$\theta = \text{a tan}\frac{G}{F} - \text{a tan}\frac{M + N}{H + L} \qquad (2)$$

where:

$$F = KP_1 - CP_2\omega$$
$$G = KP_2 - CP_1\omega$$
$$H = P_1P_5 - P_2C\omega - m_1K_1P_3\omega^2$$
$$L = m_1C_1C_2\omega^4 + \left(m_2K_2P_4\omega^2 - m_2C_1C_2\omega^4\right)$$

$$M = P_2P_5 - CP_1\omega - \left(m_1C_1P_3 - m_1C_2k_1\right)\ \omega^3$$
$$N = m_2C_2P_4\omega^3 + m_2K_2C_1\omega^3$$
$$P_1 = m_1m_2\omega^4 + K_1K_2 - \left(m_1K_2 + m_2K_1 + C_1C_2\right)\ \omega^2$$

$$P_2 = \left(C_1K_2 + C_2K_1\right)\ \omega - \left(m_1C_2 + m_2C_1\right)\ \omega^3$$
$$P_3 = K_2 - m_2\omega^2$$
$$P_4 = K_1 - m_1\omega^2$$
$$P_5 = K - m\omega^2$$

Substituting seat parameters (*k and c*) and seated human body model parameters (k_1, c_1 , k_2 , c_2 , *m*, m_1 *and* m_2) into equation 1 and 2 gives seat transmissibility predictions.

11. Reporting of results

The following information shall be given:

a) Name and address of the seat manufacturer;

b) Model of seat, product and serial number;

c) Date of test;

d) Duration of run-in period;

e) Characteristics of the simulated input vibration test;

f) The name of the person responsible for the test;

g) Identification of test laboratory.

h) Calculation of seat stiffness and damping (e.g. using a MATLAB program in Annex A).

i) Prediction of seat transmissibility (e.g. using a MATLAB program in Annex B).

12. References

Whitham,E.M., Griffin,M.J. (1977) Measuring vibration on soft seats. Society of Automotive Engineers, SAE Paper 770253, International Automotive Engineering Congress and Exposition, Detroit, 28 February - 4 March.

L. Wei, M.J. Griffin (1998), Mathematical model for the apparent mass of the seated human body exposed to vertical vibration, Journal of Sound and Vibration, 212(5), 855-874.

L. Wei, M.J. Griffin (1998), The prediction of seat transmissibility from measures of seat impedance, Journal of Sound and Vibration, 214(1), 121-137.

Dierckx,C. (1995) *Oxford Science Publications.* Curve and surface fitting with splines.

13. Figures

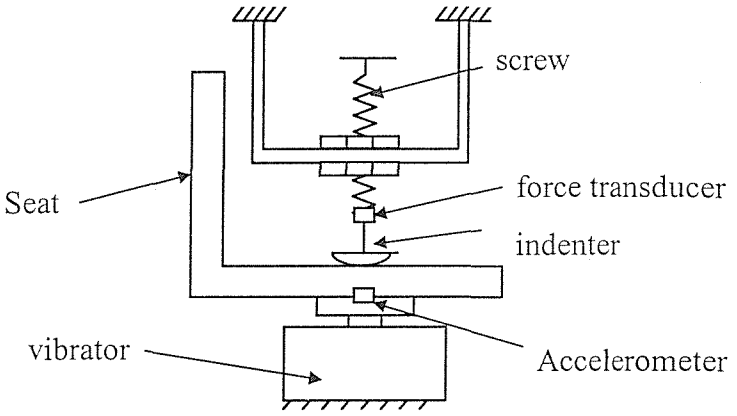

Figure 1 Seat test using indenter rig

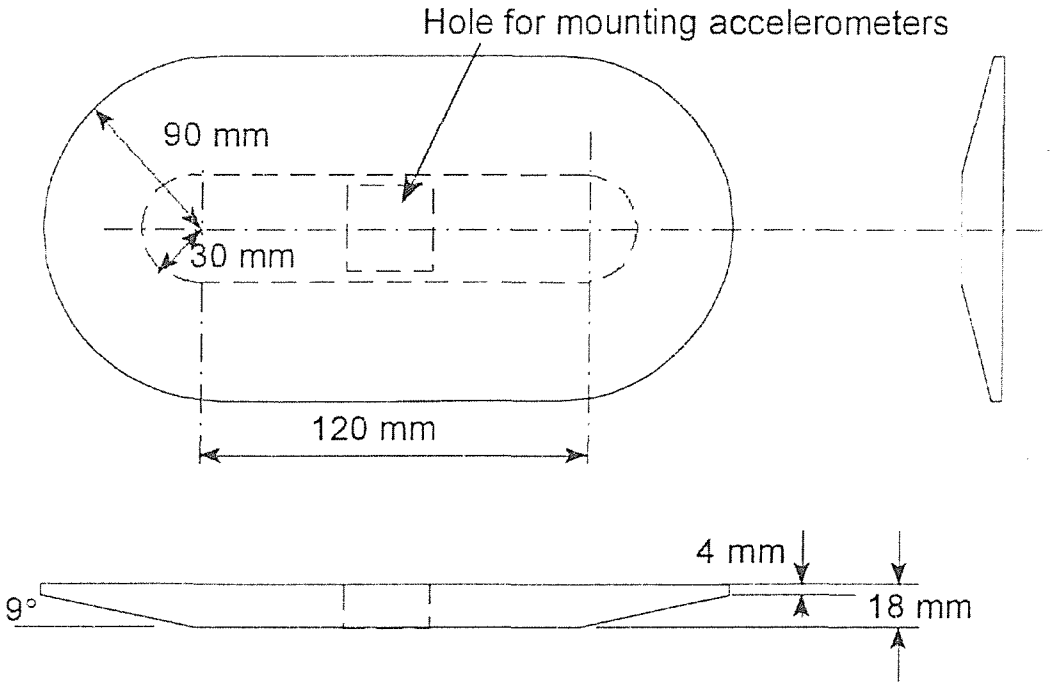

Figure 2 Design of the SIT-BAR (Whitham and Griffin 1977).

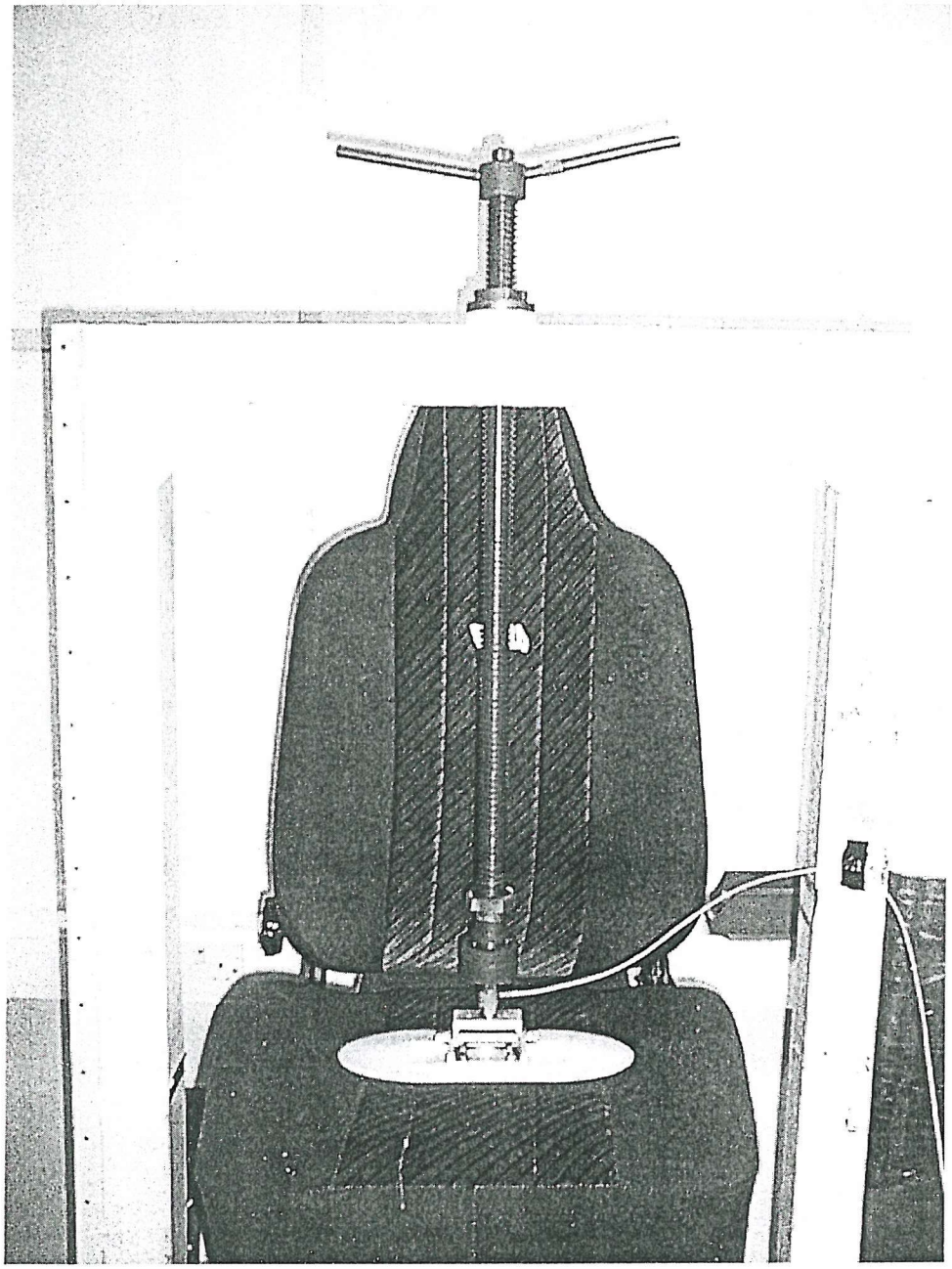

Figure 3 Use of load cell to measure force applied by the indenter (using SIT-BAR as indenter head).

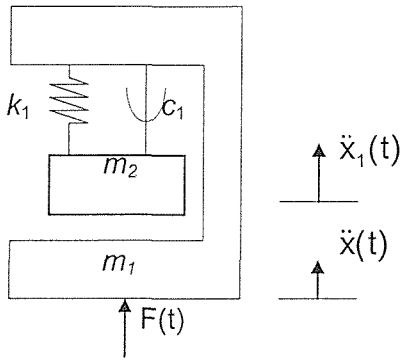

Figure 4 A single degree-of-freedom model with rigid support (model 1b)

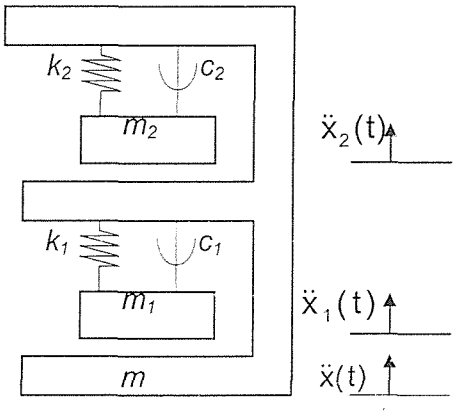

Figure 5 A two degree-of-freedom model with rigid support

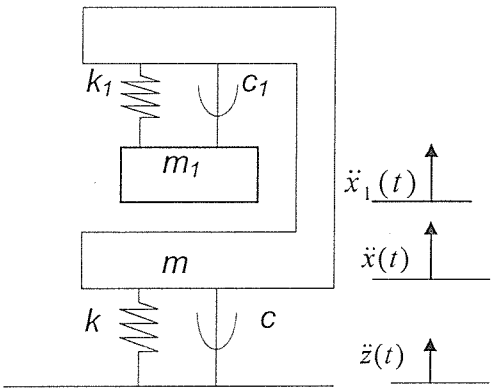

Figure 6 Two degree-of-freedom seat/person system model.

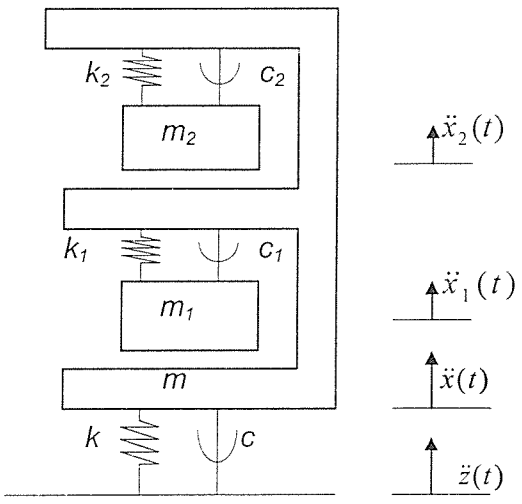

Figure 7. Three degree-of-freedom seat/person system model.

Annex A Programmes to calculate seat stiffness and damping from measured seat impedance (using MATLAB)

The purpose of this Section is to calculate seat impedance using recorded experimental data (see Section 8.1, using measured force and displacement) and then calculate seat stiffness, k, and damping, c, using the obtained seat impedance.

(1) *HVLab* routines (calculate seat impedance):

1. Seat dynamic stiffness calculation
2. Seat dynamic stiffness ASCII data output from *HVLab* system.

(2) MATLAB routines (calibrate seat model stiffness, k, and damping, c using obtained seat impedance):

A) Obtain seat stiffness.

Fk.m is a MATLAB program to fit seat stiffness curve and Fk1.m is a subprogram to calculate the least square error. When these programs are used, the only thing needed to do is that change **ascii file name** in the program to real data file name (i.e., the measured ascii data file name).

Fk.m (MATLAB file name to calculate seat stiffness)

```
clc
% Seat stiffness curve fitting
%
%
load ascii file name
% load seat stiffness ascii file


h= ascii file name;
% using h represent seat stiffness ascii file


t=h(2:60,1);
a=h(2:60,2);
b=h(2:60,3);
w=2*pi*t;
y0=a;y=y0;
z0 = [32500];
% z0 - a random estimate value for seat stiffness
```

```
f=fmins('fk1',z0,[0 1.e-4 1.e-4],[],t,y);
k=f(1);

y=k*t./t;

plot(t,y0,'w',t,y,'w*')
title('Road 1')
xlabel('Frequency Hz')
ylabel('Stiffness (N/m)')
k=k
```

fk1.m (MATLAB subprogram file name to calculate the least square error)

```
function  err = fitfun(z, t, y0)
k = z(1);
w=2*pi*t;
y=k*t./t;
N = length(t);
err = sqrt(sum((y - y0).^2)/N);
```

B) Obtain seat damping.

Fc.m is a MATLAB program to fit seat damping curve (imaginary part of measured seat dynamic stiffness) and Fc1.m is a subprogram to calculate the least square error. When these programs are used, the only thing needed to do is that change **ascii file name** in the program to real data file name (i.e., the measured ascii data file name).

.

Fc.m (MATLAB file name to calculate seat damping)*:*

```
clc
% Seat damping curve fitting
%
%
load ascii file name
% load seat stiffness ascii file
```

```
h= ascii file name;
% using h represent seat damping ascii file

t=h(2:90,1);
a=h(2:90,2);
b=h(2:90,3);
w=2*pi*t;
y0=b;y=y0;
z0 = [500];
f=fmins('fc1',z0,[0 1.e-4 1.e-4],[],t,y);
c=f(1);
y=w*c;
plot(t,y0,'w',t,y,'w*')
title('Road 1')
xlabel('Frequency Hz')
ylabel('Damping (Ns/m)')
c
```

fc1.m (MATLAB subprogram file name to calculate the least square error)

```
function  err = fitfun(z, t, y0)
 c = z(1);
w=2*pi*t;
y=w*c;
N = length(t);
err = sqrt(sum((y - y0).^2)/N);
```

Annex B Programmes to predict seat transmissibility (using MATLAB)

The purpose of this section is to calculate seat transmissibility using the seat-person model (see Section 10.2.1 as well as Figure 6 and 7). Model parameters of the person are listed in Table 1 (see Section 10.1) and model parameters of seat are obtained in Annex B.

A) Predict seat transmissibility using two degree-of-freedom model (Figure 6) without backrest

```
load Ascii file name
%  Load Ascii file (i.e., measured seat transmissibility)
t= Ascii file name (3:125,1);
e1= Ascii file name (3:125,2);
y0=e1; y=y0;

k=67317;c=172;
% input seat stiffness and damping coming from Annex A

m=6; m1=45.6; k1=44943;  c1=1390;
% input body model parameters (see Table 1)

w=2*pi*t;
h=sqrt((k*k1-(m2*k+c*c1)*w.^2).^2+((k*c1+k1*c-m2*c*w.^2).*w).^2);
i=((k-60*w.^2)*k1+(m1*m2*w.^2-k*m2-c*c1).*w.^2).^2;
j=((k*c1+k1*c-(m1*c1+m2*c+m2*c1)*w.^2).*w).^2;
l=sqrt(i+j);
y=h./l;

plot(t,y0,'o',t,y)
title('Predict seat transmissibility ')
xlabel('Frequency Hz')
ylabel('Transmissibility')
gtext('*  Measured seat transmissibility ')
```

```
gtext('-  predict seat transmissibility ')
```

B) Predict seat transmissibility using three degree-of-freedom model (Figure 7) without backrest

```
load Ascii file name
%   Load Ascii file (i.e., measured seat transmissibility)
 t= Ascii file name (3:125,1);
 e1= Ascii file name (3:125,2);

y0=e1; y=y0;

k=67317;c=172;
% input seat stiffness and damping coming from Annex A
m=5.6;m1=36.2;m2=8.9;k1=35007;c1=815;k2=33254;c2=484;
% input body model parameters (see Table 1)

w=2*pi*t;
p1=m1*m2*w.^4-(m1*k2+m2*k1+c1*c2)*w.^2+k1*k2;
p2=(c1*k2+c2*k1)*w-(m1*c2+m2*c1)*w.^3;
p3=k2-m2*w.^2;
p4=k1-m1*w.^2;
p5=k-m*w.^2;
aa=p5.*p1-c*w.*p2-[(m1*k1*w.^2).*p3-m1*c1*c2*w.^4]-[(m2*k2*w.^2).*p4-
m2*c1*c2*w.^4];
bb=(p5.*p2+c*p1.*w)-(m1*c1*p3.*w.^3+m1*c2*k1*w.^3)-
(m2*c2*p4.*w.^3+m2*k2*c1*w.^3);
cc=k*p1-c*w.*p2;
dd=k*p2+c*w.*p1;
h=sqrt(cc.^2+dd.^2);
j=sqrt(aa.^2+bb.^2);

y=h./j;
```

```
plot(t,e1,'w*',t,y,'w-')
title('Predict seat transmissibility ')
xlabel('Frequency Hz')
ylabel('Transmissibility')
gtext('*  Measured seat transmissibility ')
gtext('-  predict seat transmissibility ')
```

APPENDIX B SOME EXPERIMENT RESULTS

1. *Dynamic stiffness of three car seats (Mondeo, Fiesta and Jaguar see Section 8.3.2.1)*

Three car seats (Mondeo, Fiesta and Jaguar) dynamic stiffnesses were measured in the laboratory using the indenter. Floor vibrations in four cars were adopted as the input vibration to represent the four different roads. Three random vibrations were also used to measure seat dynamic stiffnesses. Figures b1 to b3 show measured results. A curve fitting technique was used to obtain seat stiffness and damping (see Section 4.2.2).

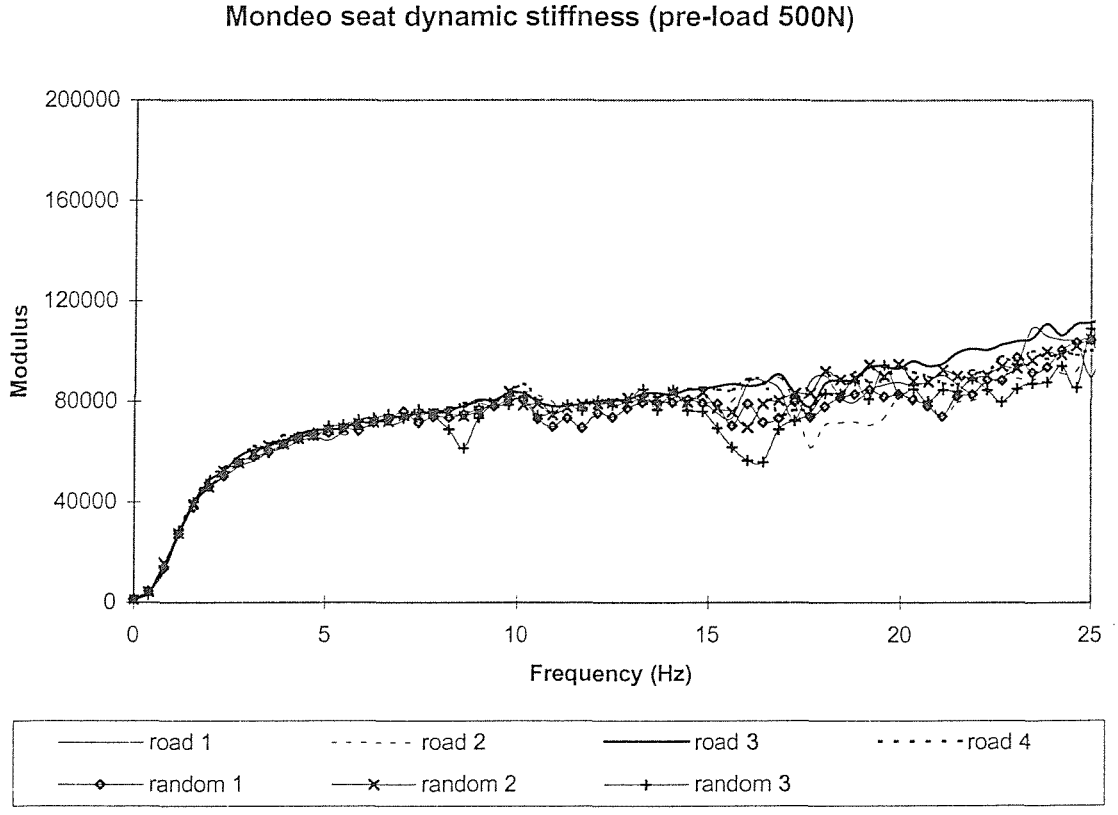

Figure b1. Mondeo seat dynamic stiffness with different input vibrations.

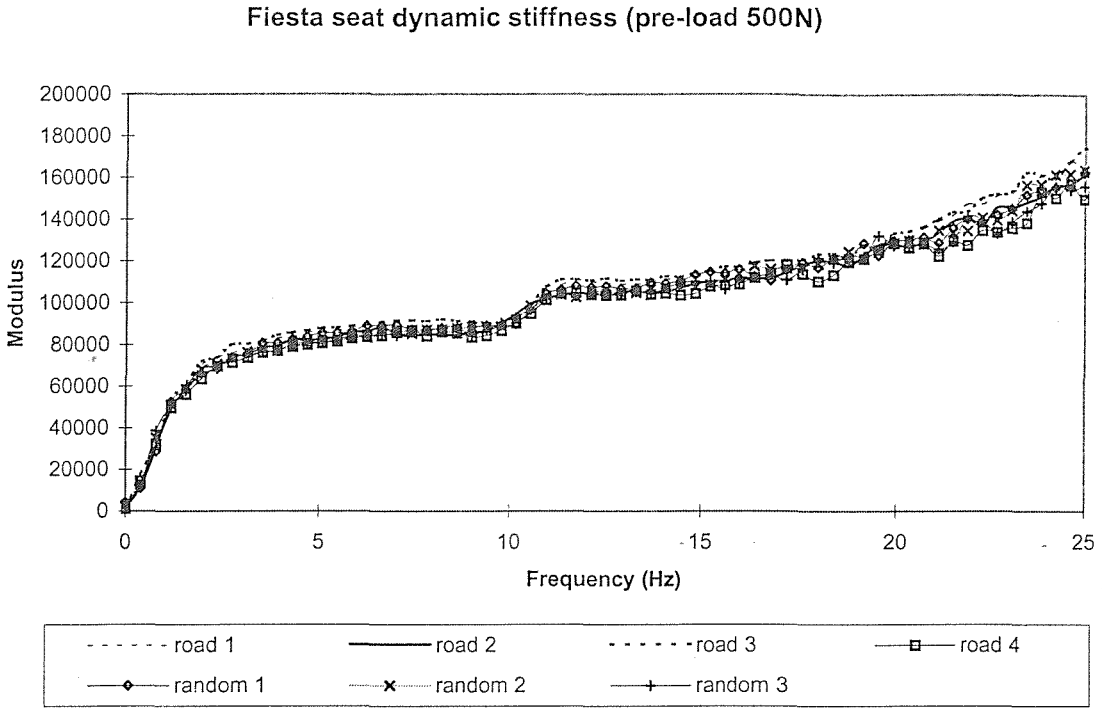

Figure b2. Fiesta seat dynamic stiffness with different input vibrations.

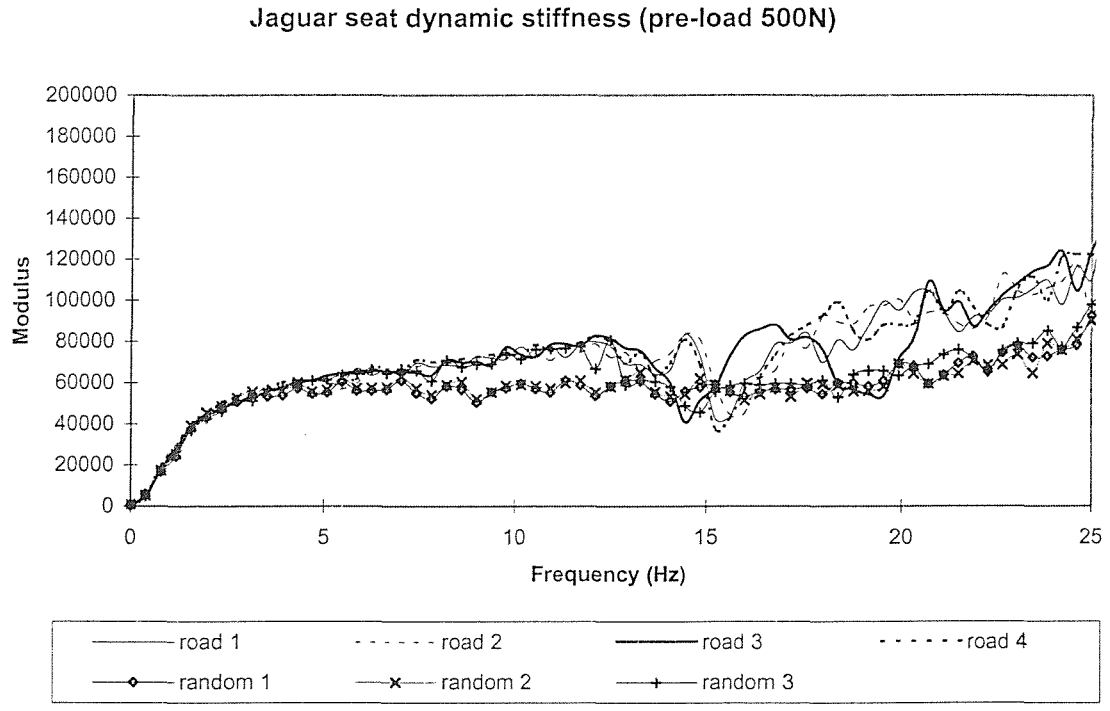

Figure b3. Jaguar seat dynamic stiffness with different input vibrations.

2. *Transmissibility of three car seats (Mondeo, Fiesta and Jaguar see Section 8.3.2.1)*

Figures b4 to b6 show transmissibilities of three car seat (Mondeo, Fiesta and Jaguar). The experimental conditions are described in Section 8.3.2.1. The mean measured transmissibilities of the three seats with six subjects are shown in Figure 8.17.

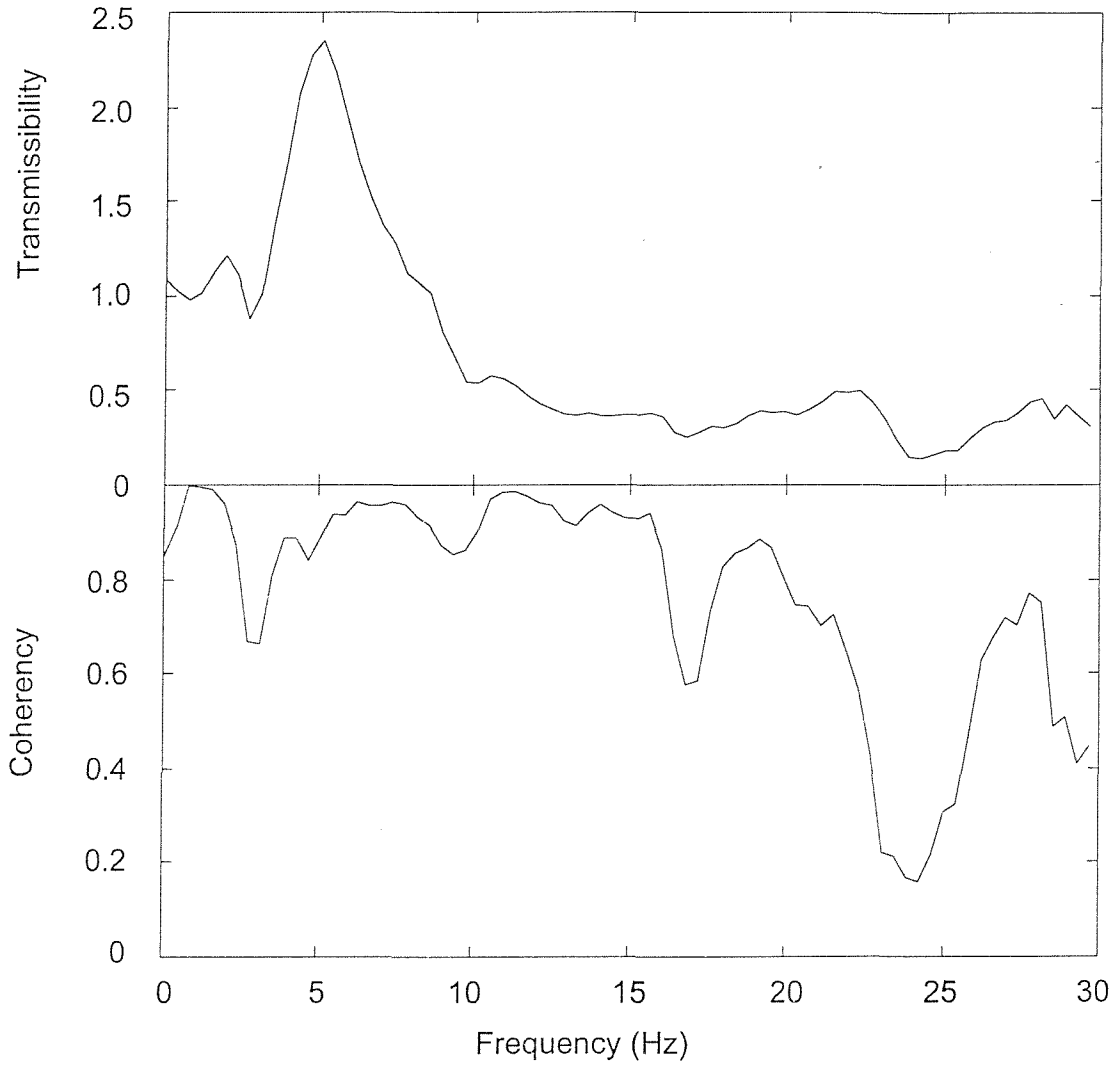

Figure b4. Measured Fiesta seat transmissibility on one road with one subject.

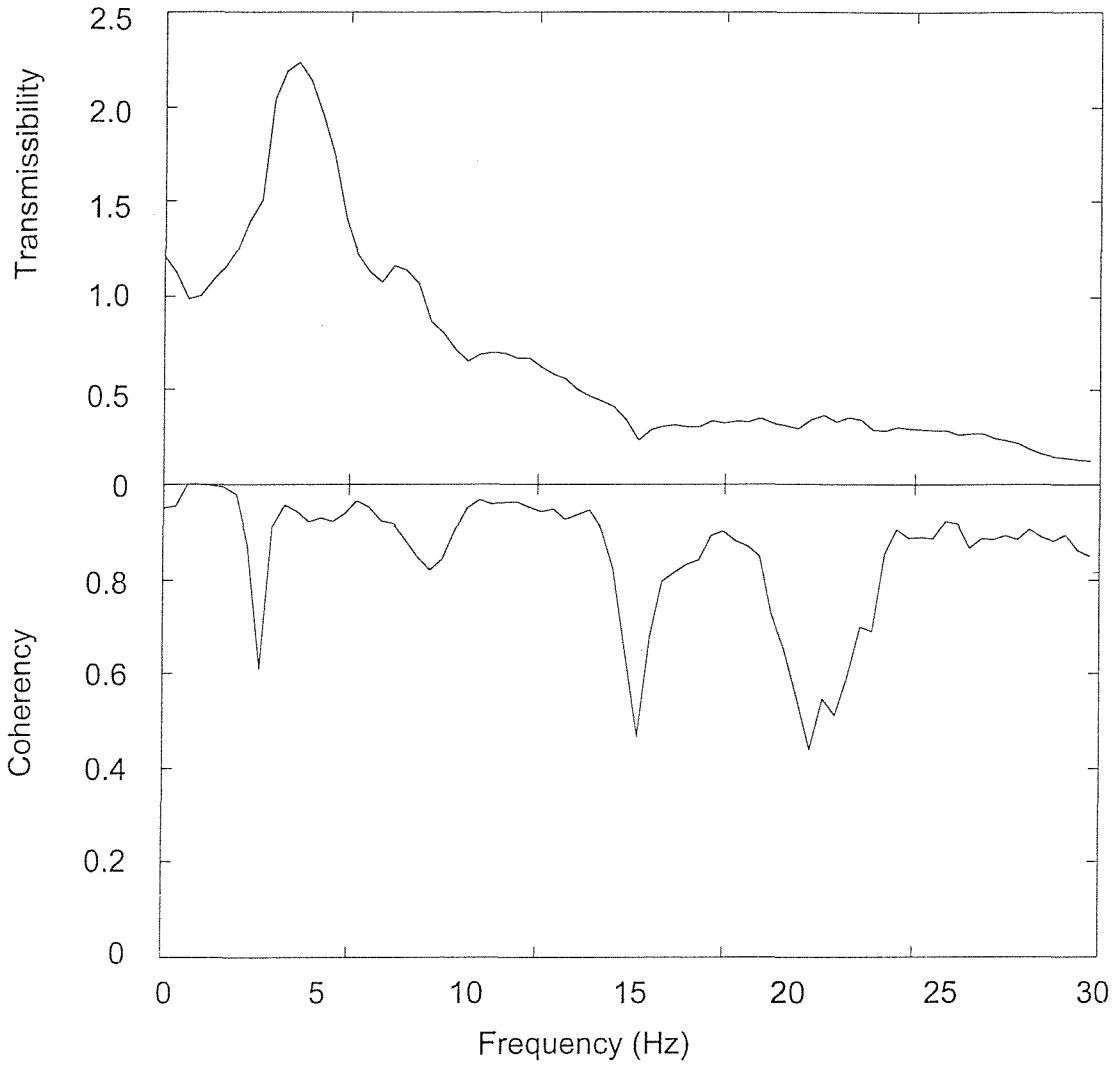

Figure b5. Measured Mondeo seat transmissibility on one road with one subject.

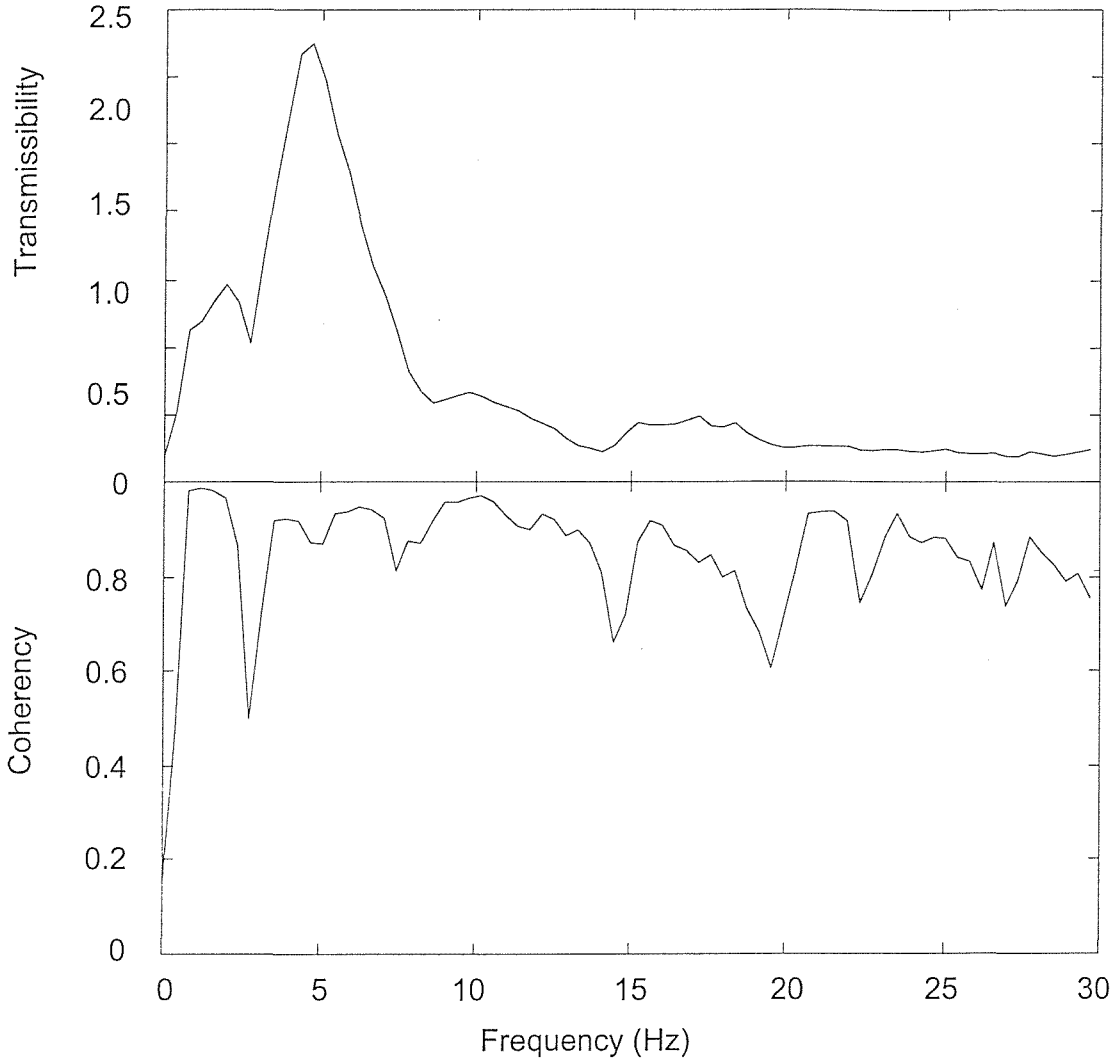

Figure b6. Measured Jaguar seat transmissibility on one road with one subject.

3. *Apparent mass of human body measured in laboratory (see Section 7.4)*

Figures b7 to b9 show measured apparent masses for three subjects. The experimental conditions are described in Section 7.4.1. The mean measured apparent mass of ten subjects is shown in Figure 7.9.

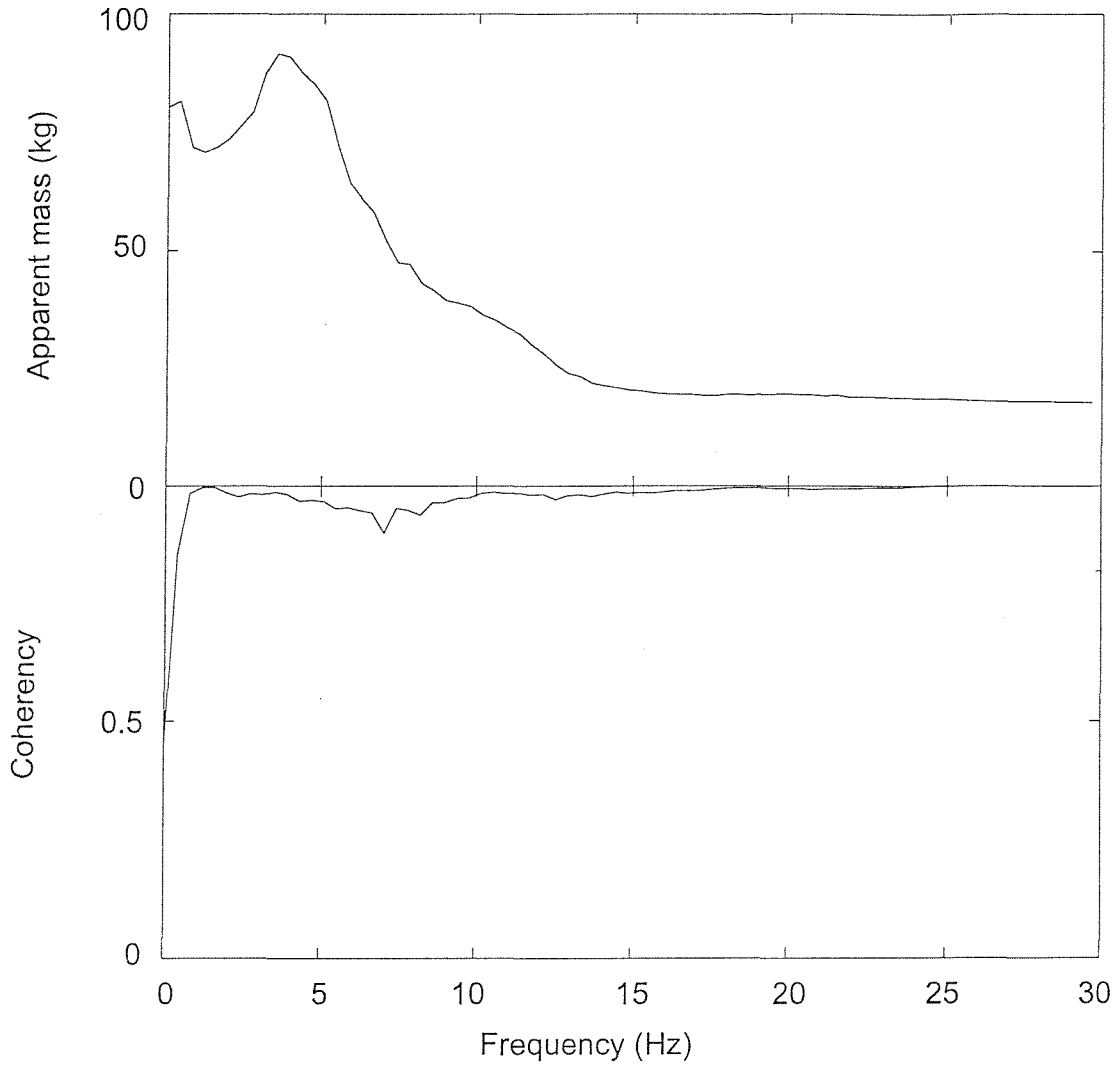

Figure b7. Measured apparent mass for subject 1 with random vibration at 0.5 ms^{-2} r.m.s.

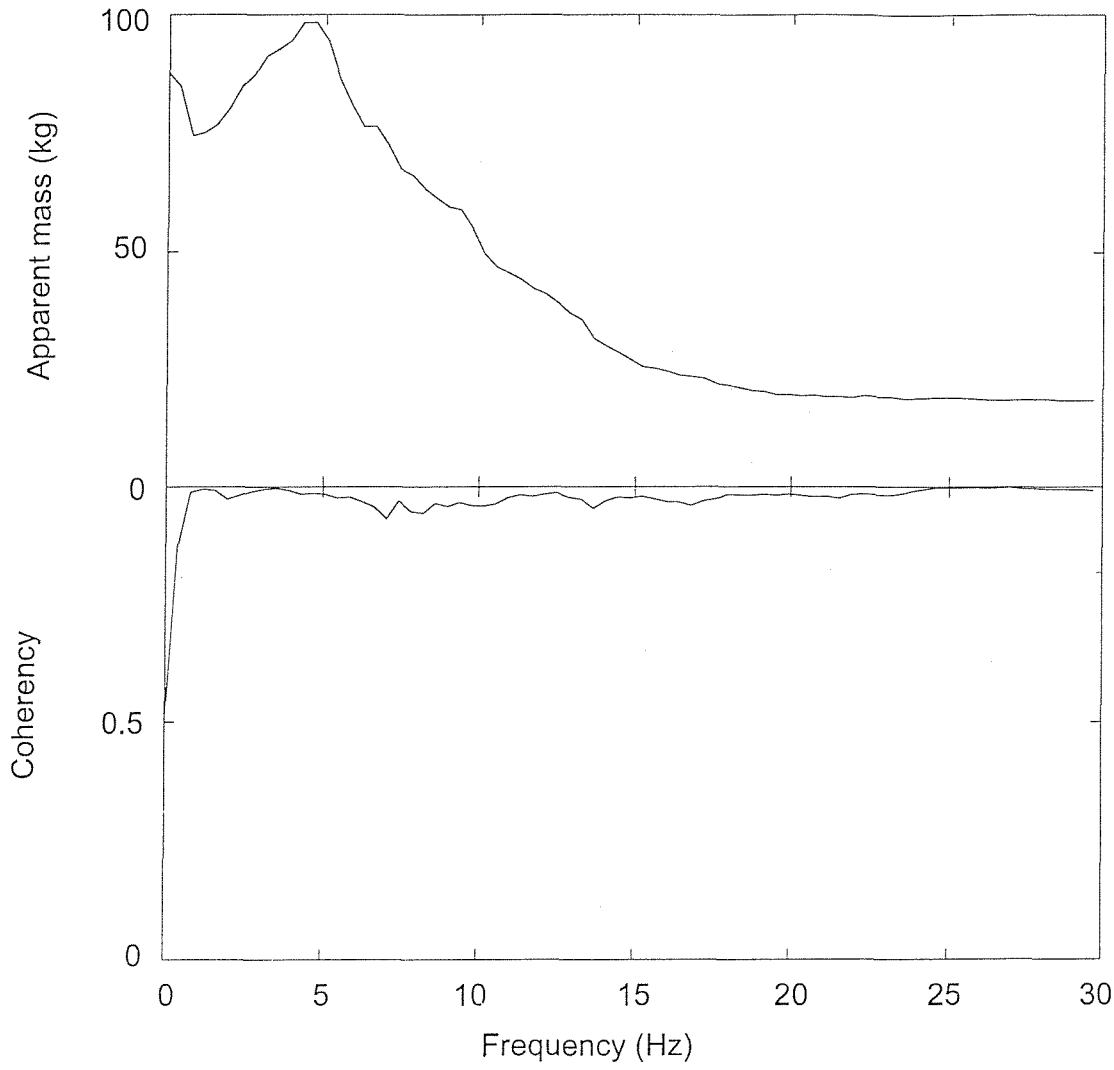

Figure b8. Measured apparent mass for subject 2 with random vibration at 0.5 ms^{-2} r.m.s.

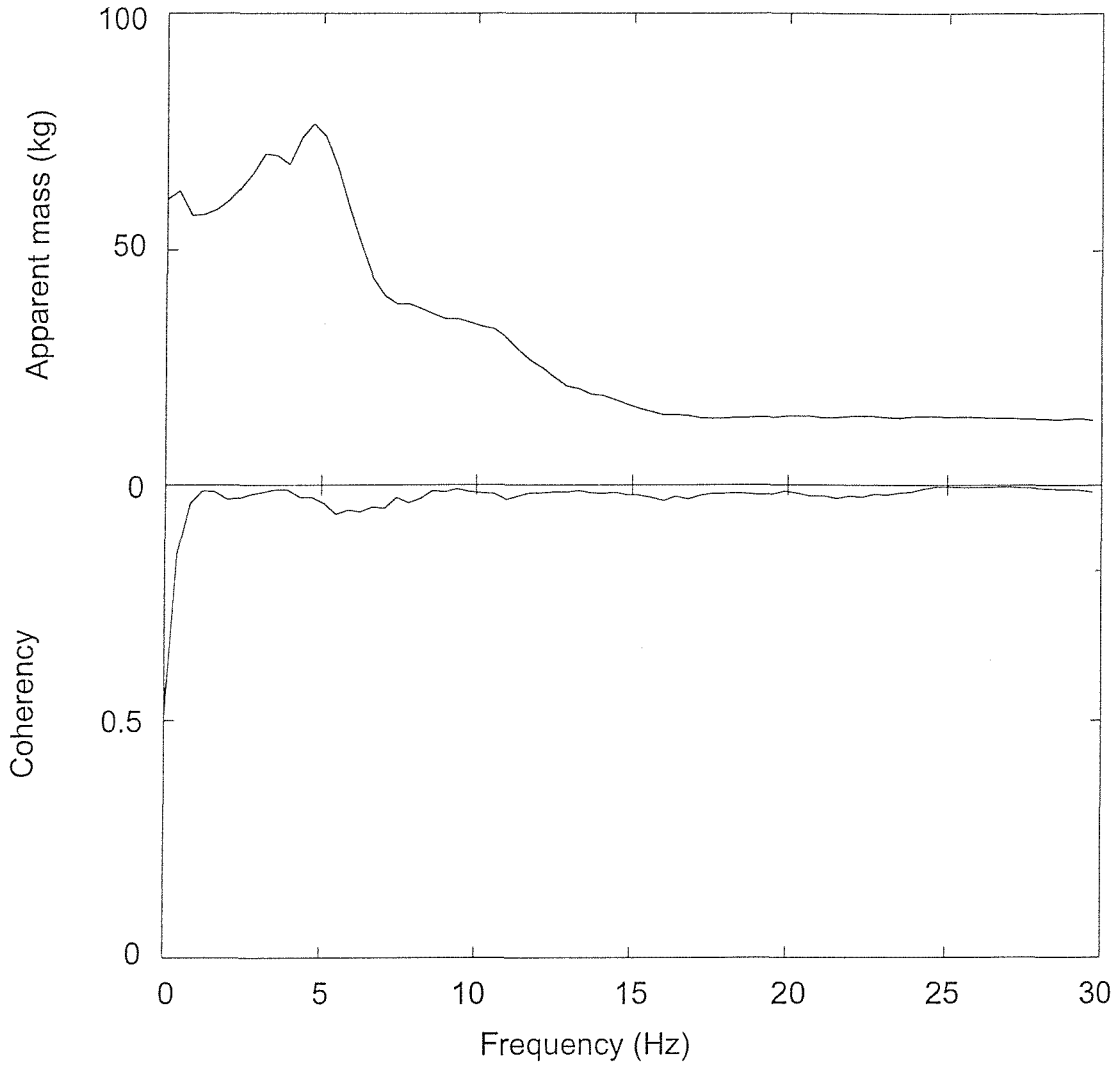

Figure b9. Measured apparent mass for subject 3 with random vibration at 0.5 ms^{-2} r.m.s.

REFERENCES

Ashley, C. (1976), Work vehicle suspension seating, Proceedings of the United Kingdom Informal Group Meeting on Human Response to Vibration, Shrivenham, Swindon: The Royal Military College of Science.

British Standards Institution (1987), British Standard guide to measurement and evaluation of human exposure to whole-body mechanical vibration and repeated shock, BS 6841, London: British Standards Institution.

British Standards Institution (1989), Guide to safety aspects of experiments in which people are exposed to mechanical vibration and shock, BS 7085, London: British Standards Institution.

British Standards Institution (1991), Instrumentation for the measurement of vibration exposure of human beings, BS 7482, London: British Standards Institution.

British Standards Institution (1994), Calibration of vibration and shock pick-ups, BS 6955, London: British Standards Institution.

Broman, H., Pope, M.H., Benda, M., Svensson, M., Ottosson, C. and Hansson, T. (1991), The impact response of the seated subject, Journal of Orthopaedic Research 9(1): 150-154.

Bruns, H.J. and Ronitz, R. (1971), Optimizing ride comfort, Part one: The basic theoretical approach, Automobile engineer 61(3): 26-28.

Bruns, H.J. and Ronitz, R. (1971), Optimizing ride comfort, Part two: The effects of the engine mass, and some results obtained on the simulator *Automobile engineer* 61(4) 45-47.

Burdorf, A. and Swuste, P. (1993), The effect of seat suspension on exposure to whole-body vibration of prefessional drivers, Annals of Occupational Hygiene, 37(1): 45-55.

Bush, T.R., Mills, F.T., Thakurta, K., Hubbard, R.P. and Vorro, J. (1995), The use of electromyography for seat assessment and comfort evaluation, SAE technical paper series 950143, Society of Automotive Engineers, Automotive Engineering Congress and Exposition, Detroit, Michigan, 27 February – 2 March 1995.

Catherines, J.J., Clevenson, S.A. and Scholl, H.F. (1972), A method for the measurement and analysis of ride vibrations of transportation system, N72-24939, National Aeronautics and Spice Administration, Washington, D.C., NASA TN D-6785.

Caventer, K.D. and Kinkelaar, M.R. (1996), Real time dynamic comfort and performance factors of polyurethane form in automotive seating, SAE technical paper series 960509, Society of Automotive Engineers, Automotive Engineering Congress and Exposition, Detroit, Michigan, 26-29 February 1996.

Coermann, R.R. (1962), The mechanical impedance of the human body in sitting and standing positions at low frequencies, Human Factors 4(10): 227-253.

Coermann, R.R., Ziegenruecker, G.H., Witter, A.L. and von Gierke, H.E. (1960), The

passive dynamic mechanical properties of the human thorax-abdomen system and of the whole body system, Aerospace Medicine 31:441-455.

Corbridge, C. (1981), Effect of subject weight on suspension seat vibration transmissibility: suspension in and out, Proceeding of the United Kingdom Informal Group Meeting on Human Response to Vibration, Heriot-Watt University, Edinburgh, 9-11 September l981. 78-91.

Corbridge, C. (1984), A comparison of the vertical and for-and-aft dynamic performance of six suspension seats, Proceeding of the United Kingdom Informal Group Meeting on Human Response to Vibration, Heriot-Watt University, Edinburgh, 21-22 September 1984, 154-167.

Corbridge, C. and Griffin, M.J. (1986), Vibration and comfort: vertical and lateral motion in the range 05 to 5.0 Hz, Ergonomics 29: 249-272.

Corbridge, C. (1987), Vertical vobration transmitted through a seat: effect of vibration input, subjects' postures and subjects' physical characteristics, Informal Group Meeting on Human Response to Vibration, Royal Military College of Science, Shrivenham, 21 –22 September 1987.

Corbridge, C. and Griffin, M.J. (1989), Seat dynamic and passenger comfort, F01388, IMechE.

Corbridge, C. and Griffin, M.J. (1991), Dynamic and static seat comfort, In Contemporary Ergonomics, 1991 Proceedings of the Ergonomics' Society's annual conference, Ergonomics Design for performance, Editor: Lovesey, E.J. Published: Taylor and Francis, London, ISBN: 0-74840-007-9, 20-25.

Cramer,H.J., Liu,Y.K., Rosenberg,D.U.von, 1976, A distributed parameter model of the inertially loaded human spine, Journal of Biomechanics, 9, 15-130.

Crandall, S.H., (1963) Random Vibration in Mechanical System, Massachusetts institute of Technology Cambridge, Massachusetts, Academic Press New York and London

Dierckx,C. (1995) Curve and surface fitting with splines, Oxford Science Publications.

Donati, P.M. and Boldero, A.G., Whyte, R.T. and Styner R.M., (1983), A pilot experiment for seat assessments under dynamic and static conditions, Div, Note DN/1183, natn. Inst. Agric. Engng., Silsoe.

Donati, P.M. and Bonthoux, C. (1983), Biodynamic response of the human position when subjected to vertical vibration, Journal of Sound and Vibration 90(3), 423-442.

Ebe, K. (1993), Effect of foam pad construction on vibration transmission, Proceedings of the United Kingdom informal Group Meeting on Human Response to vibration, Ministry of Defence, Farnborough, Hampshire, England, 20-22 September 1993.

Ebe, K. (1994), The effect of polyurethane foam composition on dynamic comfort of automotive seats, Proceedings of the Japan informal Group Meeting on Human Response to vibration, National Institute of Industrial Health, 6-21-1, Nagao, Tamaku, Kawasaki, 214, Japan, 1st to 3rd July 1994.

Ebe, K. (1995), Effect of foam pad construction on vibration transmission Proceedings of the United Kingdom informal Group Meeting on Human Response to vibration, Silsoe Research Institute, Wrest Park, Silsoe, Bedford, 18-20 September 1995.

Ebe, K. (1998), Predicting the overall discomfort of seats from their static and dynamic characteristics, PhD thesis, University of Southampton.

Fairley, T.E. (1983), The effect of vibration input characteristics on seat transmissibility, Proceedings of the United Kingdom Informal Group Meeting on Human Response to Vibration, National Institute of Agricultural Engineering, Silsoe, Bedford, 14-16 September 1983.

Fairley, T.E. and Griffin, M.J. (1983), Application of mechanical impedance method to seat transmissibility, Internoise 83: 533-537.

Fairley, T.E. and Griffin, M.J. (1984), Modelling a seat person system in the vertical and fore and aft axes, Institute of Mechanical engineers Conference C149/84. 83-89.

Fairley, T.E. (1986), Predicting the dynamic performance of seats, PhD thesis, University of Southampton.

Fairley, T.E. and Griffin, M.J. (1986), A test method for the prediction of seat transmissibility, Society of Automotive Engineers International Congress and Exposition, Detroit, 24-28 February 1986, SAE paper 860046.

Fairley, T.E. (1988), Predicting seat transmissibilities: the effect of the legs, Proceedings of the Joint French-British meeting, Groupe Francais des Etudes des Effets des Vibrations sur l'Homme and United Kingdom Informal Group on Human Response to Vibration, INRS, Vandoeuvre, France 26-28 September 1988.

Fairley, T.E. and Griffin, M.J. (1989), The apparent mass of the seated human body: vertical vibration, Journal of Biomechanics 22: 81-94.

Fairley, T.E. and Griffin, M.J. (1990), The apparena mass of the seated human body in the fore-and-aft and lateral directions, Journal of Sound and Vibration (1990) 139(2), 299-306

Fairley, T.E. (1990), Predicting the transmissibility of a suspension seat, Ergonomics, Vol. 33, No. 2, 121-135.

Fothergill, L.C. and Griffin, M.J. (1977), The subjective magnitude of whole-body vertical vibration, Journal of Biomechanicacs, 22: 81-94.

Fothergill, L.C. and Griffin, M.J. (1977), The use of an Intensity matching technique to evaluate human response to whole-body vibration, Ergonomics, Vol. 20, No.3, 249-261.

Frolov, K.V. (1970), Dependence on position of the dynamic characteristics of a human operator subjected to vibration In: Dynamic Response of Biomechanical Systems, Editor: Perrone, N. American Society of Mechanical Engineers 146-150.

General Motors (1978), HYBRID III exterior body General Motors Corporation Proving Ground, May 1978.

Giacomin, J. (1997), In-vehicle measurement of the apparent mass of small children, Proceedings of the United Kingdom Group Meeting on Human Response to Vibration Institute of Sound and Vibration Research, University of Southampton, 17-19 September I997.

Griffin, M.J. (1975), Vertical vibration of seated subjects: effects of posture, vibration level, and frequency, Aviation Space and Environmental Medicine 46(3): 269-276.

Griffin, M.J. (1978), The evaluation of vehicle vibration and seats, Applied ergonomics 9: 15-21.

Griffin, M.J. (1990), Handbook of human vibration, Academic Press Limited, ISBN 0-12-303040-4.

Griffin, M.J., Lewis, C.H., Parsons, K.C. and Whitham, E.M. (1979), The biodynamic response of the human body and its application to standards, AGARD conference proceedings CP-253, In: Models and Analogues for the Evaluation of Human Biodynamic Response, Performance and Protection, Paris, 6-10 November 1978 (von Gierke, HE ed.) Paper A28, Advisory Group on Aerospace Research and Development.

Guignard, F.L.J.C., (1960), Effects of low-frequency vibration on man, Engineering Vol. 190, No. 4925, 364-367.

Gurram, R and Vertiz, A., (1995), Non-linear vibration response of automotive seat system, Automotive Body Interior & Safty System, IBEC '95,

Hilyard, N.C., Collier, P., Douglass, D. and McNulty, G.J. (1983), Influence of seat cushions on vibration in earth moving vehicles, Internoise 83: 527-531.

Hilyard, N.C., Collier, P. and Care, C. M. (1984), Influence of the mechanical properties of cellular plastic cushions meterials on ride comfort. Coference on "Dynamics in automotive engineering" held at Granfield Institute of Technology, Granfield, Bedford, 5-6 April 1984

Hinz, B. and Seidel, H. (1987), The nonlinearity of the human body's dynamic response during sinusoidal whole body vibration, Industrial Health 25: 169-181.

Hopkins, G.R. (1971), Non-linear lumped parameter mathematical model of dynamic response of the human body, Symposium on Biodynamic Models and their Applications, Dayton, Ohio. 26-28 October 1971, Paper 25: 649-669, AMRL-TR-71-29.

International Organization for Standardization (1981), Vibration and shock-Mechanical driving point impedance of the human body, ISO 5982, Intentional Organization for Standardization, Geneva.

International Organization for Standardization (1985), Evaluation of human exposure to whole-body vibration - Part 1: General requirements, ISO 2631/1- 1985, Intentional Organization for Standardization, Geneva.

International Organization for Standardization (1986), Polymetric materials, cellular flexible – Determination of stress-strain characteristics in compression – Part 1: Low-density materials ISO 3386/1:1986, Intentional Organization for Standardization, Geneva.

International Organization for Standardization (1987), Mechanical vibration and shock – mechanical transmissibility of the human body in the z-direction. ISO 7962, Intentional Organization for Standardization, Geneva.

International Organization for Standardization (1990), Human response to vibration-Measuring instrumentation, ISO 8041 Intentional Organization for Standardization, Geneva.

International Organization for Standardization (1992), Mechanical vibration laboratory method for evaluating vehicle seat vibration, Part 1 basic requirements ISO 10326-1 Intentional Organization for Standardization, Geneva.

International Organization for Standardization (1993), Calibration of vibration and shock pick-ups Part 5: Method of calibration by Earth's gravitation ISO 5347 Intentional Organization for Standardization, Geneva.

International Organization for Standardization (1997), Mechanical vibration and shock-evaluation of human exposure to whole-body vibration - Part 1, General requirements ISO 2631-1 Intentional Organization for Standardization, Geneva.

Jacobson, I.D., Richards, L.G. and Kuhlthau, A.R. (1980), Models of human comfort in vehicle environments, Human Factors in Transportation Research Volume 2, User Factors Comfort, The Environment and Behaviour: 24-32.

Janeway, R.N., (1975), Human vibration tolerance criteria and application to ride evaluation, SAE technical paper series 750166, Society of Automotive Engineers, Automotive Engineering Congress and Exposition, Detroit, Michigan, 24-25 February 1975.

Ji, T.J., (1995), A continuous model for the vertical vibration of the human body in a standing position, Paper presented at the United Kingdom informal group meeting on human response to vibration held at the Silsoe Research Institute 18-20 September I995.

Jolly, A. (1983), Study of ride comfort using a nonlinear mathematical model of a vehicle suspension, Int. J. of Vehicle Design, Vol. 4, No. 3, 233-244.

Kaleps, I., Weiss, E.B. and von Gierke, H.E. (1971), A five degree-of-freedom mathematical model of the body Symposium on Biodynamic Models and their Applications, Dayton, Ohio 26-28 October, 1970, Paper No. 8. 211-231, AMRL-TR-71-29.

Kamijo, K., Tsujimura, H., Obara, H. and Katsumata, M. (1982), Evaluation of seating comfort, SAE technical paper series 820761, Society of Automotive Engineers, Passenger Car Meeting, Troy, Michigan, 7-10 June 1982.

Kitazaki, S. (1992), Application of experimental modal analysis to the human whole-body vibration, Proceedings of United Kingdom Informal Group Meeting on Human Response to Vibration, Institute of Sound and Vibration Research, University of Southampton, 28-30 September 1992.

Kitazaki, S. (1994), Modelling mechanical responses to human whole-body vibration, PhD. thesis, University of Southampton.

Kitazaki, S. and Griffin, M.J. (1997), A modal analysis of whole-body vertical

vibration, using a finite element model of the human body, Journal of Sound and Vibration 200(1): 83-103.

Kitazaki, S. and Griffin, M.J. (1998), Resonance behaviour of the seated human body and effects of posture, Journal of Biomechanics 31: 143-149.

Lakie, M. (1986), Vibration causes stiffness changes (thixotropic behaviour), in relaxed human muscles Proceedings of United Kingdom Informal Group Meeting on Human Response to Vibration, Loughborough University of Technology, 22-23 September 1986.

Latham, F. (1957), A study in body ballistics seat ejection. Proceeding of the Royal Sociaty, B, !47: 121-139.

Leatherwood, J.D. (1975), Vibrations transmitted to human subjects through passenger seats and considerations of passenger comfort, NASA technical note TN D-7929, National Aeronautics and Space Administration.

Lee, J., Ferraiuolo, P. and Temming, J. (1993), Measuring seat comfort, Automotive Engineering, July 1993: 25-30.

Lee, R.A. and Pradko, F. (1968), Analytical analysis of human vibration, Automotive Engineering Congress, Detroit, Michigan, 8-12 January 1968, SAE paper 680091, Society of Automotive Engineers.

Lee, H.G. and Dobson, B.J., (1991), The direct measurement of structural mass, stiffness and damping properties, Journal of Sound and Vibration 145 (1), 61-81.

Lewis, C.H., Griffin, M.J. (1996), The transmission of vibration to the occupants of a car seat with a suspended backrest, D00895, IMechE.

Lewis, C.H., (1998), the implementation of an improved anthropodynamic dummy for testing the vibration isolation of vehicle seat, Proceedings of United Kingdom Group Meeting on Human Response to Vibration, Health and Safty Executive, Buxton, Derbyshire, England, 16-18 September 1998.

Li, T.K., Advani, S. H. and Lee, Y.C., (1971), The effect of initial curvature on the dynamic response of the spine to axial axxeleration, Symposium on biodynamic models and their applications, 26-28 October 1970

Liu, Y.K. and Murray, J.D., (1966), A theoretical study of the effect of impulse on the human torso, Proc. Ame. Soc. Mech. Engineers, Symp. Biomechanics, New York, Nov. 30.

Liu,Y.K., Cramer, H.J., Rosenberg,D.U. von, 1973, A distributed parameter model of the inertially loaded human spine: a finite difference solution, Aerospace Medical Research Laboratory, Wright-Patterson Air Force Base, Ohio, AMRL-TR-73-65. AD-773 859,

Lowe, F.G. (1972), Practical aspects of suspension seat design Vibration isolation symposium, Society of Environmental Engineers, 5 January 1972.

Lundström, R. Holmlund, P. and Lindberg, L. (1995), Absorption of energy during exposure to whole-body vibration, Proceeding of the United Kingdom Informal Group Meeting on Human Response to Vibration, Silsoe Research Institute, Wrest Park,

Silsoe, Bedford, 18-20 September 1995.

Lundström, R. Holmlund, P. and Lindberg, L. (1998), Absorption of energy during vertical whole-body vibration exposure, Journal of Biomechanics 31, 317-326.

Mansfield, N.J. (1993), Test methods for the prediction of the transmissibility of vehicle seats, Paper presented at the Engineering Integrity Society Symposium on "Prectical NVH solutions to real problems" Peugeot-Talbot Social Centre, England, 6th October l993.

Mansfield, N.J. (1994), The apparent mass of the human body in the vertical direction – the effect of vibration magnitude, Proceedings of the United Kingdom informal Group Meeting on Human Response to vibration, Silsoe Research Institute, Wrest Park, Silsoe, Bedford, 18-20 September 1995.

Mansfield,N.J., Griffin,M.J. 1996 Inter-noise '96, Proceedings of 25th Anniversary Congress, Liverpool, Book 4, Published: Institute of Acoustics, ISBN: 1-873082 91 6, 1725-1730. Vehicle seat dynamics measured with an anthropodynamic dummy and human subjects.

Mansfield, N.J. (1997), A consideration of alternative non-linear lumped parameters models of the apparent mass of a seated person, Paper presented at international Conference on Whole Body Vibration Injuries, Institute of Sound and Vibration Research, University of Southampton 15-17 September l997.

Mansfield, N.J. (1998), Non-linear dynamic response of the seated person to whole body vibration. PhD thesis, University of Southampton.

Matsumoto, Y. (1996), The influence of posture on the apparent mass of standing subjects exposed to vertical vibration, Proceedings of the United Kingdom Informal Group Meeting on Human Response to Vibration, Motor Industry Research Association, Watling Street, Nuneaton, Warwickshire, 18-20 September 1996.

Matsumoto, Y. and Griffin, M.J. (1997), Movement of the upper-body of seated subjects exposed to vertical whole-body vibration at the principal resonance frequency, Paper presented at international Conference on Whole Body Vibration Injuries, Institute of Sound and Vibration Research, University of Southampton 15-17 September l997.

Matsumoto, Y. and Griffin, M.J. (1998), Dynamic response of the standing human body exposed to vertical vibration: influence of posture and vibration magnitude, Journal of Sound and Vibration 212 (1), 85-107.

Matsumoto, Y. (1998) An investigation of linear lumped parameter models with rotational degrees of freedom to represent the dynamic response of the human body. Proceedings of the United Kingdom Group on Human Response to Vibration, organized by the Health and Safety Executive, Buxton, 16-18 September.

Matsumoto, Y. (1999), Dynamic response of the standing and seated persons to whole-body vibration: principal resonance of the body. PhD thesis, University of Southampton.

Matthews, J. (1966), Ride comfort far tractor operators IV: Assessment of the ride quality of seats Journal of Agricultural Engineering Research 11(1): 44-57.

Matthews, J. (1967), Progress in the application of ergonomics to agricultural engineering, Proceedings of Engineering Symposium of the institution of Agricultural Engineers, National College of Agricultural Engineering, Silsoe, 12 September 1967.

Mertens, H. (1978), Nonlinear behaviour of sitting humans under increasing gravity Aviation Space and Environmental Medicine 49(1) Section 11: 287-298.

Mertens, H. and Vogt, L. (1979), The response of a realistic computer model for sitting humans to different types of shocks AGARD conference proceedings CP-253 In Models and Analogues for the Evaluation of Human Biodynamic Response, Performance and Protection, Paris, 6-10 November 1978 (von Gierke. HE ed.) Paper A26, Advisory Group on Aerospace Research and Development.

Messenger, A.J. (1988), The effects of modifications to a helicopter seat on the transmission of vertical vibration through seat and occupant, Proceedings of the Joint French-British meeting, Groupe Francais des Etudes des Effets des Vibrations sur lHomme and United Kingdom Informal Group on Human Response to Vibration, INRS, Vandoeuvre, France 26-28 September 1988.

Messenger, A.J., Stratford, R. and Griffin, M.J. (1992), Design guide for the Ergonomic Aspects of Helicopter Crew Seating Institute of Sound and Vibration Research, University of Southampton. Technical Report 209.

Miwa, T. (1975), Mechanical Impedance of Human Body in various postures Industrial Health 13(1): 1-22.

Miwa, T. and Yonekawa, Y. (1971), Evaluation methods for vibration effect part 10 Measurement of Vibration attenuation effect of Cushions, industrial Health 9: 81-98.

Muksian, R. and Nash, C.D. (1974), A model for the response of sealed humans to sinusoidal displacements of the seat Journal of Biomechanics 7: 209-215.

Muksian, R. and Nash, C.D. (1976), On frequency dependant damping coefficients in lumped parameter models of human beings, Journal of Biomechanics 9: 339-342.

Ng, D., Cassar, T. and Gross, C.M. (1995), Evaluation of an intelligent seat system, Applied Ergonomics, 26(2): 109-116.

Nigam, S.P. and Malik, M., (1987), A study on a vibratory model of a human body, Journal of Biomechamical Engineering, 109, pp. 148-153.

Paddan, G.S. and Griffin, M.J. (1988), The transmission of translational seat vibration to the head. I. Vertical seat vibration. Journal of Biomechanicals 21: 199-206

Paddan, G.S. and Griffin, M.J. (1996), Transmission of mechanical vibration through the human body to the head. Technical report 260, ISVR, The University of Southampton.

Parsons, K.C. and Griffin, M.J. (1983), Method for predicting passenger vibration discomfort, Society of Automotive Engineers Technical Paper Series 831029.

Parsons, K.C. and Griffin, M.J. (1988), Whole-body vibration perception thresholds, Journal of Sound and vibration 121(2): 237-258.

Patten, W.N., Sha, S. and Mo, C., (1998), A vibration model of open celled

polyurethane foam automotive seat cushion, Journal of Sound and Vibration 217(1), 145-161.

Payne, P.R. (1965), Personnel restraint and support system dynamics, Technical Report AMRL-TR-65-127 Aerospace Medical Research Laboratory, Aerospace Medical Division, Air Force Systems Command, Wright-Patterson Air Force Base, Ohio.

Payne, P.R. and Band, E.G.U. (1971), A four degree-of-freedom lumped parameter model of the seated human body technical Report AMRL-TR-70-35, Aerospace Medical Research Laboratory, Aerospace Medical Division, Air Force Systems Command, Wright-Patterson Air Force Base, Ohio.

Pope, M.H., Broman, H. and Hansson, T. (1990), Factors affecting the dynamic response of the seated subject, Journal of spinal disorders 3(2): 135-142.

Pope, M.H., Kaigle, A.M., Magnusson, M., Broman, H. and Hansson, T. (1991), Intervertebral motion during vibration, Proceedings of the institution of Mechanical Engineering Part FI, Journal of Engineering in Medicine 205 (1).

Pope, M.H., Wilder, D.G., Jorneus, L., Broman, H., Svensson, M. and Andersson, G. (1986), How the seated human responds to vibration and impact, Proceedings of the Winter Annual Meeting of the American Society of Mechanical Engineers, Anaheim California, 7-12 December 1986.

Pope, M.H., Wilder, D.G., Jorneus, L., Broman, H., Svensson, M. and Andersson, G. (1987), The response of the seated human to sinusoidal vibration and impact Journal of Biomechanical Engineering 109: 279-284.

Potemkin, B.A. and Frolov, K.V. (1979), Non-linear effects connected with the spatial vibrations of biomechanical systems, Man under vibration: suffering and protection Studies ill Environmental Science 13: 228-234, ISBN 0-444-99743-1.

Potemkin, B.A. and Frolov, K.V. (1971), Representation by models of the biomechanical system 'man-operator' under the action of random vibrations DAN, SSSR 197(6): 1284-1287 (Royal Aircraft Establishment Library Translation 1651 1972).

Pradko. F. (1965), Human response to random vibration, Shock and Vibration bulletin 34: 173-190.

Pradko, F., Lee, R. and Kaluza, V. (1966), Theory of human vibration response Proceedings of the Winter Annual Meeting of the Human Factors, Chicago, 7-11 November ASME Paper 66-WA/BHF-I5.

Radke, O.A. (1956), The application of human engineering data to vehicular seat design Paper presented to participants in Project 335, European Productivity Agency, Purdue University, October 1 1956.

Roberts, V.L., Terry, C.T. and Stech. E.L. (1966), Review of Mathematical Models Which Describe Human Response to Acceleration Paper presented at Winter Annual Meeting and Energy Systems Exhibition, New York, 27 November - 1 December American Society of Mechanical Engineers, BB-WA/BHF-13.

Robertson, C.D. and Griffin, M.J. (1989), Laboratory studies of the electromyographic

response to whole-body vibration Institute of Sound and Vibration Research, University of Southampton Technical Report 184.

Sandover, J. (1970), Some current biomechanical research in the United Kingdom related to the effects of impact and vibration an man Symposium on biodynamic models and their applications 25-28 October 1970, AMRL-TR-71-29 105-123.

Sandover, J. (1971), Study of human analogues Part 1: a survey of the literature Department of Ergonomics and Cybernetics, Loughborough University of Technology.

Sandover, J. (1978), Modelling Human Responses to Vibration, Aviation Space and Environmental Medicine 49(1): 335-339.

Seidel, H. and Heide, R.(1986), Long term effects of whole-body vibration: a critical survey of the literature international Archives of Occupational and Environmental Health 58: 1-26.

Seroussi, R.E., Wilder, D.G. and Pope, M.H. (1989), Trunk muscle electromyography and whole-body vibration Journal of Biomechanics 22: 219-229.

Siegal, S. and Castellan, N.J. (1988), Nonparametric statistics for the behavioural sciences. McGraw-Hill ISBN 0-07-100326-6

Smith, S.D. (1994), Nonlinear resonance behaviour in the human exposed to whole-body vibration, Shock and Vibration 1(5): 439-450.

Smith, C.C. and Kwak, Y.K. (1978), Identification of the dynamic characteristics of a bench type automotive seat for the evaluation of ride quality Transactions of the American Society of Mechanical Engineers, Journal of Dynamic Systems, Measurement and Control 100: 42-49.

Snowdon, J.C., (1968) Vibration and Shock in Damped Mechanical System , JOHN WILEY & SONS.

Society of Automotive Engineers (1978), Vehicle dynamics terminology, Society of Automotive Engineers 3670e.

Society of Automotive Engineers (1974), Measurement of whole body vibration to the seated operator of agricultural equipment Society of Automotive Engineers J1013.

Society of Automotive Engineers (1985), Manikins for use in defining vehicle seating accommodation, Society of Automotive Engineers J826.

Stayner, R.M. (1971), Aspects of the development of a test code for tractor suspension seats, British Acoustical Society Paper 71SA8.

Stayner, R.M. (1973), Ride vibration on agricultural tractors Proceedings of the United Kingdom informal Group Meeting on Human Response to Vibration, University of Salford, 17-19 September.

Stech, E.L. (1965), A review of restraint systems test methods American Society of Mechanical Engineers 63-WA-179.

Suggs, C.W., Abrams, C.F. and Stikeleather, L.F. (1968), Development of a dynamic

simulator from the mechanical impedance of seated man Biomechanics 32(6) 21st ACEMB, Shamrock Hilton Hotel, Houston, Texas.

Suggs, C.W., Abrams, C.F. and Stikeleather, L.F. (1969), Application of a damped spring-mass human vibration simulator in vibration testing of vehicle seats, Ergonomics 12: 79-80.

Suggs, C.W., Stikeleather, L.F., Harrison, J.Y. and Young, R.E. (1969), Application of a dynamic simulator in seat testing, Annual Meeting American Society of Agricultural Engineers Purdue University, 22-25 June. Paper No. 69-172.

Suggs, C.W., and Abrams, C.F. (1971), Mechanical impedance techniques for evaluating the dynamic characteristics of biological materials, Journal of Agricultural Engineering, 16: 307-315.

Tomlinson, R.W. and Kyle, D.J. (1970), The development of a dynamic model of the seated human operator, Departmental note: Tractor and Machine Performance Division, National Institute of Agricultural Engineering, Wrest Park, Silsoe, Bedford, DN/TE/037/1445.

Varterasian, J.H. (1981), On measuring automobile seat ride comfort Research Publication, General Motors Research Laboratories, Warren, Michigan 48090, GMR-3679.

Varterasian, J.H. (1982), On measuring automobile seat ride comfort, Society of Automotive Engineers Technical Paper Series International Congress and Exposition, Detroit, Michigan, February 22-26,1982 SAE paper 820309.

Varterasian, J.H. and Thompson, R.R. (1977), The dynamic characteristics of automobile seats with human occupants, Society of Automotive Engineers, international Automotive Engineering Congress and Exposition, Coo Hall, Detroit February 28 - March 4, 1977, SAE paper 770249.

Vogt, H.L., Coermann, R.R. and Fust, H.O. (1968), Mechanical impedance of the sitting human subject under sustained acceleration Aerospace Medicine, July 1968, 675- 679.

Vogt, H.L., Krause, H.E., Hohlweck, H. and May, E. (1973), Mechanical impedance of supine humans under sustained acceleration Aerospace Medicine 44: 123-128.

Vogt. H.L, Mertens, H and Krause. H.E. (1977), Model of the supine human body and Its reaction to external forces, Aviation Space and Environmental Medicine 29(1): 270-278.

Wambold, J.C. (1986), Vehicle ride quality, measurement and analysis Society of Automotive Engineers Technical Paper Series 861113.

Wambold, J.C. and Park. W.H. (1976), A human model for measuring ride quality, *Mechanical Engineering*, July 1976. 30-34.

Wei,L., Griffin,M.J. (1995) A Method of Predicting Seat Transmissibility, United Kingdom Informal Group Meeting on Human Response to Vibration held at the Silsoe Research Institute, September 1995.

Wei,L., Griffin,M.J. (1997) The influence of contact area, vibration magnitude and

static force on the dynamic stiffness of polyurethane seat foam, Presented at the United Kingdom Group Meeting on Human Response to Vibration held at the ISVR, University of Southampton, Southampton, SO17 1BJ, England, 17-19 September 1997.

Wei,L., Griffin,M.J. (1998a) Mathematical model for the mechanical impedance of the seated human body exposed to vertical vibration, Journal of Sound and Vibration 212(5), 855-874

Wei,L., Griffin,M.J. (1998b) The prediction of seat transmissibility from measures of seat impedance, Journal of Sound and Vibration, 214 (1), 121-137.

Whitham, E.M. and Griffin, M.J. (1977), Measuring vibration on soft seats Society of Automotive Engineering, International Automotive Engineering Congress and Exposition, Cobo Hall, Detroit, February 28 March 4, 1977, SAE 770253.

Wilcoxon, F. (1945), individual comparisons by ranking methods, Biometrics 1:80-83.

Wilcoxon, F. (1947), Probability tables for individual comparisons by ranking methods Biometrics 3: 119-122.

Wilcoxon, F. (1949), *Some rapid approximate statistical procedures* Stamford, CT: American Cyanamid.

Wittman, T.J. and Phillips, N.S. (1969), Human body nonlinearity and mechanical *impedance analyses, journal of Biomechanics* 2: 281-288.

Wu, X. (1994), A method of testing suspension seats for end-stop impacts Proceedings of the United Kingdom informal Group Meeting on Human Response to Vibration, Institute of Naval Medicine, Alverstoke, Gosport, Hants, P012 2DL, 19-21 September l994.

Wu, X. and Griffin, M.J. (1995), Simulation study of factors influencing the severity of suspension seat end-stop impacts Proceeding of the United Kingdom informal Group Meeting on Human Response to Vibration, Silsoe Research Institute, Wrest Park, Siisoe, Bedford, 18-20 September 1995.

Wu, X., Rakheja, S. and Boileau, P.E. (1997), Study of biodynamic functions of human response to whole-body vibration Proceeding of the United Kingdom Group Meeting on Human Response to Vibration Institute of Sound and Vibration Research, University of Southampton 17-19 September 1997 195-208.

Zimmermann, C.L. and Cook, T.M. (1997), Effect of vibration frequency and postural changes on human response to seated whole-body vibration exposure, International Archive of Occupational and Environmental Health, 69: 165-179.